CHALMERS

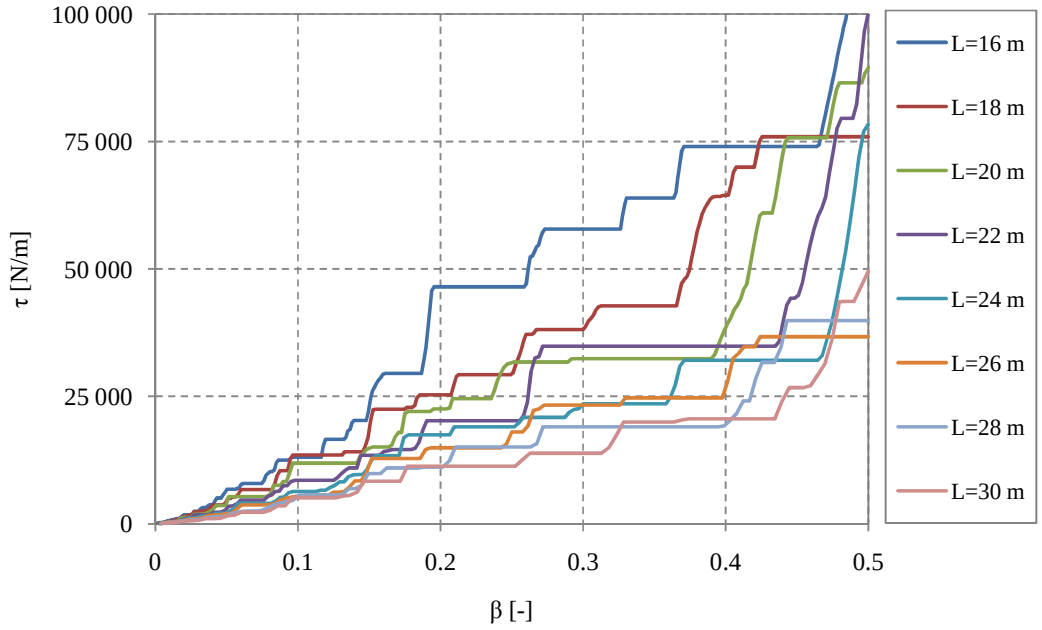

Dynamic design of high-speed railway bridges

Simplifications and guidelines

Master's Thesis in the International Master's Programme Structural Engineering and Building Performance Design

PATRIK ERIKSSON
EMANUEL TROLIN

Department of Civil and Environmental Engineering
Division of Structural Engineering
Concrete Structures
CHALMERS UNIVERSITY OF TECHNOLOGY
Göteborg, Sweden 2010
Master's Thesis 2010:37

MASTER'S THESIS 2010:37

Dynamic design of high-speed railway bridges

Master's Thesis in the International Master's Programme Structural engineering and Building Performance Design

PATRIK ERIKSSON

EMANUEL TROLIN

Department of Civil and Environmental Engineering
Division of Structural Engineering
Concrete Structures
CHALMERS UNIVERSITY OF TECHNOLOGY

Göteborg, Sweden 2010

Dynamic design of high-speed railway bridges

Simplifications and guidelines

Master's Thesis in the International Master's Programme Structural Engineering and Building Performance Design

PATRIK ERIKSSON
EMANUEL TROLIN

Examensarbete / Institutionen för bygg- och miljöteknik,
Chalmers tekniska högskola 2010:37

Department of Civil and Environmental Engineering
Division of Structural Engineering
Concrete Structures
Chalmers University of Technology
SE-412 96 Göteborg
Sweden
Telephone: + 46 (0)31-772 1000

Cover:
Design curves for a two-span bridge in 2D, Figure 4.51.

Chalmers reproservice / Department of Civil and Environmental Engineering Göteborg, Sweden 2010

Dynamic design of high-speed railway bridges

Simplifications and guidelines

Master's Thesis in the International Master's Programme Structural Engineering and Building Performance Design

PATRIK ERIKSSON
EMANUEL TROLIN
Department of Civil and Environmental Engineering
Division of Structural Engineering
Concrete Structures
Chalmers University of Technology

ABSTRACT

In 2006 the bridge code was updated to include a demand of dynamic analysis of railway bridges subjected to high-speed trains. This analysis includes several complex loads to be examined for a large range of train velocities and is therefore complicated and time consuming. The dynamic analysis' complexity also makes it hard to establish guidelines for the early bridge design even with increased experience. There is hence a need today to introduce both guidelines for the early bridge design and simplifications for the advanced dynamic analysis of railway bridges. This master thesis provides an extensive study of railway bridges' dynamic behavior and presents a method of guidance for the dynamic design.

As a continuation of previous master theses, carried out at Reinertsen Sverige AB, a method for transforming a railway bridge into a single-degree-of-freedom (SDOF) system is examined in this thesis. It is shown that a railway bridge of several spans can be successfully transformed into a SDOF system that provides accurate results compared to a finite element analysis.

A parameter study is performed in this thesis with the purpose of studying the individual bridge parameters' effect on the dynamic response. It is shown that material parameters exert an describable effect, while the effect of geometric parameters is more complicated. The increased understandings concerning bridge parameters' effect on the dynamic response and resonance phenomenon in railway bridges are used in the creation of a graphical calculation tool, referred to as a design curve. A design curve is a comprehensible presentation of an extensive number of finite element analyses from which it possible to obtain the designing vertical acceleration, independent of the choice of train velocity, material parameters and cross-section geometry.

A comparison between 2D and 3D analyses of railway bridges is performed in this thesis. It is shown how the designing acceleration is altered as 3D geometry and hence bridge torsion and load eccentricity is considered. A discussion is presented on the possibility of creating guidelines and simplifications of railway bridges' dynamic design with consideration to 3D effects.

Keywords: Dynamics, Railway bridges, high-speed trains, HSLM, SDOF, eccentric loading, resonance, vibrations

Dynamisk design av järnvägsbroar utsatta för höghastighetståg

Förenklingar och riktlinjer

Examensarbete inom det Internationella mastersprogrammet Structural Engineering and Building Performance Design

ERIKSSON PATRIK
TROLIN EMANUEL
Institutionen för bygg- och miljöteknik
Avdelningen för betongbyggnad

Chalmers tekniska högskola

SAMMANFATTNING

År 2006 uppdaterades bronormen till att inkludera krav på den dynamiska analysen av järnvägsbroar som är utsatta för höghastighetståg. En sådan analys inkluderar flera komplexa lastfall som ska undersökas för ett stort spann av hastigheter, vilket gör analysen komplicerad och tidskrävande. Komplexiteten i den dynamiska analysen gör det svårt att upprätta riktlinjer för brokonstruktionen i ett tidigt skede, även med ökad erfarenhet i ämnet. Idag finns det därför ett behov av riktlinjer för den tidiga designen och förenklingar av den avancerade dynamiska analysen av järnvägsbroar. Detta examensarbete består av en omfattande studie av järnvägsbroars dynamiska beteende och presenterar en metod med riktlinjer för dynamisk design.

Som fortsättning på tidigare examensarbeten, utförda på Reinertsen Sverige AB, har en metod för att omvandla en järnvägsbro till ett enfrihetsgradssystem (SDOF) undersöks. Det visas att en järnvägsbro i flera span framgångsrikt kan förvandlas till ett SDOF system som ger tillförlitliga resultat jämfört med finita element analyser.

En parameterstudie har genomförts med syfte att studera individuella broparametrars inverkan på den dynamiska responsen. Det visas att materialparametrar har beskrivbar inverkan medan effekten av de geometriska parametrarna är mer komplicerad. Den ökade förståelsen för hur olika broparametrar påverkar den dynamiska responsen och resonansfenomen i järnvägsbroar används för att skapa ett grafiskt beräkningsverktyg som kallas designkurvor. En designkurva är en jämförbar presentation av ett stort antal finita element analyser från vilka det är möjligt att erhålla den vertikala dimensionerande accelerationen oberoende av val av tåghastighet, materialparametrar och sektionens geometri.

En jämförelse mellan 2D och 3D analyser av järnvägsbroar utförs i detta examensarbete. Det visas hur den dimensionerande accelerationen förändras med olika geometrier, varför vridning och lastexcentricitet har undersökts. Slutligen presenteras en diskussion kring möjligheten att skapa riktlinjer och förenklingar för den dynamiska dimensioneringen av järnvägsbroar med hänsyn till 3D-effekter.

Nyckelord: Dynamik, Järnvägsbroar, höghastighetståg, HSLM, enfrihetsgradssystem, excentrisklast, resonans, vibrationer

Contents

ABSTRACT I

CONTENTS III

PREFACE VI

NOTATIONS VII

1 INTRODUCTION 1

1.1 Background 1

1.2 Previous work 1

1.3 Aim 2

1.4 Method 2

1.5 Limitations 2

1.6 General layout 3

2 BASIC DYNAMICS 5

2.1 SDOF systems 5

2.2 Analytical solution of an SDOF 6

2.2.1 Undamped SDOF system 6

2.2.2 Damped SDOF system 8

2.3 Resonance 10

2.4 MDOF systems 11

2.4.1 Eigenfrequencies and eigenmodes 13

2.4.2 Properties of natural modes 13

2.5 Mode superposition 14

2.5.1 Rayleigh damping 15

2.5.2 Modal damping 16

2.5.3 Advantages with mode superposition 16

2.6 Numerical integration 17

2.7 Inverse iteration 18

2.8 Transverse vibration of Bernoulli-Euler Beams 19

3 RAILWAY BRIDGE CODE 23

3.1 High-speed load models (HSLM) 23

3.1.1 HSLM-A 23

3.1.2 HSLM-B 25

3.2 Demands on vertical acceleration 25

3.3 Limitation of considered eigenmodes 26

3.4 Structural damping 26

4 ANALYSIS IN 2D 27

4.1 Geometric definitions 28
4.1.1 Cross section 28
4.1.2 Definitions of span relation parameters 29

4.2 Eigenfrequencies for multi-span bridges 30
4.2.1 Two-span bridges 31
4.2.2 Three-span bridges 36
4.2.3 Comparison to single-span bridges 39
4.2.4 Remarks 40

4.3 Load frequency and resonance effects 40

4.4 The SDOF model 44
4.4.1 Theory 44
4.4.2 Verification 46

4.5 Amplitude of the acceleration response 51
4.5.1 Method 52
4.5.2 Extent of the study 54
4.5.3 Results 55
4.5.4 Conclusions 66

4.6 Case studies 67
4.6.1 Development of the design curves 67
4.6.2 The design curves area of use 71
4.6.3 Limitations of the design curves 73
4.6.4 Design curves for the three case studies 74
4.6.5 Two calculation examples 78

5 ANALYSIS IN 3D 81

5.1 Performed calculations and limitations 81
5.1.1 Geometry 81
5.1.2 Method 82

5.2 Eigenmodes and eigenfrequencies 83

5.3 Variation of width 87
5.3.1 Influence on bending modes 88
5.3.2 Influence on torsion modes 90
5.3.3 Combined response 92

5.4 Variation of load eccentricity 95
5.4.1 Influence on bending modes 95
5.4.2 Influence on torsion modes 96
5.4.3 Combined response 98

5.5 Design curves 99

5.6 Conclusions from the analysis in 3D 102

6 DISCUSSION 105

6.1 Analysis in 2D 105

6.2 Analysis in 3D 107

6.3 Practical use of design curves 108
6.4 Advanced dynamic analysis 108

7 CONCLUDING REMARKS 111
7.1 Conclusions 111
7.2 Suggestions of continued work 112

8 REFERENCES 115

APPENDIX A - Analytical eigenfrequencies for multi-span bridges 116

APPENDIX B - Parameter study 118

APPENDIX C - Design curves 133

APPENDIX D - Matlab programs 169

APPENDIX E - Solution of SDOF system 199

APPENDIX F - Tabled values of eigenfrequency functions and design curves 214

Preface

The dynamic design of high-speed railway bridges have been studied in this master thesis with the aim of producing guidelines and simplifications in the design process. This thesis has been performed at Reinertsen Sverige AB in co-operation with the Department of Civil and Environmental Engineering at Chalmers University of Technology.

Mario Plos, PhD, at Concrete Structures at Chalmers University of Technology was the examiner and Ginko Gueorguiev, MSc, at Reinertsen Sverige AB, was the supervisor of this thesis.

The authors thank Mario Plos, PhD, for his remarks on the thesis. The authors also thank Morgan Johansson, PhD, at Reinertsen Sverige AB, which been greatly involved in this project and supplied many appreciated comments and ideas.

The authors would like to thank the opposition group, Max Fredriksson and Håkan Yhlén, whom continuously supplied feedback for the project.

And finally, but foremost, the authors give there sincere thanks and gratitude to Ginko Gueorguiev for his great support and guidance throughout this thesis.

Göteborg Juni 2010

Patrik Eriksson and Emanuel Trolin

Notations

Roman upper case letters

A	Cross-section area [m^2]
2D	Two-dimensional
3D	Three-dimensional
C	Viscosity of the dashpot [Ns/m]
$\boldsymbol{C}$	Damping matrix [Ns/m]
$\widehat{\boldsymbol{C}}$	Modal damping matrix
$\widehat{\boldsymbol{C}}_{red}$	Reduced modal damping matrix
$D(r)$	Dynamic magnification factor [-]
D	Coach length [m]
$\boldsymbol{D}$	Dynamical matrix
DOF	Degrees of freedom
E	Young's Modulus [N/m^2]
FE	Finite Element
FEM	Finite Element Method
HSLM	High-speed load model
I	Moment of inertia [m^4]
K	Stiffness of the SDOF model spring [N/m]
$\boldsymbol{K}$	Stiffness matrix [N/m]
$\widehat{\boldsymbol{K}}$	Modal stiffness matrix
$\widehat{\boldsymbol{K}}_{red}$	Reduced modal stiffness matrix
L	Beam/bridge length [m]
L_{tot}	Beam/bridge total length [m]
M	Mass [kg], mass of the SDOF model [kg]
$\boldsymbol{M}$	Mass matrix [kg]
$\widehat{\boldsymbol{M}}$	Modal mass matrix
$\widehat{\boldsymbol{M}}_{red}$	Reduced modal mass matrix
N	Number of intermediate coaches [-]
P	Point force [kN]
R^2	Least square values [-]
SDOF	Single Degree Of Freedom
U	Amplitude [m]
$\boldsymbol{U}$	Amplitude vector [m]
U_0	Static amplitude [m]
$U(r)$	Dynamic amplitude [m]

Roman lower case letters

a	Design acceleration
b	Width of bridge [m]
c_{cr}	Critical damping coefficient
c_i	Viscosity of the dashpot [Ns/m]
d	[m]
e	Eccentricity [m]
f_i	Forces [N]
f_i	Eigenfrequency [Hz]
$f_{i,single}$	Eigenfrequency for single-span bridge [Hz]
$g_i(\mu)$	Eigenfrequency function

h	Height [m]
l	Length of beam/bridge [m]
m_i	Mass [kg]
n	Number of eigenvalue
$p(t)$	Time dependent load [N]
$p_y(x,t)$	Load per unit length in location *x* at time *t* [N/m]
$\boldsymbol{p}(t)$	Time dependent load vector [N]
p_0	[N]
r	Frequency ratio [-]
u	Displacement/deflection [m]
$p(t)_{sdof}$	Load acting on SDOF model [N]
$\boldsymbol{u}$	Displacement vector [m]
$\boldsymbol{u_s}$	Eigenvector for iteration s
$\dot{u}$	First derivative of *u* with respect to time t, velocity [m/s]
$\dot{\boldsymbol{u}}$	First derivative of $\boldsymbol{u}$, velocity vector [m/s]
$\ddot{u}$	Second derivative of *u* with respect to time t, acceleration [m/s^2]
$\ddot{\boldsymbol{u}}$	Second derivative of $\boldsymbol{u}$, acceleration vector [m/s^2]
$u(t)$	Total displacement in time [m]
$u_c(t)$	Homogenous solution of the general equation of motion [m]
$u_p(t)$	Particular displacement solution of the general equation of motion [m]
$u(t)_{sdof}$	Displacement of SDOF system [m]
$u(t)_{bridge}$	Critical displacement in a bridge [m]
$\dot{u}_p$	First derivative of u_p with respect to time t, velocity [m/s]
$\ddot{u}_p$	Second derivative of u_p with respect to time t, acceleration [m/s^2]
x	Space coordinate
$\bar{s}$	Root to the equation of motion for a SDOF system
v	Velocity [m/s], Poisson's ratio [-]
$v(x_e,t)$	Displacements of a beam
$\boldsymbol{v_s}$	Un-scaled eigenfrequency for iteration s
$v_{resonance}$	Train velocity at which resonance effects occur [m/s]
vcr	Critical velocity [m/s]
v_{cr}	Critical velocity [m/s]

Greek upper case letters

Ω	Load frequency [Hz]
Δt	Time step [s]
$\boldsymbol{\Phi}$	Modal matrix [-]
$\boldsymbol{\Phi}_{red}$	Reduced modal matrix [-]

Greek lower case letters

α	Phase angle [-]
β	
β*	
η	Describes the span relation of a three-span bridge
η_i	Modal coordinate of mode i
$\boldsymbol{\eta}$	Modal coordinates
$\boldsymbol{\eta}_{red}$	Reduced modal coordinates
$\dot{\boldsymbol{\eta}}$	Modal velocity vector

$\ddot{\boldsymbol{\eta}}$	Modal acceleration vector
κ	Describes the geometry of a three-span bridge
λ_i	Eigenvalue
ζ	Viscous damping factor [%]
μ	Span ratio for a two span bridge
π	Mathematical constant 3.14159…
ρ	Density of material [kg/m^3]
τ	
ω_n	Undamped natural frequency [rad/s]
ω_i	Natural frequency or Eigenfrequency [rad/s]
ω_d	Damped natural frequency [rad/s]
ω_{sdof}	
$\boldsymbol{\phi_i}$	Natural mode or eigenvector [-]

1 Introduction

1.1 Background

The interest in design of railway bridges that allows travelling of high-speed trains has increased in recent years. In 2006 the Swedish railway administration updated their bridge code regarding the dynamic design of these railway bridges. Before this update the dynamic aspects were only considered through a dynamic amplification factor in static analysis. The new requirements though demand an additional extensive dynamic analysis to be performed for all bridges subjected to high-speed trains travelling in a speed faster than 200 km/h. The demand is in line with the requirements and recommendations from the annex used in connection with Eurocode.

The additional requirement of dynamic analyses means that both static and dynamic analyses are required for the design of railway bridges today. It is possible that bridges that are structural sound when statically loaded are not acceptable when considering its dynamic response. If the dynamic analysis proves unsatisfactory both static and dynamic analyses have to be re-made making the design process time consuming and expensive.

Dynamic analysis is very time consuming to execute since the code specifies several complex train loads to be used for a range of train velocities. Hence, there is a need for simplifications and guidelines for the dynamic analysis to make it more time efficient. There is also a need for guidelines in the design process that considers the dynamic aspects, to be used parallel to static analysis and to prevent complications that arise when dynamic criteria proves unfulfilled.

1.2 Previous work

This master thesis is a continuation from three projects carried out at Reinertsen Sweden AB during 2007 and 2008. In these theses it has been shown that it is possible to simplify a single-span bridge structure with a single-degree-of-freedom system (SDOF) and attempts have been made to create guidelines for the dynamic analysis of railway bridges through FE-analyses, graphical presentation and the SDOF model.

In Ekström and Kieri (2007) focus was put on the comparison of displacements and accelerations for a SDOF system subjected to various types of loading. It was shown that a SDOF system can be used to approximate the acceleration response by comparing the result with a FE-model. The continuation of this thesis, performed by De Leon and Lasn (2008), treated the transformation procedure of railway bridges into a SDOF model by using an alternative procedure called the force scaling approach. This approach is more compatible with complex structures and was also successfully applied on portal frames. De Leon and Lasn (2008) also made an attempt to establish a graphical guideline with its basis in the SDOF model. In both Ekström and Kieri (2007) and De Leon and Lasn (2008) calculations were made to increase the understanding of the dynamic response behaviour of railway bridges.

In Gustafsson (2008) an attempt to build a 2D FE-model in Matlab was successfully made. It was stated that the FE program reduces the calculation time required to make

a 2D analysis with a certain set of predefined geometrical and material parameters and hence could be used to simplify the dynamic calculations. Different methods of modelling the train load were also examined.

1.3 Aim

The overall aim of this master thesis was to find guidelines and simplifications for the dynamic response for railway bridges subjected to high speed trains. This includes easier and faster calculations procedures, guidance to suitable parameter combinations and tools for verification of the advanced calculations.

This thesis aims to investigate the compatibility of the previous developed SDOF model on multi-span bridges. The investigation includes how such a simplification shall be carried out and what possibilities and limitations the model has.

The thesis aims also to increase the understanding of the dynamic response in railway bridges and the differences between 2D and 3D analysis.

1.4 Method

An extensive literature study has been performed in the beginning of the master thesis to increase the knowledge about design and dynamic behaviour of railway bridges. Several master theses have been written at the technical universities of Chalmers, KTH and Lund about dynamic design of railway bridges during the last years which all have been studied. Further, Swedish and European design codes have been studied to increase the knowledge of demands and requirements for the dynamic behaviour of railway bridges subjected to high-speed trains.

The advances made in creating a SDOF system by Ekström and Kieri (2007) and De Leon and Lasn (2009) was used as a basis for the development of a SDOF model that is compatible with multi-span bridges.

Examination of the individual influence of bridge parameters on the dynamic response was made to increase the understanding of the dynamic behaviour in railway bridges. This increased understanding together with accumulated knowledge of simplified FE modelling, the possibilities in SDOF systems and graphical presentation was used in the development of possible guidelines and simplifications of the dynamic calculations.

Differences between the dynamic response in 2D and 3D were studied by examining single-span bridges subjected to eccentric loading and with variation in width.

Matlab was used to create programs for the required SDOF and FE calculations. The commercial software ADINA was used to verify the created Matlab programs.

1.5 Limitations

To manage the thesis over the limited time schedule several limitations have been made. Some of these limitations are defined by the national bridge code BV Bro Banverket (2006) as this thesis is limited to the required calculation procedure described in this code.

The train load was assumed to be the HSLM model described in BV Bro. This model treats the train load as moving point loads and consequently the train mass, rail irregularities and interaction between train and rail have not been considered.

In the bridge code there are demands on the dynamic response of railway bridges concerning vertical deflection, vertical acceleration, horizontal transverse deflection, twist of the bridge deck and uplifting of the bearings. Here the studied response was the vertical acceleration as this design criterion often governs the dynamic aspect of railway bridge design.

Throughout the thesis the material parameters are chosen to resemble concrete. A linear viscoelastic material model is consequently used. The section is hence treated as uncracked and the reinforcement in the bridge is neglected.

1.6 General layout

The outline of the report consists of three major Chapters. Chapter 2 and 3 are together an introduction to the field of structural dynamics and the railway bridge code relevant to this thesis.

In Chapter 4 dynamic analyses in 2D for railway bridges are investigated extensively. The Chapter treats the determination of eigenfrequencies for multi-span bridges, the transformation of multi-span bridges to a SDOF model, individual examinations of bridge parameters effect on the acceleration response and finally an attempt to create guidelines for the dynamic design of railway bridges considering 2D analyses.

Chapter 5 treats dynamic analysis of railway bridges in 3D. The Chapter shows the additional complications that arise when 3D geometry is considered.

More extensive presentations of the layouts in Chapter 4 and 5 are presented in the introduction of each Chapter. A summary, discussion and suggestions for further studies are presented in the end of the thesis.

2 Basic Dynamics

This chapter treats fundamental theory of structural dynamics that is vital for the examinations made in this thesis. Theory behind discrete parameter models described by one and multiple degrees of freedom is presented, together with application of the so called mode superposition method which is very important for model reduction with consideration to railway bridge dynamics. Some short comments on numerical integration and continuous models are also presented and the dynamic resonance phenomenon is explained.

2.1 SDOF systems

A system that consists of a single-degree-of-freedom is called a SDOF system. The SDOF system is a good application for understanding the fields of dynamics. Since mode superposition (which is introduced in section 2.5) basically is a way to transform larger systems into independent SDOF systems, its solution is also vital for the fields of dynamics. A mass-spring-dashpot model is a good example of a SDOF system and will be used in the following section, see Figure 2.1.

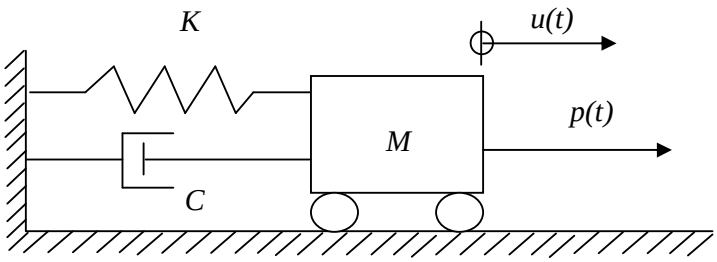

Figure 2.1 SDOF system in the form of a mass-spring-dashpot model.

Newton's second law is required for the derivation of the equation of motion for the SDOF system and is defined as

$$\sum F = M\ddot{u} \tag{2.1}$$

Figure 2.2 shows all forces acting on the mass in Figure 2.1.

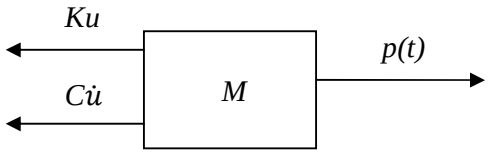

Figure 2.2 Forces acting on the mass in the mass-spring-dashpot model

The forces in Figure 2.2 and Newton's second law in equation (2.1) give together the equation of motion for a single degree of freedom system as

$$M\ddot{u} + C\dot{u} + Ku = p(t) \tag{2.2}$$

Solving the equation of motion can be done either analytically or numerically. Often it is not possible to solve more complex systems analytically. However it is possible for a SDOF system subjected to a sinusoidal load, and this analytical solution will for the purpose of explaining the fundamentals in structural dynamics be presented in the upcoming section.

2.2 Analytical solution of an SDOF

The analytical solution to a SDOF system subjected to a sinusoidal load differs whether damping is considered or not. The derivation procedure is also somewhat different and therefore independent sub-sections will treat the undamped and damped case respectively in this section.

2.2.1 Undamped SDOF system

Consider the SDOF system in Figure 2.1 without damping subjected to a sinusoidal load. This system has the equation of motion in the form

$$M\ddot{u} + Ku = p_0 \cos(\Omega t) \tag{2.3}$$

Where the solution can be divided in two parts: the particular and complementary solution. In the field of structural dynamics the terms forced and natural motion are used, respectively, and they together form the total response, i.e.

$$u(t) = u_p(t) + u_c(t) \tag{2.4}$$

Consider first the natural motion u_c or, as it is also called, the free vibration. The natural motion is the general solution to the equation of motion when the loading is absent. It is convenient to rewrite equation (2.3) for solving the natural motion as

$$\ddot{u} + \omega_n^2 \cdot u = 0 \tag{2.5}$$

where

$$\omega_n = \sqrt{\frac{K}{M}} = undamped\ natural\ frequency$$

The general solution to equation (2.5) can be written in the form of trigonometric functions as

$$u_c(t) = A_1 \cdot \cos(\omega_n \cdot t) + A_2 \cdot \sin(\omega_n \cdot t) \tag{2.6}$$

where A_1 and A_2 are constants that are determined by initial conditions.

Consider now the forced motion of the system created by the sinusoidal load. It is seen that the forced motion from equation (2.3) will have the form

$$u_p(t) = U \cdot \cos(\Omega t) \tag{2.7}$$

where U is the amplitude of the forced motion. By inserting equation (2.7) into (2.3) an expression for the amplitude U can be derived as

$$U = \frac{p_0}{K - M\Omega^2} \tag{2.8}$$

This expression can (for a pedagogical reason of the upcoming examination of resonance effects) be rewritten as

$$U = \frac{U_0}{1 - \mathrm{r}^2} \tag{2.9}$$

where

$$U_0 = \frac{p_0}{K} \tag{2.10}$$

is the static displacement and

$$r = \frac{\Omega}{\omega_n} \tag{2.11}$$

is the frequency ratio. The total response for the undamped SDOF system as the sum of the forced and natural motion can now be concluded to be

$$u(t) = \frac{U_0}{1 - \mathrm{r}^2} \cdot \cos(\Omega t) + A_1 \cdot \cos(\omega_n \cdot t) + A_2 \cdot \sin(\omega_n \cdot t) \tag{2.12}$$

2.2.2 Damped SDOF system

The derivation of the analytical solution for a damped SDOF system is more advanced than the derivation without consideration to damping in section 2.2.1. However, the approach is the same and as for the case without damping the total response is divided in forced and natural motion which solutions are solved separately.

The equation of motion for the SDOF system that considers damping and is subjected to a sinusoidal load has the appearance

$$M\ddot{u} + C\dot{u} + Ku = p_0 \cos(\Omega t) \tag{2.13}$$

As for the case without damping it is convenient to rewrite this equation for the derivation of the natural motion as

$$\ddot{u} + 2\zeta\omega_n\dot{u} + \omega_n^2 u = 0 \tag{2.14}$$

where

$$\omega_n = \sqrt{\frac{K}{M}} = undamped\ natural\ frequency$$

$$\zeta = \frac{c}{c_{cr}} = viscous\ damping\ factor$$

$$c_{cr} = 2\sqrt{KM} = critical\ damping\ coefficient$$

To solve the natural motion the form of the solution is assumed as

$$u(t) = \bar{C}e^{\bar{s}t} \tag{2.15}$$

By inserting equation (2.15) into (2.14) we obtain the characteristic equation

$$\bar{s}^2 + 2 \cdot \zeta \cdot \omega_n + \omega_n^2 = 0 \tag{2.16}$$

which roots can be solved as

$$\bar{s}_{1,2} = -\zeta \cdot \omega_n \pm \omega_n\sqrt{\zeta^2 - 1} \tag{2.17}$$

The size of ζ can be divided in three cases:

- $0 < \zeta < 1$: underdamped
- $\zeta = 1$: critically damping

- $\zeta > 1$: overdamped

The solution to the natural motion will differ depending on which case that is considered. In this thesis only the underdamped case will be treated as the viscous damping factor usually lies in the range of 0 to 0.05 for real life structures (like railway bridges). For information of the other cases, see for example Craig and Kurdila (2006).

By the use of Euler's formula the solution of the underdamped case can be derived to be

$$u(t) = e^{-\zeta\omega_n t}(A_1 \cdot \cos(\omega_d t) + A_2 \cdot \sin(\omega_d t)) \tag{2.18}$$

where

$$\omega_d = \omega_n\sqrt{1-\zeta^2} \tag{2.19}$$

is called the damped natural frequency.

Consider now the forced motion of equation (2.13). The solution can be written as

$$u_p = U \cdot \cos(\Omega t - \alpha) \tag{2.20}$$

where U is the amplitude and α is the phase angle. The velocity and acceleration of the forced response then become

$$\dot{u}_p = -\Omega U \cdot \sin(\Omega t - \alpha) \tag{2.21}$$

$$\ddot{u}_p = -\Omega^2 U \cdot \cos(\Omega t - \alpha) \tag{2.22}$$

The expressions for the displacement, velocity and acceleration of the forced response, inserted into equation (2.13), give that

$$-M\Omega^2 U \cdot \cos(\Omega t - \alpha) - C\Omega U \cdot \sin(\Omega t - \alpha) + \tag{2.23}$$
$$+ KU \cdot \cos(\Omega t - \alpha) = p_0 \cos(\Omega t)$$

from which it is obtained that

$$U = \frac{p_0}{\sqrt{(K - M\Omega^2)^2 + (C\Omega)^2}} = \frac{U_0}{\sqrt{(1 - \mathrm{r}^2)^2 + (2\zeta r)^2}} \tag{2.24}$$

and

$$\tan\alpha = \frac{C\Omega}{K - M\Omega^2} = \frac{2\zeta r}{1 - \mathrm{r}^2} \tag{2.25}$$

The total response of the damped SDOF system can now be written as

$$\begin{aligned} u(t) = &\frac{U_0}{\sqrt{(1 - \mathrm{r}^2)^2 + (2\zeta r)^2}} \cdot \cos(\Omega t - \alpha) + \\ &+ e^{-\zeta\omega_n t}(A_1 \cdot \cos(\omega_d t) + A_2 \cdot \sin(\omega_d t)) \end{aligned} \tag{2.26}$$

2.3 Resonance

The reason why a dynamic analysis is required in structures subjected to frequency loading is because of the so called resonance effects. Resonance occurs when $r \approx 1$, i.e. when the loading frequency is approximately equal to the natural or damped natural frequency. Resonance can cause very large amplitudes of the response compared to the corresponding static loading. To examine this consider the dynamic magnification factor defined as the ratio between dynamic and static amplitude, i.e.

$$D(r) = \frac{U(r)}{U_0} \tag{2.27}$$

With U defined as in equations (2.9) and (2.24) the dynamic magnification factor becomes

$$D(r) = \frac{1}{1 - \mathrm{r}^2} \tag{2.28}$$

for an undamped SDOF system and

$$D(r) = \frac{1}{\sqrt{(1 - \mathrm{r}^2)^2 + (2\zeta r)^2}} \tag{2.29}$$

for a damped SDOF system. Figure 2.3 shows the dynamic magnification factor for different values of the viscous damping factor and variation of frequency ratio.

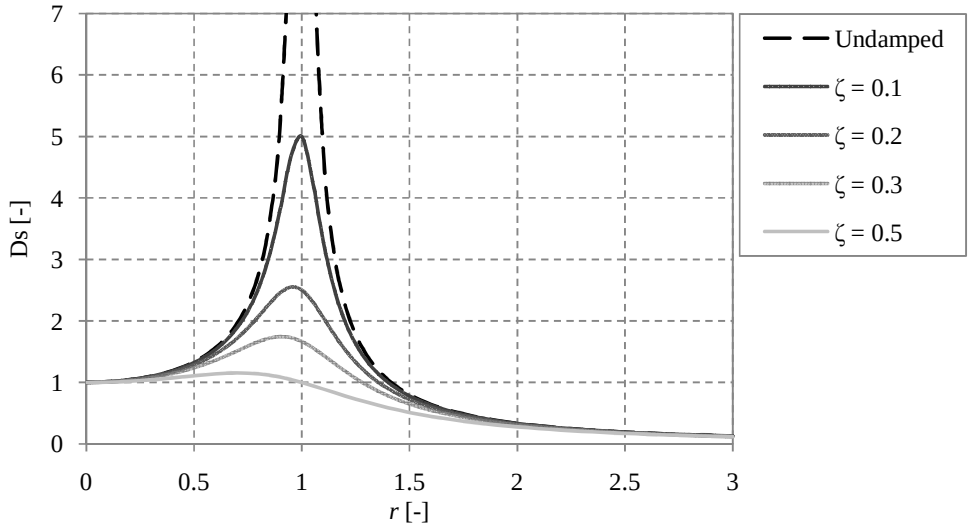

Figure 2.3 Dynamic magnification factor for variation in damping and frequency ratio.

Higher values of damping cause large differences between the natural and damped natural frequency. It can hence be seen in Figure 2.3 that resonance occurs for lower values of the frequency ratio for higher damping. For the undamped system the dynamic magnification factor will go towards infinity as $r \rightarrow 1$.

2.4 MDOF systems

The dynamic analyses of most real structures are based on multiple-degree-of-freedom systems, MDOF system. To show how the equation of motion for a MDOF system is assembled consider the lumped mass model shown in Figure 2.4.

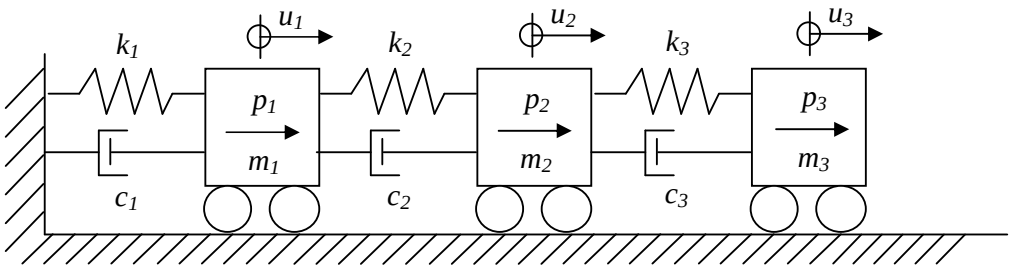

Figure 2.4 A three-degree-of-freedom system with lumped mass and viscous damping

Figure 2.5 shows all forces acting on the three masses in Figure 2.4.

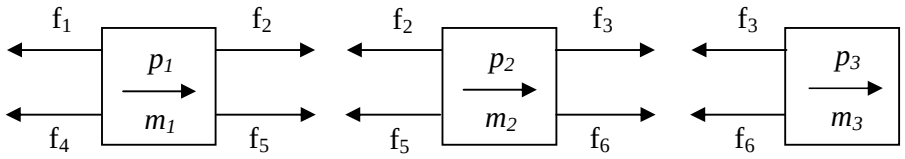

Figure 2.5 Free-body diagram for the masses in Figure 2.4.

By use of Newton's Second law three force equilibriums can be established as

$$\begin{aligned} m_1\ddot{u}_1 &= p_1(t) + f_2 + f_5 - f_1 - f_4 \\ m_2\ddot{u}_2 &= p_2(t) + f_3 + f_6 - f_2 - f_5 \\ m_3\ddot{u}_3 &= p_3(t) - f_3 - f_6 \end{aligned} \tag{2.30}$$

where the forces in Figure 2.5 are defined as

$$\begin{aligned} f_1 &= k_1 u_1 \\ f_2 &= k_2(u_2 - u_1) \\ f_3 &= k_3(u_3 - u_2) \\ f_4 &= c_1\dot{u}_1 \\ f_5 &= c_2(\dot{u}_2 - \dot{u}_1) \\ f_6 &= c_3(\dot{u}_3 - \dot{u}_2) \end{aligned} \tag{2.31}$$

By combining equations (2.30) and (2.31) the force equilibrium can be written in matrix form as

$$\begin{pmatrix} m_1 & 0 & 0 \\ 0 & m_2 & 0 \\ 0 & 0 & m_3 \end{pmatrix}\begin{pmatrix} \ddot{u}_1 \\ \ddot{u}_2 \\ \ddot{u}_3 \end{pmatrix} + \begin{pmatrix} c_1 + c_2 & -c_2 & 0 \\ -c_2 & c_2 + c_3 & -c_3 \\ 0 & -c_3 & c_3 \end{pmatrix}\begin{pmatrix} \dot{u}_1 \\ \dot{u}_2 \\ \dot{u}_3 \end{pmatrix} + \cdots \tag{2.32}$$

$$+\begin{pmatrix} k_1 + k_2 & -k_2 & 0 \\ -k_2 & k_2 + k_3 & -k_3 \\ 0 & -k_3 & k_3 \end{pmatrix}\begin{pmatrix} u_1 \\ u_2 \\ u_3 \end{pmatrix} = \begin{pmatrix} p_1(t) \\ p_2(t) \\ p_3(t) \end{pmatrix}$$

or using matrix format as

$$\boldsymbol{M\ddot{u} + C\dot{u} + Ku = p}(t) \tag{2.33}$$

Equation (2.33) represents the equation of motion of a MDOF system. The appearance of equation (2.33) is the same for two- and three-dimensional analysis and forms the basis to the finite element method and hence also dynamic analysis of railway bridges.

2.4.1 Eigenfrequencies and eigenmodes

Consider now the free vibration of a MDOF system with *N* degrees of freedom. The corresponding equation of motion for the free vibration is defined as

$$\boldsymbol{M\ddot{u} + Ku = 0} \tag{2.34}$$

where $\boldsymbol{M}$ is the mass matrix and $\boldsymbol{K}$ is the stiffness matrix. Both $\boldsymbol{M}$ and $\boldsymbol{K}$ have the size *N* x *N*. As for a SDOF system a harmonic solution to equation (2.34) is assumed, i.e.

$$\boldsymbol{u}(t) = \boldsymbol{U}\cos(\omega_n t - \alpha) \tag{2.35}$$

which inserted in equation (2.34) gives that

$$[\boldsymbol{K} - \omega_n^2 \boldsymbol{M}]\boldsymbol{U} = \boldsymbol{0} \tag{2.36}$$

Since $\boldsymbol{U} \neq 0$ it is required that

$$\det(\boldsymbol{K} - \omega_n^2 \boldsymbol{M}) = \boldsymbol{0} \tag{2.37}$$

which is the characteristic equation of the MDOF system. There are *N* roots to equation (2.37) , *N* eigenvalues, each corresponding to a squared eigenfrequency. For each eigenvalue there is a corresponding eigenvector, or natural mode. The determination of the eigenfrequencies and natural modes for a MDOF system is most commonly made numerically.

2.4.2 Properties of natural modes

The solution to mode superposition, presented in section 2.5, is based on two properties of the natural modes, scaling and orthogonality, which will be presented in this section.

2.4.2.1 Scaling

The natural modes' shapes are unique, i.e. for a specific value of one mode's first element the remaining elements are fixed. However the amplitudes of the natural modes are arbitrary and they can hence be scaled in any appropriate manner. A scaled mode is in this thesis referred to as $\boldsymbol{\phi_i}$, where *i* = 1...*N*. A common procedure is to scale the modes so that the modal mass, which is defined as

$$M_i = \boldsymbol{\phi_i^T M \phi_i} \tag{2.38}$$

becomes equal to one. This scaling procedure has been used in this thesis and is assumed for all modes in the remainder of the thesis. If equation (2.36) is multiplied by $\boldsymbol{\phi_i}^T$ it is obtained that

$$\boldsymbol{\phi}_i^{\mathrm{T}}\boldsymbol{K}\boldsymbol{\phi}_i = \omega_r^2\left(\boldsymbol{\phi}_i^{\mathrm{T}}\boldsymbol{M}\boldsymbol{\phi}_i\right) \tag{2.39}$$

and hence that the modal stiffness can be defined as

$$K_i = \boldsymbol{\phi}_i^{\mathrm{T}}\boldsymbol{K}\boldsymbol{\phi}_i = \omega_i^2 M_i = \omega_i^2 \tag{2.40}$$

2.4.2.2 Orthogonality

A very important property of natural modes is that they are orthogonal to each other. It can be shown that

$$\boldsymbol{\phi}_i^{\mathrm{T}}\boldsymbol{K}\boldsymbol{\phi}_j = 0 \tag{2.41}$$

$$\boldsymbol{\phi}_i^{\mathrm{T}}\boldsymbol{M}\boldsymbol{\phi}_j = 0$$

where $\boldsymbol{\phi}_i$ and $\boldsymbol{\phi}_j$ are two different natural modes.

2.5 Mode superposition

Mode superposition is extensively used in dynamic analysis, and can be used for both solving dynamic problems analytically and simplifying numerical calculations. To employ mode superposition the modal matrix must first be defined as a matrix which columns represent the scaled natural modes, i.e.

$$\boldsymbol{\Phi} = [\boldsymbol{\phi_1} \quad \boldsymbol{\phi_2} \quad \ldots \quad \boldsymbol{\phi_N}] \tag{2.42}$$

The concept of mode superposition lies in the possibility of representing the true response as

$$\boldsymbol{u}(t) = \sum_{i=1}^{N} \boldsymbol{\phi}_i \eta_i(t) = \boldsymbol{\Phi}\boldsymbol{\eta}(t) \tag{2.43}$$

Where η_i is called the modal coordinate of mode *i*. If the equation of motion is multiplied with $\boldsymbol{\Phi}^{\mathrm{T}}$ and combined with equation (2.43) it is obtained that

$$\widehat{\boldsymbol{M}}\ddot{\boldsymbol{\eta}} + \widehat{\boldsymbol{C}}\dot{\boldsymbol{\eta}} + \widehat{\boldsymbol{K}}\boldsymbol{\eta} = \boldsymbol{\Phi}^{\mathbf{T}}\boldsymbol{p}(t) \tag{2.44}$$

where

$$\begin{aligned}\widehat{\boldsymbol{M}} &= \boldsymbol{\Phi}^{\mathrm{T}}\boldsymbol{M}\boldsymbol{\Phi} = \mathrm{diag}(M_1, M_2, \dots, M_N) = \boldsymbol{I} \\ \widehat{\boldsymbol{K}} &= \boldsymbol{\Phi}^{\mathrm{T}}\boldsymbol{K}\boldsymbol{\Phi} = \mathrm{diag}(K_1, K_2, \dots, K_N) = \mathrm{diag}(\omega_1^2, \omega_2^2, \dots, \omega_N^2) \\ \widehat{\boldsymbol{C}} &= \boldsymbol{\Phi}^{\mathrm{T}}\boldsymbol{C}\boldsymbol{\Phi}\end{aligned} \tag{2.45}$$

are denoted the modal mass matrix, modal stiffness matrix and modal damping matrix respectively. It should be note that the modal mass and stiffness matrix are diagonals because of the orthogonality of the natural modes. This means that the modal coordinates are uncoupled with regard to stiffness and mass.

Whether the modal coordinates are uncoupled with regard to damping depends on the damping's definition. In several design cases it is not possible to establish a diagonal modal damping matrix, for example when there is a presence of energy absorbers or viscous damping. However for many structures (including railway bridges) it is not possible to define such a damping mechanisms. In those cases it is common to use damping definitions that lead to a diagonal modal damping matrix. Two such methods will be presented in this thesis and are referred to as Raleigh damping and modal damping.

2.5.1 Rayleigh damping

In Rayleigh damping the damping matrix is defined as a linear combination of the stiffness and mass matrix, i.e.

$$\boldsymbol{C} = a_o\boldsymbol{M} + a_1\boldsymbol{K} \tag{2.46}$$

where a_o and a_1 are constants.

The modal damping matrix then becomes

$$\widehat{\boldsymbol{C}} = \boldsymbol{\Phi}^{\mathrm{T}}\boldsymbol{C}\boldsymbol{\Phi} = \mathrm{diag}((a_0 + a_1\omega_i^2)M_i) = \mathrm{diag}(2\zeta_i\omega_i M_i) \tag{2.47}$$

where ζ_i is called the modal damping factor and corresponds to the viscous damping factor defined for the SDOF system. For the last step in equation (2.47) to be true it is required that

$$\zeta_i = \frac{1}{2}\left(\frac{a_0}{\omega_i} + a_1\omega_i\right) \tag{2.48}$$

Basically Rayleigh damping is utilized by choosing two modal damping factors and calculating a_0 and a_1 based on these values.

2.5.2 Modal damping

Rayleigh damping has the obvious disadvantage of only having the possibility of specifying the modal damping factor for two natural modes. However the modal damping method allows specification of all modal damping factors. A disadvantage compared to Rayleigh damping is the somewhat more complicated calculation of the damping matrix. However, when using mode superposition the damping matrix is commonly not required but only the modal damping matrix. In the modal damping method the modal damping matrix is basically assumed to satisfy

$$\widehat{\boldsymbol{C}} = \boldsymbol{\Phi}^{\mathrm{T}}\boldsymbol{C}\boldsymbol{\Phi} = \mathrm{diag}(2\zeta_i\omega_i M_i) \tag{2.49}$$

It can be shown that the damping matrix based on this assumption can be calculated as

$$\boldsymbol{C} = \sum_{\mathrm{i}=1}^{\mathrm{N}} \frac{2\zeta_{\mathrm{i}}\omega_{\mathrm{i}}}{\mathrm{M_i}} (\boldsymbol{M}\boldsymbol{\phi}_r)(\boldsymbol{M}\boldsymbol{\phi}_r)^{\mathrm{T}} \tag{2.50}$$

2.5.3 Advantages with mode superposition

The modal coordinates become completely uncoupled in the use of mode superposition if a definition of damping that gives a diagonal modal damping matrix is used. Basically *N* SDOF systems are obtained in the form

$$M_i\ddot{u}_i + 2\zeta_i\omega_i M_i\dot{u}_i + K_i u_i = \boldsymbol{\phi}_i^{\mathrm{T}}\boldsymbol{p}(t) \tag{2.51}$$

If a simple load acts on the system it may be possible to solve the dynamic problem analytically. As an example consider the case where a sinusoidal load acts on the system. The solution then becomes similar to that of equation (2.26). However in many situations the load is so complex that numerical integration procedures still are preferred, see section 2.6.

However, even when the calculations are solved numerically there is a great use in mode superposition in the form of model reduction. Model reduction using mode superposition is made by only including a specific number of eigenmodes. It is assumed that

$$\boldsymbol{u}(t) = \sum_{i=1}^{M} \boldsymbol{\phi}_i\eta_i(t) = \boldsymbol{\Phi}_{red}\boldsymbol{\eta}_{red}(t) \tag{2.52}$$

where $M < N$ and

$$\boldsymbol{\Phi}_{red} = [\boldsymbol{\phi_1} \quad \boldsymbol{\phi_2} \quad \dots \quad \boldsymbol{\phi_M}] \tag{2.53}$$

is the reduced modal matrix and

$$\boldsymbol{\eta}_{red} = [\eta_1 \quad \eta_2 \quad \dots \quad \eta_M]^{\mathrm{T}} \tag{2.54}$$

contain the reduced modal matrix's corresponding modal coordinates. If the equation of motion is multiplied with $\boldsymbol{\Phi}_{red}^{\mathrm{T}}$ and combined with equation (2.52) it is obtained that

$$\widehat{\boldsymbol{M}}_{red}\ddot{\boldsymbol{\eta}}_{red} + \widehat{\boldsymbol{C}}_{red}\dot{\boldsymbol{\eta}}_{red} + \widehat{\boldsymbol{K}}_{red}\boldsymbol{\eta}_{red} = \boldsymbol{\Phi}_{red}^{\mathrm{T}}\boldsymbol{p}(t) \tag{2.55}$$

where

$$\begin{aligned} \widehat{\boldsymbol{M}}_{red} &= \boldsymbol{\Phi}_{red}^{\mathrm{T}}\boldsymbol{M}\boldsymbol{\Phi}_{red} = \mathrm{diag}(M_1, \dots, M_M) = unit\ matrix = \boldsymbol{I} \\ \widehat{\boldsymbol{K}}_{red} &= \boldsymbol{\Phi}_{red}^{\mathrm{T}}\boldsymbol{K}\boldsymbol{\Phi}_{red} = \mathrm{diag}(\omega_1^2, \dots, \omega_M^2) \\ \widehat{\boldsymbol{C}}_{red} &= \boldsymbol{\Phi}_{red}^{\mathrm{T}}\boldsymbol{C}\boldsymbol{\Phi}_{red} = \mathrm{diag}(2\zeta_1\omega_1, \dots, 2\zeta_M\omega_M) \end{aligned} \tag{2.56}$$

It should be noted that equation (2.52) is an estimation of the true response. But the error will be small in many design situations as modes of higher order tend to give very low contribution to the dynamic response. Say that the response can be well estimated using twenty eigenmodes. Then a system containing perhaps several hundred degrees of freedom can be reduced to only twenty, which greatly reduces calculation time for the numerical integration procedures.

2.6 Numerical integration

To obtain the acceleration response over time there are in many design situations a need for numerical integration. Such procedures do not require any transformation of the equation of motion and are therefore commonly referred to as direct integration. The procedures are required in many design situations, for example when uncoupled modal coordinates cannot be established, when the system contains nonlinearities or when the load has a complicated time history.

There are several direct integration procedures used in the field of structural dynamics and these can be divided in two general groups. The first group directly treats the second order differential equation (the equation of motion) and the other group handles it through an equivalent set of first order differential equations. In the first group some of the most commonly used integration procedures are the central difference method, the Newmark-β method and the Wilson-θ method. One example from the second group is the Sub-zero order hold method.

In this section focus have been put on the presentation of the Newmark-β method which is the only numerical integration procedure used in this thesis. The reader is referred to Craig and Kurdila (2006) and Abrahamsson (2000) for insight in the other mentioned numerical integration procedures.

2.6.1.1 Newmark-β method

The main assumption in the Newmark-β method is that the systems displacement and velocity can be written as

$$\dot{\boldsymbol{u}}_{n+1} = \dot{\boldsymbol{u}}_n + [(1-\gamma)\ddot{\boldsymbol{u}}_n + \gamma\ddot{\boldsymbol{u}}_{n+1}]\,\Delta t \tag{2.57}$$

$$\boldsymbol{u_{n+1}} = \boldsymbol{u}_n + \dot{\boldsymbol{u}}_n h + [(1-2\beta)\ddot{\mathbf{u}}_{\mathrm{n}} + 2\beta\ddot{\mathbf{u}}_{\mathrm{n+1}}]\frac{\Delta t^2}{2} \tag{2.58}$$

where the parameters β and γ are the integration coefficients and used to obtain integration stability and accuracy. Newmark introduced an unconditionally stable scheme with the relation $\beta = 0.5$ and $\gamma = 0.25$ and the method is therefore said to be an unconditionally stable implicit integration scheme. The Newmark-β method using this relation for β and γ is called the Constant Average Acceleration method (or the trapezoidal rule). The Constant Average Acceleration method has no demand on the incremental time step to reach a stable solution, the acceleration variation is shown in Figure 2.6.

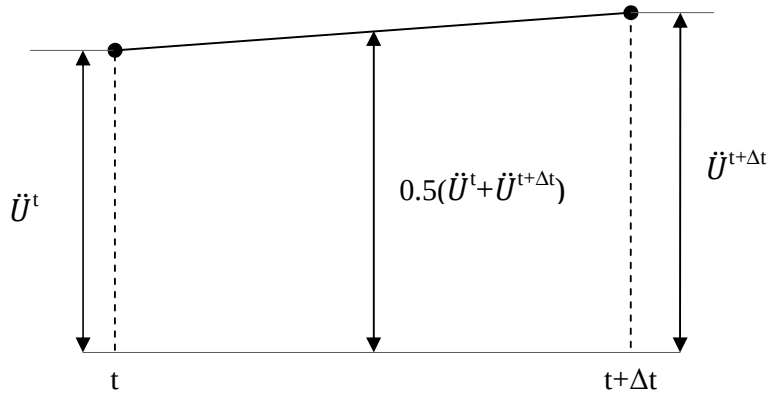

Figure 2.6 Newmark's constant-average-acceleration scheme.

2.7 Inverse iteration

In section 0 it was mentioned that the eigenfrequencies and eigenvectors of MDOF systems in general are calculated numerically. In many situations more general procedures for solving eigenvalue problems are utilized. However when only a few of the lowest eigenvalues are required there are simpler and less time consuming alternatives. Inverse iteration is a procedure for calculating the first eigenfrequency and eigenvector. Consider again the eigenvalue problem

$$(\boldsymbol{K} - \lambda_{\mathrm{i}}\boldsymbol{M})\boldsymbol{\phi}_{\mathrm{i}} = 0 \tag{2.59}$$

where $\lambda_i = \omega_i^2$. The inverse iteration method is in the subgroup of vector iterations methods of solving eigenvalue problems and directly employs equation (2.59). It is possible to write the equation in the form

$$\boldsymbol{\phi} = \lambda \boldsymbol{D}\boldsymbol{\phi} \tag{2.60}$$

where

$$\boldsymbol{D} = \boldsymbol{K}^{-1}\boldsymbol{M} \tag{2.61}$$

is called the dynamical matrix. The iterative procedure of the inverse iteration method follows a few specific steps. A first guess of the eigenvector $\boldsymbol{u}_s$, is initially assumed and then a new vector $\boldsymbol{v}_{s+1}$ is calculated using the dynamical matrix as

$$\boldsymbol{v}_{s+1} = \boldsymbol{D}\boldsymbol{u}_s \tag{2.62}$$

The new guess for the next iteration is then calculated as

$$\boldsymbol{u}_{s+1} = \lambda_{s+1}\boldsymbol{v}_{s+1} \tag{2.63}$$

where $\lambda_{s+1}$is a scaling factor for $\boldsymbol{v}_{s+1}$ chosen in a consistent manner, for example to get the highest value equal to one. According to equation (2.60) $\boldsymbol{u}_{s+1}$ becomes equal to $\boldsymbol{u}_s$ and the scaling factor becomes the corresponding eigenvalue, if an iteration is made using the correct eigenvector. When the initial guess deviates from the true eigenvector this result is achieved after some iterations.

An alternative for the definition of the scaling factor is to use the Rayleigh quotient, i.e.

$$\lambda_{s+1} = \frac{\boldsymbol{v}_{s+1}^{\mathrm{T}}\boldsymbol{M}\boldsymbol{u}_s}{\boldsymbol{v}_{s+1}^{\mathrm{T}}\boldsymbol{K}\boldsymbol{v}_{s+1}} \tag{2.64}$$

which gives a faster convergence.

2.8 Transverse vibration of Bernoulli-Euler Beams

In section 2.2 it was shown how the eigenfrequency and eigenvector can be calculated analytically for a SDOF system and in Section 2.4 it was said that numerical procedures often are required for solving the eigenfrequencies and eigenvectors of a

MDOF system. SDOF and MDOF systems are similar as they belong to the same group, as discrete parameter models. In this section an example of a continuous model will be presented, namely a simply supported beam. Continuous models can be used to derive the exact analytical solution for free vibration of structures, which presented as a discrete parameter model would require a MDOF system. The simply supported beam is of special interest as it can be seen as representation of a single-span railway bridge.

It can be shown that beams that are relatively long and thin, i.e. are applicable of Bernoulli-Euler beam theory, have the differential equation of motion for governing vertical vibration as

$$\frac{\partial^2}{\partial x^2}\left(EI\frac{\partial^2 v}{\partial x^2}\right)+\rho A\frac{\partial^2 v}{\partial t^2}=p_y(x,t), \qquad 0<x<L \tag{2.65}$$

where *EI* is the bending stiffness, ρA is the mass per meter length, *x* is the length coordinate and *v* is the vertical deflection. If it is assumed that *EI* is constant along the beam the differential equation of motion becomes

$$EIv'''' + \rho A\ddot{v} = 0 \tag{2.66}$$

As for the discrete parameter models a harmonic solution is assumed as

$$v(x,t) = V(x)\cdot\cos(\omega t-\alpha) \tag{2.67}$$

and with this solution inserted in equation (2.66) it is obtained that

$$\frac{d^4V}{dx^4}-\lambda^4 V=0 \tag{2.68}$$

where

$$\lambda^4=\omega^2\frac{\rho A}{EI} \tag{2.69}$$

The general solution to equation (2.68) can be written as

$$V(x)=A_1\sinh(\lambda x)+A_2\cosh(\lambda x)+A_3\sin(\lambda x)+A_4\cos(\lambda x) \tag{2.70}$$

where $A_{1,2,3,4}$ are constants determined by the boundary conditions. The boundary conditions for a simply supported beam are

$$v(x=0,t)=0 \qquad v(x=L,t)=0$$

$$\left.\frac{\partial^2 v}{\partial x^2}\right|_{x=0}=0 \qquad \left.\frac{\partial^2 v}{\partial x^2}\right|_{x=L}=0 \tag{2.71}$$

By combining equations (2.70) and (2.71) it can be shown that the eigenfrequencies and eigenvectors of a simply supported beam has the analytical solution

$$V_{(n)}(x)=\sqrt{\frac{2}{ml}}sin\frac{n\pi x}{l} \tag{2.72}$$

$$\omega_{(n)}=(n\pi)^2\sqrt{\frac{EI}{ml^4}} \tag{2.73}$$

where

$$n=1,2,3\ldots$$

The shapes of the first three eigenmodes are shown in Figure 2.7.

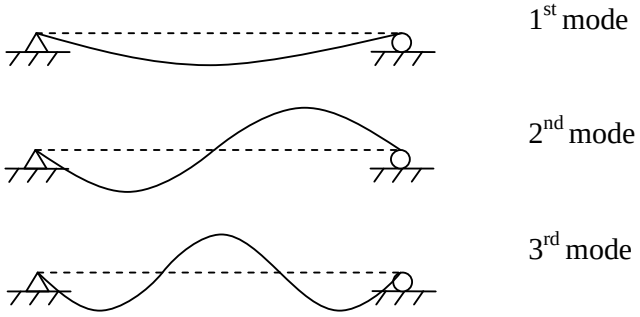

Figure 2.7 First three eigenmodes for a simply supported beam

3 Railway bridge code

In Sweden railway bridges subjected to high speed trains are design according to BV Bro (Banverket, 2006), with regulations set by the Swedish railway administration. This code is similar to the regulations set by Eurocode but differs in some aspects. In this Chapter the demands of dynamic design of railway bridges set by both BV Bro (Banverket, 2006) and Eurocode will be presented.

3.1 High-speed load models (HSLM)

Eurocode 1, CEN (2003), states that in a dynamic analysis of a bridge, characteristic values shall be used for the specified trains. The choice of train shall regard every permitted train configuration for each high speed train configuration that is expected to operate the bridge with velocities over 200 km/h. The dynamic analysis shall on international lines also include high-speed load models (HSLM). Load model HSLM consist of two separate universal train models, HSLM-A and HSLM-B, where the length of the coaches varies.

In BV Bro (Banverket, 2006) there are no demands on additional permitted train configurations to the HSLM loads suggested by Eurocode, and the HSLM loads are hence the only loads used in the dynamic design of railway bridges in Sweden. The HSLM load model consists of two separate universal train configurations, HSLM-A and HSLM-B, where the coach length varies. From Table 3.1 it is possible determine which train configuration that should be applied depending on the total length of the bridge.

Table 3.1 Load models for different structural configurations.

Structural configuration	Span	
	$L < 7$ m	$L \geq 7$ m
Simply supported one span	HSLM-B	HSLM-A
Continuous bridge	HSLM-A: trains A1 to A10 inclusive	HSLM-A: trains A1 to A10 inclusive

3.1.1 HSLM-A

The HSLM-A load model consist of a load geometry determined by the coach length *D*, the bogie axle spacing *d* and the numbers of coaches *N* between the power cars, se Figure 3.1. There is also an intermediate coach after the power car in each train configuration.

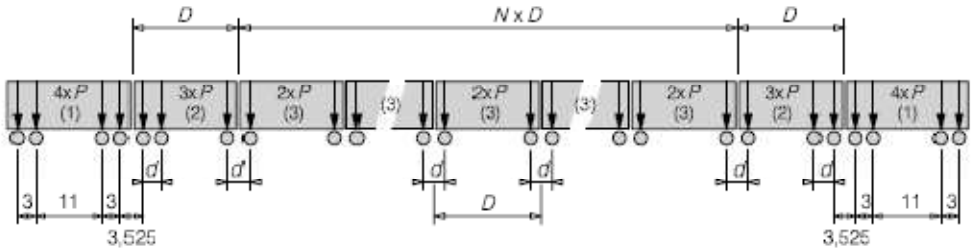

Figure 3.1 The load geometry for the train model HSLM-A.

The HSLM-A train load defined in Eurocode 1, CEN (2003), include ten different train configurations, see Table 3.2. The designing dynamic response should be the most critical considering all ten load configurations.

Table 3.2 Train configurations for train HSLM-A.

Train load	Intermediate coaches N [-]	Coach length D [m]	Boogie axel spacing d [m]	Point force P [kN]
A1	18	18	2.0	170
A2	17	19	3.5	200
A3	16	20	2.0	180
A4	15	21	3.0	190
A5	14	22	2.0	170
A6	13	23	2.0	180
A7	13	24	2.0	190
A8	12	25	2.5	190
A9	11	26	2.0	210
A10	11	27	2.0	210

3.1.2 HSLM-B

The HSLM-B train load consists of equally spaced point loads. Depending on the total span length, Eurocode defines the number of loads *N* and the spacing *d*, as in Figure 3.2 and Figure 3.3.

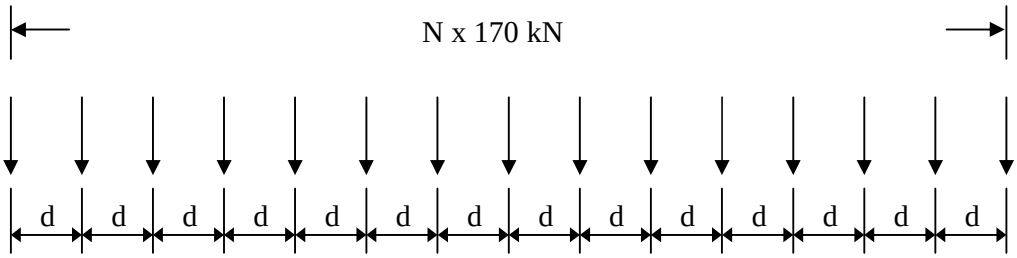

Figure 3.2 *The load distribution for train model HSLM-B.*

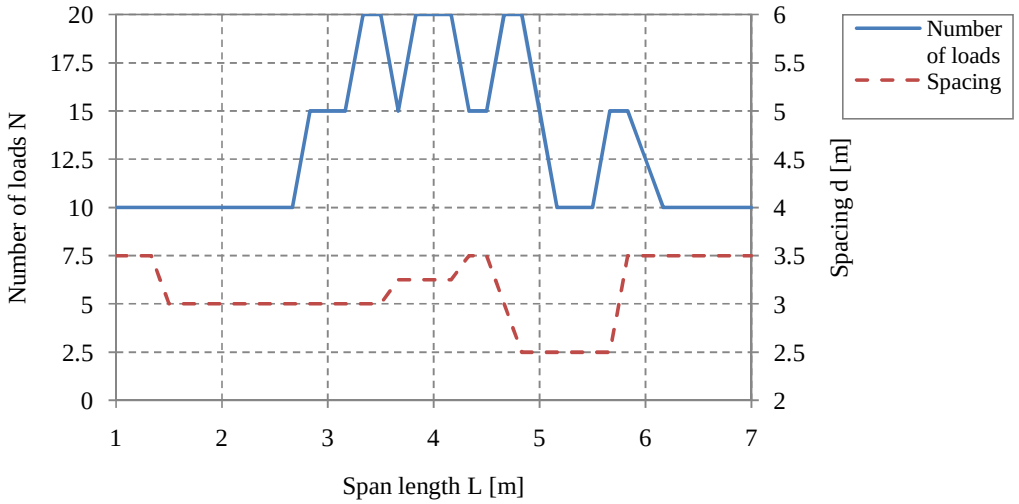

Figure 3.3 *The spacing and number of loads for HSLM-B.*

3.1.2.1 Speeds to consider

According to Eurocode 1, CEN (2003), dynamic calculations of railway bridges should be considered from 40 m/s (144 km/h), with a series of speed steps, up to the 1.2 x maximum design speed. It is mentioned that speed steps should be smaller at speeds where resonance is likely to occur, but no specific value is given.

BV Bro (Banverket, 2006) requires that the dynamic response is examined for a speed interval of 100 km/h to the maximum design speed + 20%. The speed steps should be 5 km/h in general and 2.5 km/h close to resonance effects.

3.2 Demands on vertical acceleration

There are several requirements of the dynamic design of railway bridges for the serviceability limit state in Eurocode: Basis of Structural Design Annex A2, CEN (2003). Checks are required for vertical deflection, vertical acceleration, horizontal

transverse deflection, twist of the bridge deck and uplifting of the bearings. The scope of this Master's thesis is to investigate the vertical acceleration in the deck and therefore only this demand is presented in this section.

Bridge deck accelerations shall be limited to 3.5 m/s^2 for ballasted tracks and 5 m/s^2 for direct fastened decks according to both BV Bro (Banverket 2006) and Eurocode: Basis of Structural Design Annex A2, CEN (2003). The limit for vertical deflection along any track is L/600.

3.3 Limitation of considered eigenmodes

The criteria for traffic safety in Eurocode: Basis of structural Design Annex A2, CEN (2003), states that all members supporting the track shall consider frequencies and their associated mode shapes up to the greater of:

- 30 Hz
- 1.5 times the frequencies of the fundamental mode of vibration of the member being considered
- The frequencies of the third mode of vibration of the member

According to BV Bro (Banverket, 2006) it is enough to use the 30 Hz criteria

3.4 Structural damping

The acceleration response at resonance is highly dependent on the choice of structural damping. Therefore a lower bound value for the structural damping is suggested by Eurocode 1, CEN (2003) and the Swedish code BV Bro (Banverket, 2006). The suggested values for structural damping are shown in Table 3.3.

Table 3.3 Values of damping for different spans and type of bridges.

Bridge type	ζ Lower limit of damping [%]	
	Span $L < 20$m	Span $L \geq 20$m
Steel and composite	$\zeta = 0.5+0.125(20-L)$	$\zeta = 0.5$
Prestressed concrete	$\zeta = 1.0+0.07(20-L)$	$\zeta = 1.0$
Reinforced concrete	$\zeta = 1.5+0.07(20-L)$	$\zeta = 1.5$

4 ANALYSIS IN 2D

Dynamic analysis of railway bridges is usually carried out using mode-superposition and therefore this thesis focuses solely on this method of calculation. The determination of the dynamic response in all structures when mode superposition is to be utilized is done in two steps. First the eigenfrequencies and the corresponding eigenvectors need to be determined. Secondly the response in time is determined. For simple structures this can be done analytically but for more complex structures (or complex loads) there is often a need to solve numerically.

One of the aims of this thesis is to find general guidelines for the design of railway bridges with regard to the dynamic aspects of the design process. To do that, both eigenfrequencies and the response in time have to be examined. The eigenfrequencies in relation to the load frequency applied on the bridge will affect the dynamic response behavior. The actual dynamic response will however also be affected by the configuration of geometric and material parameters of the bridge. The method applied in this thesis is to examine the effect from individual variation of material and geometric parameters to find how these affect the dynamic response. The dynamic response will throughout this thesis be referred to as the acceleration response. The reason is basically that the acceleration is the only examined outcome from the dynamic analysis performed in this thesis, since the demands on vertical acceleration govern the design process of railway bridges when considering the dynamic aspects.

A model that transforms a railway bridge seen in 2D into an SDOF model has been developed in the previous master thesis Ekström and Kieri (2007) and De Leon and Lasn (2008) carried out at Reinertsen Sverige AB. This model was shown to give accurate results for single-span bridges. The theory behind the SDOF model can be used to increase the understanding of the dynamic behavior of railway bridges. Therefore it is of interest to examine if the model is applicable on multi-span bridges. If the model can be proven to give sufficiently accurate results for multi-span bridges, it can also be a useful tool for calculating the dynamic response since it greatly reduces calculation time compared to a finite element model (FE model).

Section 4.1 will treat geometric definitions of span relation parameters and the cross-section geometry which has been kept constant for all calculations in 2D.

In Chapter 2 it was shown how the eigenfrequencies of a single-span bridge can be calculated analytically. The eigenfrequencies of multi-span bridges are examined in Section 4.2. The eigenfrequencies' complex dependence of geometric parameters is shown graphically, and also expressions for calculating the first eigenfrequencies are created empirically. These expressions allows for better examination of the acceleration response later on.

The load frequency and resonance phenomenon in railway bridges are treated in Section 4.3. It is shown that each HSLM load exerts one fundamental load frequency that dominates the dynamic response. It is also shown how the critical train speed (for which resonance in the bridge occurs) can be determined.

Section 4.4 treats the transformation of the bridge into an SDOF model. Theory behind the transformation is presented and accuracy of the model is tested.

After examining the eigenfrequencies for multi-span bridges and showing how the load frequency affect the dynamic response, a parameter study is presented in Section 4.4 treating the amplitude of the dynamic response. Geometric and material parameters' effect on the eigenfrequencies will influence the critical speed at which resonance occurs. As the examination of eigenfrequencies aim to show how the critical speeds can be determined in a simplified way, the parameter study made in Section 4.4 aims to show the acceleration amplitude at these resonance speeds depends on material and geometric parameters.

It will be shown that the geometric parameters affect the acceleration response in a rather complicated way, practically eliminating the possibility to determine single equations to express this behavior. Some simple dependencies are found though. All observations and conclusion from the previous sections are gathered in Section 4.6 and used to create a graphical calculation tool for some common railway bridge configurations. This tool can be used to determine the exact design acceleration for known material and geometric parameters, but also as a guideline of what parameter configuration that should be used to obtain a satisfying dynamic response in the bridge.

4.1 Geometric definitions

The calculations presented in this Chapter aim partly to show the effect from varying geometric and material parameters of a railway bridge. The cross-section however have been kept constant for simplicity since the effect from varying bending stiffness and bridge mass is better examined by variation of young's modulus and the density respectively.

The geometric parameters used in the 2D analysis will be presented in this section. Parameters that describe the span relations for two- and three-span bridges will also been defined.

4.1.1 Cross section

For all the examinations made in 2D analysis the same geometric parameters have been used, see Figure 4.1. The section chosen resembles the section of a portal frame bridge, with a total length of 9.5 m, designed by Reinertsen Sweden AB. The reason why a section from a real bridge design was chosen was to get an idea of how large accelerations and eigenfrequencies would get for different combinations of geometric and material parameters. For the calculations in 2D the section is treated as a rectangular cross-section, and hence the edge beams are disregarded.

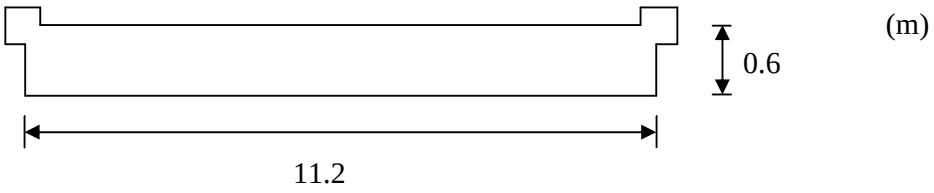

Figure 4.1 Cross section used for all analysis in this Chapter.

Since the design code of the Swedish railway administration (BV Bro, Banverket 2006) has a limit of 30 Hz for eigenmodes that needs to be considered there is a special interest for the size of the eigenfrequencies. The eigenfrequencies also have a significant influence of how large the design acceleration will be, as will be shown later in this thesis.

4.1.2 Definitions of span relation parameters

The additional geometric parameters for a multi-span bridge in comparison to a single span bridge are the relations between the span lengths. For a two-span bridge one extra parameter is required and two extra parameters are required for a three-span bridge. The span relation for a two-span bridge has been defined as the length ratio between the second and the first span, i.e.

$$\mu = \frac{L_2}{L_1} \tag{4.1}$$

where L_1 and L_2 are the lengths of the first and second span respectively. Figure 4.2 shows how the parameter μ can be used to describe the geometry of a two-span bridge.

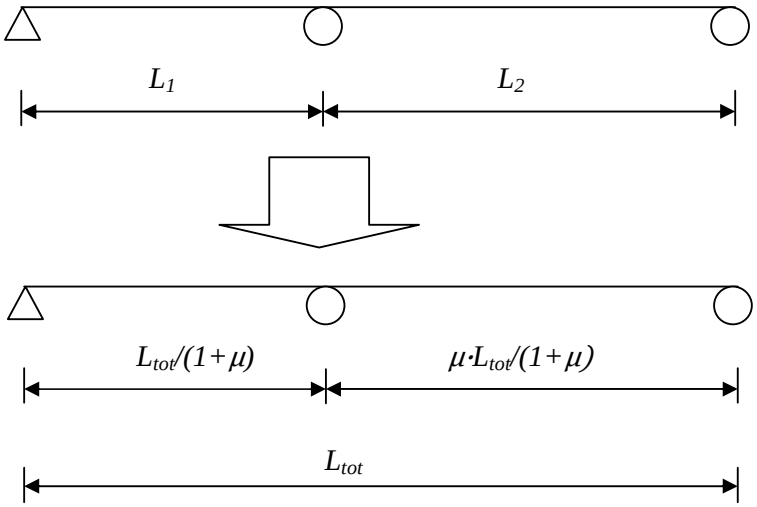

Figure 4.2 *Explanatory figure of how the geometry of a two-span bridge can be described using the parameter μ defined in equation (4.1).*

Two parameters are required to describe the geometry of a three-span bridge. These parameters are here defined as

$$\eta = L_2/(L_1 + L_3) \tag{4.2}$$

$$\kappa = L_3/L_1 \tag{4.3}$$

Figure ***4.3*** shows how these parameters can be used to describe the geometry of a three-span bridge.

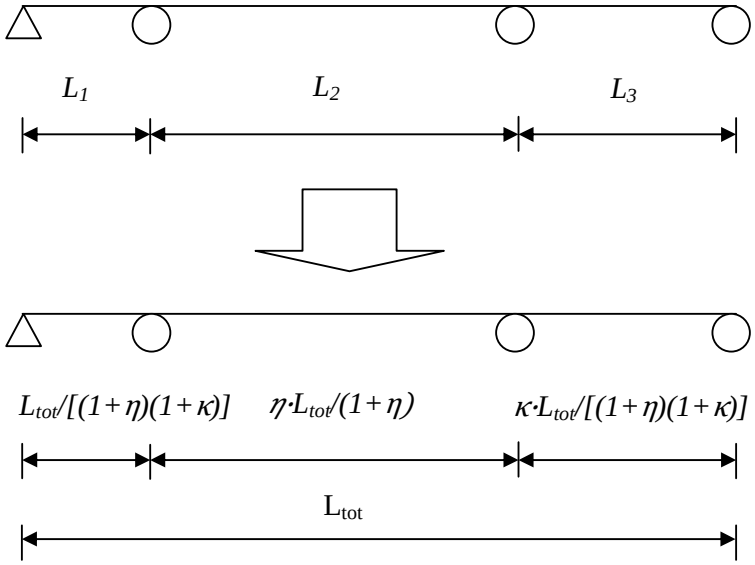

Figure 4.3 *Explanatory figure of how the geometry of a three-span bridge can be described using the parameters η and κ defined in equations (4.2) and (4.3).*

4.2 Eigenfrequencies for multi-span bridges

It is possible to derive an expression that gives the exact value of the eigenfrequencies of any degree for a single span bridge, as was shown in Chapter 2. A bridge that has two or more spans contributes to a lot more complexity in this derivation and to the knowledge of the authors it is not possible to derive an explicit expression for the frequencies analytically.

In Appendix A there is a derivation similar to that of a single-span bridge for deriving the eigenfrequency of a two-span bridge made by the authors. In litterateur you can find similar derivations that lead to similar expressions to the one derived in Appendix A, see for example Gorman (1975). But the result will always be a matrix which determinant should equal zero, resulting in a complex trigonometric expression where an explicit formulation for the eigenfrequencies is impossible to derive.

This section will treat the determination of eigenfrequencies for multi-span bridges under the variation of geometric and material parameters. As eigenfrequencies cannot be determined analytically they have instead been examined graphically. The first eigenfrequency is of special interest since it often governs the dynamic response in railway bridges. Therefore an expression to easily determine the first eigenfrequency for a two- and three-span bridge has been derived.

It is important to remember the design rule set by the Swedish railway administration, stating that only frequencies below 30 Hz need to be considered when designing a railway bridge against the dynamic response criteria. Often only a few eigenmodes need to be considered in dynamic analysis of railway bridges because of this rule, and

for many bridges only the first. Therefore only the first eigenfrequencies have been examined in the following section.

The calculation of eigenfrequencies under the variation of material and geometric parameters has been made using a Matlab program presented in Appendix D made by the authors. Matlab have been used instead of commercial FE software since it better handles iterative calculations concerning the variation of geometric parameters. However ADINA has been used to verify the Matlab program, see Appendix D.

4.2.1 Two-span bridges

As for single-span bridges the frequency of a two span bridge will depend on the bending stiffness *EI*, the mass per meter length *m* and the total length of the bridge L_{tot}. The addition to these parameters for a two span bridge is the ratio between the second and first span μ, which was defined in Section 4.1.

In Appendix A, where an attempt to derive the eigenfrequencies analytically is made, it is shown that a complicated expression is obtained when determining an explicit expression for the eigenfrequencies' dependence on bridge parameters. This complicated expression however depends solely on the geometric parameters L_{tot} and μ. The eigenvalues' dependence on material parameters is defined in the same way as for single span bridges, see equation (2.69). This means that irrespective of the complicated dependence to geometric parameters the eigenfrequencies of a multi-span bridge depends in the same simple manner on material parameters as a single-span bridge.

It can also be shown that the same dependency, as for single-span bridges, exists for the total bridge length, see Figure 4.4 and Figure 4.5.

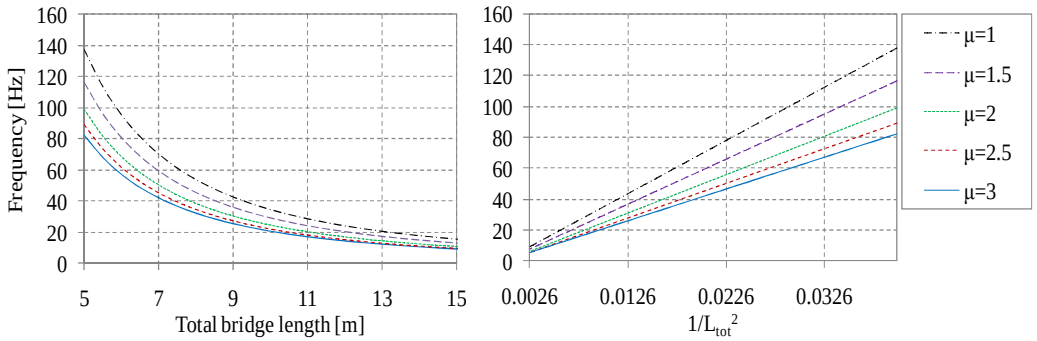

Figure 4.4 *Eigenfrequencies for the first eigenmode for a two-span bridge with μ=2, E=30GPa, ρ=3000kg/m^3.*

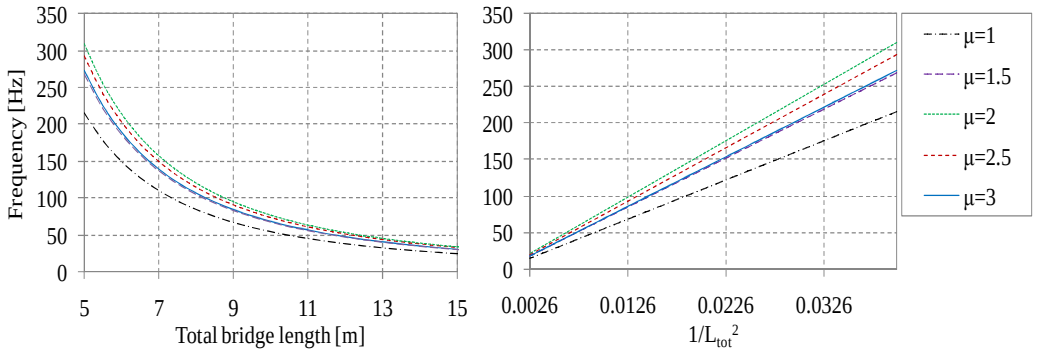

Figure 4.5 *Eigenfrequencies for the second eigenmode for a two-span bridge with μ=2, E=30GPa, ρ=3000kg/m^3.*

Figure 4.4 and Figure 4.5 show that both first and second eigenfrequency has a linear dependence against the inverse of the total bridge length in square. This means that the eigenfrequencies for a two-span bridge in a 2D analysis can be determined as

$$f_i = \frac{g_i(\mu)}{L_{tot}^{\,2}} \cdot \sqrt{\frac{EI}{m}} \tag{4.4}$$

where $g_i(\mu)$ is a different function for each eigenfrequency that depends on the span ratio. These functions will in the remainder of this thesis be referred to as eigenfrequency functions. Figure 4.6 shows how these functions vary for the first five eigenfrequencies. Note that the function is dimensionless and independent of all geometric and material parameters with the exception of μ.

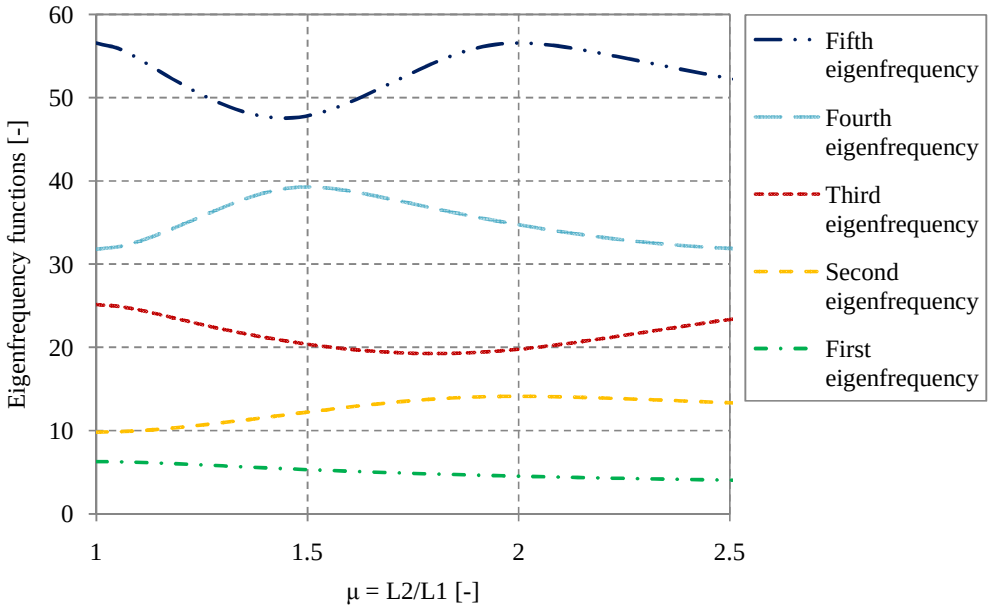

Figure 4.6 *Eigenfrequency functions for the first five frequencies for a two-span bridge.*

Examining Figure 4.6 can help understand the difficulties in deriving an analytical expression for the eigenfrequencies. As can be seen they are all affected differently by

the change of μ. Also the dependency for each individual frequency on μ is complex. This complexity can be explained by the eigenvectors corresponding to each frequency changing in shape. The shapes for the eigenvectors for the first, second and third eigenfrequency for different values of μ are shown in Figure 4.7- Figure 4.9. From Figure 4.7- Figure 4.9 it is shown that only the first eigenvector keeps a similar form when the ratio between the span lengths is altered, hence the more straight curve in Figure 4.6.

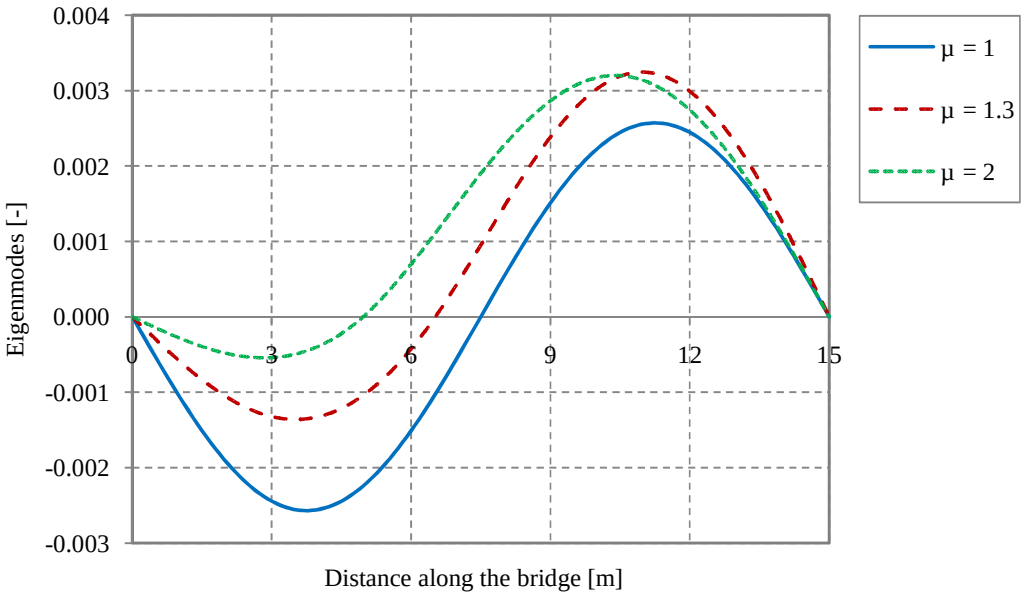

Figure 4.7 *The first eigenmode for a two-span bridge with a total length of 15 m. The mode is normalized to get the modal mass equal to one.*

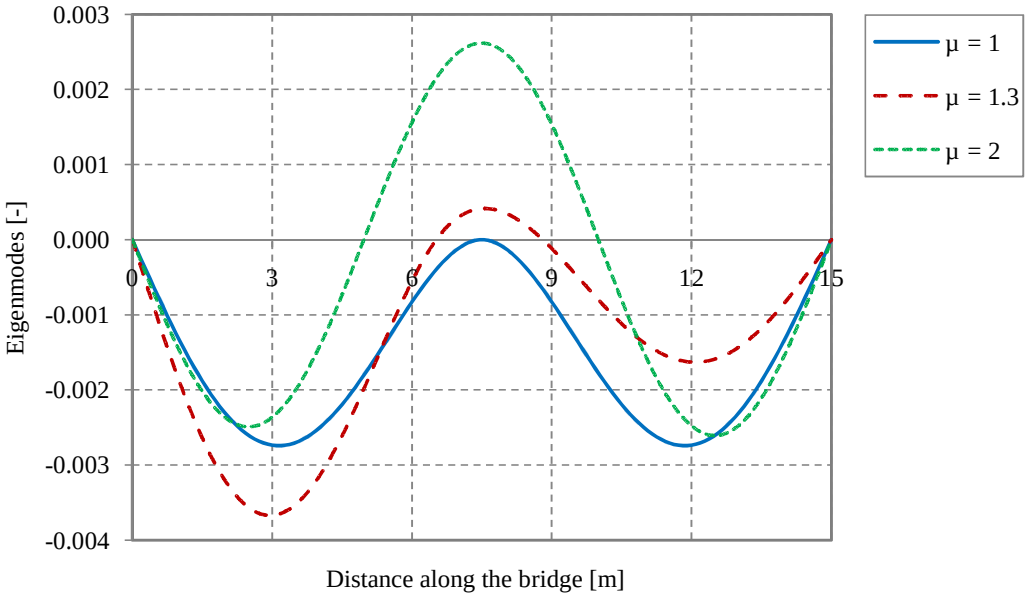

Figure 4.8 *The second eigenmode for a two-span bridge with a total length of 15 m. The mode is normalized to get the modal mass equal to one.*

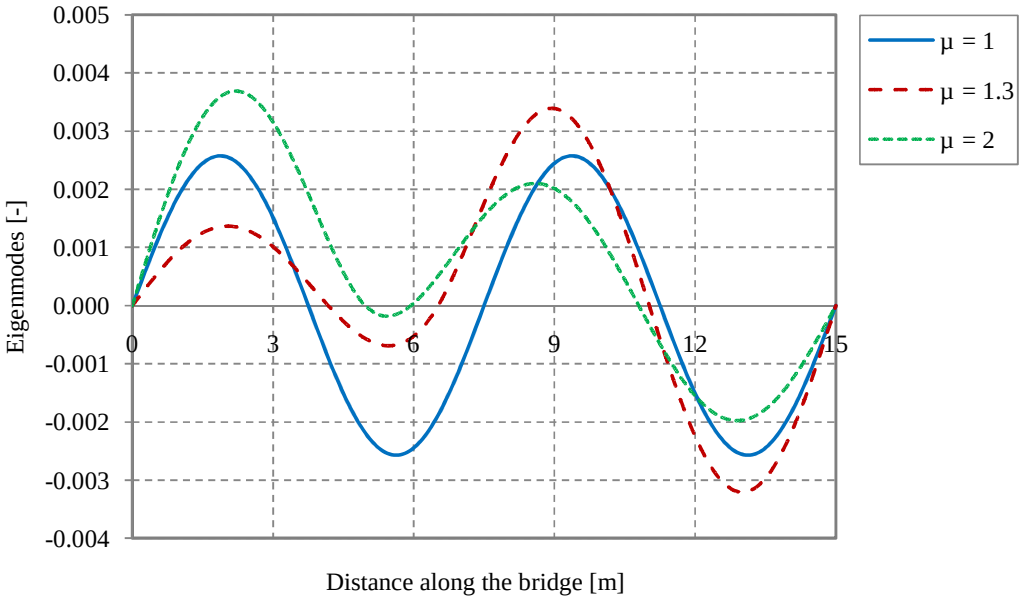

Figure 4.9 *The third eigenmode for a two-span bridge with a total length of 15 m. The mode is normalized to get the modal mass equal to one.*

It is of great value for the remaining examinations made in this thesis to have a simple expression for the first eigenfrequency. Therefore efforts have been made to create such an expression. The "curve fitting" toolbox in Matlab was used for this purpose. To get a more simple expression different equation types were fitted for different intervals of μ. The equations shown in Table 4.1 are proposed to describe the first eigenfrequency for a two-span bridge.

Table 4.1 *Proposed eigenfrequency function for determining the first eigenfrequency for a two-span bridge.*

μ	Eigenfrequency function, $g(\mu)$	R^2-value
1- 1.2	$2 \cdot \pi \cdot \sin(\pi/2 \cdot \mu)$	0.991
1.2 - 3	$8.9 \cdot e^{-\mu} + 3.34 \cdot e^{-0.00183 \cdot \mu}$	0.999

It should be noted that there is no derivation behind the expressions in Table 4.1, they have simply been chosen for their simplicity in comparison to other expressions. Figure 4.10 shows the curves fitted against the true acceleration.

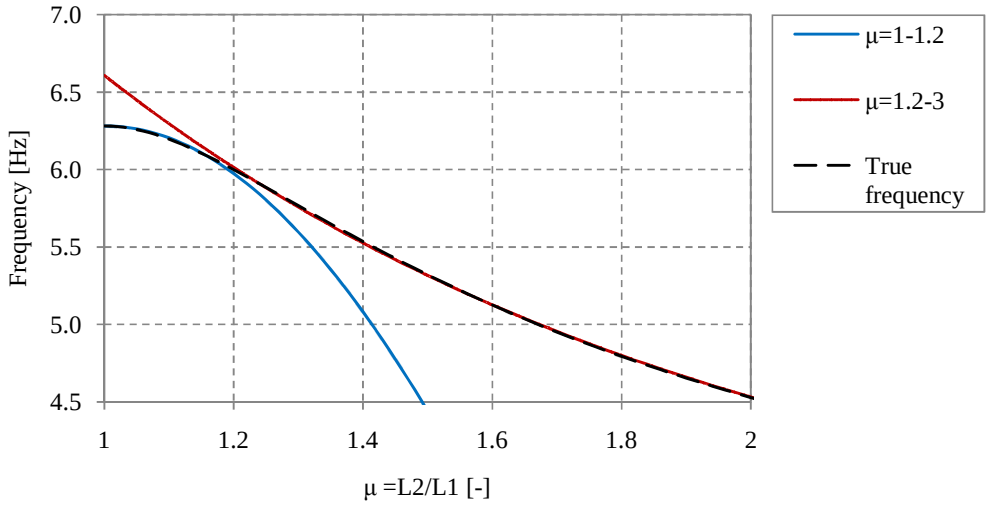

Figure 4.10 *Chosen eigenfrequency functions g for two-span bridges plotted against the true first frequency.*

Three different sets of material parameters have been chosen to show the accuracy of the expressions. Table 4.2 and Table 4.3 show these parameter sets and a comparison of eigenfrequencies calculated using the simple method presented in this section and a FE analysis.

Table 4.2 *Parameter sets used for different verifications throughout this thesis.*

Parameter	Set 1	Set 2	Set 3
E [GPa]	30	40	50
ρ [kg/m^3]	2400	2000	2800
L_{tot} [m]	25	20	15
μ [-]	1.1	2.5	1.5

Table 4.3 *Eigenfrequencies calculated using equation (4.4) and eigenfrequency functions in Table 4.1 compared to eigenfrequencies from a FE analysis.*

	Set 1	Set 2	Set 3
FE analysis	6.07	7.85	17.31
Equations	6.08	7.85	17.29

It is concluded that the frequency functions in Table 4.1 together with equation (4.4) gives satisfactory accuracy for determining the first eigenfrequency for a two-span bridge.

4.2.2 Three-span bridges

A three-span bridge have the same dependence on the bending stiffness *EI*, the mass per meter *m* and the total length of the bridge L_{tot}, with the same motivation as described in Section 4.2.1 for a two-span bridge. Two extra geometric parameters are however required to describe the relation of the three spans. In this thesis they are called η and κ and are defined in Section 4.1.

Since a two-span bridge only depends on one geometric parameter in a complex way it is possible to find expressions for describing the eigenfrequency functions for any combination of geometric and material parameters for this type of bridge. It gets more complex for a three-span bridge where two geometric parameters (η and κ) have a complex effect on the eigenfrequencies, see Figure 4.11.

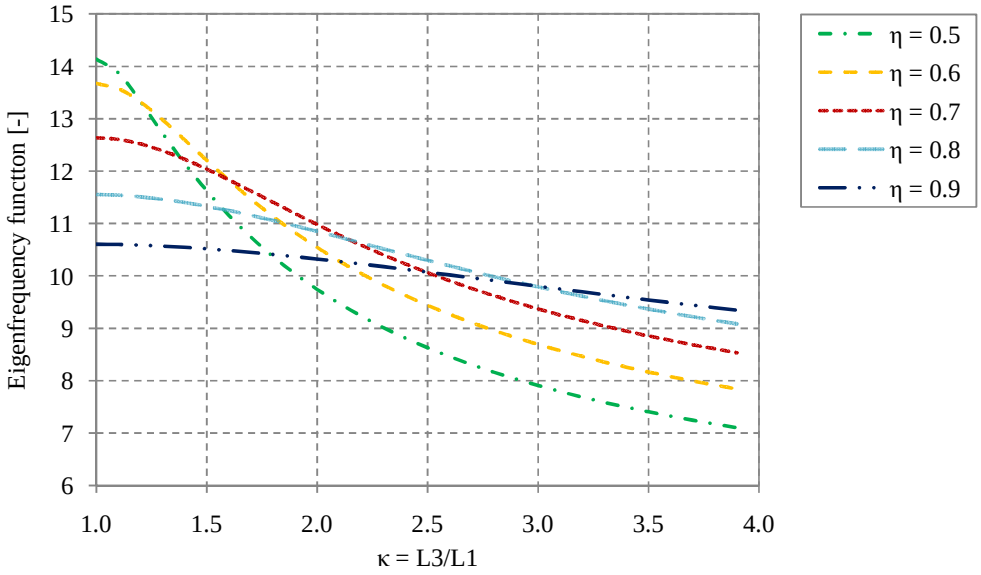

Figure 4.11 Eigenfrequency function for the first eigenfrequency for the variation of κ and η.

Figure 4.11 shows that the influence of the geometric parameter κ changes depending on the value of η. This means that it is not possible to formulate two separate equations for describing the eigenfrequencies' dependence on the two variables. Instead one equation depending on both variables is required, making it much harder to find a suitable expression.

It is rather common for three-span bridges to have κ equal to one, meaning the first and third span are equally sized while the middle span may vary in size. Since complexity in finding an expression for the frequencies depend on both η and κ a limitation has been made to bridges where κ =1.0. This type of bridge has a similar appearance of the eigenfrequencies for the variation of η as for a two span bridge, see Figure 4.12.

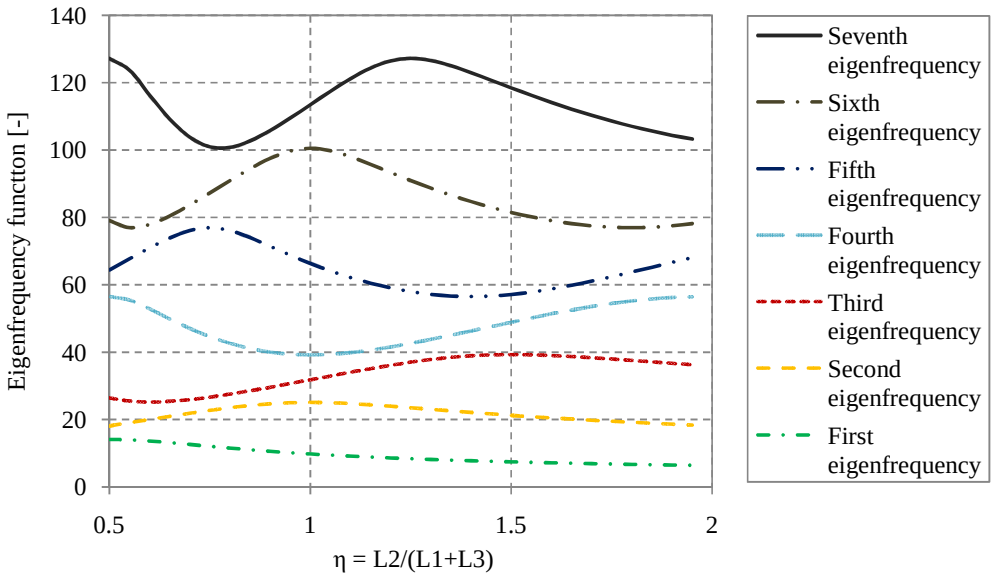

Figure 4.12 *Eigenfrequency functions for the first seven eigenfrequencies for a three-span bridge with $\kappa = 1.0$.*

As for a two-span bridge it is of great value for further examinations to have a simplified expression for calculating only the first eigenfrequency for variations in μ. Again the Matlab curve fitting toolbox was used for this purpose, and the expressions in Table 4.4 are proposed for different intervals of μ.

Table 4.4 *Proposed expressions for the eigenfrequency function for the first eigenfrequency of a three-span bridge with κ=1.0.*

Mode	$\eta = L2/(L1+L3)$ [-]	Eigenfrequency function, $g(\eta)$	R^2-value
First mode	0.5- 0.8	$1.6 \cdot \sin(7.2 \cdot \eta - 1.95) + 12.55$	0.999
First mode	0.8-2.5	$2 \cdot pi \cdot \eta^{-1.137} + 3.511$	0.999

Figure 4.13 shows the curves fitted against the true acceleration.

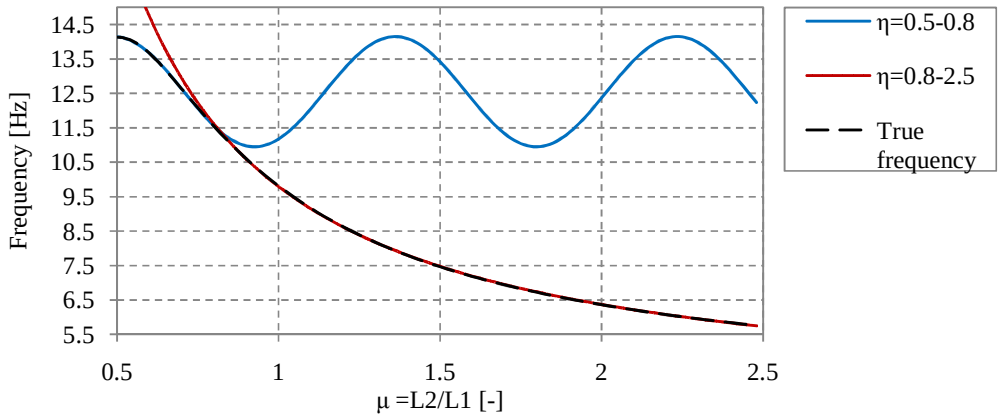

Figure 4.13 *Chosen eigenfrequency functions g for two-span bridges plotted against the true first frequency.*

A verification of the accuracy of the expressions in Table 4.4 has been made using three different parameter sets which are defined in Table 4.5. Table 4.6 shows the results from this verification.

Table 4.5 *Parameter sets used for different verifications throughout the thesis*

Parameter	Set 1	Set 2	Set 3
E [GPa]	30	40	50
M [kg/m^3]	2400	2000	2800
L_{tot} [m]	30	25	20
μ [-]	0.6	1.5	0.9

Table 4.6 *Eigenfrequencies calculated using equation (4.4) and eigenfrequency functions in Table 4.4 compared to eigenfrequencies from a FE analysis.*

	First eigenfrequency [Hz]		
	Set 1	Set 2	Set 3
FE analysis	9.301	9.254	19.402
Equations	9.298	9.262	19.385

4.2.3 Comparison to single-span bridges

Single-span railway bridges are very common and their first eigenfrequency can as mentioned be calculated analytically. Hence it may be of interest to know the increase in eigenfrequency that the additional spans of a multi-span bridge contribute with compared to a single-span bridge corresponding to the largest span length. The eigenfrequency of a multi-span bridge can alternatively be calculated as

$$f_i = U \cdot f_{i,single} \tag{4.5}$$

where $f_{i,single}$ is the i:th eigenfrequency of a single-span bridge corresponding to the largest span length of the multi-span bridge and

$$U = \frac{2 \cdot g_i(\mu) \cdot (1+\mu)^2}{\pi \cdot \mu^2} \tag{4.6}$$

for a two-span bridge and

$$U = \frac{2 \cdot g_i(\eta) \cdot (1+\eta)^2}{\pi \cdot \eta^2} \tag{4.7}$$

for a three-span bridge. Figure 4.14 shows the appearance of U for calculation of the first eigenfrequency of a two- and three-span bridge.

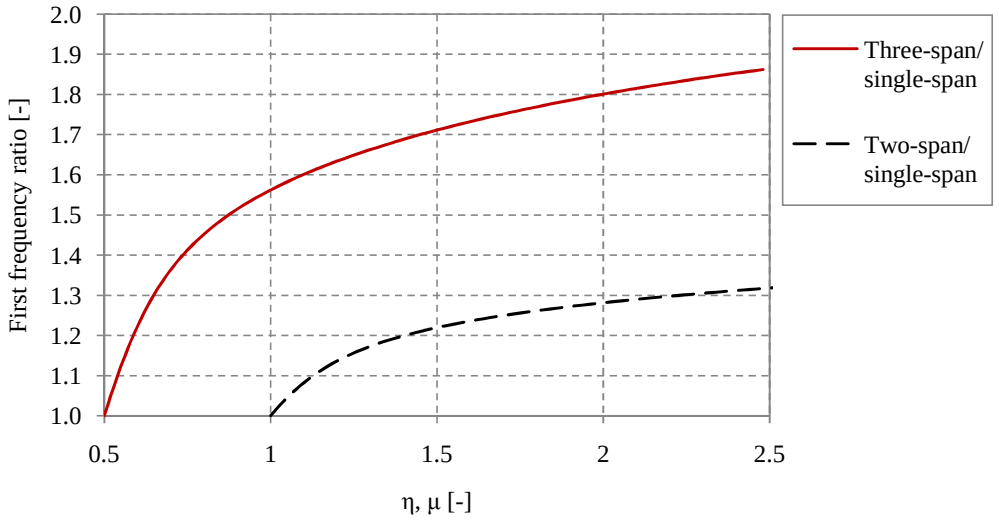

Figure 4.14 *Appearance of the factor U for determining the first eigenfrequency for a two- and three span bridge through the eigenfrequency of a single-span bridge corresponding to the largest span length.*

4.2.4 Remarks

By examining the derivation of eigenfrequencies for single- and multi-span bridges it was seen that the eigenfrequencies for a multi-span bridge depend on material parameters in the same way as a single-span bridge. By graphic examination it was seen that this also is true for the total length of the bridge. One important feature to note is that all frequencies have the same dependence on these parameters. This means the eigenfrequencies have the same relation to each other for any combination of material parameters and total bridge length. This is important in later calculations since it allows searching for simpler dependencies that the acceleration response has on these parameters. However the geometric span relation parameters affect the eigenfrequencies differently for all multi-span bridges. This means that the dynamic response behavior will be affected in a different way when span relations are altered depending on which eigenmode that is examined. It is therefore not possible to define exactly how the dynamic response depends on the span relation parameters since each eigenmode has its own effect on the dynamic response, and the number of eigenmodes in a continuous structure is infinitely large.

4.3 Load frequency and resonance effects

According to BV Bro (Banverket 2006) all railway bridges with a total length above 7 m have to be designed to withstand the HSLM-A train loads in terms of maximum allowed vertical acceleration in the superstructure of the bridge, see Chapter 3. As shown in Chapter 3 all HSLM-A loads have different load parameters in the term of coach length D, bogie axel length d and the number of coaches. In this section it is discussed how the train loads will affect a railway bridge is presented. The main load frequency is defined and it is shown how it in relation to the eigenfrequencies of a bridge affects the dynamic response due to resonance.

To understand the meaning of load frequency of a train load it is convenient to start with a single point load moving over a single-span bridge with a fixed velocity, see Figure 4.15.

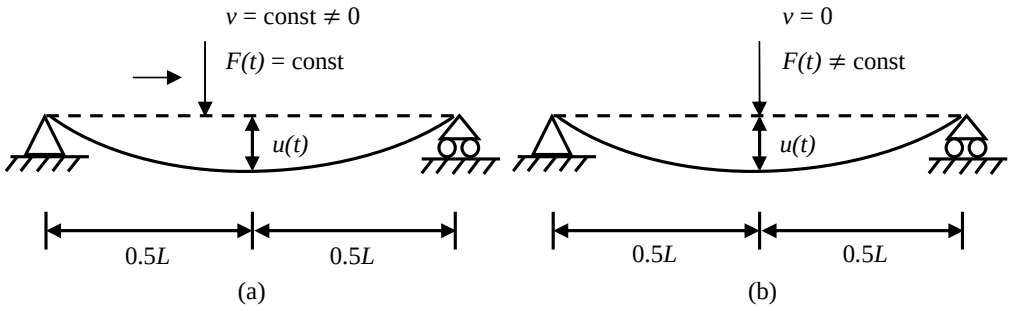

Figure 4.15 *A single-span bridge subjected to one point load. (a): constant load moving over the bridge with constant velocity. (b): point load that varies in time acting in the middle of the bridge.*

Figure 4.15 implies that a point load moving over a single-span bridge can be transformed from a load varying in the space domain to a stationary load varying in the time domain. The transformed load in Figure 4.15 will hence vary in time and if

several loads with equal distance moves over the bridge there will be a load effect on the bridge varying with a certain frequency affected by the speed of the loads and the distance between them. As an example let us consider the static analysis of the bridge in Figure 4.15. The influence line for the mid-span deflection caused by one point load as it moves over the bridge is very close to a sinusoidal curve. If several influence lines are superpositioned in the time domain a resulting influence of the loads is received, see Figure 4.16.

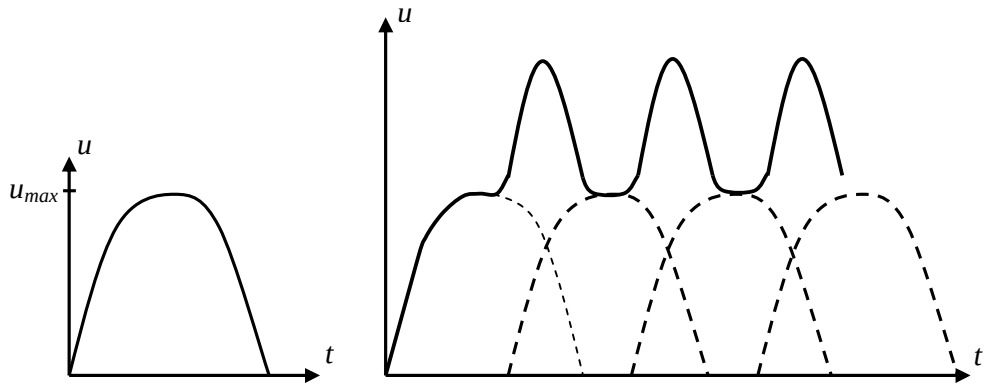

Figure 4.16 *The influence line for static displacement in a single-span bridge subjected to several equally distanced point loads travelling over the bridge with constant speed.*

The static response shown by Figure 4.16 gives an idea of how a bridge will be affected by moving point loads, even though the full complexity in a dynamic analysis is not considered. It should be noted that the appearance of the total influence line differ as the load distance is altered or bridge spans are added. For more information about the reliability/possibility to describe load effect on the dynamic response using a static model, see Section 4.4.

The train load models HSLM-A are all a combination of point loads traveling with different distances in between, namely the coach length *D* and the boogie axel length *d*. However, the coach length *D* can be considered as the "main" distance between the loads, as it serves as the distance between the resultants of the boogie axle loads of the train, see Figure 3.1. In Figure 4.16 it can been seen that the time between peaks in the total load influence is equal to the time between the traveling loads. As the frequency is the inverse of this time it can then be concluded that the "main" frequency of a HSLM-A train load can be defined as

$$\Omega = \frac{v}{D} \tag{4.8}$$

where

Ω = *Load frequency*

D = *Coach length of considered HSLM-A load*

v = *Train velocity*

Resonance will occur when the load frequency coincides with one of the eigenfrequencies of any structure, see Chapter 2. However, for railway bridges resonance will also occur when an eigenfrequency coincides with any multiple of the load frequency, i.e.

$$\Omega = \frac{f_i}{k} \tag{4.9}$$

where

f_i = *Eigenfrequency of the i:th degree*

k = *1, 2, 3…*

The behavior behind equation (4.9) can be understood by looking at a spring-weight SDOF system without damping. Say the system is vibrating with its eigenfrequency. If we tap the weight (put a small impulse load on it) every time it is in its highest position we will increase the amplitude of the vibration every cycle and the amplitude goes to infinity with time, see Figure 4.17. If we tap the weight every second time it is in its highest position the amplitude also goes to infinity in time but it increases slower. These two examples correspond to adding a load with a frequency coinciding with the eigenfrequency and the eigenfrequency divided by two. In a real structure the first of these most often gives the largest dynamic responses since the structure has less time to damp out the vibrations.

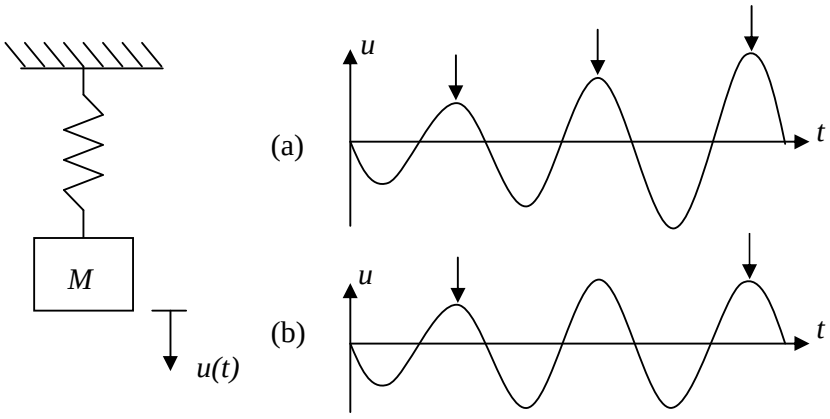

Figure 4.17 *Illustrative figure of how the displacement increases for a SDOF model when an impulse load is applied with a frequency corresponding to the systems eigenfrequency and half the eigenfrequency in (a) and (b) respectively*

The ratio between the load frequency and the first eigenfrequency is defined as

$$\beta = \frac{\Omega}{f_1} \tag{4.10}$$

This parameter will be frequently used in this thesis since it can be used to describe all bridge parameters and the train velocities' effect on the maximum acceleration response.

FE analyses have been performed on a two-span bridge to show how the dynamic response in a railway bridge is dominated by resonance phenomenon. Three different data sets have been used, see Table 4.2. In the analyses mode superposition is used and limited to the first two eigenmodes. The examined result is the maximum acceleration for the variation of train velocity, see Figure 4.18.

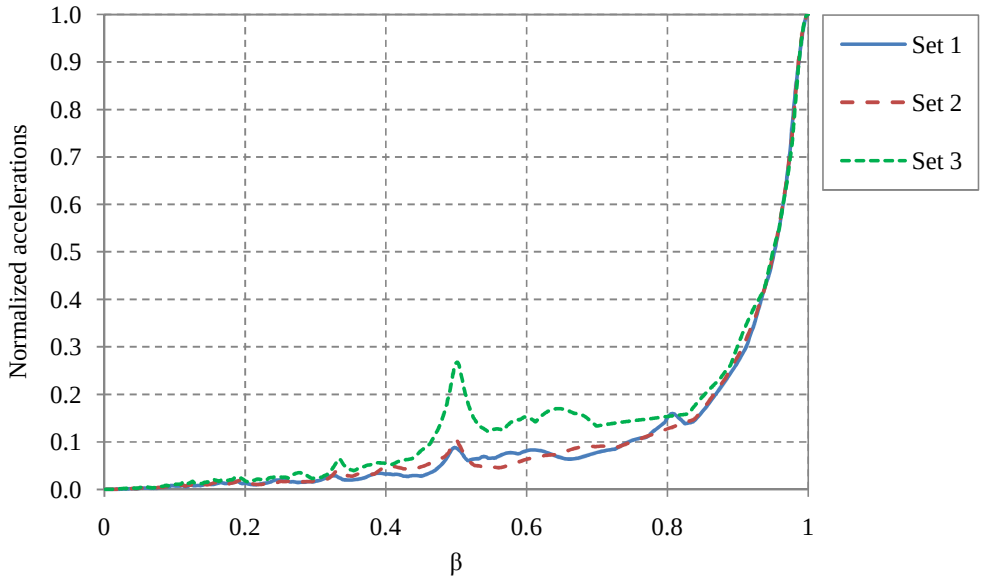

Figure 4.18 *Maximum acceleration response for the variation of train velocity using the three parameter sets defined in Table 4.2, two eigenmodes and a modal damping of 2%. The train load HSLM-A1 is used for all three parameter sets.*

It can be seen in Figure 4.18 that resonance effects occur at $\beta = 1$ and 1/2 for all three parameter sets and thus confirming the correctness of equation (4.9).

An additional parameter denoted the critical speed is defined before proceeding to the following sections.

$$v_{cr} = D \cdot f_1 \tag{4.11}$$

Where:

v_{cr} = *The critical speed for a specific bridge configuration and HSLM-A load*

The critical speed is the speed resulting in $\beta = 1.0$ for a given coach length D and consideration to the first eigenfrequency. In reality this speed is never reached as it is unadvisable considering dynamic aspects of railway bridge design. Figure 4.18 gives an understanding of how much larger the accelerations become if the speed is

reached. It serves nevertheless as a good reference value and it will be used frequently in the remainder of the thesis.

By combining equation (4.8), (4.9) and (4.11) the resonance speed can be shown to be

$$v_{resonance} = \frac{v_{cr}}{k} \tag{4.12}$$

where

$v_{resonance}$ = *train velocity at which resonance effects occur in a railway bridge*

Finally by combining equations (4.4), (4.11) and (4.12) an analytical expression for calculating the resonance speeds by hand is obtained as

$$v_{resonance} = \frac{D}{k} \cdot \frac{g_i}{{L_{tot}}^2} \cdot \sqrt{\frac{EI}{m}} \tag{4.13}$$

4.4 The SDOF model

A model meant for describing the dynamic response of multi-span bridges consisting of only one degree of freedom has been established. The purpose of creating such a model is partly because it describes the complex dynamic response in a simple way which may increase the understanding of this complexity, but also because it greatly decreases calculation time and gives an analytical equation of the response that could be used for finding guidelines in the design process of railway bridges.

In this section the theory behind the creation of the SDOF model will be explained. This is followed by a verification of the SDOF model's accuracy.

4.4.1 Theory

The examination of a SDOF model that resembles a railway bridge is a continuation from previous master carried out at Reinertsen Sweden AB, namely Ekström and Kieri (2007) and De Leon and Lasn (2008).

In Ekström and Kieri (2007) the transformation of a single-span railway bridge was made using transformation factors which was first introduced by Nyström (2006), also a master thesis carried out at Reinertsen Sweden AB. The transformation factor approach creates a transformation factor for stiffness, mass and load respectively. These factors are defined so that kinetic energy stored in the beam and SDOF system becomes equal, the moved mass and the load exerts the same amount of work. The transformation factors are based on the assumption that the beam deforms as a sinusoidal curve.

De Leon and Lasn (2008) compared the transformation factor approach to an additional method of transformation, called the force scaling approach. The force scaling approach requires considerably less calculations and is also easier to apply on

more complex structures. The method was proven to give accurate results for a single-span bridge.

One of the aims of this thesis is to examine if it is possible to transform also a multi-span bridge into a SDOF model. Because of the complexity in multi-span bridges the force scaling approach has hence been chosen for this task, and its theory will be presented in this section. The interested reader is referred to Nyström (2006) for theory on the transformation factor approach.

A SDOF model has the equation of motion shown in equation (2.2). To establish this model the stiffness *K*, mass *M*, damping *C* and load *p(t)* needs to be determined. The force scaling approach has the following calculation procedure:

- Chose an arbitrary mass of the SDOF model
- Calculate the stiffness of the SDOF model so the first frequency of the SDOF model and the railway bridge becomes equal
- Determine the damping
- Scale the load acting on the bridge to use on the SDOF model so that the static deflection of the bridge and SDOF model becomes equal

Let us go through the four steps in more detail. First an arbitrary mass of the SDOF model is chosen as

$$M = T \cdot M_{bridge} \ , \ where \ \mathrm{T} > 0 \tag{4.14}$$

In Section 4.3 it was shown that the response in railway bridges is governed by the ratio between load frequency and first eigenfrequency. It is hence important that the SDOF model has a frequency that corresponds to the first eigenfrequency of the bridge. The fact that an SDOF model only has one eigenfrequency limits the model since only the first eigenfrequency of the bridge can be regarded. Resonance effects that occur with regard to higher eigenmodes are not given consideration in the model. By combining the expression for the eigenfrequency in equation (2.5) and equation (4.4) an expression for determining the stiffness is obtained as

$$K = M \cdot \frac{f_i(\mu)}{{L_{tot}}^2} \cdot \sqrt{\frac{EI}{m}} \tag{4.15}$$

The SDOF model is made to resemble the dynamic response using the first eigenmode. The damping should therefore be chosen to resemble the modal damping of the first eigenmode. Equation (4.16) shows how the damping *C* can be calculated from a known modal damping.

$$C = 2 \cdot \zeta \cdot M \cdot \omega_{sdof} \tag{4.16}$$

where

$$\omega_{sdof} = \sqrt{\frac{K}{M}}$$

Finally the load acting on the bridge is scaled so that the static deflection of the bridge and SDOF model becomes equal. The static displacement of the SDOF model is defined as

$$u(t)_{sdof} = \frac{p(t)_{sdof}}{K} \tag{4.17}$$

Setting the static displacement in equation (4.17) equal to the static displacement of the bridge gives an expression for determining the load acting on the SDOF model as

$$p(t)_{sdof} = K \cdot u(t)_{bridge} \tag{4.18}$$

The force scaling approach has its name since equation (4.18) re-written forms a relation between the load acting on the bridge and on the SDOF model equal to K/K_{bridge} which in De Leon and Lasn (2008) has been called the scaling factor.

A point in which the largest accelerations are assumed to occur in the bridge needs to be chosen before the deflection of the bridge can be calculated. It is assumed in this thesis that the largest acceleration will occur in the middle of the largest span. The static deflection in time is calculated by using influence lines for the deflection in the critical point with consideration to one point load. The influence lines are based on the coordinate of the point load which can be replaced with velocity of the point loads times the time to get the static deflection in time. By superpositioning the influence of point loads in a correct manner a HSLM-A train load can be resembled. The added complications with applying the force scaling approach on a multi-span bridge compared to on a single-span bridge, as has been made in De Leon and Lasn (2008), lies solely in the calculation of the static deflection of the bridge.

4.4.2 Verification

The whole concept of the SDOF model is based on the limit of required eigenmodes in BV Bro Banverket (2006). As described in Chapter 3 this limit is 30 Hz. It means that the eigenmodes that has an eigenfrequency above 30 Hz can be excluded when calculating the dynamic response.

The SDOF model created is meant for calculating the dynamic accelerations. These accelerations are strongly affected by higher eigenmodes, as shown by Figure 4.19. The only time the SDOF model is capable of describing a more accurate dynamic acceleration response is when only the first eigenmode has to be considered. However, this is often the case for multi-span bridges.

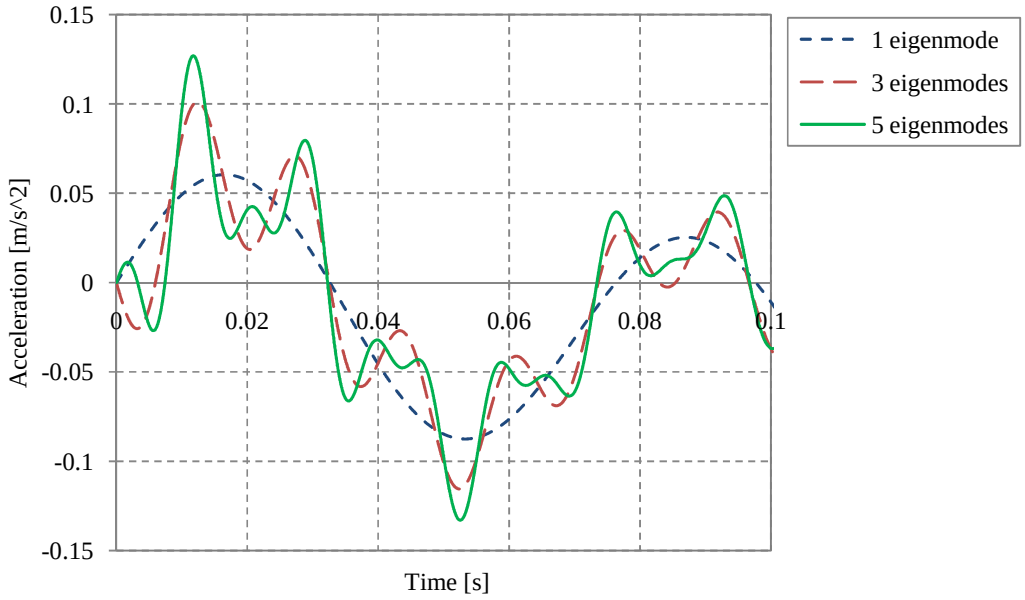

Figure 4.19 *Comparison of the maximum acceleration response in a two-span bridge subjected to a point load of 100 kN moving with v=50 m/s using different number of eigenmodes. The used parameters are E=40 GPa, ρ=2400 kg/m^3, L=15 m, μ=2, c=0.02.*

A SDOF model based on the theory presented in Section 4.4.1 has been established and its Matlab code can be found in Appendix D. The SDOF model's accuracy have been verified against a FE program that also can be found in Appendix D. In the verification only the first eigenmode was used in the FE analysis since this corresponds to what the SDOF model describes. Table 4.7 shows two sets of parameters that have been used in the verification. Figure 4.20 and Figure 4.21 shows the acceleration response in time for the SDOF model and the FE analysis using data set 1 in Table 4.7.

Table 4.7 *Two parameter sets used in the verification of the SDOF models accuracy. Both parameter sets concern a two-span bridge.*

Bridge type	E [GPa]	ρ [kg/m^3]	L [m]	μ [-]	c [-]	HSLM-A	v [m/s]
Set 1	40	2400	15	2.0	0.02	A1	50
Set 2	40	2400	15	2.0	0.02	A4	75

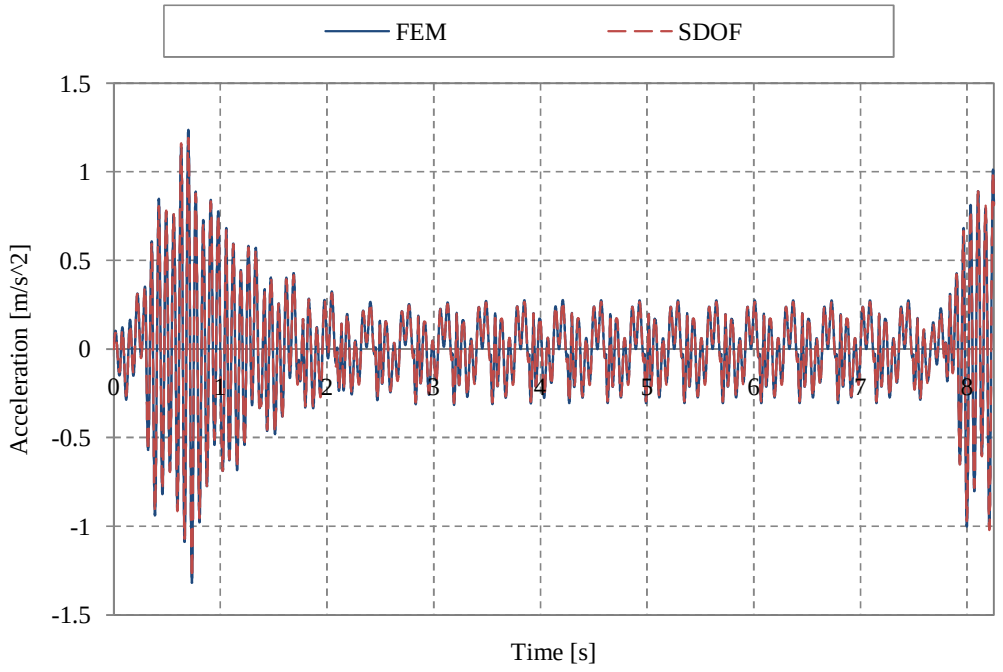

Figure 4.20 *Acceleration response in the middle of the second span using data set 1 in Table 4.7.*

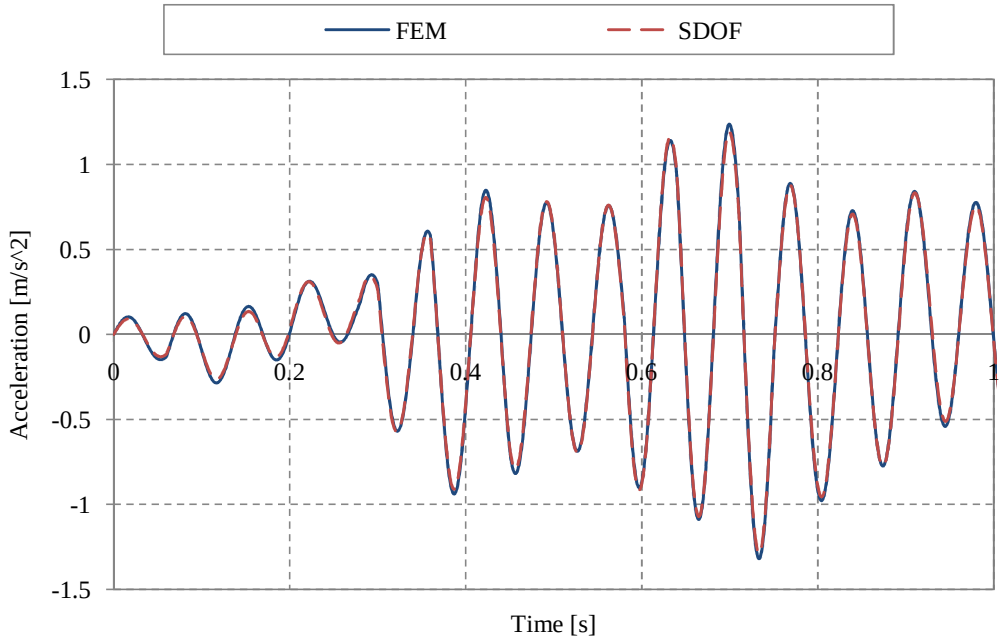

Figure 4.21 *Acceleration response from Figure 4.20 during the first second.*

Figure 4.22 and Figure 4.23 shows the acceleration response in time for the SDOF model and the FE analysis using data set 2 in Table 4.7.

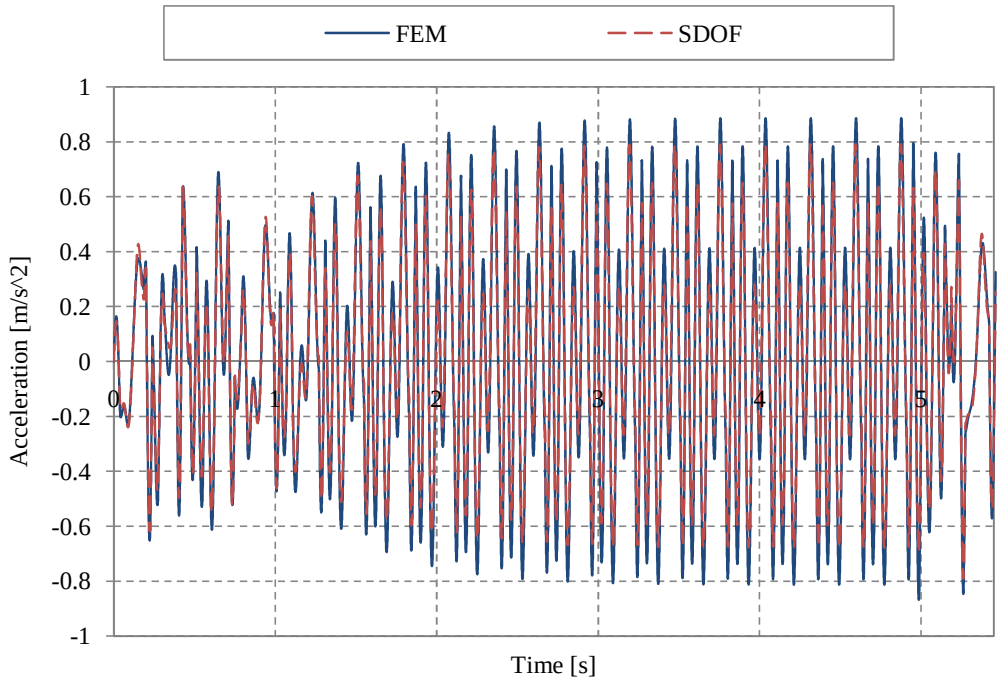

Figure 4.22 *Acceleration response in the middle of the second span using data set 2 in Table 4.7.*

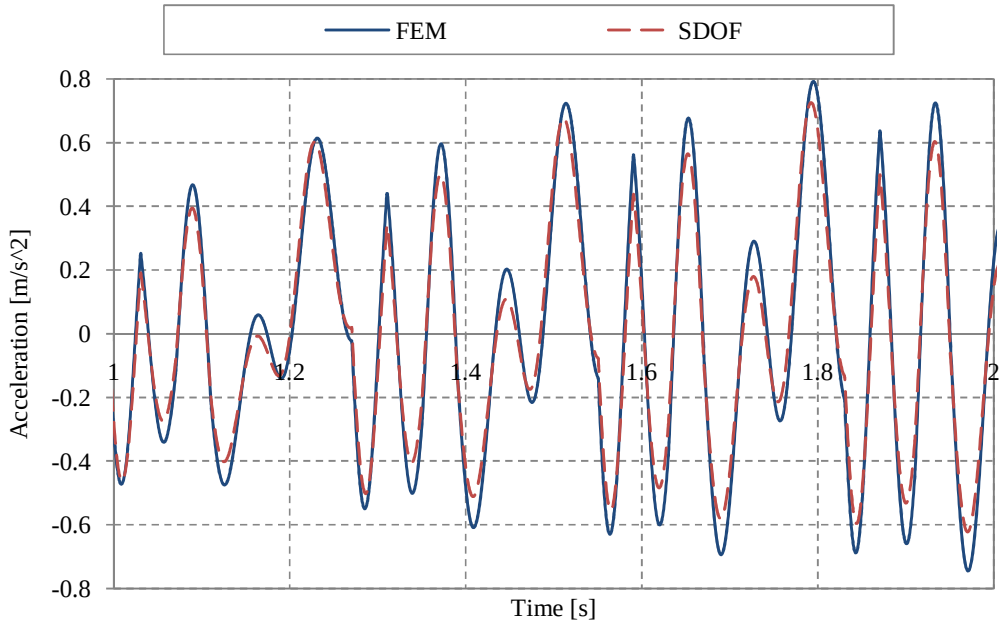

Figure 4.23 *Acceleration response from Figure 4.22 during the 2: nd second.*

For the first data set in Figure 4.20 and Figure 4.21there is a close resemblance between the SDOF model and the FE analysis. Both the appearance and the amplitude of the acceleration response are similar. For the second data set Figure 4.22 and Figure 4.23 there is however some lack in accuracy when it comes the amplitude of the accelerations, even though the appearance is accurate.

A more extensive comparison of the acceleration amplitude has been made by examining the variation of maximum acceleration in time for different train velocities, see Figure 4.24 and Figure 4.25. A comparison between the acceleration response in the middle of the largest span (in this case the second span) and the maximum acceleration response in the whole bridge is also made in Figure 4.24 and Figure 4.25.

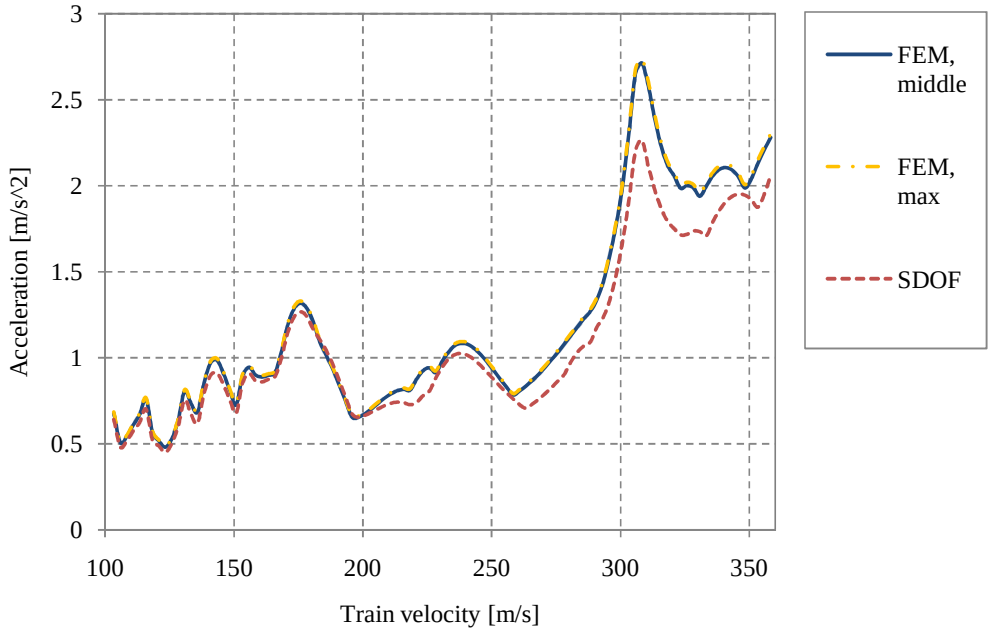

Figure 4.24 *Maximum acceleration response using data set 1 in Table 4.7 with variation in the train velocity.*

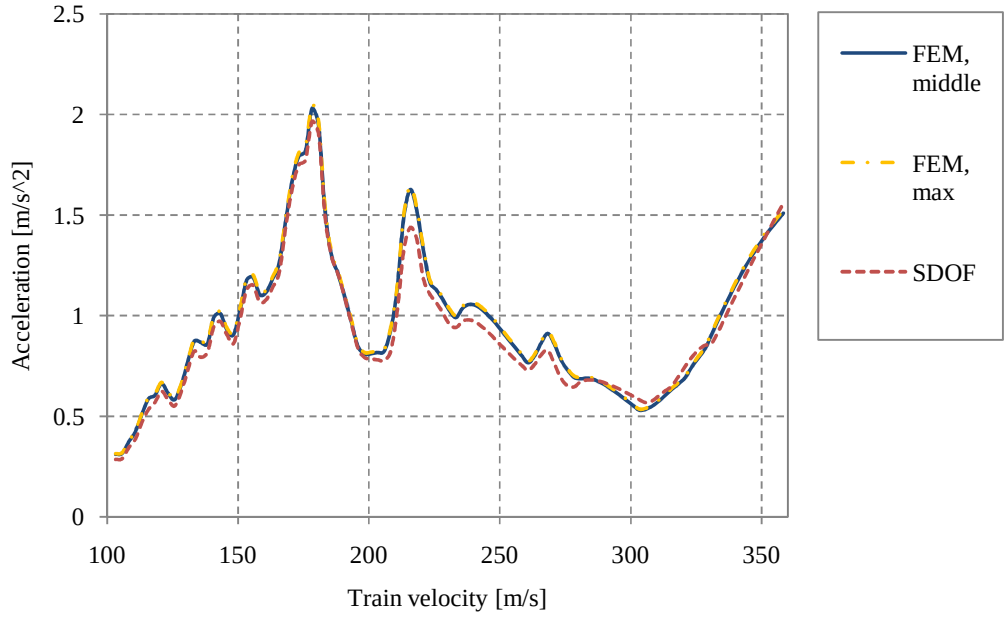

Figure 4.25 *Maximum acceleration response using data set 2 in Table 4.7 with variation in the train velocity.*

When higher modes are included the maximum acceleration is likely to occur somewhat off the center of the largest span. When only one mode is included however Figure 4.24 and Figure 4.25 show that the maximum acceleration occurs in the middle of the largest span with just a small error. This is good for the SDOF model since it is based on the maximum acceleration appearing in the middle of the largest span. This makes the acceleration behavior in the SDOF model more correct. Figure 4.24 and Figure 4.25 do however also show that the SDOF model lack accuracy and also that this lack of accuracy is not consist for the variation of train velocity.

In the following section calculations have been made to capture different material and geometric parameters dependence on the acceleration amplitude. For the possibility of finding such dependencies it is necessary to use a calculation tool that can show if the dependencies are consistent for the variation of train velocity. It was stated in the beginning of this Chapter that the SDOF model could be used to decrease the calculation time for the upcoming calculations if proven accurate enough. But since the accuracy varies depending on train velocity the SDOF model has not been used further in this thesis.

It can however be stated that the accuracy of the SDOF model is remarkably good considering the models simplicity even for multi-span bridges.

4.5 Amplitude of the acceleration response

By calculating the eigenfrequencies of a railway bridge, as shown in Section 4.2, it is possible to decide the critical speeds at which resonance occur for a certain train load. In Section 4.3 it was also shown that resonance effects occurs for multiples of the critical speed for railway bridges and how the resonance speeds can be calculated.

The equations in Sections 4.2 and 4.3 give together an exact formulation of how the resonance speed is calculated. They do not however give any guidance to how large the dynamic response will be at this resonance speed. As this thesis partly aims to give guidelines for how to estimate the dynamic response it is required to further examine the variation in acceleration amplitude of the dynamic response.

In this section the results from a parameter study made on two- and three span bridges is presented. In this parameter study the amplitude of the dynamic response in terms of acceleration has been examined at different resonance speeds for the variation of both material and geometric parameters. Section 4.5.3 will present the results from the parameter study for the individual variation of each material and geometric parameter, respectively. A discussion and the conclusions made concerning the amplitude of the dynamic acceleration response are presented in Section 4.5.4.

The dynamic response in the parameter study has been calculated using a Matlab FE program developed within this thesis by the authors, see Appendix D. For details about meshing, element choice, load application and time integration the reader is referred to Appendix D. In comparison to commercial FE software the variation of geometric parameters is substantially easier to handle in Matlab. It is also easier to apply train loads and variation of train velocity in Matlab.

Equation (4.13) has been used for calculating the resonance speeds both in the Matlab program and when handling the data from it. In the FE calculations mode superposition was used utilizing only the first eigenmode to save calculation time.

Parameter behaviors that differ for different eigenmodes are beyond the time limit of this thesis and therefore the use of additional eigenmodes is unnecessary.

In this section a selection of figures are presented to give the reader a comprehensible presentation of the results from the parameter study. For the interested reader a more extensive gathering of figures from all the analysis made can be found in Appendix B.

4.5.1 Method

In this section the method behind the parameter study will be presented. The section is meant to clarify what calculations that have been performed and how the data for the figures that will be presented have been extracted.

The time response of the vertical acceleration when a train runs over a bridge is complex. However the shape of this response is not of interest in the process of designing a railway bridge. Only the maximum acceleration in time is of interest. Therefore there is no necessity in examining the actual response in time, but rather only the maximum acceleration. When designing a railway bridge a range of train velocities need to be considered however, see Chapter 3. Changing the train velocity may result in a completely different acceleration response in time and hence also a different maximum acceleration.

The process of creating the Matlab programs that have been used for the parameter study can be divided in steps. First a program that calculates the response in time for a fixed train velocity and parameter set was created and verified against ADINA. Then this program was modified to calculate the response in time for every train velocity of interest and from these extracting the maximum acceleration response, see Figure ***4.26***.

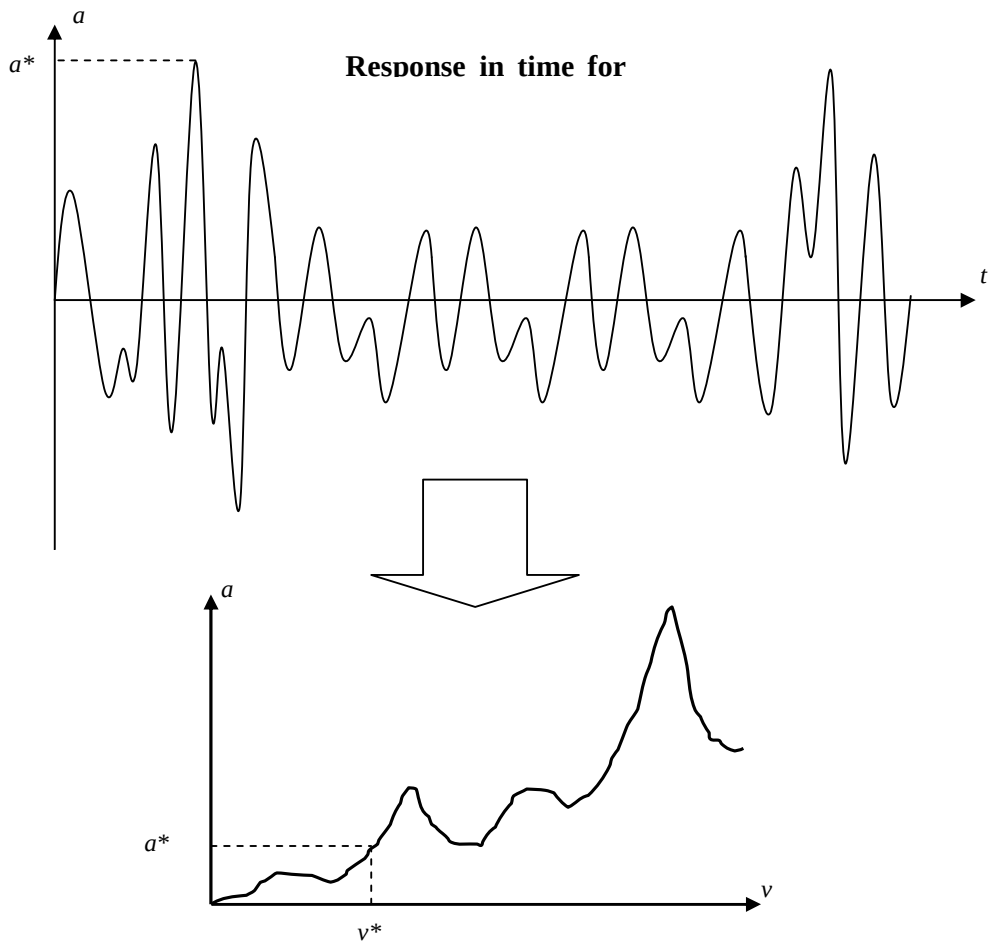

Figure 4.26 *Illustrative figure of how the acceleration response in time has been gathered in a v-a plot.*

The method applied in the parameter study has been to first calculate the maximum acceleration response in time for the variation of train velocity with a certain train load and set of material and geometric parameters, as shown by Figure 4.26 procedure is then repeated with the independent variation of one variable. The variation in amplitude of the acceleration response for changing that variable can then be studied by examining the amplitude for fixed values of β. Since the acceleration response at resonance often governs the determination of design acceleration in real life projects the β values 0.5, 0.33, 0.25 and 0.2 have been examined which corresponds to resonance speeds. Figure 4.27 shows how the data at a constant value of β have been extracted to show the accelerations dependence upon a variable of interest.

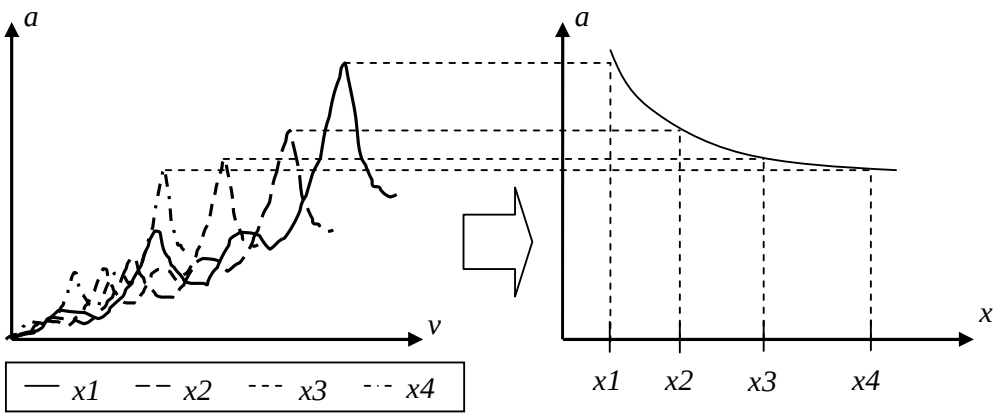

Figure 4.27 *Illustrative figure of how the acceleration at a β value have been extracted and gathered in a figure that shows the accelerations dependence on the examined variable.*

4.5.2 Extent of the study

In this section an overview of all the performed calculations will be presented. The section is meant to show the extent of the parameter study together with the required performance to achieve this extent.

The examined parameters are the Young's modulus, E, the density, ρ, the total bridge length, L_{tot}, the span relation, μ, and the modal damping c. Calculations have been performed on both two- and three-span bridges. Table 4.8 shows the extent of the parameter study.

Table 4.8 *Extent of the parameter study*

Variable	Step length	Two-span bridge			Three-span bridge		
		A1	A4	A8	A1	A4	A8
E [GPa]	5	15-60	15-60	-	15-60	-	-
ρ [kg/m^3]	200	2800-4600	-	-	2200-4000	-	-
L_{tot} [m]	0.5	13-22.5	13-22.5	15-24.5	-	-	-
μ [-], η [-]	0.05	1-1.95	1-1.95	1-1.95	0.5-1.45	0.5-1.45	0.5-1.45
c [-]	0.001	0.01-0-029	-	-	-	-	-

It is seen in Table 4.8 that the train loads HSLM-A1, -A4 and -A8 have been chosen for the parameter study. These loads have been chosen as they have different values of every parameter that defines the HSLM-A train loads.

The calculations behind the parameter study are very time consuming. As mentioned in Section 4.5.1 the response in time must be calculated for every train velocity of interest to receive the response from one single set of parameters. Table 4.8 show that this calculation procedure has been repeated 250 times using different parameter sets. This is despite limiting the parameter study to three HSLM-A train loads.

For the examination of every parameter the train velocity has been varied within the interval of 100- 360 km/h. Both the interval of the train velocity and the size of the examined parameters shown by Table 4.8 have been chosen to resemble realistic values.

When examining one variable the remaining data set have been chosen to capture the resonance peaks of interest, namely at β=0.5, 0.33, 0.25 and 0.2. This means that different data sets have been chosen for the examination of different variables. The data set used is shown in the caption of every figure presented from the parameter study later on.

4.5.3 Results

The effect on the acceleration amplitude in railway bridges from varying different material and geometric parameters have been examined. Each parameter has been examined individually and the results are presented in this section in a corresponding way. The cross-section defined in Section 4.1 have been used for all analysis presented in this section.

4.5.3.1 Variations of mass

The mass has been varied by changing the density. When the mass per meter of a bridge length is increased the eigenfrequencies, and consequently the resonance speeds, will decrease. As can be seen in equation (4.13) the critical speed depends on the inverse of the square root of the mass. Figure 4.28 shows an example of the maximum acceleration response in a bridge for different train velocities and it is seen how the resonance speeds decrease as the mass increase.

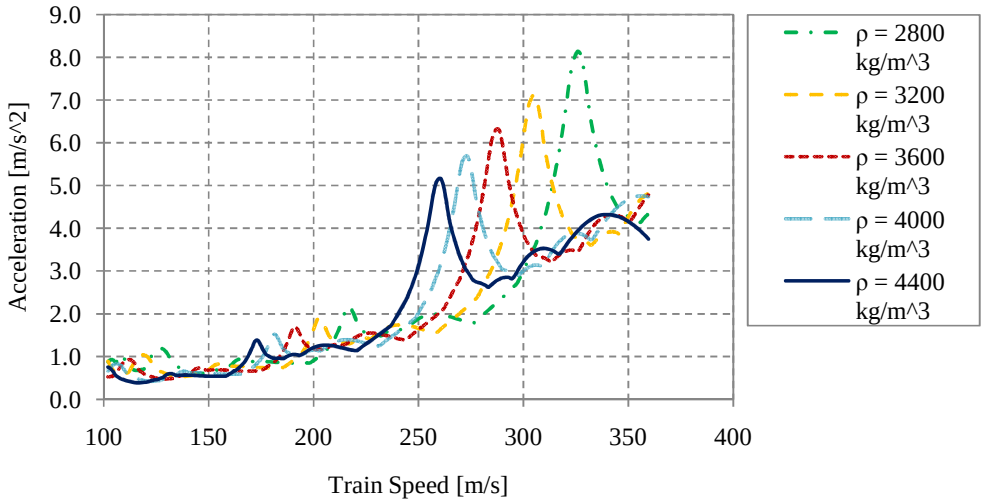

Figure 4.28 *Acceleration response for a two-span bridge subjected to HSLM-A1 using E = 30 GPa, Ltot = 16 m, μ = 2 and ζ = 0.02.*

In Figure 4.28 it can be seen that the shape of the acceleration response curve is kept as the mass of the examined bridge varies. The accelerations at the resonance speeds have been collected and plotted against each respective density in Figure 4.29.

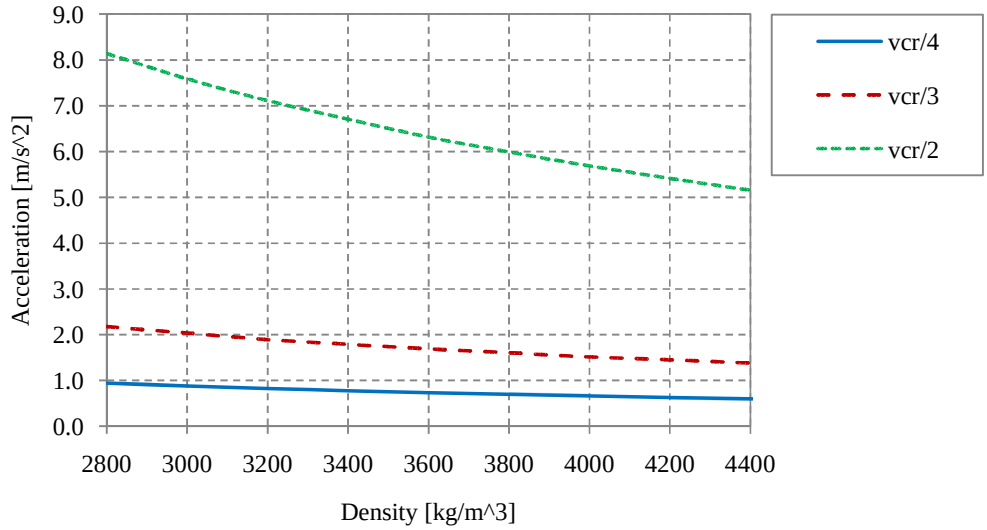

Figure 4.29 *Acceleration response for a two-span bridge subjected to HSLM-A1 using E = 30 GPa, Ltot = 16 m, μ = 2 and ζ = 0.02 at three resonance speeds.*

Eurocode states that the amplitude of the acceleration response has an inverse proportionality against the mass. Figure 4.30 shows the normalized curves from Figure 4.29, plotted against the inverse of each respective density. Here it can be seen that the statement in Eurocode is true. It is important to note that the acceleration amplitude has the same dependence for any speed, and hence only one line can be seen in Figure 4.30.

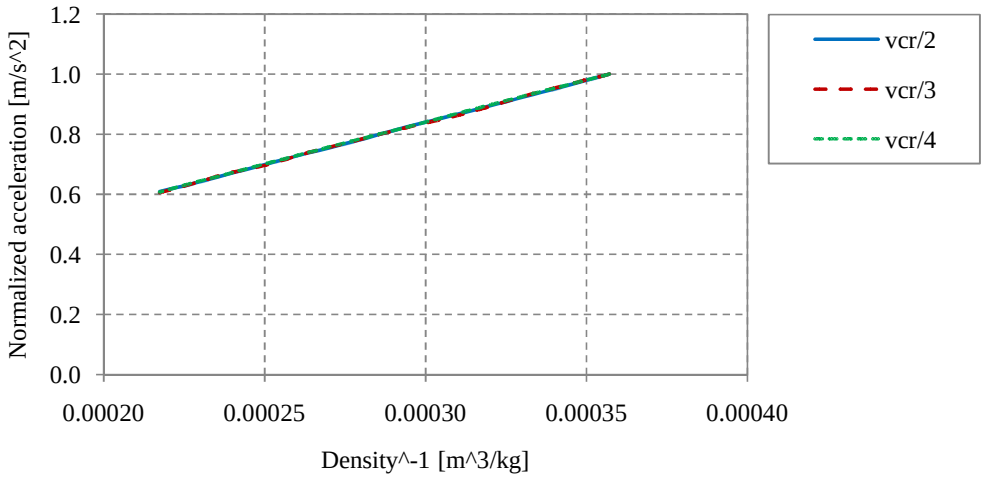

Figure 4.30 Acceleration from Figure 4.29 plotted against the inverse of the density.

4.5.3.2 Variation of bending stiffness

From equation (4.13) it is known that the resonance speeds depend on the square root of the bending stiffness. An increase in the bending stiffness thus leads to the resonance peaks appearing at higher speeds. In this thesis the variation of bending stiffness has been examined by varying the module of elasticity. Figure 4.31 and Figure 4.32 shows examples of the acceleration response for the variation of train velocity for a two- and three-span bridge respectively.

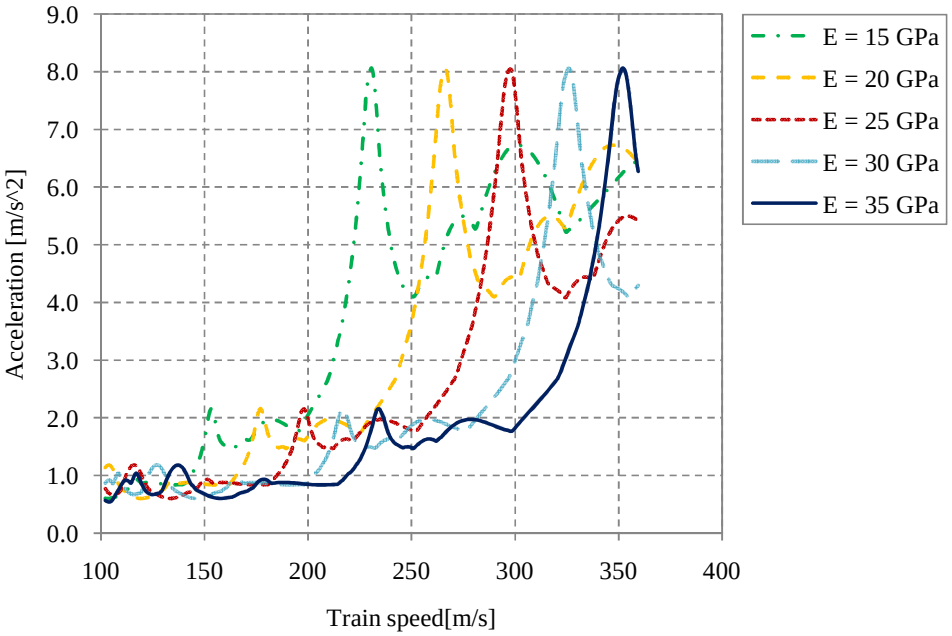

Figure 4.31 Acceleration response for a two-span bridge subjected to HSLM-A1 using = 2800 kg/m^3, Ltot = 16 m, = 2 and = 0.02.

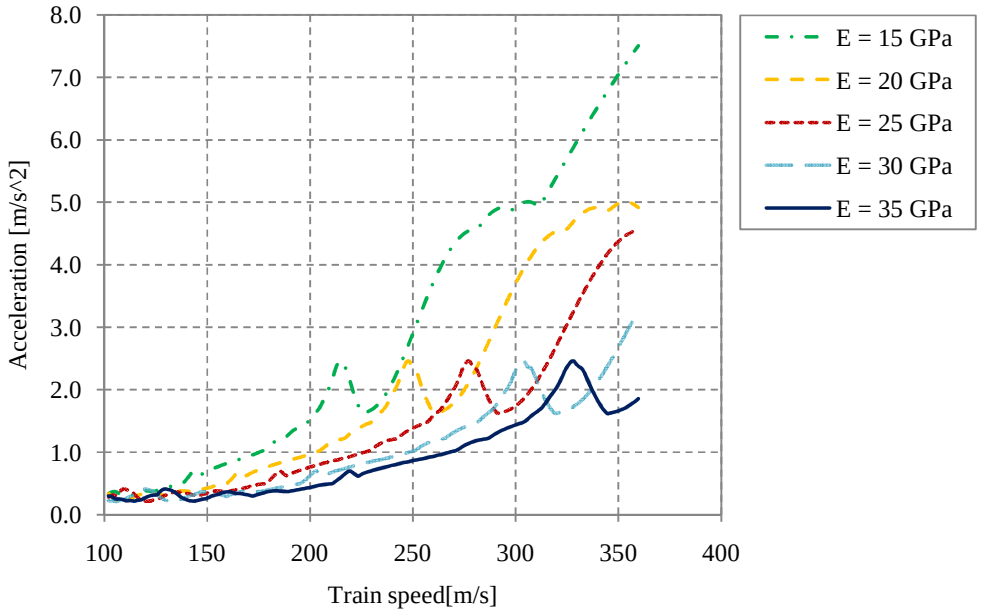

Figure 4.32 *Acceleration response for a three-span bridge subjected to HSLM-A1 using ρ = 3000 kg/m^3, η = 1, Ltot = 25 m, , κ = 1 and ζ = 0.02.*

It can be seen in Figure 4.31 and Figure 4.32 that both the acceleration amplitude and shape are completely independent of the choice of module of elasticity and hence also independent of the bending stiffness. For the purpose of giving more credibility to this shown phenomenon and give further insight in the response for the reader that is not too acquainted with the fields of dynamics additional calculations have been made in ADINA, see Figure 4.33 and Figure 4.34.

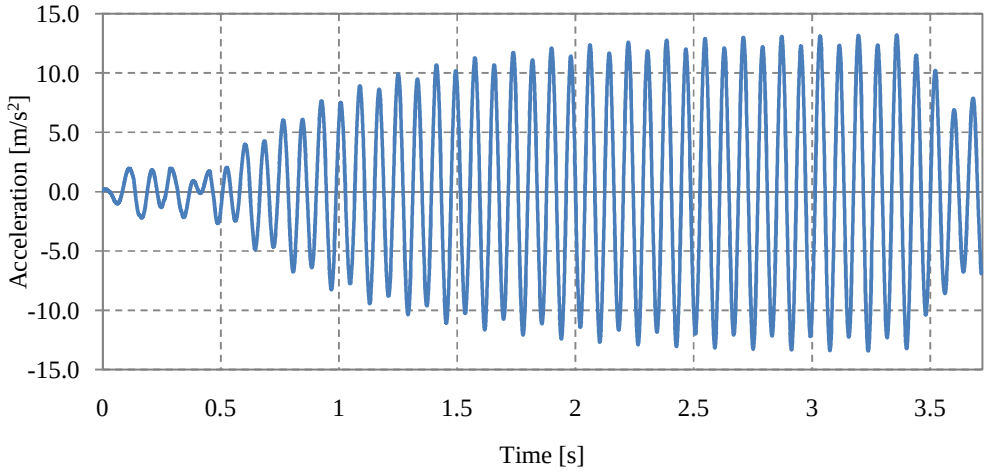

Figure 4.33 *Acceleration response in time using HSLM-A1 and E = 30 GPa, ρ = 2400 kg/m^3, Ltot = 15 m, μ = 2, ζ = 0.02 and v = 399 km/h. The response is calculated in ADINA.*

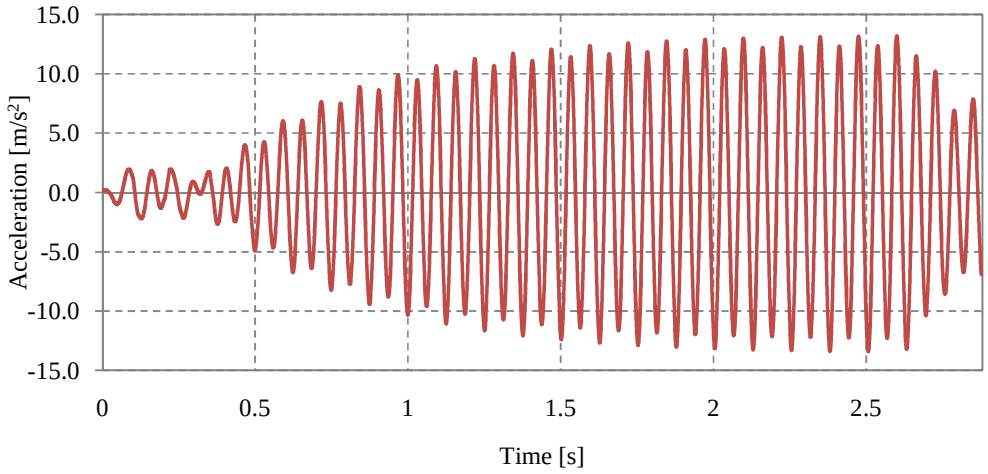

Figure 4.34 *Acceleration response in time using HSLM-A1 and E = 50 GPa, ρ = 2400 kg/m^3, Ltot = 15 m, μ = 2, ζ = 0.02 and v = 516 km/h. The response is calculated in ADINA.*

Figure 4.33 and Figure 4.34 shows the acceleration response in time using two different sets of module of elasticity and train velocity. The choice of parameter sets have been made to capture the response in time at $v_{cr}/2$ or $\beta = 0.5$. The figures show identical response curves but with different time axis implying that the maximum acceleration response are the same using the two different parameter sets. To show why the response in time becomes identical the analytical solution for a SDOF model has been examined, see Appendix E.

4.5.3.3 Variations of geometric parameters

The determination of dynamic acceleration response in railway bridges is a complex problem. The examinations of material parameters in Sections 4.5.3.1 and 4.5.3.2, though showed that the dynamic response has a simple relation to these parameters, which implies that the complexity solely lies in the variation of geometry.

How the acceleration response depends on geometric parameters cannot be expressed in separate expressions as for the material parameters. Instead they depend on each other. The geometric parameters for a bridge exist of the total bridge length and span relations. The reader should acknowledge however that the geometric parameters does not only include the total bridge length and span relation. There are also additional geometric parameters in the load in the form of bogie axle length and coach length. And it is a combination of these four geometric parameters together that affects the dynamic response.

With the goal of capturing the general variation trend of the acceleration response, examinations have still been performed on the geometric parameters. Variations in the load parameters have not been performed. Instead different HSLM-A loads have been used to examine the dynamic response during the variation of total bridge length and span relations independently.

4.5.3.4 Variation of total bridge length

The variation of total bridge length has been examined for two-span bridges only. The variation of total bridge length on two-span bridges will be shown to affect the dynamic response in such a complex way that no additional conclusions are presumed to be gained from analysis on three-span bridges. Figure 4.35 and Figure 4.36 shows examples of the acceleration response for a two-span bridge subjected to a HSLM-A load for different bridge lengths.

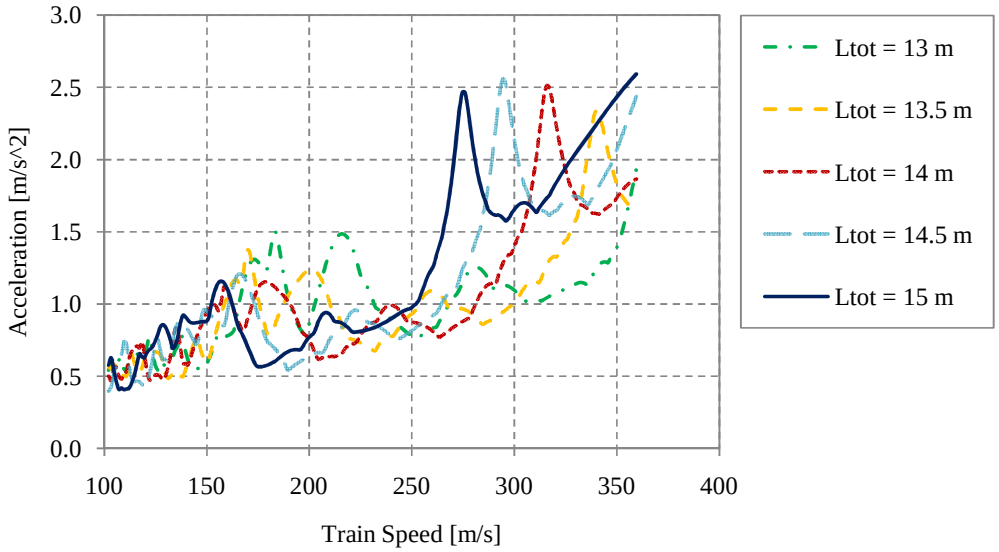

Figure 4.35 *Acceleration response for a two-span bridge subjected to HSLM-A1 using E = 40 GPa, μ = 2, ρ = 3000 kg/m^3 and ζ = 0.02.*

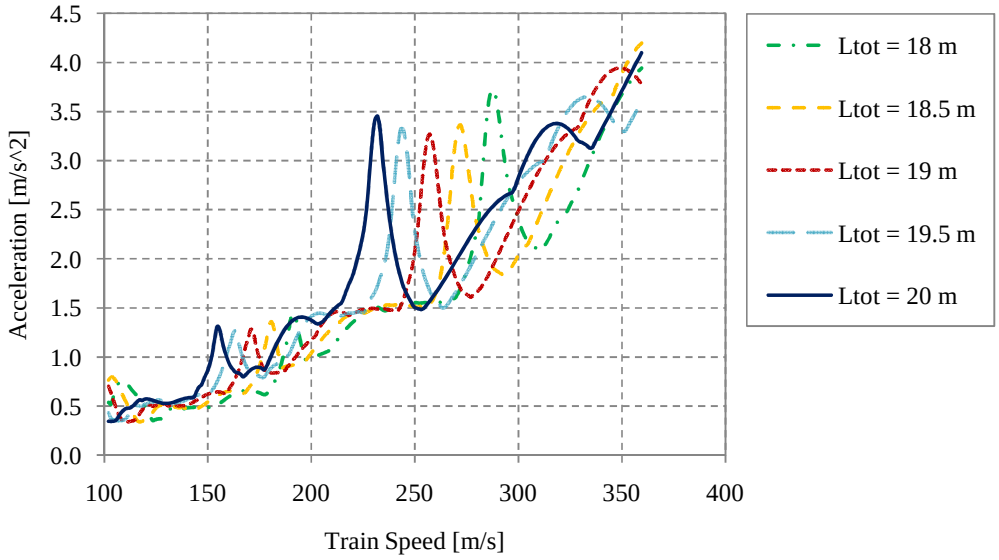

Figure 4.36 *Acceleration response for a two-span bridge subjected to HSLM-A1 using E = 40 GPa, μ = 2, ρ = 3000 kg/m^3 and ζ = 0.02.*

Just by examining Figure 4.35 and Figure 4.36 it can be seen that the acceleration response due to bridge length variation is not consistent. This means that the

acceleration has different dependencies on the bridge length for different values of β, i.e. the acceleration amplitude varies differently in different resonance peaks when the bridge length is changed, see Figure 4.35- Figure 4.38. More figures, similar to Figure 4.35- Figure 4.38 are presented in Appendix B.

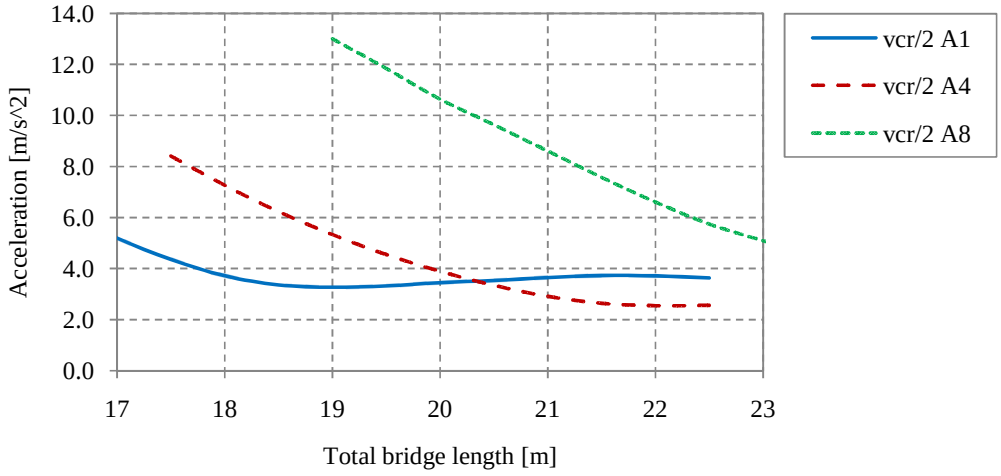

Figure 4.37 *Acceleration response in resonance peak at $v_{cr}/2$ for different train loads and a two-span bridge using E = 40 GPa, μ = 2, ρ = 3000 kg/m^3 and ζ = 0.02.*

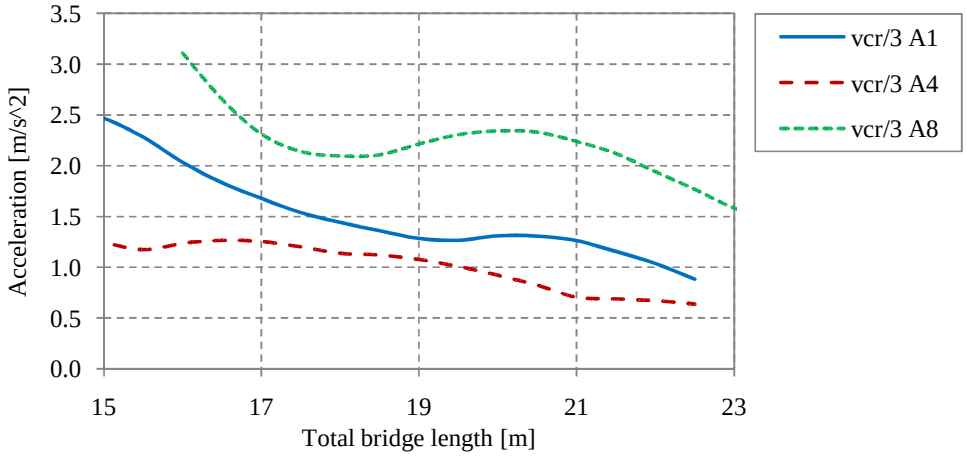

Figure 4.38 *Acceleration response in resonance peak at $v_{cr}/3$ for different train loads and a two-span bridge using E = 40 GPa, μ = 2, ρ = 3000 kg/m^3 and ζ = 0.02.*

The following conclusions can be made concerning the acceleration amplitudes dependence of the total bridge length:

- The dependence differs for different β values, meaning that the design velocity of the bridge considered will affect the dependence.

- The dependence will differ between eigenmodes for a constant train velocity since these correspond to different β values.

- The dependence will differ between HSLM-A train loads for a constant train velocity since these correspond to different β values.

These conclusions together make it difficult to derive an expression for how the acceleration amplitude will depend on the total bridge length, since the number of possible β values and eigenmodes for a continuous structure are both infinitely large.

The general trend from varying the total bridge length that was found during the parameter study was that the acceleration amplitude decrease when the total bridge length is increased. However if this decrease depends on the combination of geometric parameters is unclear since increasing the total bridge length also increases the total bridge mass.

4.5.3.5 Variation of span relation for a two-span bridge

The eigenfrequencies for a two-span bridge was shown in Section 4.2 to be affected differently by the variation of span relation μ depending on the examined eigenmode. This knowledge alone makes it impossible to derive an expression for the acceleration amplitudes dependence on μ. Each eigenfrequency will have a different dependence and the β value will hence be affected differently for each eigenmode. Therefore the eigenmodes individual response is super-positioned differently for different values of μ.

The variation of the span relation μ has still been examined with the purpose of capturing the general effect on the acceleration amplitude. Three different HSLM-A loads have been used in this examination, namely A1, A4 and A8. These three HSLM-A loads have been chosen as they differ in every load parameter that defines their appearance. Figure 4.39 and Figure 4.40 shows examples of the acceleration response for a two-span bridge for different values of the span relation using A1 and A8 respectively.

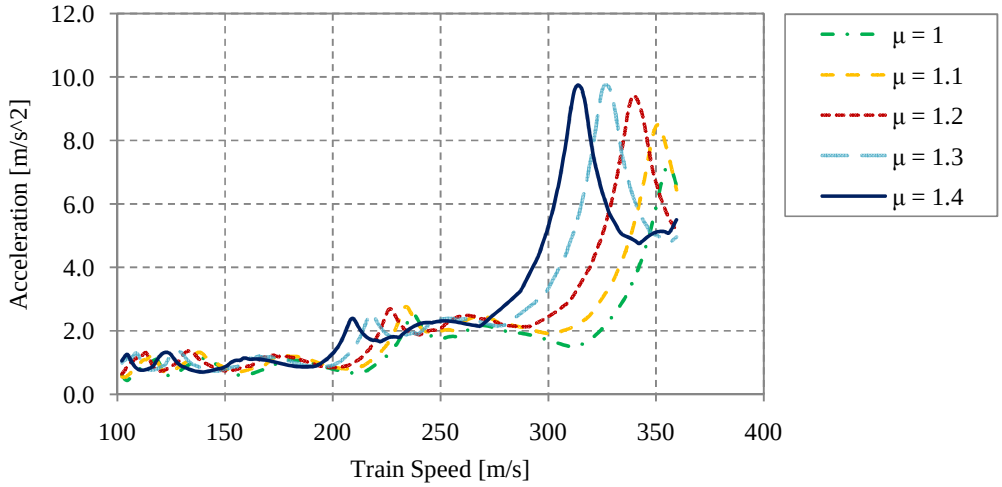

Figure 4.39 *Acceleration response for a two-span bridge subjected to HSLM-A1 using E = 20 GPa, L_{tot} = 16 m, ρ = 3000 kg/m^3 and ζ = 0.02.*

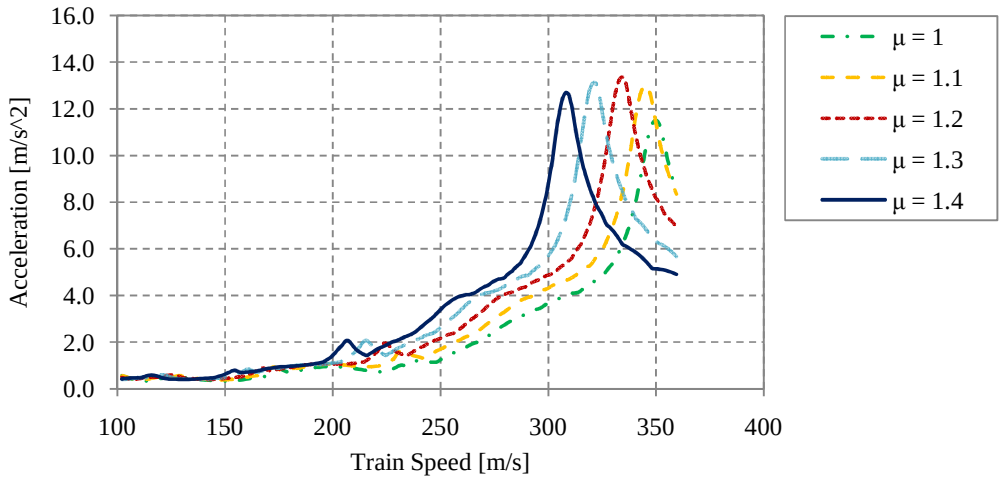

Figure 4.40 *Acceleration response for a two-span bridge subjected to HSLM-A8 using E = 20 GPa, L_{tot} = 16 m, ρ = 6000 kg/m^3 and ζ = 0.02.*

The acceleration amplitude has been gathered for constant β values corresponding to resonance speeds, namely 0.5, 0.33, 0.25 and 0.2. Figure 4.41 and Figure 4.42 shows the variation of acceleration amplitude for β equal to 0.5 and 0.33. More detailed results are presented in Appendix B.

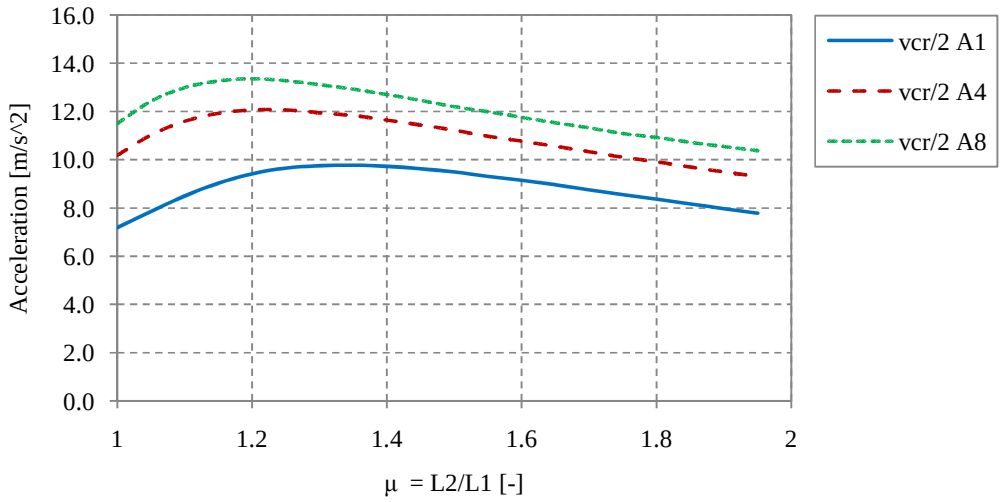

Figure 4.41 *Acceleration response in resonance peak at vcr/2 (β=0.5) for different train loads using E = 20 GPa, L_{tot} = 16 m, ζ = 0.02 and ρ = 3000,4000 and 6000 kg/m^3 for A1, A4 and A8 respectively.*

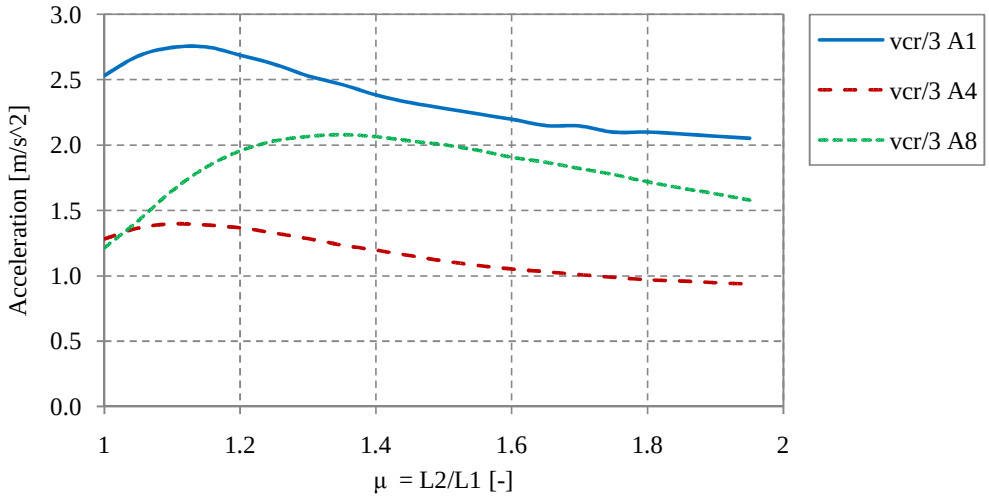

Figure 4.42 *Acceleration response in resonance peak at vcr/3 (β = 0.33) for different train loads using E = 20 GPa, L_{tot} = 16 m, ζ = 0.02 and ρ = 3000,4000 and 6000 kg/m^3 for A1, A4 and A8 respectively.*

The acceleration amplitude seems to have a similar dependence on the span relation μ for all examined values of β and all examined train loads. An interesting observation is that the acceleration amplitude increases when small the asymmetry is created in the bridge. For a two-span bridge it was shown in Section 4.2.1 that when asymmetry was increased the first eigenfrequency decreased while the second increased. The criterion set by the Swedish railway administration stating that only eigenfrequencies up to 30 Hz need to be considered then raises an interesting discussion. Because of this criterion there is often only need for considering the first, or first and second eigenmode. If creating small asymmetry always leads to increased accelerations this means that an increase of μ that puts the second eigenfrequency above 30 Hz may lead to lower design acceleration while the true acceleration increase. There might not be any conclusions to make of this observation, except that the 30 Hz criterion set by the Swedish railway administration might be considered questionable.

4.5.3.6 Variation of span relation for a three-span bridge

For the same reason as for a two-span bridge it is not possible to derive an expression for the acceleration amplitudes dependence on the span relation η for three-span bridges. Examinations have still been performed with the purpose of capturing the general dependence. Resulting figures from this examination can be found in Appendix B. Figure 4.43 and Figure 4.44 show the variation of acceleration amplitude at β=0.5 and β=0.33 from the examination.

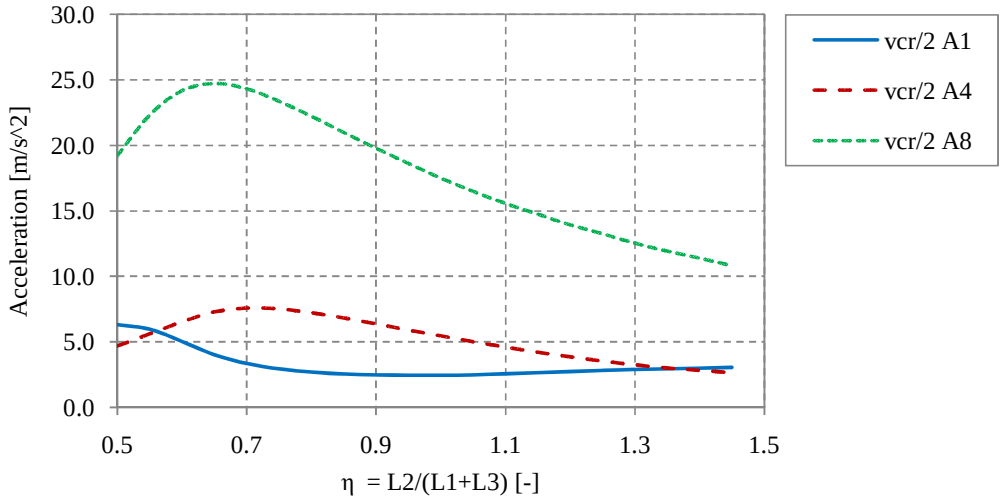

Figure 4.43 *Acceleration response in resonance peak at vcr/2 (β = 0.5) for different train loads using ρ = 2500 kg/m^3, L_{tot} = 20m, ζ = 0.02, κ = 1 and E = 20,14 and 10 GPa for A1, A4 and A8 respectively.*

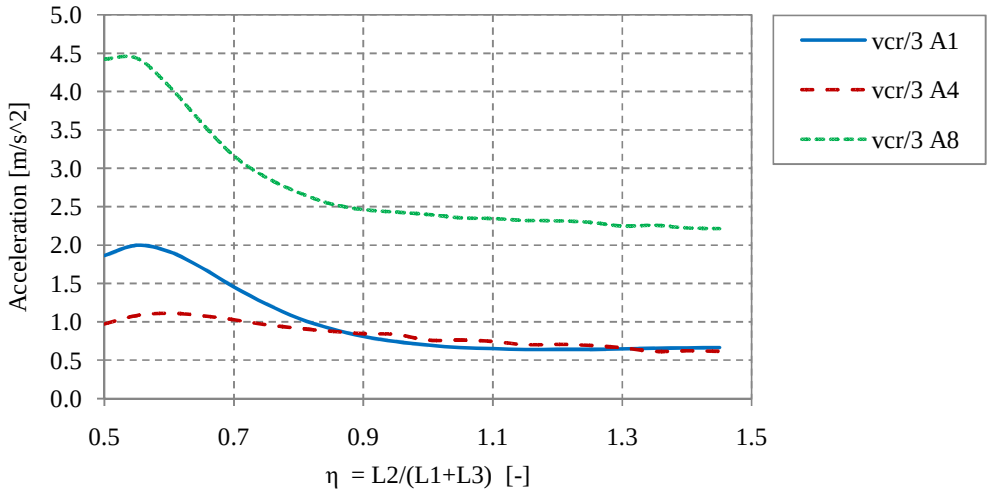

Figure 4.44 *Acceleration response in resonance peak at vcr/3 (β = 0.33) for different train loads using ρ = 2500 kg/m^3, L_{tot} = 20 m, ζ = 0.02, κ = 1 and E = 20,14 and 10 GPa for A1, A4 and A8 respectively.*

The same conclusion as for a two-span bridge can be made for three-span bridges concerning the span relation η. The acceleration amplitude seems to increase when small asymmetry is created. However one deviating result was obtained in the analysis which increases the uncertainties in this conclusion, see Figure 4.43.

4.5.3.7 Variations of damping

The damping is the only examined variable that does not affect the eigenfrequencies and hence the resonance speeds. It does however affect the acceleration amplitude. The damping effect is not consistent but instead varies for different values of β. The largest effect occurs for β values corresponding to resonance speeds while β values in between these values can be unaffected, see Figure 4.45. The damping always lowers the acceleration response.

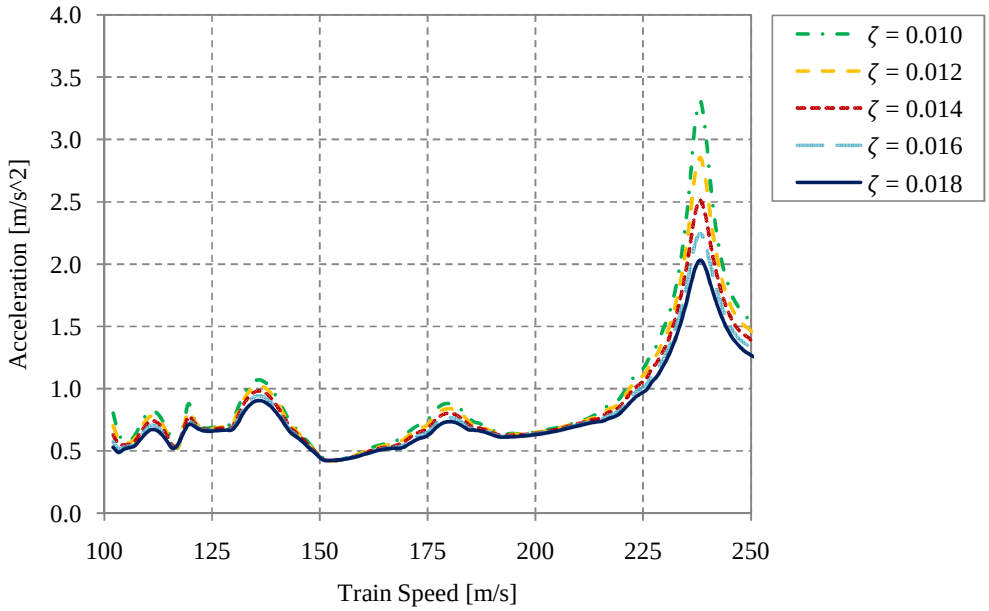

Figure 4.45 *Acceleration response for a two-span bridge subjected to HSLM-A1 using E = 40 GPa, μ = 2, ρ = 4000 kg/m^3 and L_{tot} = 15 m.*

4.5.4 Conclusions

In Section 4.5.3 the results from the individual examinations of material and geometric parameters where presented. Several conclusions where made already in this section but will be gathered here for a more comprehensible presentation. Also some complementary observations will be presented concerning the general dynamic response behavior in railway bridges.

The following observations were made during the parameter study:

- The acceleration amplitude is independent of the module of elasticity.
- The acceleration amplitude is proportional to the inverse of mass.
- The total bridge length's effect on the acceleration amplitude depends on the value of β. This makes it hard to find an expression for this dependence since different train loads and eigenmodes will have a different effect for one constant train velocity.
- When comparing the acceleration amplitude in the resonance peaks for v_{cr}/k, with k=2,3,4,5, the highest amplitude is not always ordered from lowest to highest resonance peak, i.e. the following expression

$$a\left(\frac{v_{cr}}{k_i}\right) > a\left(\frac{v_{cr}}{k_{i+1}}\right)$$

does not hold for all combinations of geometric parameters. This depends partly on the additional observation of cancellation effects that can completely remove one of the resonance peaks for some sets of geometric parameters.

- The highest acceleration amplitude does not necessarily occur in a resonance peak if a maximum limit for the examined train speed is set (This mostly occurred when cancellation effects removed the resonance peak at $v_{cr}/2$).

- The resonance effects does not always occur exactly at the critical speeds. This is especially true when cancellation effects occur but the phenomenon appears also for other speeds with small differences of around 5 km/h.

4.6 Case studies

The discussion presented in Section 4.5.4 can be seen as the result from the examination of acceleration amplitudes. In this section three special case studies will be presented where all accumulated knowledge from the observations made will be applied to create guidelines and simplifications for three common railway bridge types. Two multi-span bridges have been examined: a two-span bridge with equal span lengths and a three-span bridge with equal span. Also a single-span bridge has been examined since it is a good application for the developed calculation tools in this section and serves as a basis for the 2D/3D comparison later in Chapter 5.

The results presented in this section are in the form of diagrams, and referred to as design curves throughout this thesis. The name comes from the main concept of plotting the train velocities against the design acceleration that this velocity corresponds to instead of the actual acceleration. It is shown that the design curves can be used to decide which train loads that dominate the response for each specific bridge type. It is also possible to easily calculate the exact design acceleration for a certain set of material parameters. And as a third sector of application the curves can be used as guidance to which combination of bridge parameters that is preferable in a dynamic aspect.

4.6.1 Development of the design curves

In Section 4.5.3 and 4.5.4 it was shown that the geometric parameters of a railway bridge have a complicated effect on the acceleration response. Developing guidelines that treats an arbitrary combination of bridge length and span relations was shown to be a difficult task as the acceleration has a different dependence upon these variables for different eigenmodes and HSLM-A train loads. If a simplified model treating any combination of geometric parameters would be developed it would have to express different dependencies for every geometric parameter combination that is of interest.

In Section 4.5.4 some conclusions about the general response behavior of the accelerations were made concerning railway bridges. It was shown during the parameter study performed in Section 4.4 that it is not possible to predict which train velocity that will produce the design acceleration. Even if higher resonance peaks tend to give a higher acceleration response it is not consistently so. Also if a higher limit for the considered train velocities is set (which it always is in real life projects) it is

not necessarily the resonance peaks that contribute with the highest acceleration response.

However a discovery that contributes to increased possibility in finding guidelines for the dynamic response of railway bridges was found. The material parameters of a railway bridge have simple effect on both eigenfrequencies and the resulting acceleration amplitude. This conclusion forms the basis of the development of the design curves as the response behavior of the acceleration is kept under the variation of material parameters. Let us consider the difference in acceleration response from varying the module of elasticity (or bending stiffness), see Figure 4.31. An increase in the module of elasticity leads to increased eigenfrequencies and hence increased critical speed of the train loads, but the amplitude of the acceleration is unaffected. In Figure 4.31 the HSLM-A1 train load is used. If the different curves in Figure 4.31 are plotted against their corresponding β value for the A1 load the curves will become identical.

The same approach can be used for the variation of density (or mass per meter of the bridge) with the difference that only the shape of the curves will be identical as the amplitude will vary. The difference in acceleration amplitude is however consistent for the variation of train velocity. For this reason the parameter τ is defined as

$$\tau = m \cdot a \tag{4.19}$$

where

m = *The mass per meter length of the bridge*

a = *The acceleration response*

Figure 4.46 is an illustration of the transformations from a *v*-*a* plot to a β-τ plot.

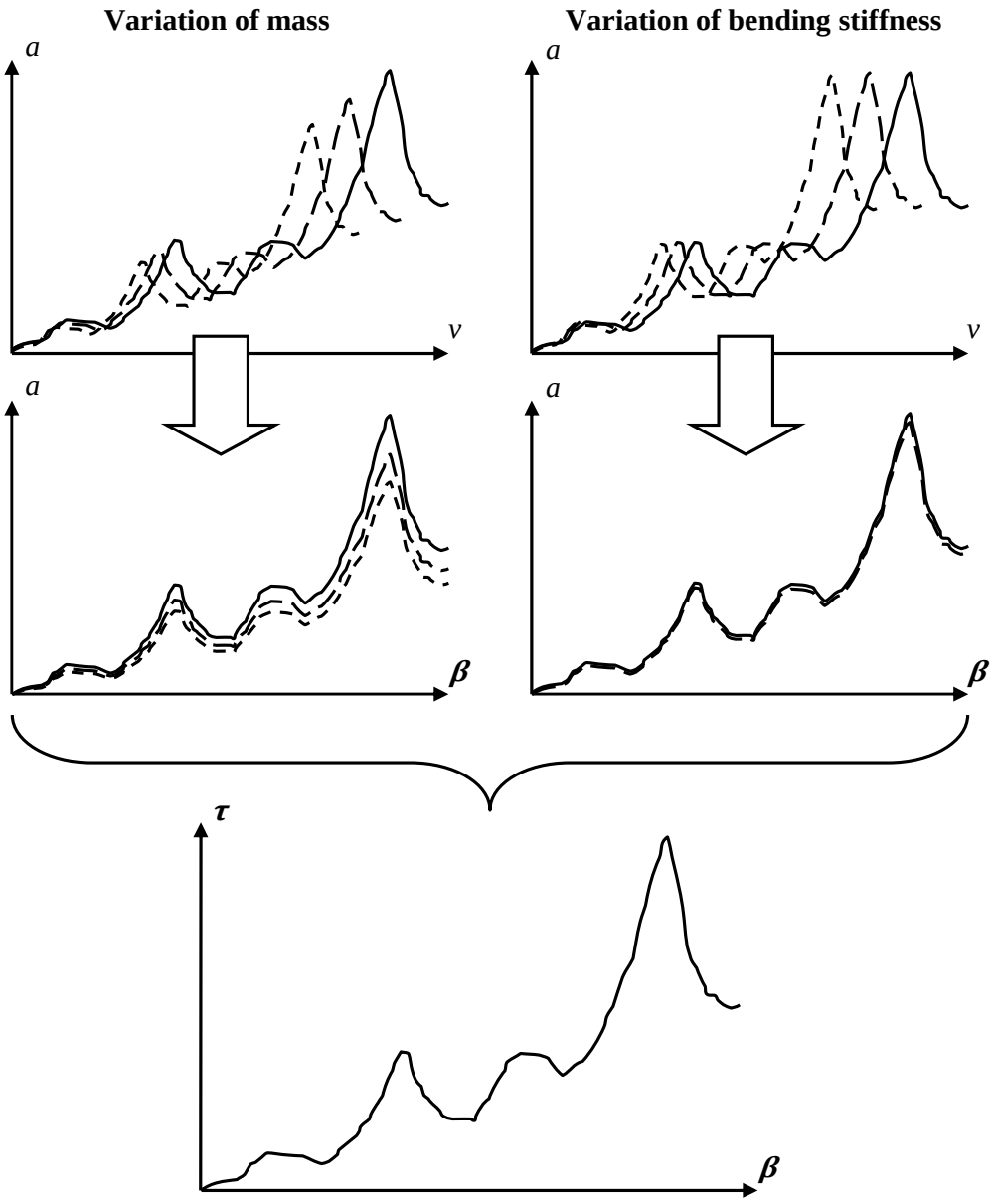

Figure 4.46 *Illustration of how different acceleration responses under the variation of material parameters can be expressed by one identical curve.*

As mentioned above it is not possible to decide which train velocity (or β value) will contribute to the highest acceleration response. Therefore it is here examined graphically. Since the material parameters' effect on the acceleration response, as shown in Figure 4.36, can be expressed by one single curve it is possible to develop one curve for each specific set of geometric parameters, from which it is possible to extract the exact acceleration response.

In the design of railway bridges the only acceleration response of interest is the highest one, the design acceleration. Therefore it is here suggested that a curve showing the corresponding design acceleration for different values of β is developed.

This type of curve will be referred to as a design curve throughout this thesis. Figure 4.47 shows the continued transformation of the illustrative curve in Figure 4.46 into a design curve.

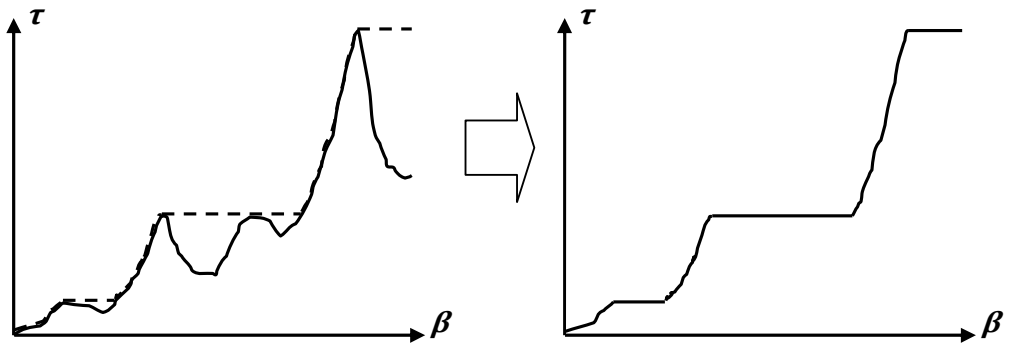

Figure 4.47 Transformation of a regular response curve into a design curve.

In Section 4.5.3 it was shown that the acceleration response has a complicated dependence on geometric parameters. The main conclusion stated was that the different dependencies for different geometric parameter sets have to be modeled separately. This is however not a possibility when the variation of several geometric parameters is of interest, since the number of different dependencies (or figures) to be developed becomes too extensive. If, on the other hand, special case studies are chosen it is possible to eliminate some of the geometric parameters. In this thesis three such case studies is made, which will be discussed later. What they all have in common is that fixed span relations have been chosen leaving only one geometric parameter for variation, namely the total bridge length. One design curve has to be developed for each length of interest for the different case studies. But if the design curves for one specific case study are gathered in one figure it would then serve as a useful comprehensive graphical calculation tool for the dynamic response of this bridge configuration.

There is however two additional complications whose solutions need to be clarified. First off the damping needs to be considered. It was shown in Section 4.5.3.7 that the damping's effect on the acceleration response varies depending on the value of β. The damping showed large change in effect at the resonance speeds but none in between. However since it was decided to create different design curves for each bridge length this is not a problem in practice. The code specifies the damping to be used for each bridge length, see Chapter 3. The design curve will hence include the effect of the considered bridge length and its corresponding damping.

Finally there are for each bridge length ten different HSLM-A train loads to account for. In real life design the only train load of interest is the one contributing to the highest acceleration response. However, it is hard to estimate which of the ten loads that will contribute to the highest acceleration, often resulting in a time consuming process where the response from all ten loads are examined. By plotting the design curves for each HSLM-A train load for a specific bridge length in one figure it is possible to graphically produce a design curve that includes the effect of all ten train

loads. One problem is that each train load corresponds to different β-τ plots since they all have different definitions of the corresponding β value because of different coach lengths *D*. In this thesis this has been solved by simply plotting all the curves against the β value of the HSLM-A1 train load. Figure 4.48 shows the final transformation of the illustrative design curve in Figure 4.47 into a design curve that includes the effect of all HSLM-A train loads.

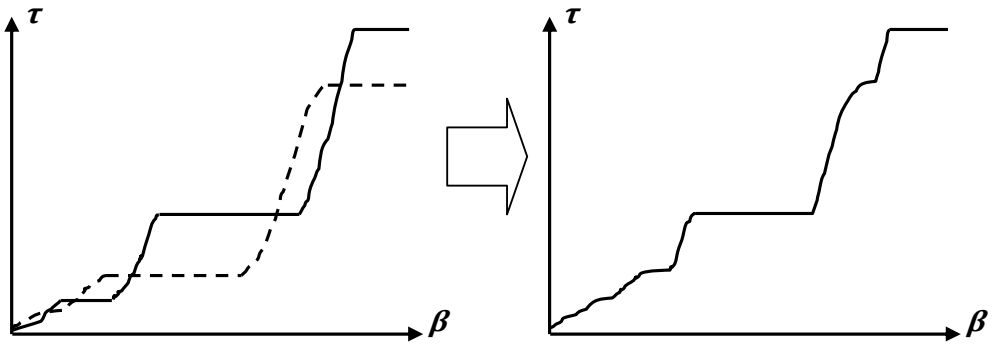

Figure 4.48 *Illustration of how the response from different HSLM-A train loads can be combined in a single design curve*

4.6.2 The design curves area of use

In real life design of railway bridges the dynamic aspect plays an important role in the design process. However, static analyses have been used in a larger extent in a historic perspective, since the requirement of dynamic analysis of railway bridges was introduced relatively recently in 2006. Static compared to dynamic analyses have in general simpler calculation procedures and engineers today possess larger experience with static aspects that govern railway bridge design. Therefore the early stage of the design process is today in a large extent still governed by calculations and guidelines based on experience from static analysis, even though the demands on dynamic criteria may prove to govern the final design. If a railway bridge is designed using guidelines based on static analysis and then shown to give unsatisfactory results in a dynamic aspect the design process becomes cumbersome and expensive.

Using the design curves it is possible to easily determine the design acceleration for a certain set of material parameters and total bridge length. It is important to note that the design acceleration determined from a design curve is not an approximation but in fact the exact design acceleration from a 2D analysis. So in the iterative process of statically designing the cross-section of a railway bridge the designer can easily check how the bridge performs in a dynamic aspect to avoid complications later in the project. The calculation is made in two steps. First the β value corresponding to the set of bridge parameters and design train velocity is calculated as

$$\beta = \frac{v}{D} \cdot \frac{L^2}{g_1} \cdot \sqrt{\frac{m}{EI}} \tag{4.20}$$

where

EI = *Bending stiffness of the bridge*

m = *Mass per meter length of the bridge*

L = *Total bridge length*

v = *Maximum allowed train velocity on the bridge*

D = *Coach length of the HSLM-A load chosen as reference for the β value.*

g_1 = *Value of the first eigenfrequency function for the given choice of span relations.*

The calculated value of β corresponds to a value of τ which is found by using the corresponding design curve. When the value of τ is known the design acceleration can be calculated using equation (4.19).

The design curves can also serve as guidance in the early design project life of a railway bridge since they basically give a complete overview of how the dynamic response change with modifications of the cross-section and changes in material parameters. Take the final design curve from the illustrative figures in the previous section as an example, see Figure 4.49.

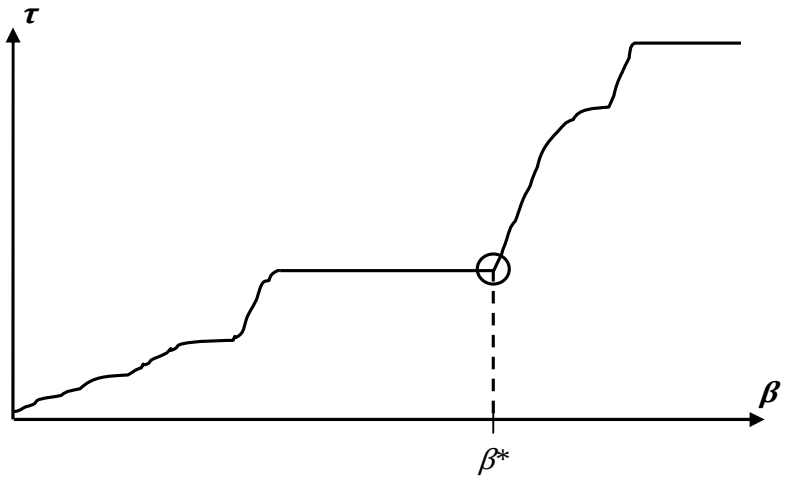

Figure 4.49 *Illustration of the value β^* which represents a value of β which is preferable to fall below in a dynamic aspect if relevant values of β are in the same range.*

It will be shown in the upcoming presentation of real developed design curves that there, in the intervals of relevant β values, often exist drastic changes in the design curves. Choosing the dimensions and materials of the cross-section with consideration to these changes greatly increases the possibility of satisfying the demands on maximum acceleration response. By combining equation (4.4), (4.8) and (4.10) an equation that gives guidance to the choice of cross-section and material parameters is obtained as

$$\frac{EI}{m} = \left(\frac{L^2 \cdot v}{D \cdot \beta^* \cdot g_1}\right)^2 \quad (4.21)$$

where

EI = *Bending stiffness of the bridge*

m = *Mass per meter length of the bridge*

L = *Total bridge length*

v = *Maximum allowed train velocity on the bridge*

D = *Coach length of the HSLM-A load chosen as reference for the β value.*

g_1 = *Value of the first eigenfrequency function for the given choice of span relations.*

β^* = *Appropriate maximum value of β according to Figure 4.49.*

As a third sector of application the design curves can be used to verify more complex FE models created in commercial software. If a 3D model has been created it can be verified by using mode superposition with just the initial eigenmodes that does not cause rotation. This is further dealt with in Chapter 5.

4.6.3 Limitations of the design curves

The damping specified in Eurocode differs between reinforced concrete bridges and pre-stressed bridges. This means that different design curves need to be developed depending on the type of bridge that is designed.

Eurocode specifies that it is not allowed to interpolate between responses using different bridge lengths. If an interpolation is made between two design curves this result can hence only be treated as a rough estimation of the true response.

The number of eigenmodes used will affect the appearance of the design curves and must hence be chosen before design curves can be developed. The chosen number of eigenmodes for the special case studies in this thesis has been estimated based on the previous examination of eigenfrequencies for multi-span bridges. These choices will be presented in the upcoming section.

The design curves developed in this Chapter are all based on 2D analysis. If a 3D geometry is considered additional accelerations can be expected, since it basically mean that more eigenmodes have to be included. More about this limitation will be presented in Chapter 5 where dynamic analysis on railway bridges in 3D are treated.

4.6.4 Design curves for the three case studies

Three different bridge configurations have been chosen for the development of real design curves. These bridge configurations are:

- Single-span bridge
- Two-span bridge with equal span lengths
- Three-span bridge with equal span lengths

As mentioned in Section 4.6.2 one design curve for each bridge length of interest has to be developed. Also the number of eigenmodes for the bridge configuration needs to be chosen. Table 4.9 shows the chosen bridge lengths taken in consideration and the choice of eigenmodes used in the calculations.

Table 4.9 Number of eigenmodes and considered bridge lengths for the four case studies

Bridge configuration	Considered lengths	Number of eigenmodes used
Single-span bridge	7-20 m	2
Two-span bridge	16-30 m	2
Three-span bridge with equal span length	30-43.5 m	5

The developed design curve are all for reinforced concrete. As mentioned pre-stress concrete corresponds to different damping according to BV Bro Banverket (2006) and their design curves must hence be developed separately.

The choices of lengths are meant to resemble common lengths for each respective bridge configuration. The creation of design curves has been limited to these length intervals since it is beyond the scope of this thesis to develop a complete calculation tool for the bridge configurations. The performed work has been restricted to the time limit of the thesis.

The chosen numbers of eigenmodes for each respective bridge configuration have been chosen based on the examination of eigenfrequencies in Section 4.2. For a single-span bridge it is known from experience at Reinertsen Sweden AB that a common value of the first eigenfrequency is above 8 Hz. In many design cases only the first eigenfrequency falls below 30 Hz since the second is four times larger, but it is not always so. For the purpose of getting design curves giving results on the safe side both the first and second eigenmode have been included in the development of design curves for single-span bridges. For the two- and three-span bridge all frequencies that fall below the 30 Hz criterion when the first frequency equals 8 Hz have been considered.

The calculation procedure presented in Section 4.5.1 has been performed for the four case studies. A comparison of design curves from each respective HSLM-A train load for each considered bridge length has been made. These design curves have then been gathered in the final design curve for each bridge length and finally the design curves for every length of each bridge configuration have been gathered in one figure, see Figure 4.50 to Figure 4.52. For the purpose of giving a comprehensive presentation of the developed design curves all figures cannot be presented in the report. The interested reader is however referred to Appendix C where an extensive presentation of all figures from the development is made.

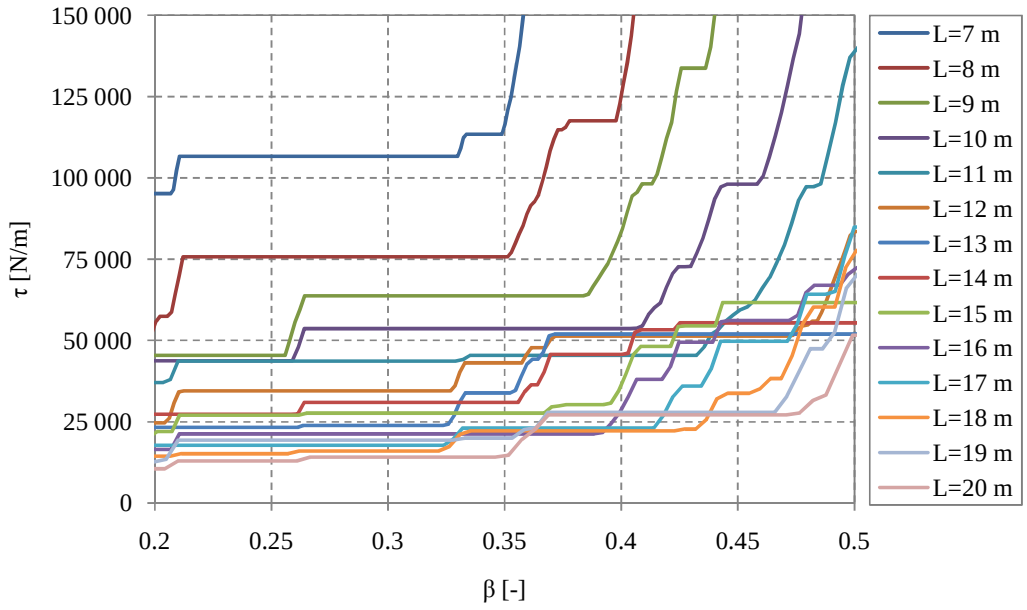

Figure 4.50 *Design curves for a single-span bridge in the bridge length range of 7-20 m*

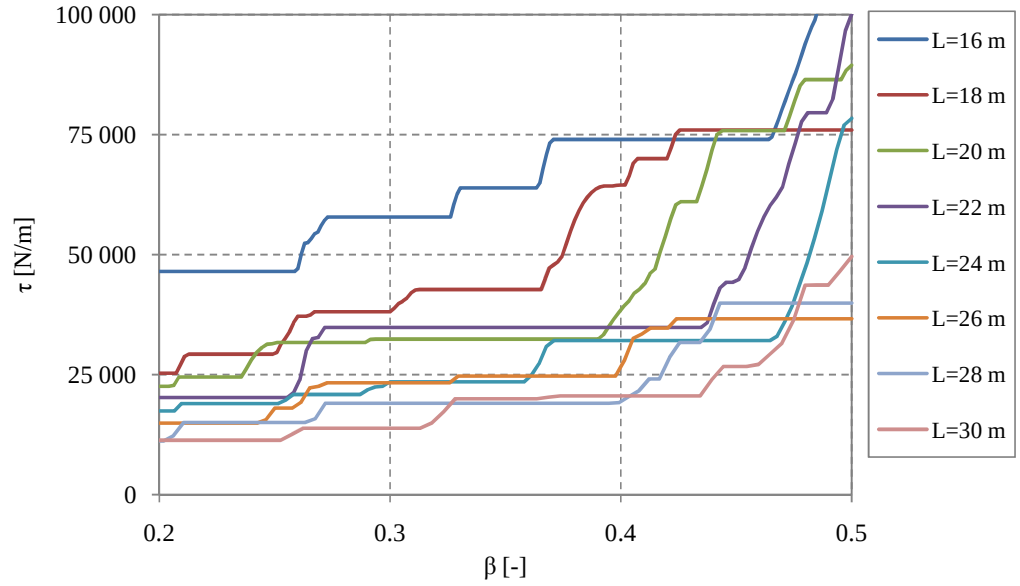

Figure 4.51 *Design curves for a two-span bridge with equal span lengths in the bridge length range of 16-30 m*

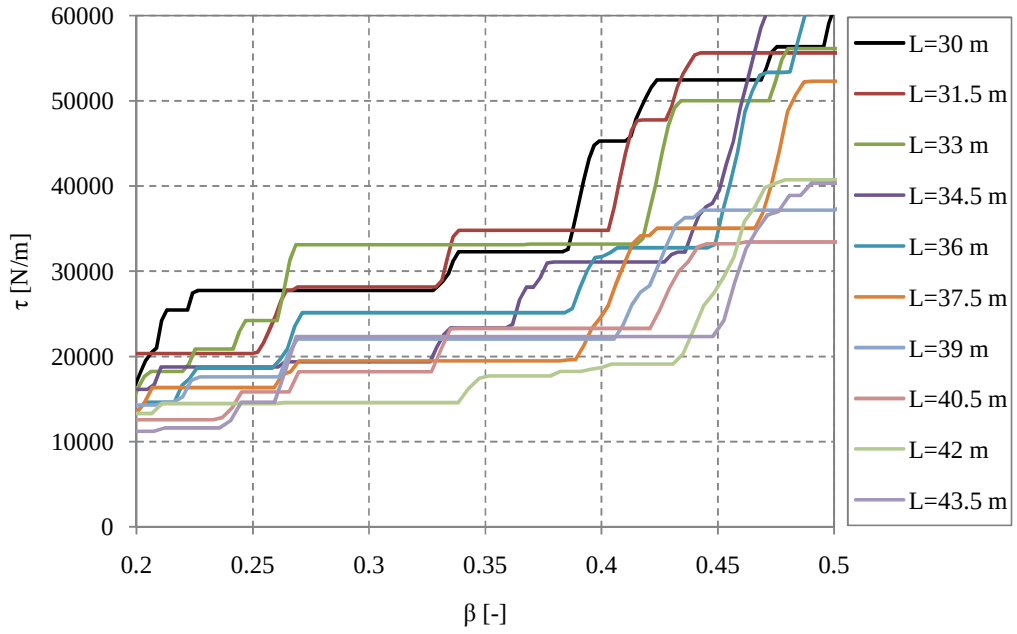

Figure 4.52 *Design curves for a three-span bridge with equal span lengths in the bridge length range of 30-43.5 m*

The developed design curves showed distinguished changes in the τ value for basically every bridge configuration and examined bridge length. This implies that there is great use in equation (4.21). This equation can be simplified for each examined bridge configuration for which the value of the eigenfrequency function is known. Also utilizing that the value of D in equation (4.21) equals 18 m since the HSLM-A1 train load have been used as reference for the β value in the design curves gives the following case specific expressions for each respective case study:

For a single-span bridge:

$$\frac{EI}{m} = \left(\frac{L^2 \cdot v}{9\pi \cdot \beta^*}\right)^2 \tag{4.22}$$

For a two-span bridge with equal span lengths:

$$\frac{EI}{m} = \left(\frac{L^2 \cdot v}{36\pi \cdot \beta^*}\right)^2 \tag{4.23}$$

For a three-span bridge with equal span lengths:

$$\frac{EI}{m} = \left(\frac{L^2 \cdot v}{81\pi \cdot \beta^*}\right)^2 \tag{4.24}$$

Every length specific design curve has been created as the maximum curve of all the corresponding load specific design curves. As mentioned above all the figures showing the load specific design curves cannot be included in the report, but as an example consider Figure 4.53.

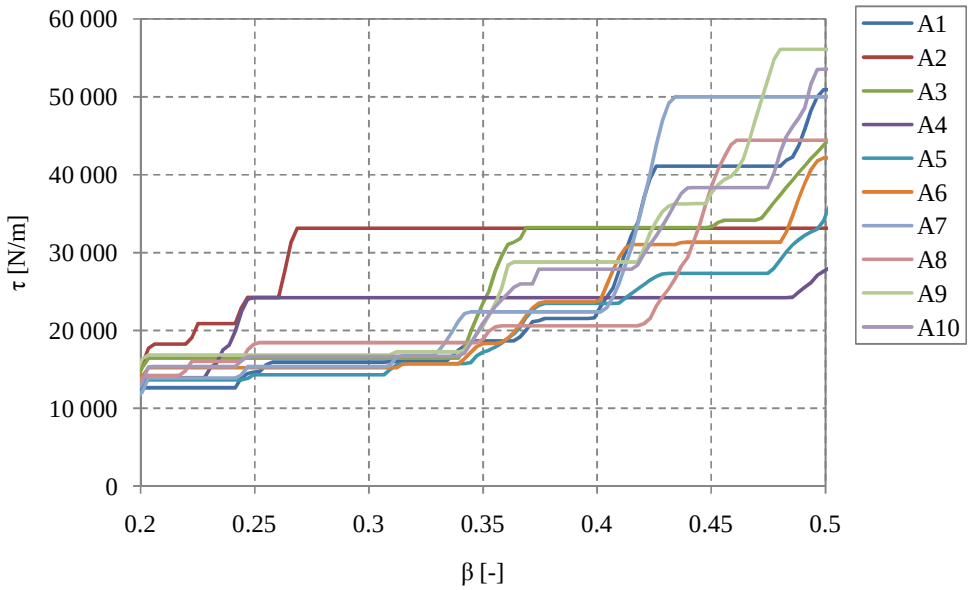

Figure 4.53 *Design curves for each HSLM-A load for a three-span bridge with equal span lengths and a total length of 33 m*

Similar curves as Figure 4.53 have been produced for every considered bridge length and bridge configuration. The curves show what HSLM-A load that governs the acceleration response. In Figure 4.53 it can be seen that A2, A7 and A9 governs the response for a three-span bridge with equal span lengths and a total length of 33 m.

It was found during the development of the design curves that there is a large variation in what HSLM-A load that governs the acceleration response. There was however one train load, namely HSLM-A8 that practically never governed the acceleration response for any length or bridge configuration. For the rare occasions when it did govern the response it was for high and short intervals of β. Another load that did not govern the response often was the A4, even if it did have influence for shorter lengths of the two-span bridge.

The HSLM-A loads that govern the acceleration response most frequently where A2 and A9. Both these loads have distinguishing load parameters compared to the other load combinations. A9 have together with A10 the largest value of the load P, namely 210 kN. A9 have however the smallest coach length of the two making resonance occur earlier. A2 has the largest bogie axle length at 3.5 m compared to the most common length of 2 m. It is interesting to note that only three HSLM-A loads have a bogie axle length larger than 2 m, and these are A2, A4 and A8. As mentioned A4 and A8 are the two HSLM-A loads that governed the acceleration response the least.

It was found that A2 governs the response for a lower interval of β for every considered length and bridge configuration, with one single exception for a single-span bridge of 17 m length.

4.6.5 Two calculation examples

In this section two examples of how to use the developed design curves is presented. The first example treats how the exact design acceleration can be calculated when all geometric and material parameters are known. The second example treats the use of a design curve as guideline in an early design stage when the cross-section is yet to be defined.

Consider first the calculation of design acceleration when all material and geometric parameters are known. Say we have a single-span bridge that is 10 m long with a rectangular cross-section that is 10 m wide and 0.6 m high. The material parameters are E=40 GPa and ρ=2400 kg/m^3. The bridge should withstand train velocities of 250 km/h. According to BV Bro Banverket (2006) the bridge should then be designed for the train velocity 1.2·250=300 km/h or 83.33 m/s, see Chapter 3. Using equation (4.20) we get that

$$\beta = \frac{v}{D} \cdot \frac{L^2}{g_1(\mu)} \cdot \sqrt{\frac{M}{EI}} = \frac{83.33}{18} \cdot \frac{10^2}{\pi/2} \cdot \sqrt{\frac{A \cdot 2400}{I \cdot 40 \cdot 10^9}} \approx 0.417$$

From Figure 4.54 we get the corresponding design curve for the studied bridge configuration.

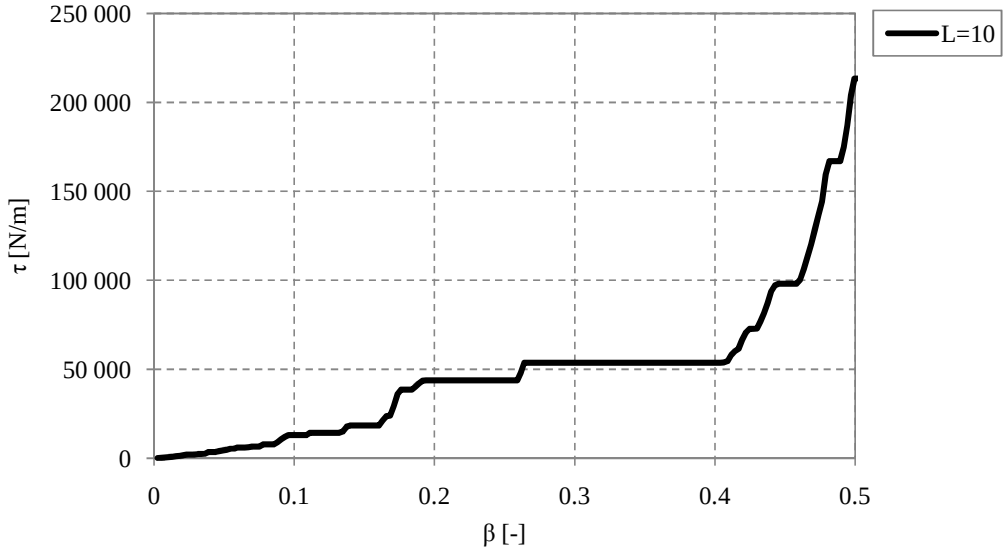

Figure 4.54 Design curve for a single-span bridge with a total length of 10 m.

The corresponding τ value for our bridge configuration and β=0.417 is approximate τ = 70000 N/m. Using equation (4.19) we can calculate the design acceleration to be

$$a = \frac{\tau}{m} = \frac{70000}{A \cdot 2400} \approx 4.34 \text{ m/s}^2$$

Consider now the following example. Say we are designing a two-span railway bridge with equal span-lengths which is supposed to be 20 m in total bridge length and have a width of 10 m. Again the bridge is designed for the train velocity 300 km/h. From Figure 4.51 we get the design curve corresponding to the bridge configuration, see Figure 4.55.

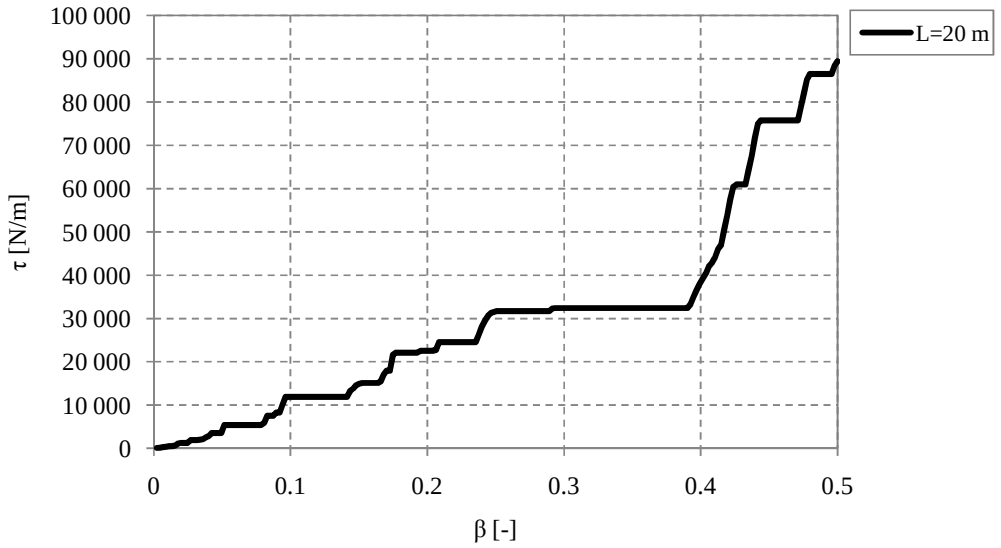

Figure 4.55 *Design curve for a two-span bridge with equal span lengths and a total length of 20 m.*

From Figure 4.55 it is seen that a drastic change in the acceleration occurs at β values higher than 0.38. Let us call this appropriate choice of β for β*. Falling below β* should be beneficial in a dynamic aspect with consideration to the demands on vertical acceleration. Using equation (4.23) we can calculate that

$$\frac{EI}{m} = \left(\frac{L^2 \cdot v}{36\pi \cdot \beta^*}\right)^2 = \left(\frac{20^2 \cdot 83.33}{36\pi \cdot 0.38}\right)^2 \approx 6 \cdot 10^5$$

correspond to an appropriate ratio between the bending stiffness and the mass per meter of the bridge to achieve this. This limit for the ratio between bending stiffness and mass per meter length is a lower limit. Increasing the ratio leads to an increased first eigenfrequency and a lower β value. Say we are interested in a rectangular cross-section. The expression can then be simplified even further since

$$\frac{EI}{m} = \frac{E\frac{bh^3}{12}}{bh\rho} = \frac{E}{\rho} \cdot \frac{h^2}{12}$$

The expression becomes independent of the width and a lower limit for allowed height is received. If we use a density of 2400 kg/m^3 and module of elasticity of 40 GPa and assume that there is no ballast we get that

$$h \approx \sqrt{6 \cdot 10^5 \cdot 12 \frac{\rho}{E}} = 0.657\, m$$

Basically we have now calculated that if we use a rectangular cross-section and a height above 0.66 m we will avoid the drastic peak in the acceleration design curve. To be sure this corresponds to the acceleration demand set by BV Bro Banverket (2006) we can calculate an upper limit for τ using equation (4.19). Say the limit for maximum allowed vertical acceleration is 5 m/s^2, which corresponds to a bridge without ballast. Then we get that

$$\tau = b \cdot h \cdot \rho \cdot a_d = 10 \cdot 0.657 \cdot 2400 \cdot 5 = 78840$$

The calculated higher limit for τ is higher than the τ value corresponding to the chosen β^* value of 0.38. It can thus be concluded that a rectangular cross-section with a height larger than 0.66 m would be satisfactory in a dynamic aspect for the considered bridge.

5 Analysis in 3D

In Chapter 4 it was shown that the design acceleration for one specific set of geometric parameters can be presented by one single curve, independent of the choice of material parameters and designing train velocity. This curve is throughout this thesis called a design curve. The design curves were shown to give great support in the design process of railway bridges with regard to the demands on vertical acceleration. There were, however, some limitations for the use of the curves. This Chapter treats the main limitation, namely that the design curves were developed through 2D analysis.

All real life structures are three-dimensional. However the designs of many structures and details are made in 2D since these analyses in many cases can be made to resemble the real behavior. 3D analyses are significantly more complicated and time consuming than 2D analyses and hence it is preferable to use a 2D analysis if possible.

This chapter treats the difference between the acceleration response in 2D and in 3D for railway bridges. The major difference comes from the fact that a 3D analysis model has eigenmodes that twist around the bridge length axis. This means that the response is be governed by eigenmodes that are affected differently by geometric changes and eccentricity of the load. The aim with the 2D/3D comparison is to get an understanding of complications that arise when three-dimensional geometry is considered. Also it is of interest to see how large difference in acceleration response that may exist between a 2D and a 3D model.

Section 5.1 presents the calculations that have been made in 3D and the corresponding assumptions for these calculations. Because of the 30 Hz criterion set by the Swedish railway administration all performed calculations and comparisons are based on FE analysis utilizing mode-superposition.

The studies of the acceleration response in 3D can be divided in three main areas. Eigenmodes and eigenfrequencies, variation in bridge width, and variation in load eccentricity. Each area is treated separately in Section 5.2 to 5.4. The difference in design acceleration is made in Section 5.5 by comparing the design curves created in 3D and 2D. Finally a discussion about the accumulated results is presented in Section 5.6.

5.1 Performed calculations and limitations

In this section all performed calculations on three-dimensional bridges is presented. Due to limit in time of this thesis several limitations have been made and these are also presented.

5.1.1 Geometry

Two different length configurations for a single-span bridge have been examined in the 3D analyses. Single-span bridges have been chosen since its geometry is simpler than multi-span bridges. The geometry is preferred since it simplifies the examination

of the added complexity that three-dimensional geometry contributes with. Two different lengths were chosen to increase the range of the examinations.

There are a number of different cross-sections used for railway bridges today. The design curves developed from 2D analysis in Chapter 4 are applicable for any form of cross-section geometry since the curves solely depend on area and moment of inertia of the cross-section, which independently affect the mass per meter length and bending stiffness respectively. However in 3D analysis when rotation around the longitudinal axis is allowed there is also an influence from bending stiffness perpendicular to the longitudinal axis and the rotational stiffness to consider. Different shapes of cross-section geometry will therefore have different effect on the acceleration response behavior and amplitude. The 3D calculations performed in this thesis have been limited to a rectangular cross-section. Cross-sections whose appearances require additional geometric parameters than cross-section height and width are presumed to add complexity in the calculations and have hence been avoided.

5.1.2 Method

Calculations have been limited to single-span bridges for variations in bridge width and load eccentricity as mentioned above. Table 5.1 shows the considered bridge lengths, widths and eccentricities in the performed calculations.

Table 5.1 Considered bridge configurations for the calculations in 3D

	Bridge length [m]	Bridge width	Load eccentricity for width of 10 m
Single-span bridge	10	5m/1m/10m	-
Single-span bridge	15	7.5m/1.5m/15m	0m/0.5m/4.5m

Table 5.1 shows that 12 different geometric configurations have been used for the variation of bridge width. For each configuration the total acceleration response and each eigenmodes separate response has been calculated in the whole bridge and in two specific nodes as shown in Figure 5.1. The calculated acceleration responses include the total and individual effect of all HSLM-A train loads.

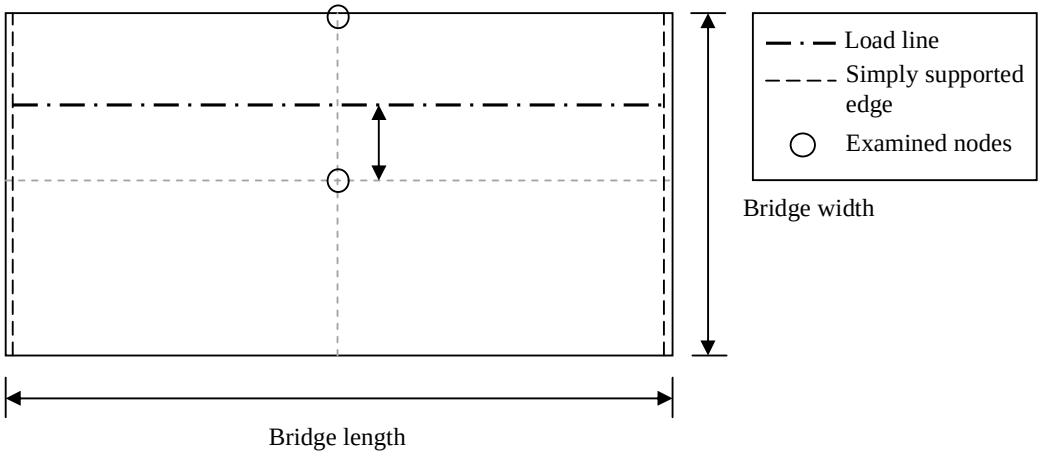

Figure 5.1 *Definition of bridge width, bridge length and load eccentricity for the calculations in 3D. Also the two nodes from where separate data has been extracted are shown.*

The effect on the acceleration response by varying the load eccentricity has been made on a single-span bridge with a length of 15 m and width of 10 m. The train load HSLM-A1 was used for the examinations on eccentricity variation.

All the 3D calculations have been made using Matlab programs created by the authors. The same main program as for the 2D analysis has been used with the difference that new function files treating the mesh and load creation have been used. All the programs used for the analysis can be found in Appendix D together with explanations of the program structures and verifications against ADINA. The reasons for using Matlab are the same as for the calculations in 2D, i.e. that the variation of geometric parameters and train velocity and the application of load are substantially easier to handle in Matlab compared to commercial FE software.

5.2 Eigenmodes and eigenfrequencies

The differences in eigenfrequencies and eigenmode shapes between 2D and 3D analyses are what make the dynamic responses differ. The change in frequencies will cause resonance to occur for different train speeds and rotation around the longitudinal axis will increase the influence of bridge width and load eccentricity.

Two different forms of eigenmodes can be distinguished in a 3D analysis, in this thesis they are referred to as bending modes and torsion modes. Bending modes are basically the eigenmodes from 2D analyses where bending in the longitudinal direction governs the eigenmode shape. Torsion modes are governed by torsion around the length coordination of the bridge and bending in the transverse direction. These eigenmodes cannot be described by 2D analyses. So basically bending and torsion modes represent eigenmodes from 2D and the additional modes in 3D respectively. It should be noted that the definitions of bending and torsion modes have been created by the authors, and are not generally accepted. The reason why they are used here is to easier explain the performed study, which is focused on differences between 2D and 3D analysis. Figure 5.2 shows the two bending and torsion modes with lowest eigenfrequency for a single-span bridge with a length of 15 m and a width of 10 m.

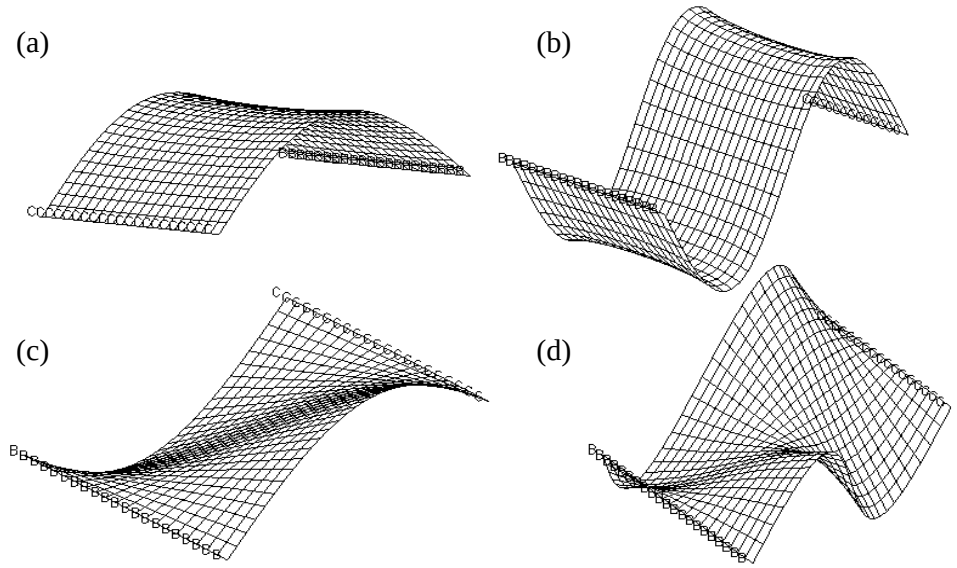

Figure 5.2 *The two bending modes (a and b) and torsion modes (c and d) with lowest corresponding eigenfrequency for a single-span bridge with a length of 15 m, width of 10 m and height of 0.6 m.*

As shown in Figure 5.2 there is small change in appearance in the bending modes compared to a 2D analysis where the section perpendicular to the length coordination remains straight. It will be shown that this bending in the cross-section plane will make the bending modes contribute to changes in acceleration with variations in bridge width and load eccentricity. The eigenfrequency is also affected but remain very close to that of a 2D analysis.

The torsion modes can have rather low eigenfrequencies and hence easily fall below the 30 Hz limit in BV Bro Banverket (2006). In most design cases the two eigenmodes with lowest corresponding eigenfrequencies are the first bending and torsion mode, respectively. If the 30 Hz criterion is considered this basically means that a larger number of eigenmodes need to be considered in a 3D analysis since the bending modes from 2D analysis in principal are kept while an addition of torsion modes is made. Consequently an increased acceleration response can be expected.

In 2D analyses an important feature of the eigenfrequencies was that the relation between eigenfrequencies of different degree was kept constant for any change in material parameters, section geometry or bridge length. A single-span bridge as an example has in a 2D analysis a second and third eigenfrequency that correspond to four and nine times the first eigenfrequency, respectively. This made the creation of design curves possible since the eigenmodes corresponding β values also had a constant relation to each other. Take Figure 4.33 and Figure 4.34 as an example. These figures show the response in time for the first eigenmode using different modules of elasticity with train velocities chosen to get β=0.5 in both cases. If similar curves for the second eigenmode where created they would both correspond to β=0.125 for the same bridge parameters, since the used eigenfrequency in the calculation of β would be four times larger in both cases. This means that the shape of the time response in the two figures would be identical also for the second eigenmode, and hence also for the total response considering both eigenmodes. If a parameter that

changes the relation between first and second eigenfrequency (the span relation μ in 2D analysis as an example) is altered instead, the nice feature of unaffected shape of the total response, considering both eigenmodes, would be lost. Choosing two train velocities that correspond to the same β value for the first eigenmode would then correspond to two different β values for the second eigenmode. Consequently it can be stated that a parameter that changes the relation between eigenfrequencies when altered affect the acceleration response in a complex way, and hence, its variation cannot be described by a design curve.

In a 2D analysis the cross-section geometry has no effect on the relation between eigenfrequencies since it only affects the moment of inertia and area of the bridge which has the same effect on all eigenfrequencies. In 3D analyses though the shape and size of the cross-section will affect the relation between eigenfrequencies. Figure ***5.3*** to Figure 5.5 shows the eigenfrequencies and the ratio between the eigenfrequencies for the eigenmodes shown in Figure 5.2 for three different length-width configurations and the variation of cross-section height. The frequencies have been calculated in ADINA.

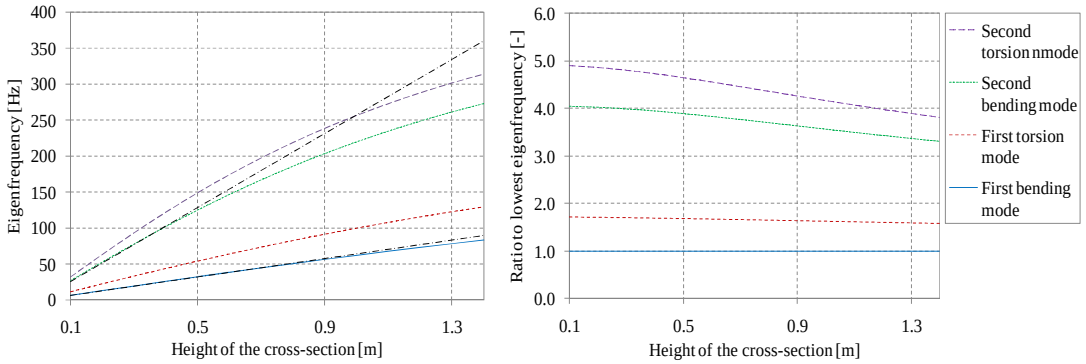

Figure 5.3 *Left: Eigenfrequencies for the eigenmodes in Figure 5.2 with L = 5m, b = 5m, E = 30 GPa, ν = 0.02, ρ = 2400 kg/m³. Straight lines correspond to the two lowest analytical calculated frequencies in 2D. Right: Corresponding rations of the frequencies to that of the first bending mode.*

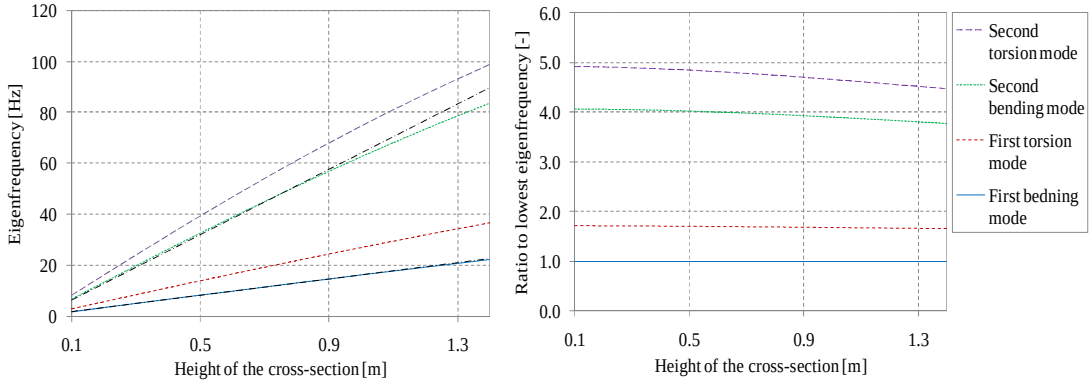

Figure 5.4 *Left: Eigenfrequencies for the eigenmodes in Figure 5.2 with L = 10 m, b = 10 m, E = 30 GPa, ν = 0.02, ρ = 2400kg/m³. Straight lines correspond to the two lowest analytical calculated frequencies in 2D. Right: Corresponding rations of the frequencies to that of the first bending mode.*

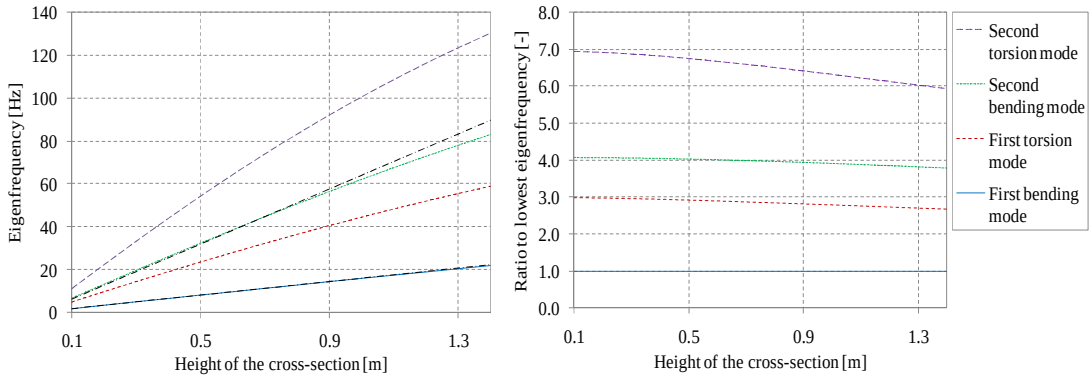

Figure 5.5 *Left: Eigenfrequencies for the eigenmodes in Figure 5.2 with L = 10 m, b = 5 m, E = 30 GPa, ν = 0.02, ρ = 2400 kg/m³. Straight lines correspond to the two lowest analytical calculated frequencies in 2D. Right: Corresponding rations of the frequencies to that of the first bending mode.*

Several observations can be made from Figure 5.3 to Figure 5.5.

- Variations in height affect the relation between eigenfrequencies and the dependence changes for different length-width configurations.
- Frequencies in 3D for bending modes deviate from the analytically calculated frequencies in 2D for larger heights.
- Increasing the width of the bridge has basically no effect on the bending modes.
- Increasing the width of the bridge decreases the frequency of the torsion modes.

For real life designs the height of rectangular cross-sections does not vary extensively but commonly lies in the range 0.5-0.8 m. Even though it is shown that the relations between eigenfrequencies are affected by changes in cross-section height they are small within the commonly used range. Therefore no further investigations on the variation of height have been made in this thesis. The height 0.6 m has been used for all remaining calculations concerning variation of bridge width and load eccentricity.

In 2D analysis the fact that all eigenmodes have the same relation to each other means that the different eigenmode shapes will be ordered in the same way for any choice of parameter set. For a single-span bridge the first eigenmode will approximately have the shape of a half sinus curve, the second a full sinus curve and so on. In 3D analysis the shape of the bending modes will come in the same order as in 2D analysis as they are very similar to these eigenmodes. The shape of the additional torsion modes may however change order. Consider Figure 5.2 where the two torsion modes with lowest corresponding eigenfrequency for a single-span bridge of 15 m length and 10 m width are shown. The first torsion mode will always be the one shown in Figure 5.2c for any choice of length-width ratio. The shape of the second eigenmode however depends on the length-width ratio of the bridge, where a smaller length-width ratio causes the appearance of the eigenmode to change. Figure 5.6 shows the second and third torsion mode of a single-span bridge with lower length-width ratio.

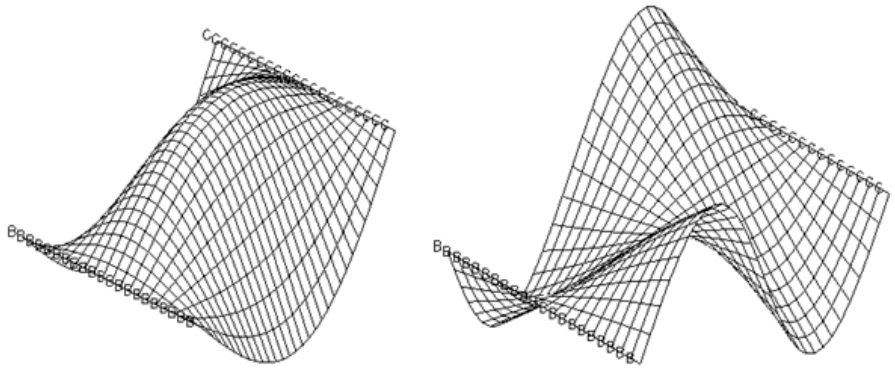

Figure 5.6 *The second and third torsion mode for a single-span bridge with a length and width of 10 m and height 0.6 m.*

As shown by Figure 5.2 and Figure 5.6 the second torsion mode becomes the third when the bridge length-width ratio is decreased. For the following examinations on bridge width and load eccentricity a choice of included eigenmodes must be made. Since the relation between torsion modes do not remain for the variation of cross-section geometry examination on width variation becomes more difficult when more torsion modes are included. Therefore a choice has been made to only include the first torsion mode in the upcoming calculations on bridge width and load eccentricity variations. However for the purpose of comparing the change in design curves in 2D and 3D for the two examined single-span bridges it is a requirement that two bending modes are used in order to be consequent with the design curves created in Chapter 4 for single-span bridges. This adds complications in the calculations since the second bending mode will change to higher eigenmode degree when width is increased because of lowered eigenfrequency of torsion modes. As a solution to this problem a Matlab program that can find the three specific eigenmodes of interest utilizing inverse iteration has been made by the authors. The Matlab program can be found in Appendix D.

5.3 Variation of width

It was mentioned in Section 5.2 that variation of cross-section geometry does not affect the relation between eigenfrequencies in 2D analysis and therefore it is possible to develop one single design curve for each length that corresponds to an arbitrary choice of cross-section. It was also shown that this is not possible for the variation of bridge width in a 3D analysis as the bridge width affect the bending and torsion modes in a more complex manner. This will be explained in more detail in this section and a graphical presentation of how the response differs for the variation of bridge width will be made.

In Section 5.1 it was shown that the calculations on bridge width variation in 3D have been made on two single-span bridges with the length of 10 and 15 m. Every figure presented in this section is a result from these calculations. As mentioned the calculations have included all the HSLM-A train loads and gathered the total acceleration response in different nodes and also the individual response of different

eigenmodes in these nodes. The results presented in this section are all for the HSLM-A1 train load and the node at the edge, in the middle of the bridge, see Figure 5.1.

5.3.1 Influence on bending modes

For a rectangular cross-section the increase of width does not affect the design curve from a 2D analysis. This is because the shape of the *v-a* plot is unaffected. Figure 5.7 shows a comparison of three *v-a* plots from 3D analysis where the only difference is the width of the cross-section.

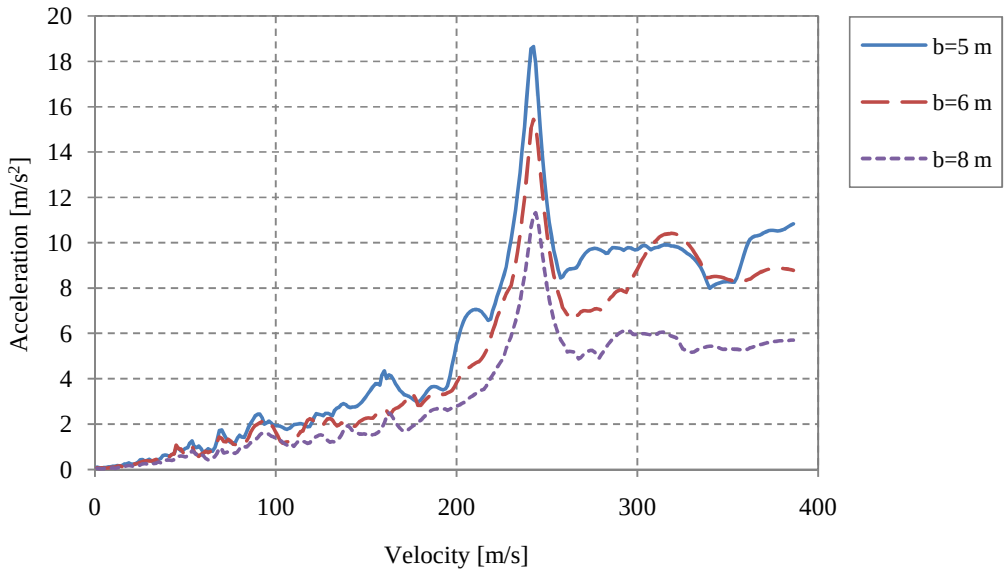

Figure 5.7 *Maximum acceleration in time for variation of train velocity for a single-span bridge with length of 10 m, height of 0.6 m and E = 30 GPa, ρ = 4000 kg/m^3, ν = 0.02 and ζ = 0.022*

As can be seen in Figure 5.7 the shape of the *v-a* plot changes with changed width, and hence also the corresponding design curve. The individual responses from the bending modes and the torsion mode have been studied for the purpose of explaining why and how the *v-a* curves change. Consider first the response from the bending modes. Figure 5.8 shows different *v-a* plots for the single-span bridge of 10 m length considering only the first bending mode.

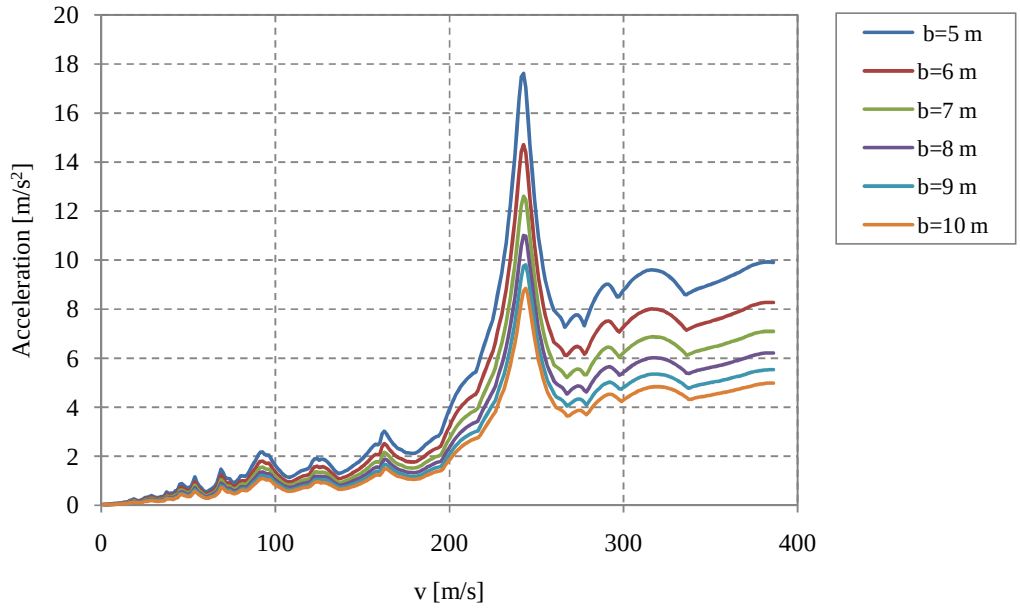

Figure 5.8 *Maximum acceleration in time for variation of train velocity considering the individual response of the first bending mode for a single-span bridge with length of 10 m, height of 0.6 m and E = 30 GPa, ρ = 4000 kg/m^3, ν = 0.02 and ζ = 0.022.*

As Figure 5.8 shows the shape of the *v-a* curve from the first bending mode remains as the width is varied. The change in amplitude can be explained by the change of bridge mass, where the amplitude was shown in Chapter 4 to have an inverse proportionality against the mass. Figure 5.9 and Figure 5.10 shows the *v-a* plots in Figure 5.8 transformed to β-τ plots.

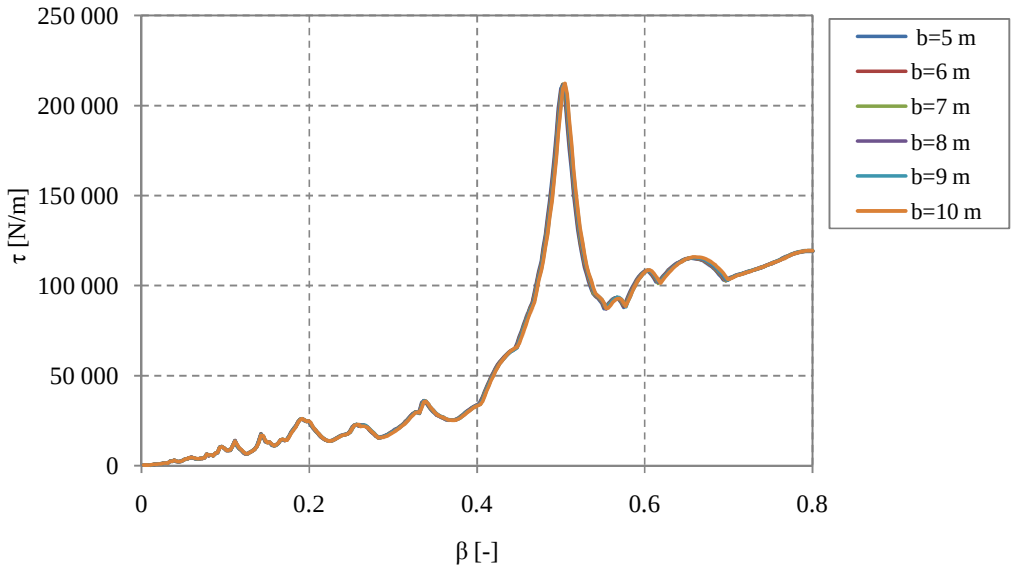

Figure 5.9 *Corresponding β-τ curves for the v-a curves in Figure 5.8.*

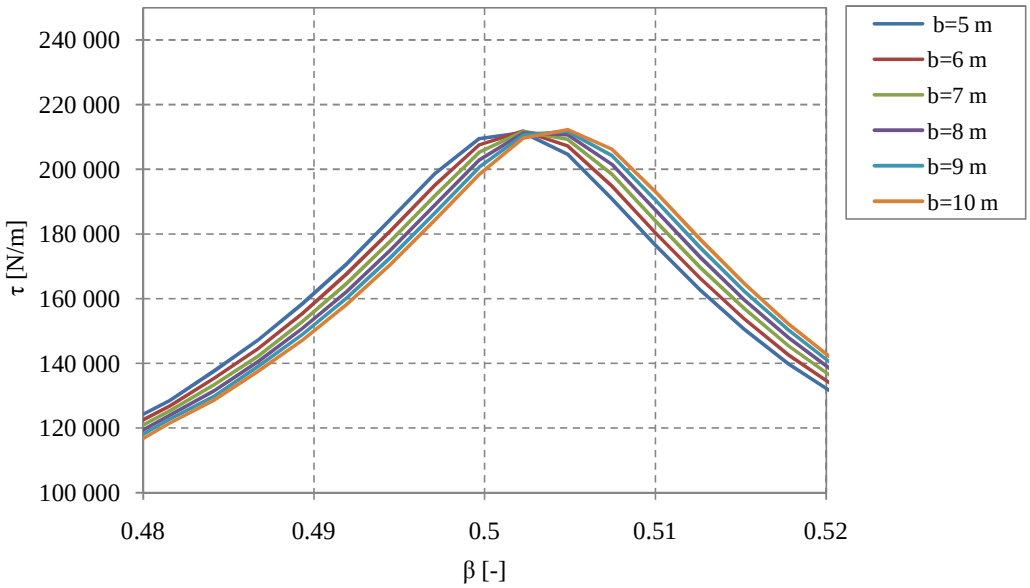

Figure 5.10 *Magnification of Figure 5.9 for the interval 0.48<β<0.52.*

It can be seen in Figure 5.10 that the β-τ curves for the bending mode do not have identical shapes for the variation of width as they would in a 2D analysis. The curves have small differences in position and amplitude. Both these observations are believed to be explained by small changes in eigenmode shape. As shown in Figure 5.2 the bending modes do include rotation around the bridge length axis, and this rotation causes the width to influence both eigenfrequency and acceleration amplitude. The widths effect on the acceleration behavior and amplitude are however small and it can be concluded that the major changes in acceleration response that were seen in Figure 5.7 are caused by the addition of a torsion mode.

5.3.2 Influence on torsion modes

Consider now the individual response of the first torsion mode. The maximum acceleration responses for different widths under the variation of train velocity are shown in Figure 5.11. A constant eccentricity of 2 m has been used in the calculations.

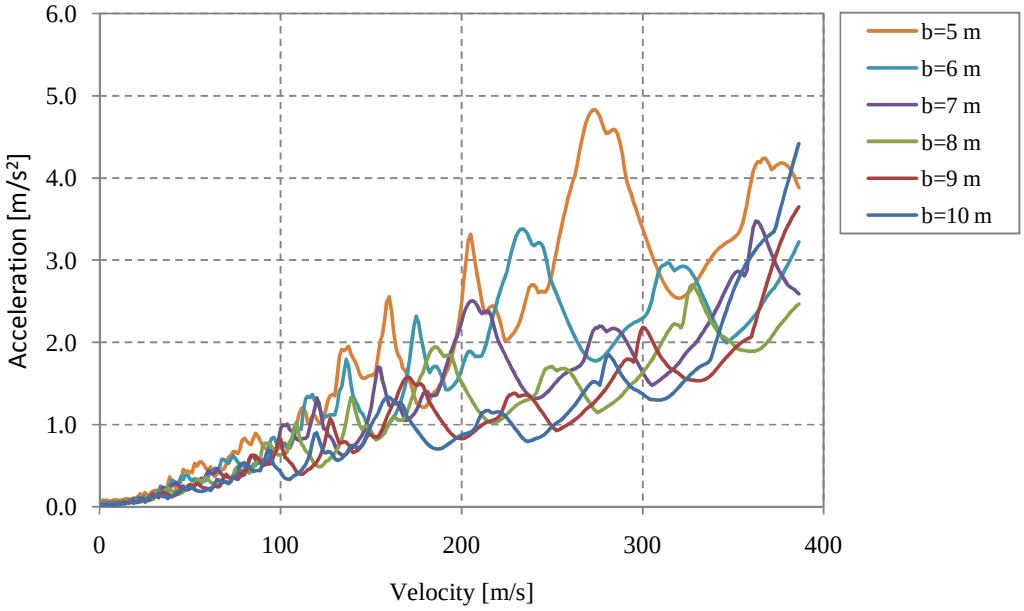

Figure 5.11 *Maximum acceleration in time for variation of train velocity considering the individual response of the first torsion mode for a single-span bridge with length of 10 m, height of 0.6 m and E = 30 GPa, ρ = 4000 kg/m^3, ν = 0.02, ζ = 0.022, e = 2 m.*

As mentioned in Section 5.2 the eigenfrequencies of the torsion modes are affected by the change in width of the cross-section. Figure 5.11 clearly shows how the placement of the response curve moves to the left because of the lowered eigenfrequency with increased width. The *v-a* curves in Figure 5.11 have been transformed to β-τ curves with the purpose of examining the acceleration response behavior for the torsion mode, see Figure 5.12.

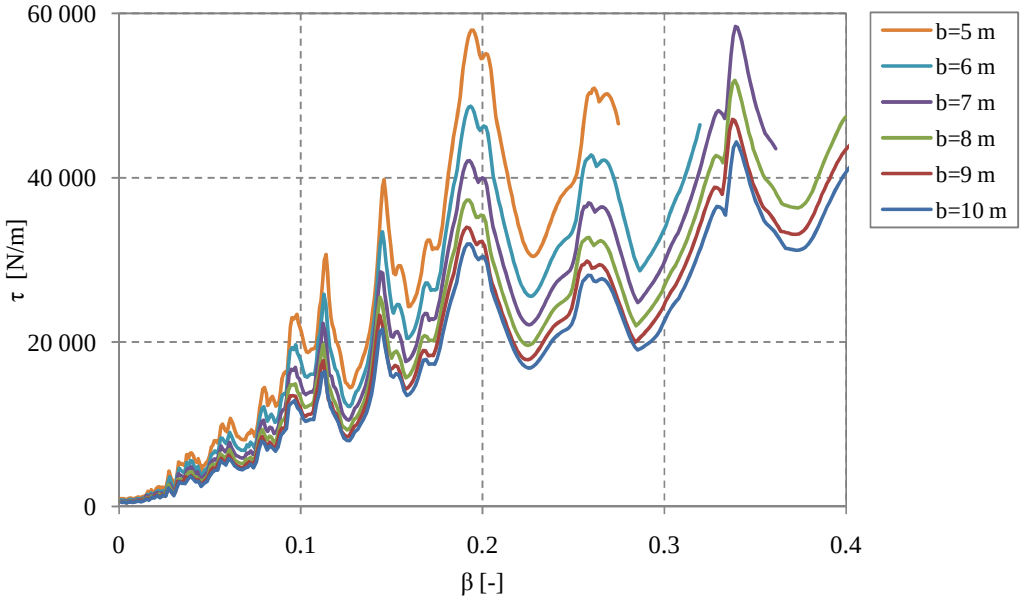

Figure 5.12 *Corresponding β-τ curves for the v-a curves in Figure 5.11.*

Figure 5.12 shows that the shape of the β-τ curve for the first torsion mode is kept as the width is increased. Also the amplitude of the acceleration is decreased with an increase in width. The change in amplitude of the accelerations seem however to have a different dependence on the increase of bridge width. The parameter τ can therefore not be used to create a curve that is independent of the bridge width as it can for bending modes. Figure 5.13 shows the acceleration for a fixed β value in Figure 5.12 plotted against the inverse of corresponding bridge width.

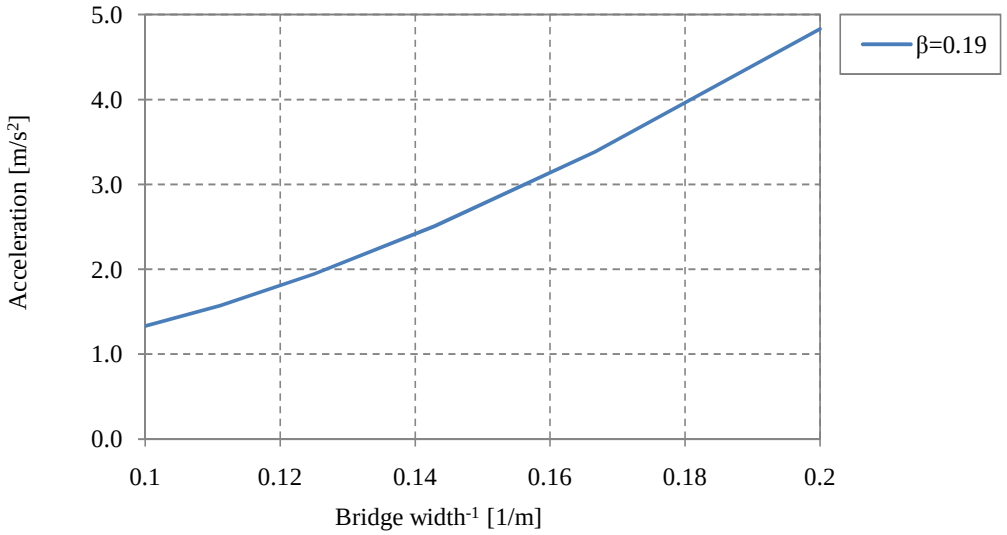

Figure 5.13 *The acceleration amplitudes relation to the inverse of the bridge width in Figure 5.12 for β=0.19.*

The curve in Figure 5.12 would have had a constant derivative of one if the torsion mode had the same dependence on the increase of bridge width as bending modes.

Basically Figure 5.12 shows that the response from the torsion mode has the same type of behavior as a bending eigenmode when plotted against its own corresponding β and an observation like resonance peaks at $\beta \approx 0.33$, 0.25 and 0.2 can be made. It would be possible to create a β curve with constant amplitude if a parameter (like τ for bending modes) were established that described the material and cross-section parameters effect on the acceleration amplitude. Additional calculations are however required to achieve this since the performed width variation affects bending stiffness, rotational stiffness and mass and hence does not give sufficient understanding of the problem.

5.3.3 Combined response

If the response from the bending modes and the torsion mode were considered separately two different design curves could be developed that gave a simple comprehensive view of the dynamic response, corresponding to an arbitrary choice of bridge width. Unfortunately the direct summation from the two curves would not correspond to the true response, considering both eigenmodes. The reason is that the two design curves would correspond to the maximum acceleration in time considering the individual response from the bending and torsion modes. Hence the *v*-*a* plots for the different eigenmodes cannot be superpositioned. In mode-superposition it is the

response in time from different eigenmodes that are superpositioned to get the total response in time. The maximum accelerations in time for different eigenmodes are likely to occur at different times. Figure 5.14 shows the superposition of the individual *v-a* plots for the different eigenmodes and the *v-a* plot considering both eigenmodes.

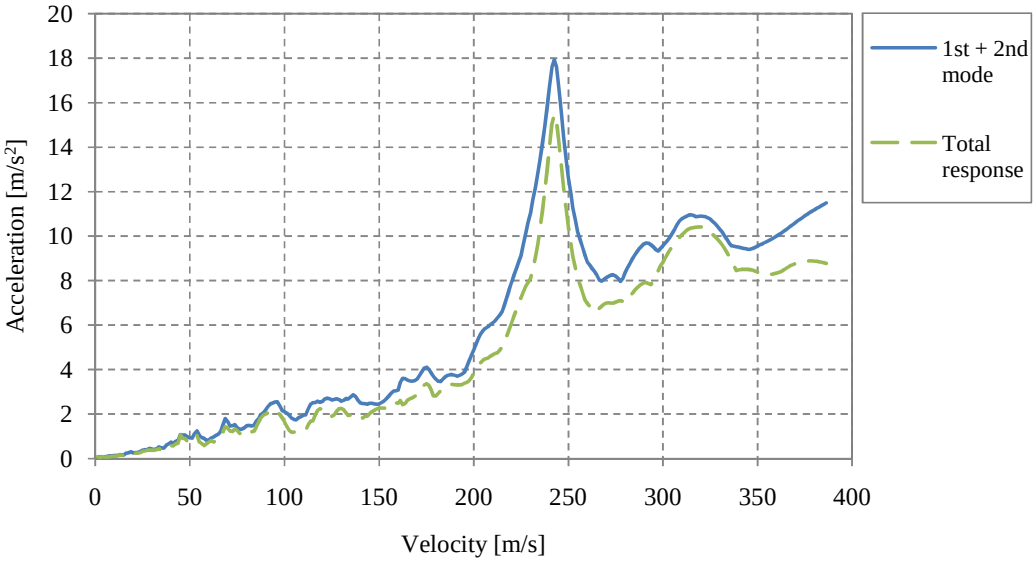

Figure 5.14 *Comparison of the total response considering both the first bending and torsion mode with the superposition of the individual response of the eigenmodes.*

The true contribution from the torsion mode is at all times equal to or smaller than the response received from superpositioning the *v-a* curves of the eigenmodes individual response. This contribution from the torsion mode is considerably more difficult to map compared to the maximum acceleration in time. The true contribution for a certain set of geometric, material and train parameters will be the contribution at the time that corresponds to the maximum acceleration for the combined response of eigenmodes. This time may occur when the torsion mode has its individual maximum but also for a time when the contribution is zero or even negative, causing a decrease of the maximum acceleration in time. Figure 5.15 shows an example of the true contribution from the torsion mode compared to the contribution if the eigenmodes individual *v-a* curve is added.

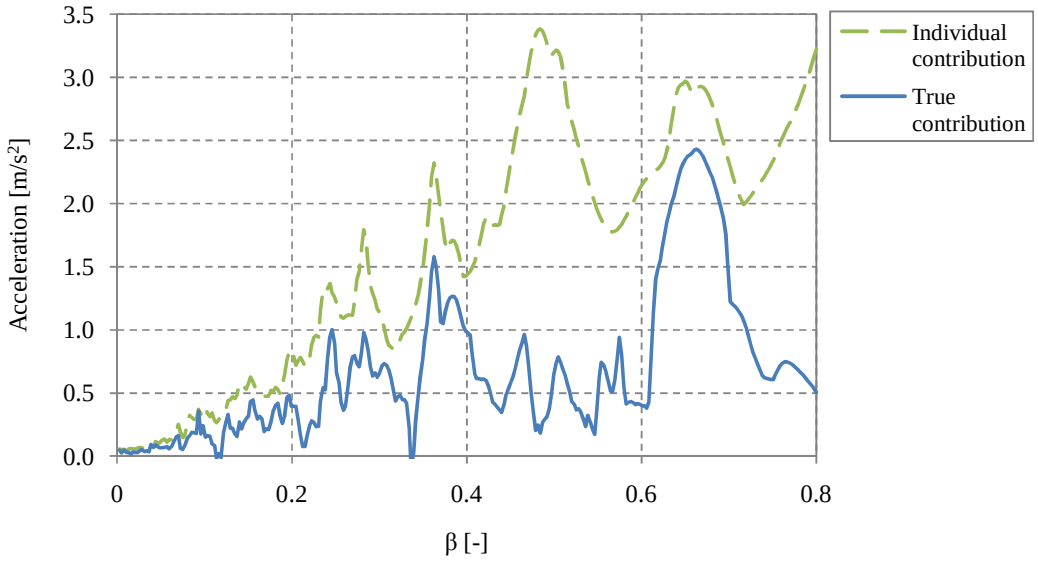

Figure 5.15 *The true contribution from the torsion mode to the total response compared to the contribution if the eigenmodes individual v-a curve is added for a single-span bridge with length 10 m, width 6 m, height 0.6 m, E = 30 GPa, ρ = 4000 kg/m^3, v = 0.02, ζ = 0.0185, e = 2 m.*

Finally Figure 5.16 shows the true contribution from the torsion mode for the variation in bridge width.

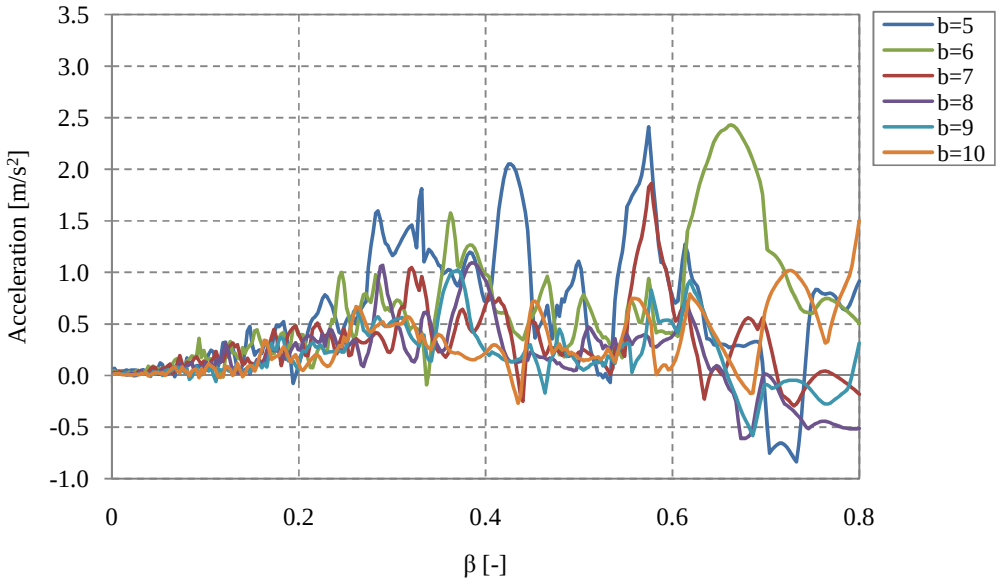

Figure 5.16 *The true contribution from the torsion mode to the response considering only the first bending mode for a single-span bridge with length 10 m, width 6 m, height 0.6 m, E = 30 GPa, ρ = 4000 kg/m^3, v = 0.02, ζ = 0.0185, e = 2 m.*

Figure 5.16 show that there are no general similarities between the true contributions from the torsion mode for different widths. Interesting to note is that the torsion mode in some cases does decrease the maximum acceleration in time. It should also be noted that the contributions shown by Figure 5.16 are for the HSLM-A1 train load in

the edge node shown by Figure 5.1. Only added complexity is presumed to be added when all HSLM-A trainloads and the maximum response for arbitrary node is considered.

5.4 Variation of load eccentricity

In a 2D analysis no consideration is given to the eccentricity of the train load. Eigenmodes that include large deformation parallel the length coordination are highly influenced by the eccentricity as it by definition decides the coordinate of load application parallel the length axis. As was shown in Section 5.2 it is mainly the torsion modes that hence is affected by eccentricity but also the bending modes to some extent.

The eccentricities' effect on each individual eigenmode will be presented initially in this section and then followed by the effect on the total response. The examinations on eccentricity variation have been in the middle line of the bridge in the two nodes shown in Figure 5.1. In these nodes there is no contribution from the second bending eigenmode and hence only responses from the first bending and torsion mode will be presented. All results presented in this section are the individual response of the HSLM-A1 train load.

5.4.1 Influence on bending modes

The bending eigenmode will be affected by the eccentricity as it includes rotation perpendicular to the length coordination. The effect is however small, see Figure 5.17.

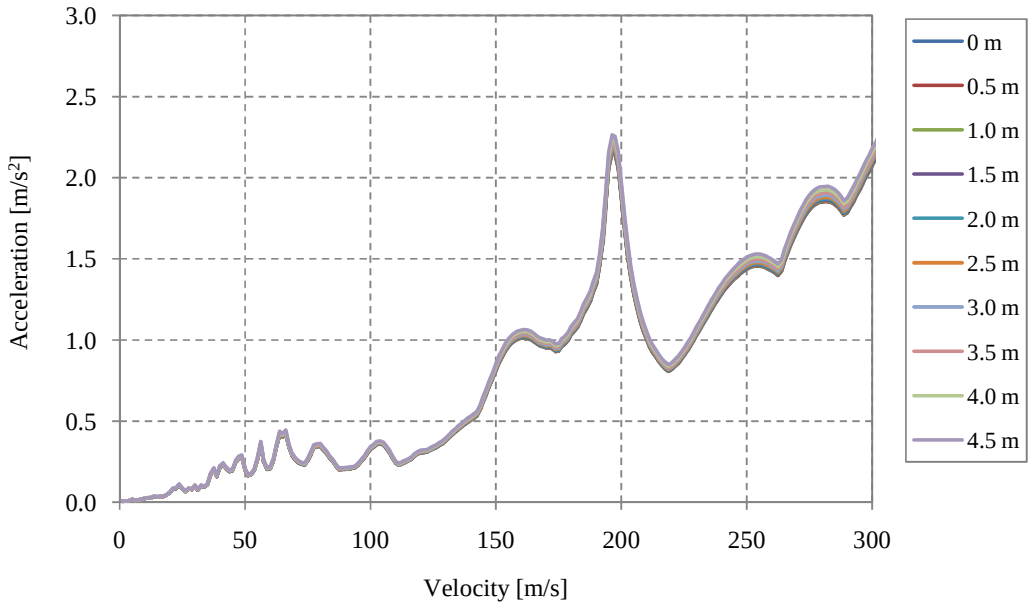

Figure 5.17 *Maximum acceleration in time for the first bending mode in the middle of the bridge for a single-span bridge with length 15 m, width 10 m, height 0.6 m, E = 100 GPa, ρ = 4000 kg/m^3, v = 0.2.The eccentricity varies from 0-4.5 m.*

The accelerations at v = 196.25 m/s (β = 0.5) have been gathered in Figure 5.18 with the purpose of examining the eccentricities' effect on the acceleration response through the first bending mode.

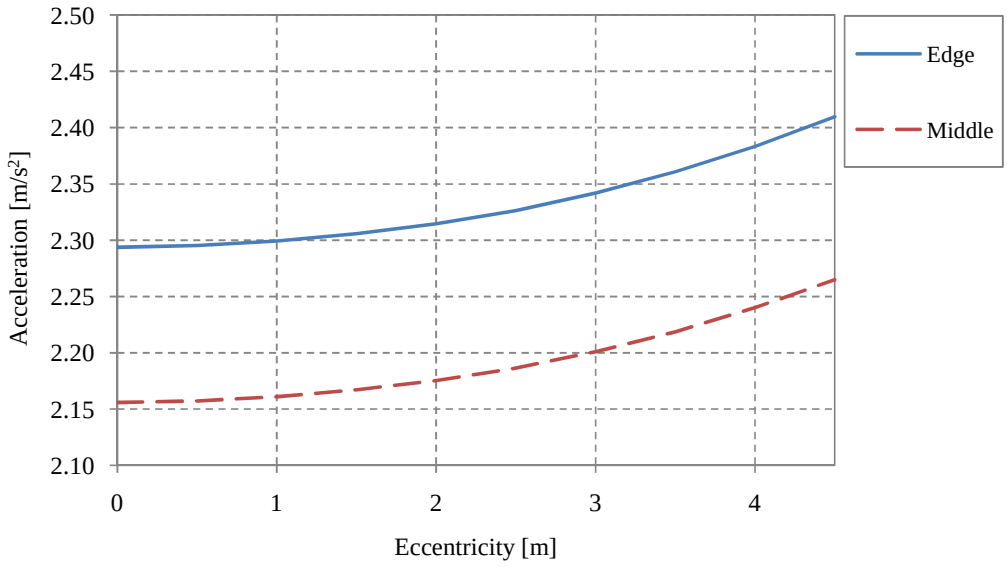

Figure 5.18 *Acceleration in the middle and edge node in Figure 5.1 from the first bending mode for a single-span bridge with length 15 m, width 10 m, height 0.6 m, E = 100 GPa, ρ = 4000 kg/m^3, ν = 0.2 and HSLM-A1with velocity of 196.25 km/h.*

An increase in acceleration with increased eccentricity is expected. The bending eigenmode can be said to be a combination of two different motions. One corresponds to the motion in 2D and is unaffected by the eccentricity and the other consist of the rotation perpendicular to the length coordination and is more influenced as the eccentricity increase. In general it can be said that the influence a load has on an eigenmode is largest when the load is placed where the eigenmode deforms the most. Larger influence on the eigenmode creates larger acceleration through it. It can be seen that the accelerations seem to increase with the same shape as the cross-section deforms for the considered bending mode, see Figure 5.2a.

5.4.2 Influence on torsion modes

The largest impact from a change in eccentricity will be through torsion modes which are governed by rotation perpendicular the length coordination. Figure ***5.19*** shows the individual response from the first torsion mode.

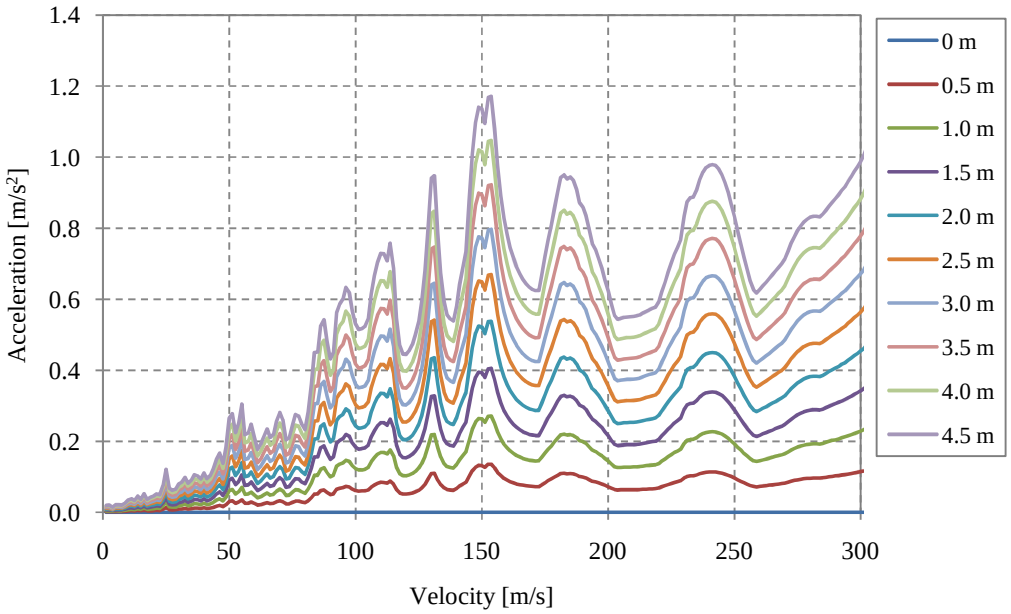

Figure 5.19 *Maximum acceleration in time for the variation of train velocity and load eccentricity for a single-span bridge with length 15 m, width 10 m, height 0.6 m, E = 100 GPa, ρ = 4000 kg/m^3, v = 0.2, ζ = 0.0185*

The accelerations at v=152.5 m/s has been gathered with the purpose of examining the eccentricities' effect on the acceleration response through the bending eigenmode, see Figure 5.20.

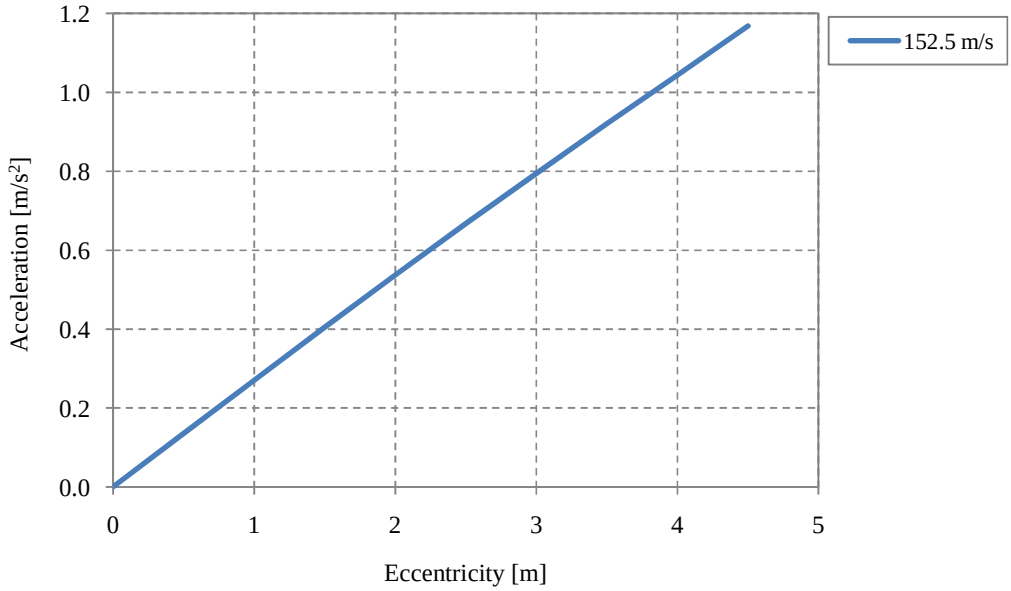

Figure 5.20 *Acceleration in the edge node in Figure 5.1 from the first torsion mode for a single-span bridge with length 15 m, width 10 m, height 0.6 m, E = 100 GPa, ρ = 4000 kg/m^3, v = 0.2 and HSLM-A1 with velocity of 196.25 km/h.*

The same arguments for why the accelerations increase with the eccentricity for the bending mode can be used for the torsion mode. It can be seen in Figure 5.20 that the accelerations seem to increase with the same shape as the cross-section deforms also for the torsion mode.

5.4.3 Combined response

Finally we consider the total response of the single-span bridge for which the individual response of the first bending and torsion mode have been presented. For the edge node, the *v-a* plots for the single-span bridge with variation in load eccentricity are shown in Figure 5.21.

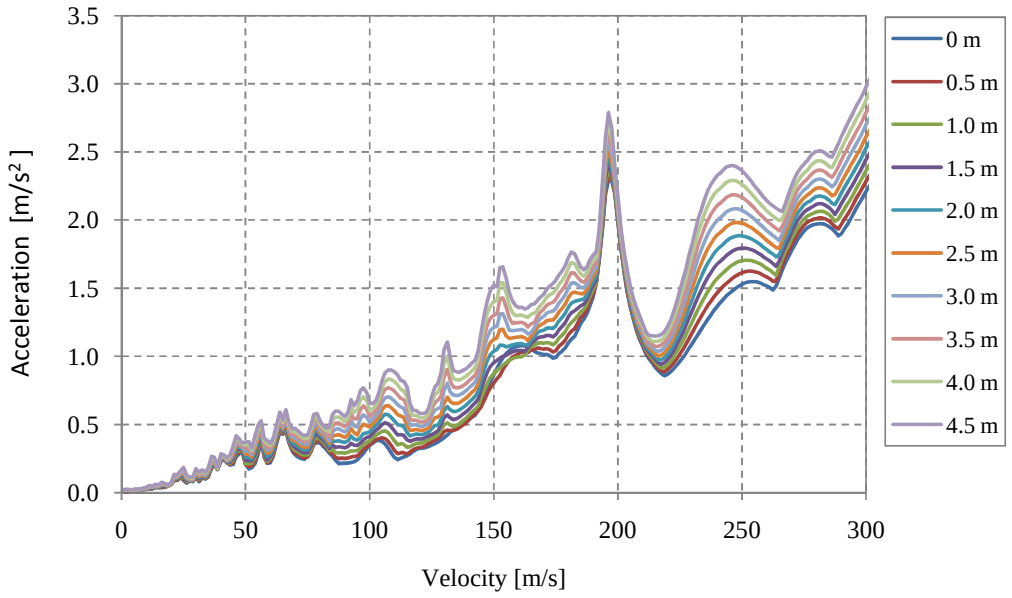

Figure 5.21 *Maximum acceleration in time for different train velocities considering the first bending and torsion mode for a single-span bridge with length 15 m, width 10 m, height 0.6 m, E = 100 GPa, ρ = 4000 kg/m^3, v = 0.2, ζ = 0.185 and HSLM-A1 with velocity of 196.25 km/h.*

The change in acceleration due to load eccentricity from Figure 5.21 for constant train velocities are shown by Figure 5.22.

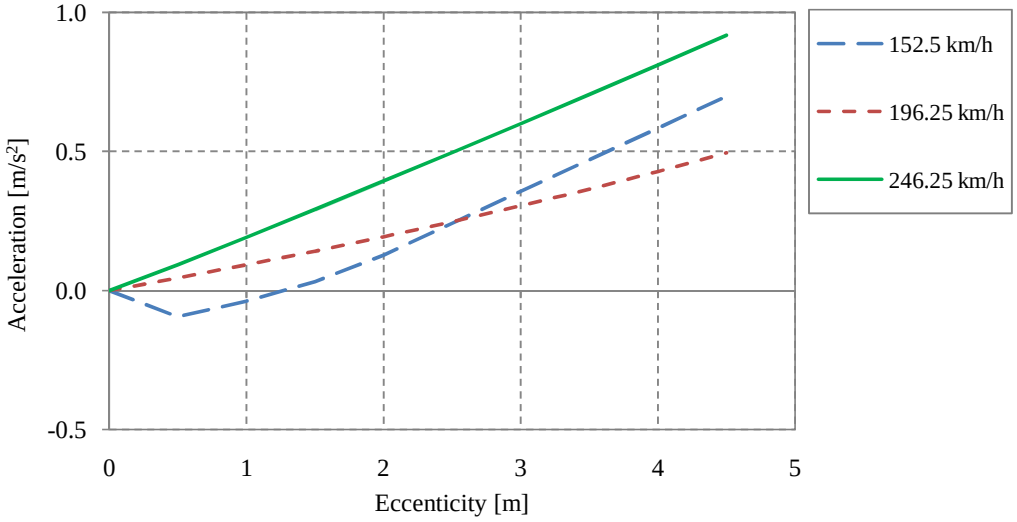

Figure 5.22 *Accelerations from Figure 5.21 for constant train velocities with increased load eccentricity.*

As seen in Figure 5.22 there is no exact influence that can be derived with regards to the eccentricity. In general the eccentricity will increase the total acceleration response in a linear manor, the same way as it affects the torsion mode. It can be seen that the increase in acceleration is linear for higher values of eccentricity for all three considered values of train velocity. But for lower values of eccentricity an increase in acceleration is not guaranteed. The reason for this is that the time for which the maximum acceleration occur shifts for lower eccentricities. If the torsion mode has an acceleration response with opposite sign at the bending modes maximum there might even be a decrease in maximum acceleration, as is the case for the train velocity 152.5 km/h in Figure 5.22.

5.5 Design curves

Last in the investigation of variation of bridge width and load eccentricity for a single-span bridge is to show the difference between design curves in 2D and 3D analysis. The design curves in 3D for each width have been compared with the 2D design curve obtained in Chapter 4, see Figure 5.23 and Figure 5.24. In both figures the 2D design curve is for all velocities the lowest design curve. It is the first torsion mode that causes different total response for the variation of bridge width, as mentioned in Section 5.3. The complexity in the response due to varying width comes from superposition of the bending and torsion modes, whose frequencies are affected differently by the variation. Figure 5.23 and Figure 5.24 show that it is not possible to predict which width that will have the largest acceleration.

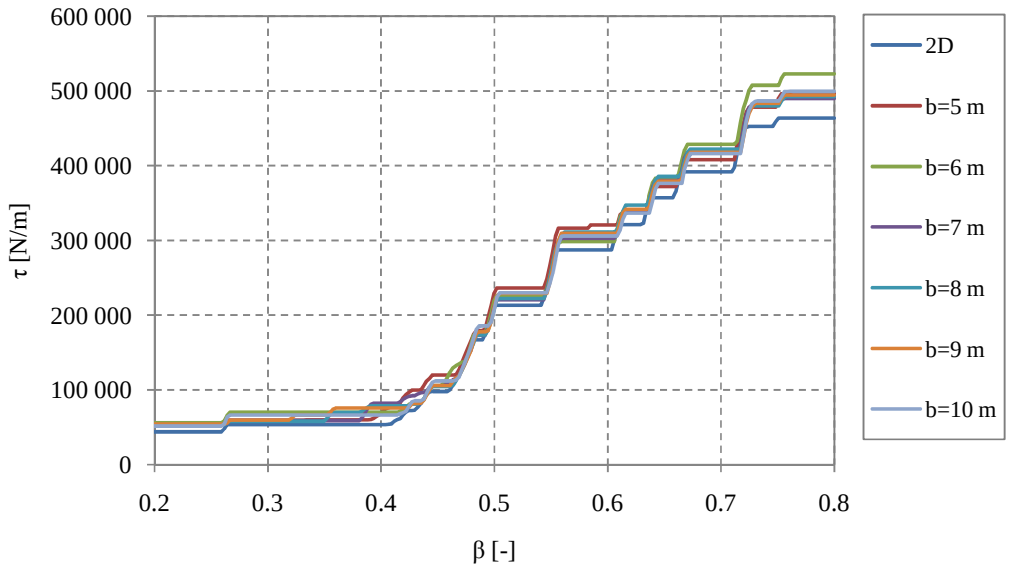

Figure 5.23 *Comparison of design curves for the variation of bridge width in 3D and the 2D design curve, with L = 10 m.*

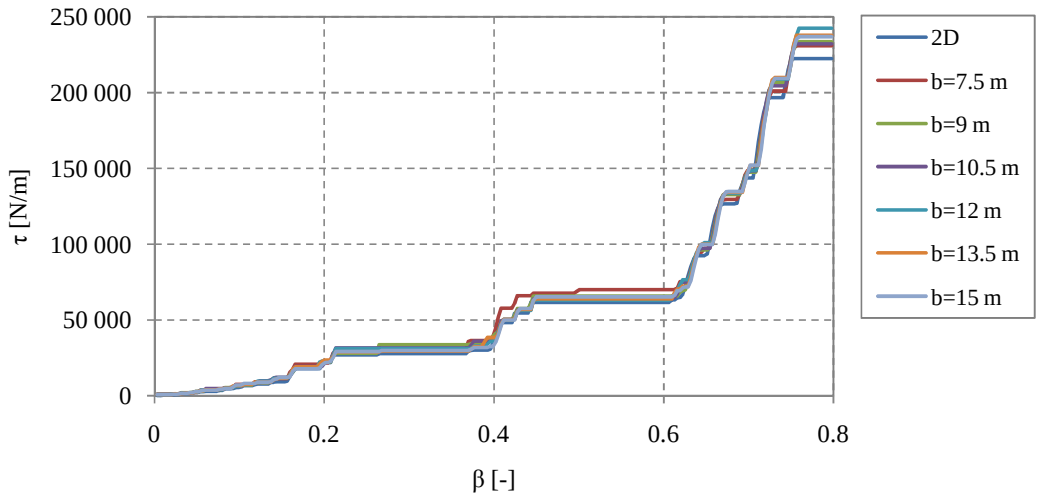

Figure 5.24 *Comparison of design curves for the variation of bridge width in 3D and the 2D design curve, with L = 15 m.*

The percental contribution from the torsion mode is shown in Figure 5.25 and Figure ***5.26***, for a bridge length of 10 and 15 m respectively. It can be concluded that the percental contribution varies for different combination of width, length and velocity. In the case of the 10 meter bridge the contribution is as high as 50 % for β=0.4, which is a β value likely to occur in a real life project. Hence the use of the design curve from 2D without consideration to 3D effects is for β=0.4 a large underestimation. In Figure 5.25 and Figure ***5.26*** it can be seen that the difference between a 2D and 3D analysis generally is smaller in percent for the longer bridge, even though the relation between length and width are the same. It is however not possible to draw any general conclusions if a longer bridge with the same length and width relation implies lower contributions from the torsion mode. For this a larger range of calculations are required.

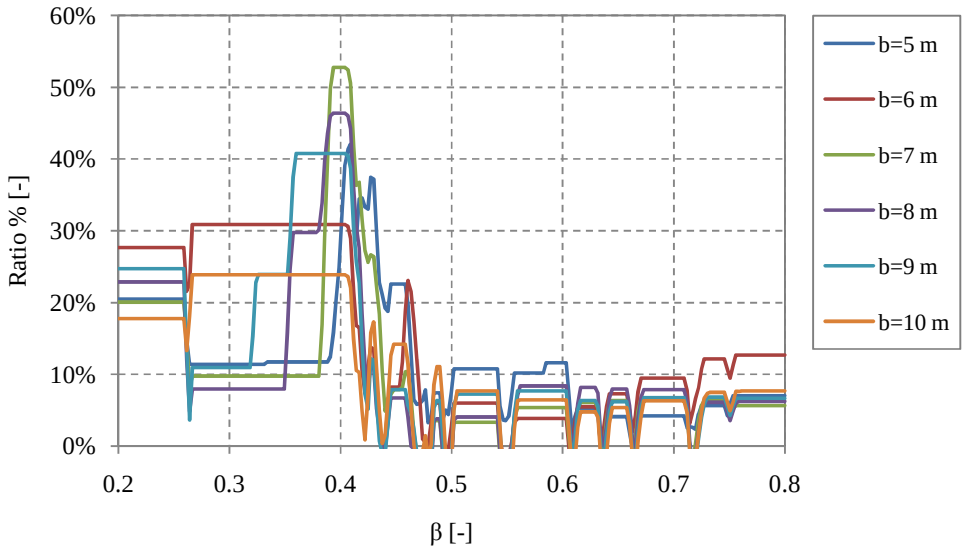

Figure 5.25 *Differences in design acceleration between 2D and 3D analysis for L = 10 m*

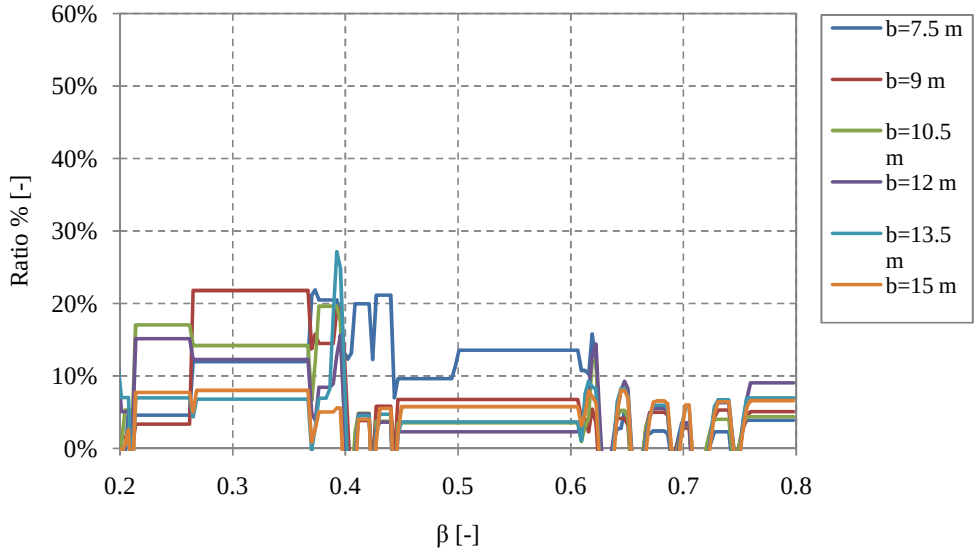

Figure 5.26 *Differences in design acceleration between 2D and 3D analysis for L = 15 m.*

The design curves for different eccentricities in 3D and the 2D design curve are compared in Figure 5.27, for a bridge with length 15 meter. It can be seen that the 2D design curve form the lower limit of the design curves and that the resulting acceleration response will increase with increasing eccentricity. This is an expected behaviour because of the increase in acceleration response from the torsion mode due to increased eccentricity that could be observed in Section 5.4. The percental increase in size of the design curves in 3D for variation of load eccentricity compared to the 2D design curve is shown in Figure 5.28.

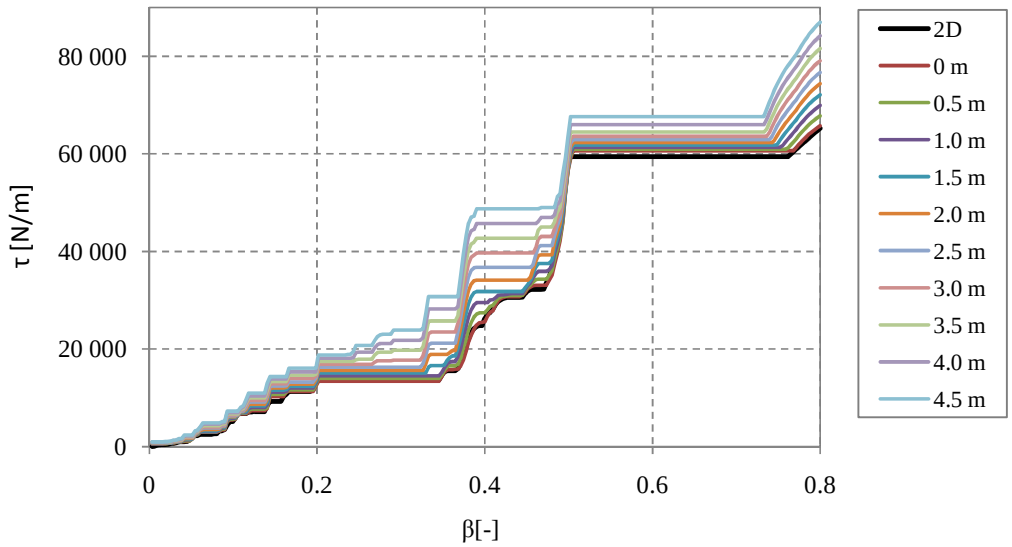

Figure 5.27 *Comparison of 3D design curves for different eccentricities in the edge node and the design curve from the 2D analysis, with L = 15 m and b = 10 m.*

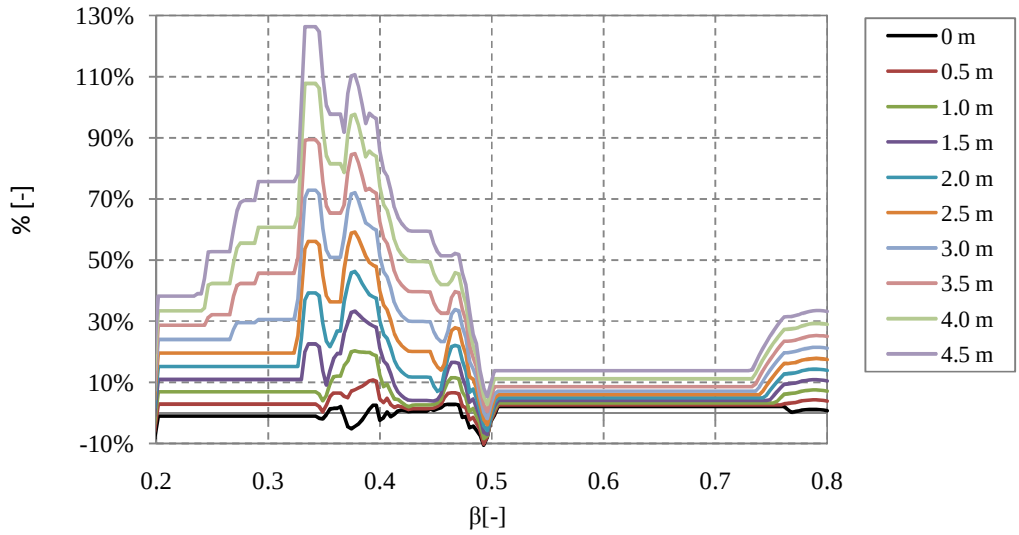

Figure 5.28 *Differences in design acceleration between 2D and 3D analysis in the edge node for L = 15 m and b = 10 m.*

5.6 Conclusions from the analysis in 3D

The main difference between 2D and 3D analysis is that torsion modes are included. In the previous sections of this Chapter it has been shown that a 3D analysis contributes with significantly more complexity compared to a 2D analysis. This complexity is mainly because of the additional torsion modes but also changes in the shape of the bending modes. Below follows the conclusions made from the 3D analysis in this thesis, with regard to single-span bridges and rectangular cross-section.

- Bending modes change in shape when going from 2D to 3D. In 3D the bending modes include torsion around the lengths coordination and the amount included depends on geometric parameters like width, height and length of the bridge.

- Torsion modes are included in 3D analysis. The eigenfrequencies of the lowest torsion modes are in range of the lowest bending modes eigenfrequencies and the two lowest eigenfrequencies seem to always be that of the first bending and torsion mode for the studied configurations.

- Cross-section height affects the relation between all eigenmodes, including bending modes. There may be a distinct deviation of the second bending modes eigenfrequency in 3D compared to the analytical from 2D for larger cross-section heights. However the height has a small influence on the ratio between the first bending and torsion mode.

- Eigenfrequencies of bending modes are in principal unaffected by variation in cross-section width but torsion modes are highly affected.

- The variation of acceleration response from the first bending mode due to changed width can be described by a design curve. The accelerations change in amplitude is in principal proportional to the cross-section width and hence also the bridge mass.

- The variation of acceleration response from the first torsion mode from changing the width cannot be described by a design curve using the parameter τ. The change in acceleration amplitude cannot be explained solely by the change in bridge mass.

- The true contribution when considering the first bending and torsion mode compared to only the first bending mode for variation in bridge width is very complex. The complexity depends mainly on the change in eigenfrequency of the torsion mode, which changes the total acceleration response in time for a fixed train velocity (or value of β for the bending mode).

- The load eccentricity's effect on bending modes is small but still present. The load's influence on the bending modes increase with increased eccentricity.

- The eccentricity has a large influence on the effect from the torsion modes. For the first torsion mode the increased acceleration is almost proportional to the eccentricity.

- The true change in design acceleration, for variation in eccentricity, is unpredictable when considering the first bending and torsion mode. A small added eccentricity may change the time for which the maximum acceleration occurs; it can even result in a decrease of the maximum acceleration.

- The increase in design acceleration in a 3D analysis compared to a 2D analysis can be as high as 100 % for large load eccentricities.

6 Discussion

As mentioned in the background to this thesis there is a need today to find guidelines and simplifications for the dynamic design of railway bridges subjected to high speed trains. Basically guidelines and simplifications cover two different areas of use, where guidelines are meant to be used parallel static analysis in an early design process and simplifications are meant to reduce calculation time for the advanced dynamic analysis.

In this thesis the main focus has been put on developing guidelines for the early design process and the main result has been the idea behind the design curves. The design curves developed in 2D do however not give an estimation of accelerations but the exact design accelerations and are hence also a first step for simplifying the time consuming advanced dynamic analysis.

The discussion presented in this chapter will attend the advances made in this thesis concerning both guidelines and simplifications in dynamic design of railway bridges. Is the design curves developed in 2D applicable in real life projects? Is it possible to develop guidelines considering 3D geometry? Is it possible to develop guidelines that completely exclude the advanced and time consuming dynamic analysis?

Discussion will also be presented on how advanced dynamic analysis could be used for a more time efficient design process.

6.1 Analysis in 2D

As mentioned in the introduction of this thesis several earlier theses have been performed regarding dynamic analysis of railway bridges within the last years. Three master theses have been carried out in cooperation with Reinertsen Sweden AB, namely Ekström and Kieri (2007), De Leon and Lasn (2008) and Gustavsson (2008). These theses are all based on 2D analysis.

One of the advances made in this thesis concerning 2D analysis is the application of the SDOF model on multi-span bridges. It was shown that the force scaling approach gives a good comparison of results to a FE analysis considering the first eigenmode. There is however some lack in accuracy which varies for different HSLM-A loads and train velocities. In De Leon and Lasn (2008) it was concluded that the SDOF model can be used for approximating the dynamic response. That thesis were however limited to single-span bridges for which the second eigenfrequency (in 2D analysis) commonly falls above 30 Hz.

So to what extent is the SDOF model applicable as a guideline or simplification in a real life design? The answer depends on the benefits of having a model that quickly can calculate an approximate response. According to the authors the use of the SDOF model as a guideline is ineffective compared to graphical alternatives like the design curves developed in this thesis. Since the model also is approximate it is difficult to implement it as a simplification of the advanced analysis, even though it could be used to verify complex models by limiting them to the first bending mode.

According to the authors the main use of the SDOF model is that the analytical expressions behind it gives an increased understanding of the influence from material, geometric and load parameters on the dynamic response. This is also the main purpose which it has served in previous master thesis. It might be possible that the added complexities when considering 3D analysis could be explained by the SDOF model. All the complications in the model are based on calculating influence lines of the travelling loads. If a SDOF model is be able to describe the dynamic behaviour in 3D depends hence on the possibility of calculating the deflection in 3D analytically.

The examinations of acceleration amplitude aimed to map the influence of geometric and material parameters. De Leon and Lasn (2008) encountered the accelerations inverse proportionality to the mass. They could however only state that there was an approximate inverse proportionality since they used their SDOF model for all calculations throughout the thesis, which as mentioned include accuracy errors compared to the response from a FE analysis. The choice in this thesis to use a FE program for the examinations of individual parameters influence on the dynamic response was made to avoid these errors. With the use of FE analysis it was stated in this thesis that both young's modulus and the density and hence also cross-section geometry has a simple influence on both eigenfrequencies and acceleration amplitude in 2D analysis.

The first idea of using a graphical tool as guideline in the design process was made by De Leon and Lasn (2008). Their idea was to create transformation graphs based on their observation of the accelerations approximate inverse proportionality to the bridge mass with the use of the SDOF model. The idea is according to the authors complicated and time consuming. Four different graphs were required for calculating an approximate result and 300 graphs had to be developed for the possibility of describing just a single-span bridge. In this thesis it has been shown that the dynamic response for single-span bridges can be illustrated by one single figure through so called design curves, and that the approach is applicable for any bridge configuration of multiple spans.

Gustavsson (2008) had a different approach compared to De Leon and Lasn (2008) as his thesis focused on developing a FE program in Matlab that performed the dynamic calculations of railway bridges subjected to HSLM-A train loads. Gustavsson meant that, using his program, it was possible to quickly determine the acceleration response for a certain set of bridge parameters, and that this approach was easier and better than the earlier ideas of simplifications through SDOF models and graphical presentation. A FE program for calculating the dynamic response of railway bridges has been created by the authors in this thesis as well. However it is not the authors' opinion that a 2D FE program alone can be used as a good guideline or simplification in the design process of railway bridges, but rather the possibilities of creating graphical calculation tools from it. As the reader is well aware of now the design curves are the way of representation created and preferred by the authors. A graphical presentation gives more than just a value of the acceleration outcome, it gives an overview and understanding of the response. As been shown the design curves can be used to easily calculate the acceleration for a certain set of bridge parameters and give guidance to a suitable choice of these parameters.

Calculating the design acceleration and giving guidance to a suitable choice of bridge parameters are the main areas of use for the design curves. However in the creation of

design curves the responses from the ten HSLM-A train loads is calculated individually, and the comparison between these individual responses serves an additional purpose as the critical load can be determined from it. In this thesis design curves were calculated for a single- two- and three-span bridge with equal span lengths. It was found that there is a large variation in what HSLM-A load that governs the acceleration response for these bridge configurations. Based on this observation it can be stated that no general exclusion rule can be established. However for the situation when it is preferable to only include a few loads for a fast approximate calculation, it was found that A2 and A9 most frequently governed the design acceleration.

6.2 Analysis in 3D

In 3D analysis eigenmodes will include torsion. As was shown eigenmodes that are governed by bending compared to those governed by torsion are affected differently by changes in cross-section geometry, and especially cross-section width. It is hence impractical to apply the design curves made for 2D analysis on 3D geometry. Too many curves have to be developed if it is not possible to create one single design curve, describing an arbitrary choice of cross-section geometry.

So what possibilities of developing guidelines and simplification for dynamic 3D analysis of railway bridges are there? The first torsion mode was shown to have the same behaviour as the bending modes when plotted against its own β-value. It showed resonance at the same values and for the width variation the shape of the acceleration response was unaffected. It was mentioned that it might be possible to develop a design curve with consideration to the first torsion mode if the effect from variation of cross-section geometry on the acceleration could be decided (as it was clear that increase in width's effect on the acceleration came from more than the increase in bridge mass). One large disadvantage with such a curve is that it does not include an arbitrary choice of torsion modes, meaning that separate curves would have to be developed for every torsion mode of interest.

The bending modes in 3D analysis can be described by one design curve, as the relation between their corresponding eigenfrequencies in principal is unaffected by cross-section geometry (the height was shown to affect the relation but it was small within the commonly used range of heights). A torsion mode cannot be included in this design curve because the relation between bending and torsion modes' eigenfrequencies changes with the cross-section geometry. For the same reason different torsion modes require individual design curves. However for the case when only one torsion mode is considered it should be possible to use a separate design curve that considers width and load eccentricity to give an estimation of the acceleration response. This estimation based on summarizing the bending modes and the first torsion mode's maximum response in time will always be on the safe side.

Another possibility could be to use the design curves developed in 2D with a safety factor considering the additional 3D effects. The design curves developed in 3D in this thesis showed large similarities with those from 2D. It was seen that the response for the examined single-span bridges was governed by the first bending mode and that distinct changes in the design curves occurred at the same values of β. The use of the design curves from 2D as a guideline could hence work even if 3D geometry is considered. If a safety factor is used for calculating the design acceleration

corresponding to a certain β value the 3D effects could be fully represented by the 2D curves. It is however complicated to establish such a safety factor. More extensive calculations in 3D are required to determine how high the addition in acceleration can be. This addition varies within a large range as already shown by the examination of the two single-span bridges in this thesis. There is a large possibility that the use of a safety factor would hence give results that is too much on the safe side for some sets of bridge parameters. If the factor is made dependent on parameters like load eccentricity this could be avoided, but further studies are required to determine if this is at all possible.

6.3 Practical use of design curves

It is the authors' opinion that the design curves are of great guidance in the 2D dynamic design of railway bridges. However the question of when 2D analyses are applicable remains. In this thesis 3D analyses were performed on two single-span bridges and the first torsion mode was included, which is highly governed by load eccentricity. The results basically showed that design curves from 2D analysis are not sufficient for describing the acceleration response for a rectangular cross-section subjected to high eccentric loading.

The case when the load has no eccentricity was not studied in this thesis. It was however still shown that the bending modes from 2D and 3D are very similar (for single-span bridges and rectangular cross-section). If only bending modes are included in the 3D analysis it might hence be possible to use 2D design curves with a small magnification factor to get accurate results for any parameter set. There are however torsion modes that are affected when the load has no eccentricity which has to be studied further.

Irrespective of when 3D effects need to be considered, it is the authors' opinion that the design curves from 2D should be used as a basis and 3D effects considered using correlation rules. This because the 2D design curves are a much more comprehensible presentation of the acceleration response, as they allow arbitrary choice of cross-section geometry. As mentioned the 2D design curves could be used for both calculating the design acceleration and as guidance when only bending modes need to be considered. The impact of 3D effects then depends on the individual torsion modes contribution, but also which torsion modes that needs to be considered.

The question of what eigenmodes that should be included could be both beneficial and unbeneficial for consideration to 3D effects. The 3D response studied in this thesis for example would become even more complicated if the code demands that an additional torsion mode should be considered. But in the situation where no torsion mode needs to be considered, which might be the case when there is no load eccentricity, the 2D design curves could be used directly.

6.4 Advanced dynamic analysis

The development of guidelines and simplifications that completely exclude the time consuming advanced dynamic analysis requires more examinations and experience of the dynamic response of railway bridges. As the analysis in 3D showed several additional complications compared to 2D analysis, such simplifications are still not in

reach, and might never be. However the advanced analysis can be gradually simplified. One such simplification is to use adequate software. As mentioned in this thesis, commercial software (like ADINA) might be unfitted for dynamic analysis of railway bridges as this analysis includes a combination of travelling point loads. Problems might for example arise when choosing the mesh size and time step for the numerical integration with consideration to a range of train velocities. The Matlab code presented in Appendix D is a good alternative to commercial software and it is preferred by the authors for iterative calculations on railway bridges. The use of a FE program that can produce a design curve also has the benefit of giving in overview of the dynamic response, which at least shows the effect of varying material parameters and design train velocity.

7 Concluding remarks

The conclusions from this master thesis and thoughts about further studies are presented in this chapter.

7.1 Conclusions

Previous master theses regarding dynamic design of railway bridges, carried out at Reinertsen Sweden AB during recent years, have all focused on single-span railway bridges. This thesis has had a more general approach, as the response of railway bridges with multiple spans also has been included. Examinations have therefore been made on the eigenmodes of multi-span bridges. It was shown to be complicated to derive the eigenfrequencies for multi-span bridges analytically. But through numerical examinations it was shown that the eigenfrequencies can be calculated through an equation that is very similar to that of single-span bridges, with the addition of so called eigenfrequency functions. These functions depend on the span relation and differ between eigenmodes.

A transformation procedure called the force scaling approach was applied on multi-span bridges as a continuation of previous master theses. The method transforms a railway bridge of interest into a SDOF model. The method have earlier been shown to give accurate results for single-span bridges and been said to be compatible with more complex structures. However, it was shown in this thesis that it lacks some accuracy for multi-span bridges. The method can still be used to approximate the dynamic response, but it will be on the unsafe side. The model was not used further in the thesis because of the lack in accuracy.

A parameter study has been performed in this thesis, with the purpose of examining the individual effect on the acceleration response due to different bridge parameters. It was found that material parameters affect the acceleration in a predictable way. The amplitude of the acceleration, for a specific frequency ratio (the ratio between load frequency and eigenfrequency), is inverse proportional against the density and independent of Young's modulus. The total bridge length and span relations were found to affect the acceleration in a way that is hard to predict, though it was seen that the accelerations tend to decrease with increased bridge length and increase for small asymmetry between spans.

During the parameter study several observations were made concerning resonance in railway bridges. It was seen that the design acceleration does not always occur in the resonance peek corresponding to the highest train velocity. It was also seen that resonance effects may disappear for some combinations of geometry, through so called cancellation effects. The summarising conclusion from these observation is that it is difficult, in advance, to determine which train speed that will govern the response, and hence the whole speed range suggested by BV Bro (Banverket, 2006) need to be considered.

The observations regarding resonance and individual parameters effect on the accelerations were gathered to create a graphical guideline, called design curves. A design curve captures the dynamic response of a railway bridge with a certain bridge configuration. It allows an arbitrary choice of train speed, material parameters and cross-section geometry and includes the effect of all ten HSLM-A train loads. It was shown that such design curves can be used to quickly calculate the design acceleration for a specific set of parameters. Also it serves as guidance in the early stage of a

project, as the graphical form gives an overview of how the response is affected by changes in bridge parameters.

The design curves main limitation is that they are based on 2D analysis. In this thesis a comparison between 2D analysis and 3D analysis was performed to show the difference in acceleration response. Calculations were made on two single-span bridges under the variation of bridge width and load eccentricity. In 2D analysis two bending modes were included and in 3D analysis one additional torsion mode was also included. The results showed that both eigenfrequencies and the acceleration response are affected differently for bending and torsion modes. The eigenfrequency of bending modes are in principal unaffected by width variation while width strongly affects the torsion modes' eigenfrequencies. The torsion modes acceleration response is also highly governed by load eccentricity, while the bending modes' response is not. The differences between eigenmodes in a 3D analysis make it more difficult to find guidelines and simplifications compared to 2D analysis. However it can be concluded that 3D effects need to be considered somehow, as it was shown that they may give a very high contribution when large load eccentricity is present. In this thesis the possibilities of producing separate design curves or magnification factors have been discussed, though additional studies are required to determine these possibilities.

7.2 Suggestions of continued work

The question of how many eigenmodes that should be included in the dynamic design of railway bridges (based on eigenfrequencies) definitely needs more attention. Developing guidelines for railway bridges, of any kind, whether it is a simplified system or a design curve requires that the number of included eigenmodes is known. In this thesis, choices were made for how many eigenmodes to include for the three bridge configurations of which design curves where created in 2D. However for the development of design curves, to be used in real life design, these choices need to be made on a larger basis.

The knowledge of which torsion modes that needs to be considered for a specific set of bridge parameters is essential when considering 3D effects. This knowledge itself might serve as guidance in the design process if it can be shown that all torsion modes can be excluded for some sets of bridge parameters. Knowing how many eigenmodes that should be included is hence an important step for the possibility of creating guidelines for the dynamic design of railway bridges considering both 2D and 3D.

To determine the required number of eigenmodes for different bridge configurations, it is suggested by the authors that a study which gather used cross-section geometry from railway bridges designed for HSLM train loads is performed. It might also be possible to use the guidance of the design curves to create a range of suitable cross-sections. However, this creates a circular reasoning as the result from the design curves depend on the included eigenmodes and vice versa.

Even if the torsion modes to include in a railway bridge design are known, there is still a question of determining these modes' contribution to the acceleration response in a simplified way. The torsion modes individual contribution could be presented by individual design curves or magnification factors as mentioned in Section 6.3. It might also be possible to develop simplified models like a rod subjected to torsion for the first torsion mode or a simply supported plate for the second torsion mode. As

different torsion modes behave in different ways it is likely that different factors/curves/models need to be developed for the respective modes.

There is also a need to increase the understanding of how both bending and torsion modes are affected by changes in cross-section shape. It was shown in this thesis that bending modes in 3D compared to 2D had small differences, but the 3D calculations in this thesis were also limited to rectangular cross-sections. For other cross-section shapes there might be larger differences between the bending modes, which then would cause larger differences between 2D and 3D analysis irrespective of the inclusion of torsion modes.

To summarize the authors would like to see further studies regarding which eigenmodes to include, individual effect of torsion modes and changes in eigenmodes regarding cross-section shape in 3D. An idea could be to examine all three areas, but for one specific bridge configuration at a time. This way useful guidance for real life projects could be continuously produced.

8 References

Abrahamsson T., (2000): *Linear System in Vibration Engineering*, skrift U72, Chalmers Solid Mechanics.

ADINA, (2004): *Theory and Modeling Guide Version 8.8.2*, ADINA R&D, Inc., Volume 1, Watertown, USA.

Austrell P.-E., et. Al., (2004): *CALFEM – A finite element toolbox version 3.4*, KFS I Lund AB, Lund.

Banverket, (2006): *BV BRO – Banverkets ändringar och tillägg till Vägverkets Bro 2004*, (Revision and additions by the Swedish Railway Administration to the Swedish bridge code, Bro 2004), inclusive supplement nr 2, Utgåva 9, BVS 583.10.

Craig R. R., Kurdila A. J. (2006): *Fundamentals of Structural Dynamics*. John Wiley & Sons, Inc., Hoboken, New Yersey, USA, 728 pp.

CEN (2003): *Eurocode 1: Actions on structures – Part 2: Traffic loads on bridges*, Comité Européen de Normalisation, Brussels, Belgium, 164 pp.

CEN (2003): *Eurocode: Basis of Structural Design Annex A2*, Comité Européen de Normalisation, Brussels, Belgium, 32 pp.

De Leon O., Lasn K. (2008): *Dynamics of railway bridges subjected to high-speed trains.* Master of Science Thesis. Department of Civil and Environmental Engineering, Chalmers University of Technology, Publication no 2008:6, Göteborg, Sweden, 152 pp.

Ekström D., Kieri L.-L. (2007): *Dynamic analysis of railway bridges.* Master of Science Thesis. Department of Civil and Environmental Engineering, Chalmers University of Technology, Publication no 2007:8, Göteborg, Sweden, 159 pp.

Gorman J. D. (1975): *Free vibration analysis of beams and shafts.* John Wiley & Sons, Inc., New York, USA, 386 pp.

Gustafsson A. (2008): *Reduced models for dynamic analysis of high-speed railway bridges.* Master of Science Thesis. Department of Construction Sciences, Lund University, Publication no 08:5160, Lund, Sweden, 86 pp.

Nyström U. (2006): *Design with regard to explosions.* Master of Science Thesis. Department of Civil and Environmental Engineering, Chalmers University of Technology, Publication no 2006:14, Göteborg, Sweden, 205 pp.

A. Appendix A

Attempt of analytically deriving an explicit expression for the eigenfrequencies of a two-span bridge

The procedure of deriving an analytical expression for the eigenfrequencies of a single span bridge is rather simple and results in an explicit expression for eigenfrequencies of any degree. For two span bridges it gets more complicated however and an explicit expression is impossible to derive. This appendix is meant to give the reader an idea of why.

The differential equation of motion for transverse vibration is shown by equation (A.1).

$$\frac{\partial^2}{\partial x^2} * \left(EI \frac{\partial^2 v}{\partial x^2} \right) + \rho A \frac{\partial^2 v}{\partial t^2} = p_y(x,t) \quad \text{(A.1)}$$

For free vibrations with constant bending stiffness equation (A.1) reduces to:

$$EIv'''' + \rho A \ddot{v} = 0 \quad \text{(A.2)}$$

If we assume the following solution to equation (A.2):

$$v(x,t) = V(x) * \cos(\omega t - \alpha) \quad \text{(A.3)}$$

We get:

$$\frac{d^4 V}{dx^4} - \lambda^4 V = 0 \quad \text{(A.4)}$$

Where:

$$\lambda^4 = \omega^2 \frac{\rho A}{EI} \quad \text{(A.5)}$$

The general solution to (A.4) can be written as:

$$V(x) = A_1 \sinh(\lambda x) + A_2 \cosh(\lambda x) + A_3 \sin(\lambda x) + A_4 \cos(\lambda x) \quad \text{(A.6)}$$

This equation has four variables which must be determined. For a single span bridge we could simply use the boundary condition $V = d^2V/dx^2 = 0$ at both ends. This gives us that $A_2 = A_4 = 0$ and the two remaining linear equations gives us that:

$$\begin{vmatrix} \sin(\lambda L) & \sin(\lambda L) \\ \lambda^2 \sin(\lambda L) & -\lambda^2 \sin(\lambda L) \end{vmatrix} = 0 \quad \text{(A.7)}$$

Which because of the simplicity of the matrix gives us an explicit expression for $\lambda = r*\pi/L$ for r= 1, 2, 3 and so on.

For a two span bridge we have two beams connected together. This means we instead have eight variables and eight boundary conditions. The boundary conditions at the middle support will connect the two beams together.

Figure (A-1) defines two different parameters along the bridge. The definitions of these parameters are made to give as simple result as possible.

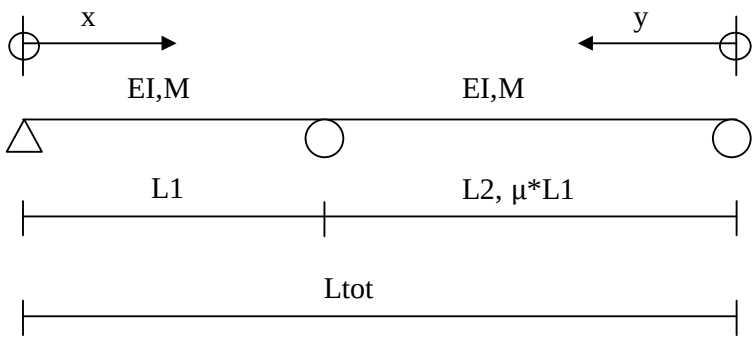

Figure A-1 Definition of the variables x and y

We have the following general solutions for the displacement of beam 1 and 2:

$$V_1(x) = A_1 \sinh(\lambda x) + A_2 \cosh(\lambda x) + A_3 \sin(\lambda x) + A_4 \cos(\lambda x) \quad \text{(A.8)}$$

$$V_2(x) = B_1 \sinh(\lambda y) + B_2 \cosh(\lambda y) + B_3 \sin(\lambda y) + B_4 \cos(\lambda y) \quad \text{(A.9)}$$

With the definition of x and y we have the following boundary conditions:

$$V_1(0) = V''_1(0) = 0 \quad V_2(0) = V''_2(0) = 0$$

$$V_1(L1) = 0 \qquad V_1(L2) = 0$$

$$V'_1(L1) = -V'_2(L2) \quad V''_1(L1) = V''_2(L2) \quad \text{(A.10)}$$

This gives us that:

$$A_2 = A_4 = B_2 = B_4 \quad \text{(A.11)}$$

And the following linear equations give us that:

$$\begin{vmatrix} \sinh(\lambda L1) & 0 & \sin(\lambda L1) & 0 \\ 0 & \sinh(\lambda L2) & 0 & \sin(\lambda L2) \\ \cosh(\lambda L1) & \cos(\lambda L1) & \cosh(\lambda L2) & \cos(\lambda L2) \\ \sinh(\lambda L1) & -\sin(\lambda L1) & -\sinh(\lambda L2) & \sin(\lambda L2) \end{vmatrix} = 0 \quad \text{(A.12)}$$

And this results in a complicated expression where there is no possibility of deriving an explicit analytical expression for λ.

The last steps can be better performed. The first two rows in (12) could be used to eliminate two variables. But even if we get that the determinant should be zero for a two times two matrix we still get a very complicated expression. The interested reader is referred to Gorman (1975).

B. Appendix B

Results from a parameter study on multi-span railway bridges

The following document contains figures showing the results from a parameter study made on continuous railway bridges. The parameter study covers two- and three-span bridges.

The parameter study aims to show the effect from different parameters on the dynamic response. The studied parameters are:

- E = Module of elasticity
- Ltot = Total bridge length
- μ = L2/L1 for two-span bridges
- η = L2/(L1+L3) for three-span bridges
- ρ = density
- c = damping

Two different types of figures are presented. The first type shows different acceleration responses with the variation of train speed. The second type shows the variation of acceleration amplitude around resonance peeks.

The corresponding parameter set for the variation of a certain variable are presented in the figure explanation. Different parameter sets have been chosen for different comparisons.

Table of content

B. APPENDIX B 118

B.1 Variation of module of elasticity, E, for a two-span bridge 119

B.2 Variation of density, ρ, for a two-span bridge 120

B.3 Variation of span relation, μ, for a two-span bridge 121

B.4 Variation of total bridge length, Ltot, for a two-span bridge 125

B.5 Variation of damping, c, for a two-span bridge 128

B.6 Variation of module of elasticity, E, and density, ρ, for a three-span bridge 129

B.7 Variation of span relation, η, for a three-span bridge 130

B.1 Variation of module of elasticity, E, for a two-span bridge

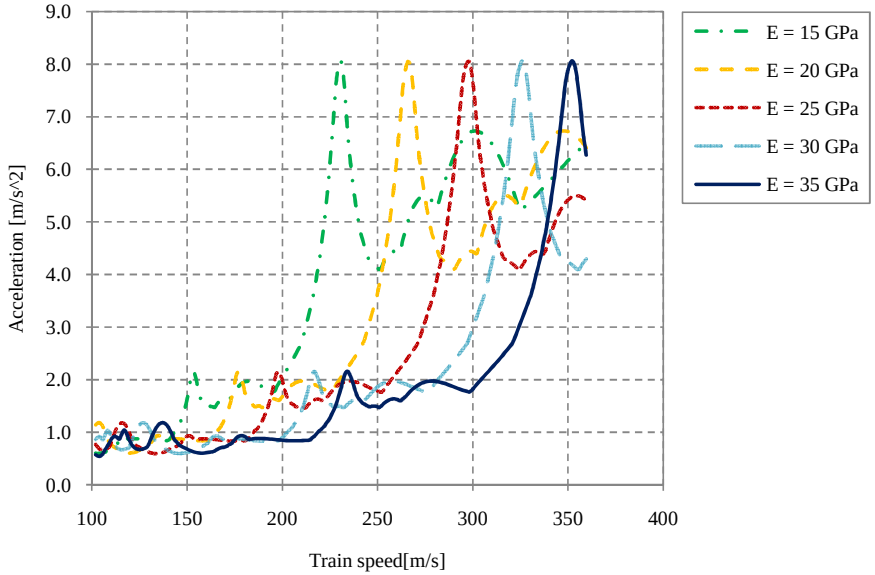

Figure B-1 *Acceleration response for a two-span bridge subjected to HSLM-A1 using ρ=2800 kg/m^3, Ltot=16m, μ=2 and c=0.02*

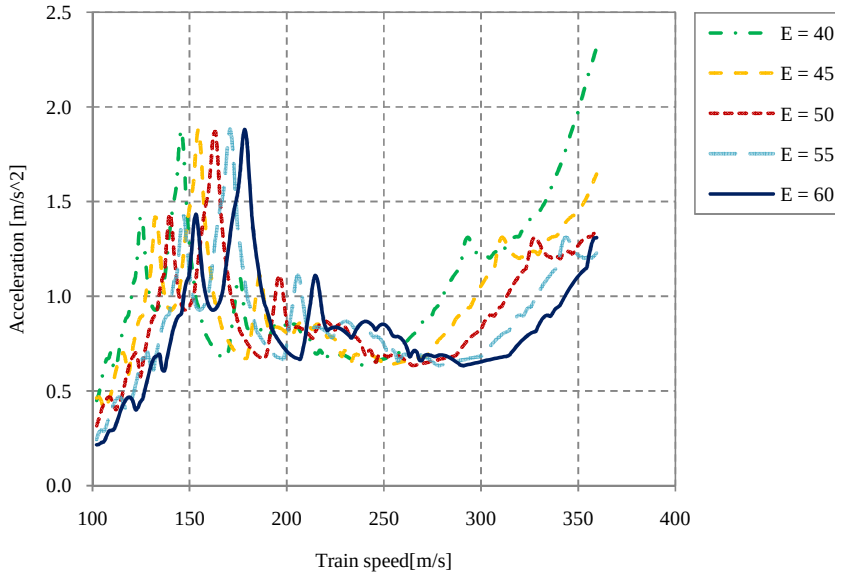

Figure B-2 *Acceleration response for a two-span bridge subjected to HSLM-A4 using ρ=2800 kg/m3, Ltot=16m, μ=2 and c=0.02*

B.2 Variation of density, ρ, for a two-span bridge

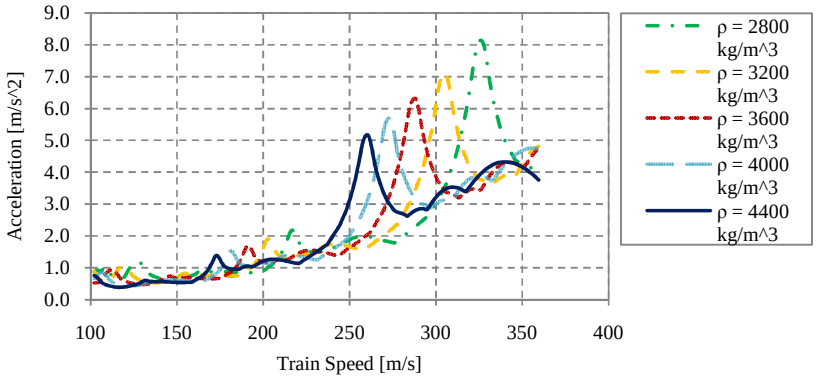

Figure B-3 *Acceleration response for a two-span bridge subjected to HSLM-A1 using E=30 GPa, Ltot=16m, μ=2 and c=0.02*

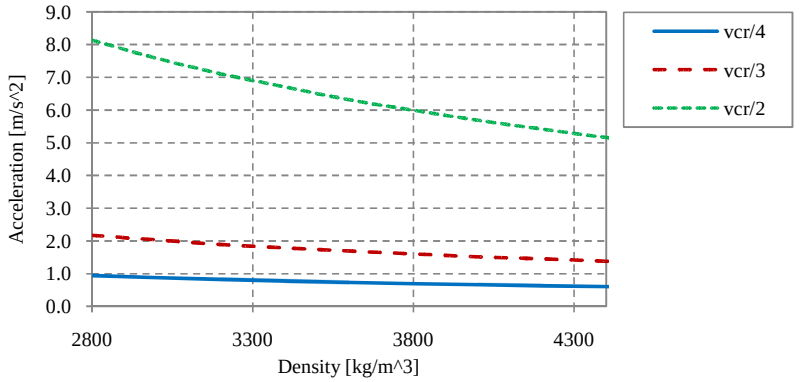

Figure B-4 *Acceleration response for a two-span bridge subjected to HSLM-A1 using E=30 GPa, Ltot=16m, μ=2 and c=0.02*

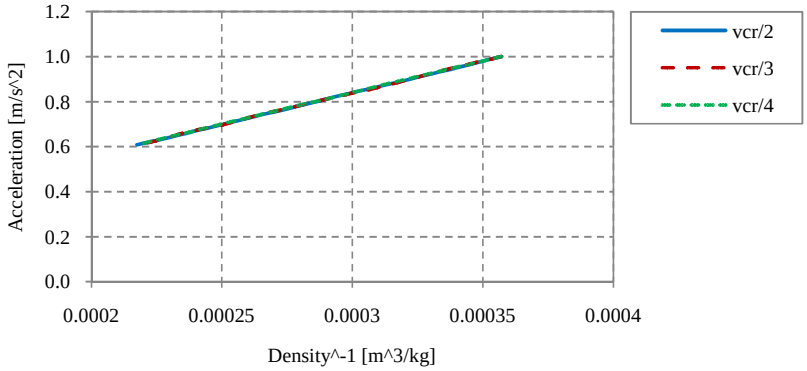

Figure B-5 *Acceleration from figure B-4 plotted againsst the inverse of the density*

B.3 Variation of span relation, μ, for a two-span bridge

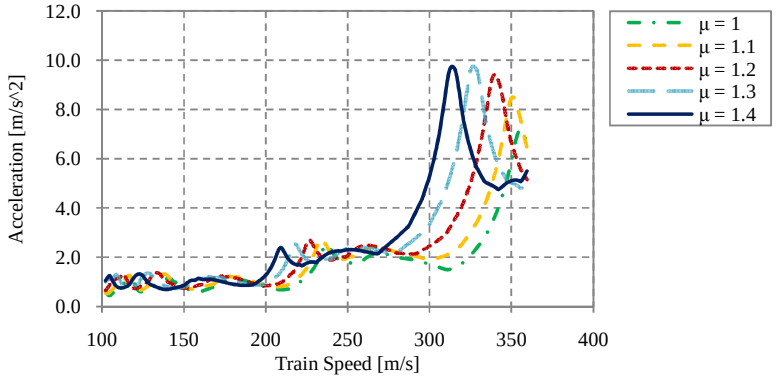

Figure B-6 *Acceleration response for a two-span bridge subjected to HSLM-A1 using E=20 GPa, Ltot=16m, ρ=3000 kg/m^3 and c=0.02*

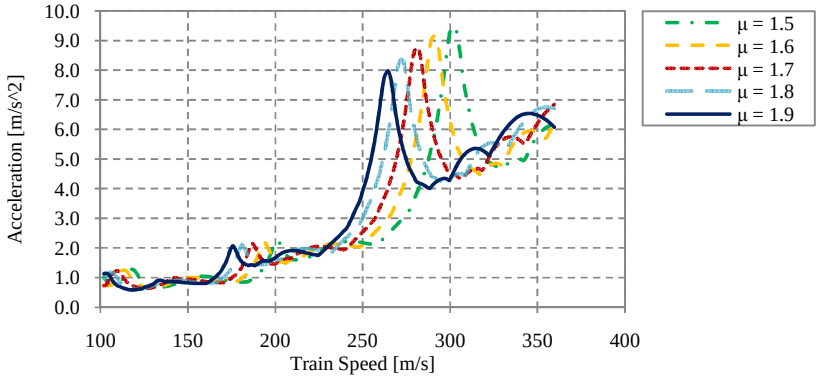

Figure B-7 *Acceleration response for a two-span bridge subjected to HSLM-A1 using E=20 GPa, Ltot=16m, ρ=3000 kg/m^3 and c=0.02*

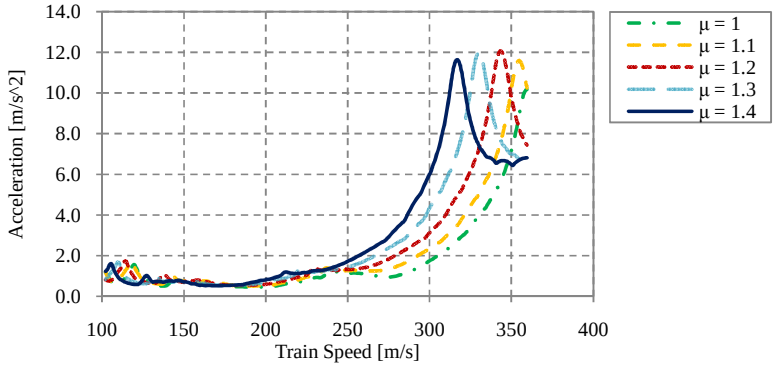

Figure B-8 *Acceleration response for a two-span bridge subjected to HSLM-A4 using E=20 GPa, Ltot=16m, ρ=4000 kg/m^3 and c=0.02*

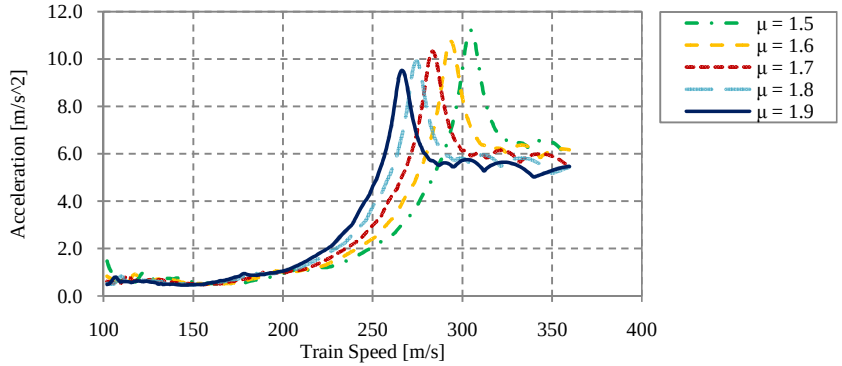

Figure B-9 *Acceleration response for a two-span bridge subjected to HSLM-A4 using E=20 GPa, Ltot=16m, ρ=4000 kg/m^3 and c=0.02*

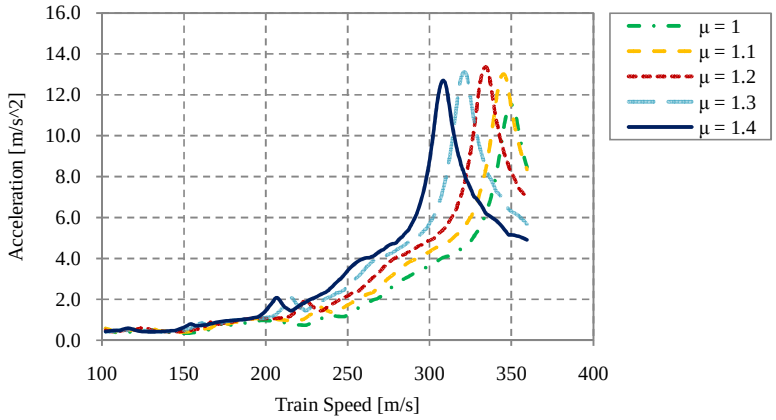

Figure B-10 *Acceleration response for a two-span bridge subjected to HSLM-A8 using E=20 GPa, Ltot=16m, ρ=6000 kg/m^3 and c=0.02*

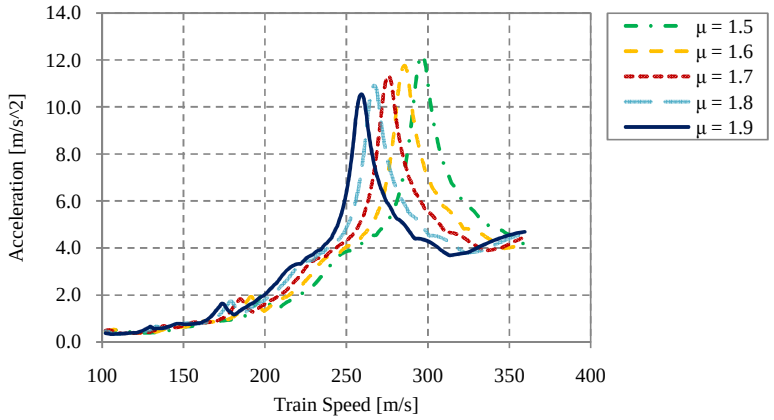

Figure B-11 *Acceleration response for a two-span bridge subjected to HSLM-A8 using E=20 GPa, Ltot=16m, ρ=6000 kg/m^3 and c=0.02*

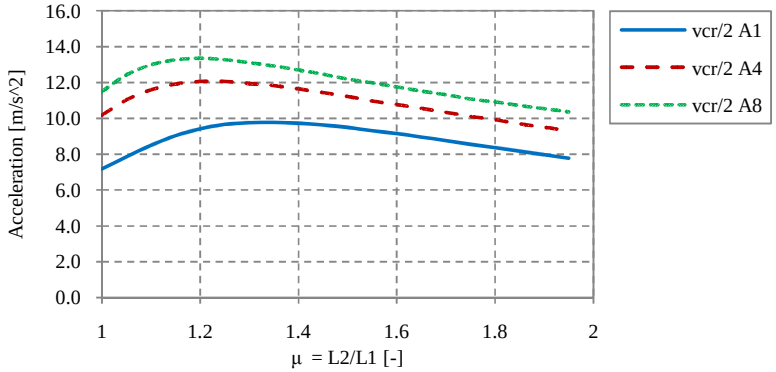

Figure B-12 *Acceleration response in resonance peek at vcr/2 from the response shown by figures B-6-11*

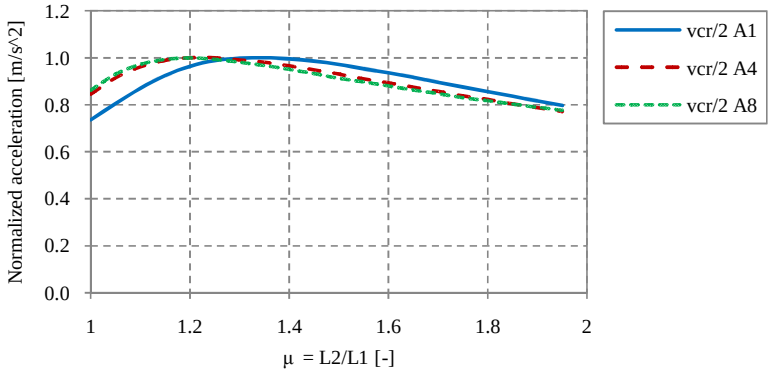

Figure B-13 *Normalized acceleration response in resonance peek at vcr/2 from the response shown by figures B-6-11*

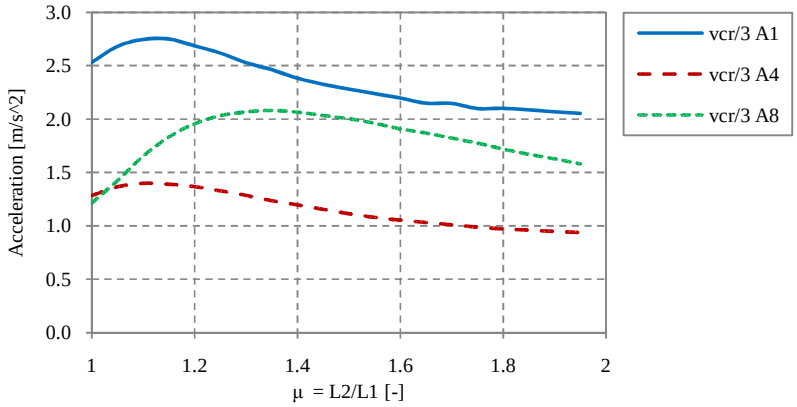

Figure B-14 *Acceleration response in resonance peek at vcr/3 from the response shown by figures B-6-11*

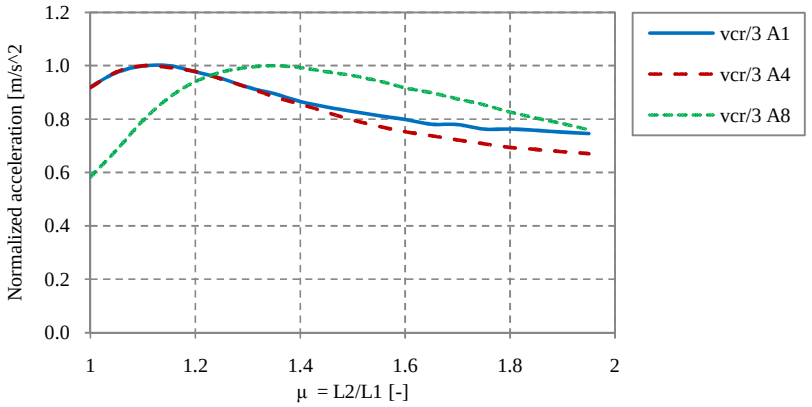

Figure B-15 *Normalized acceleration response in resonance peek at vcr/3 from the response shown by figures B-6-11*

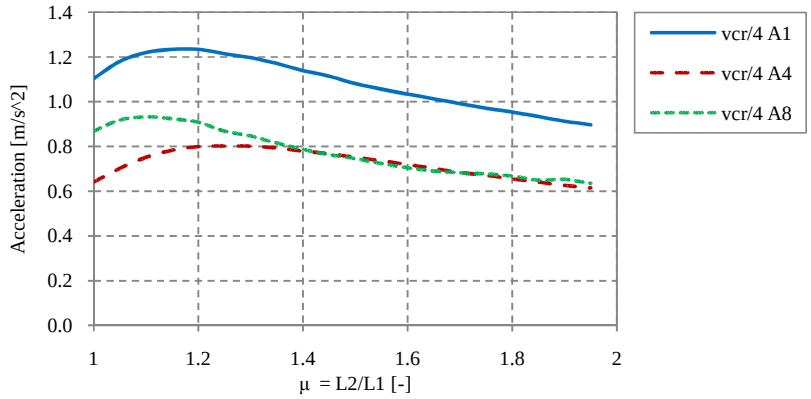

Figure B-16 *Acceleration response in resonance peek at vcr/4 from the response shown by figures B-6-11*

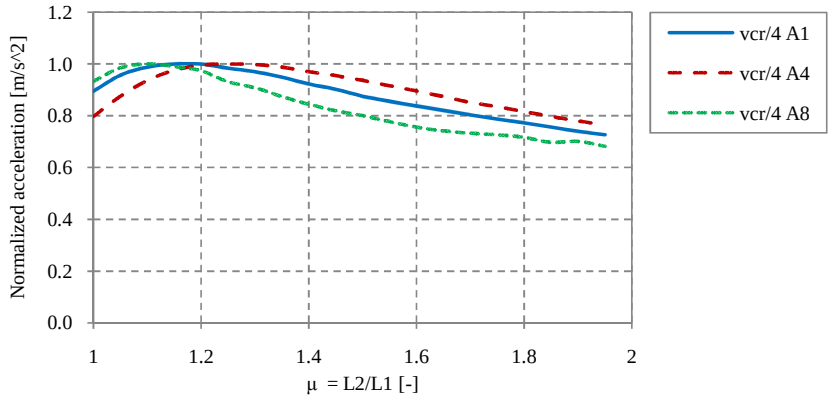

Figure B-17 *Normalized acceleration response in resonance peek at vcr/4 from the response shown by figures B-6-11*

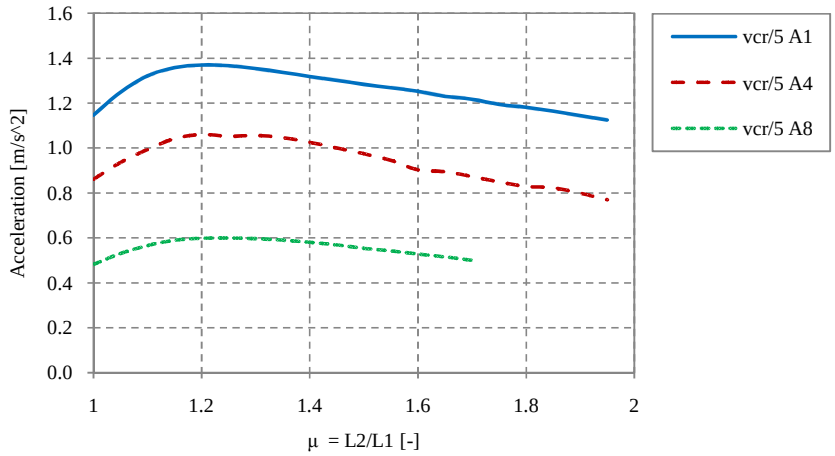

Figure B-18 *Acceleration response in resonance peek at vcr/5 from the response shown by figures B-6-11*

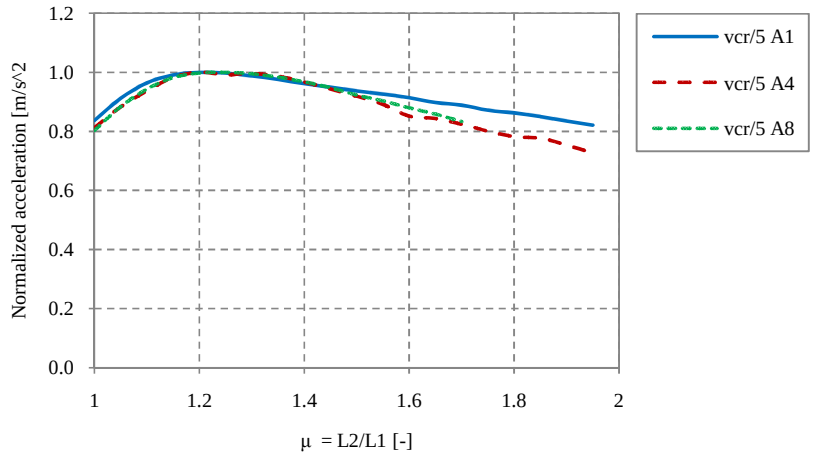

Figure B-19 *Normalized acceleration response in resonance peek at vcr/5 from the response shown by figures B-6-11*

B.4 Variation of total bridge length, Ltot, for a two-span bridge

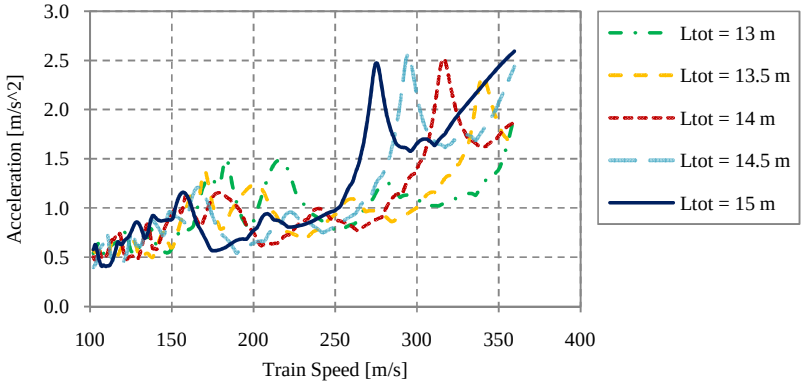

Figure B-20 *Acceleration response for a two-span bridge subjected to HSLM-A1 using E=40 GPa, μ=2, ρ=3000 kg/m^3 and c=0.02*

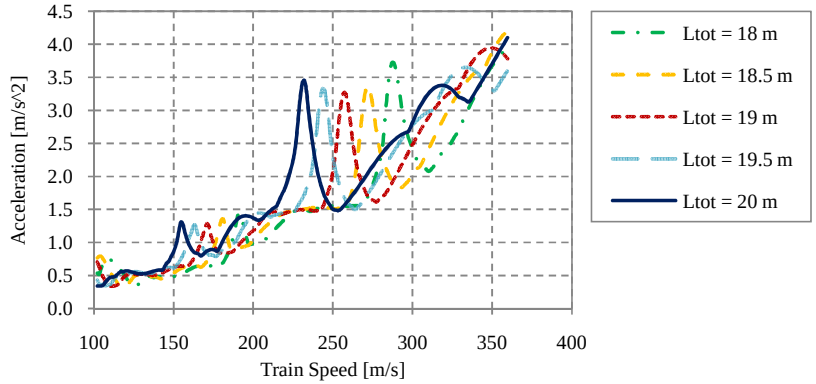

Figure B-21 *Acceleration response for a two-span bridge subjected to HSLM-A1 using E=40 GPa, μ=2, ρ=3000 kg/m^3 and c=0.02*

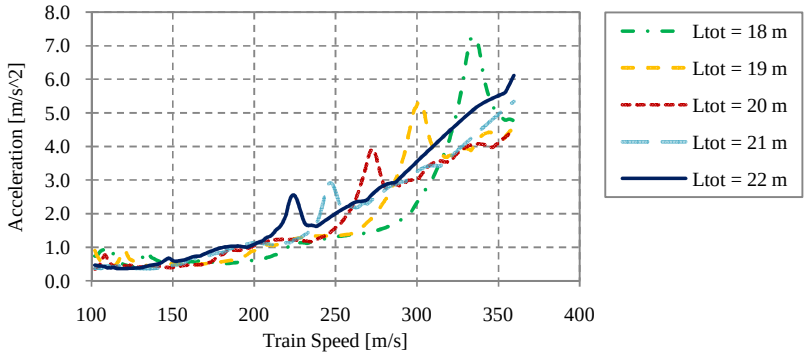

Figure B-22 *Acceleration response for a two-span bridge subjected to HSLM-A4 using E=40 GPa, μ=2, ρ=3000 kg/m^3 and c=0.02*

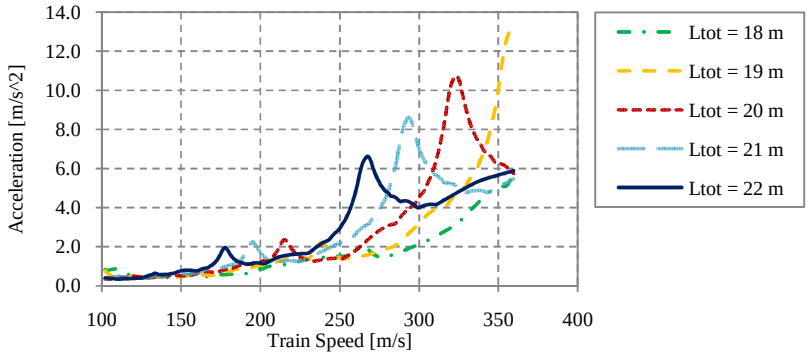

Figure B-23 *Acceleration response for a two-span bridge subjected to HSLM-A8 using E=40 GPa, μ=2, ρ=3000 kg/m^3 and c=0.02*

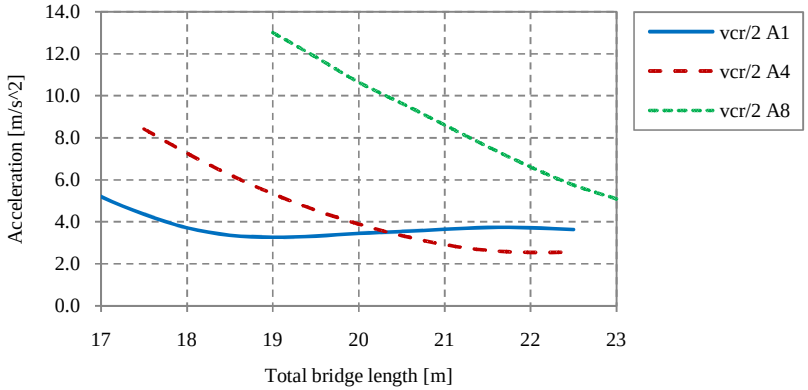

Figure B-24 *Acceleration response in resonance peek at vcr/2 from the response shown by figures B-20-23*

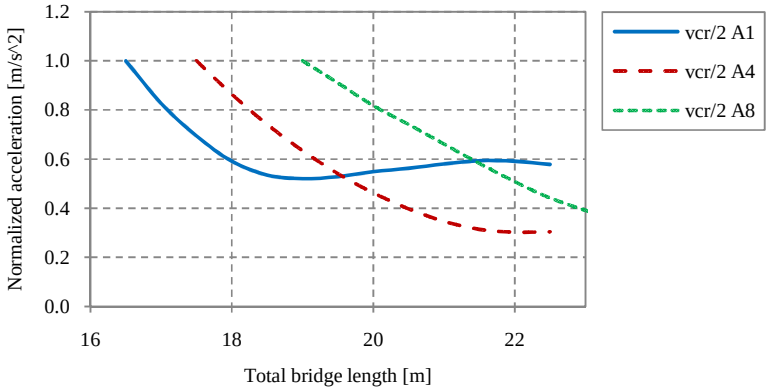

Figure B-25 *Normalized acceleration response in resonance peek at vcr/2 from the response shown by figures B-20-23*

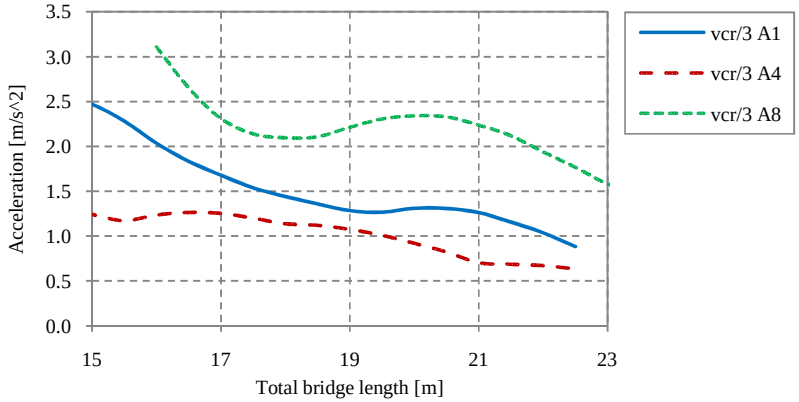

Figure B-26 *Acceleration response in resonance peek at vcr/3 from the response shown by figures B-20-23*

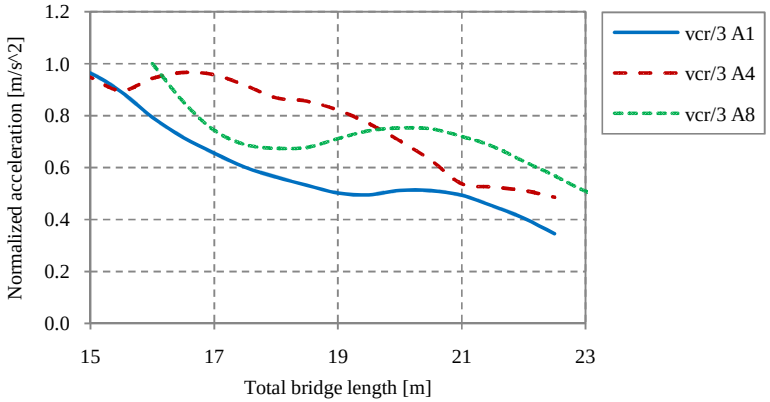

Figure B-27 *Normalized acceleration response in resonance peek at vcr/3 from the response shown by figures B-20-23*

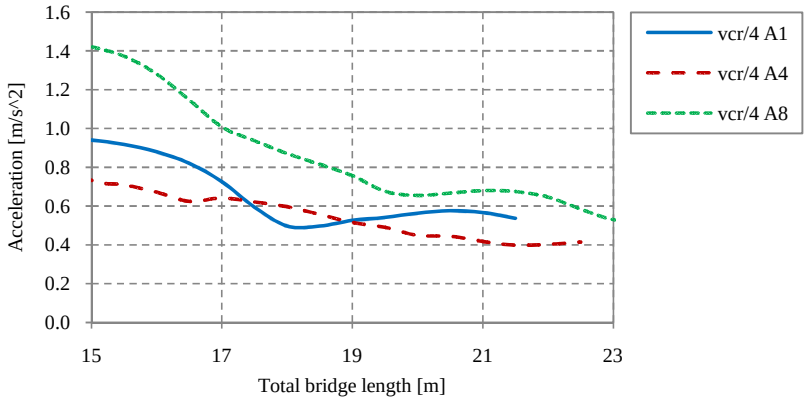

Figure B-28 *Acceleration response in resonance peek at vcr/4 from the response shown by figures B-20-23*

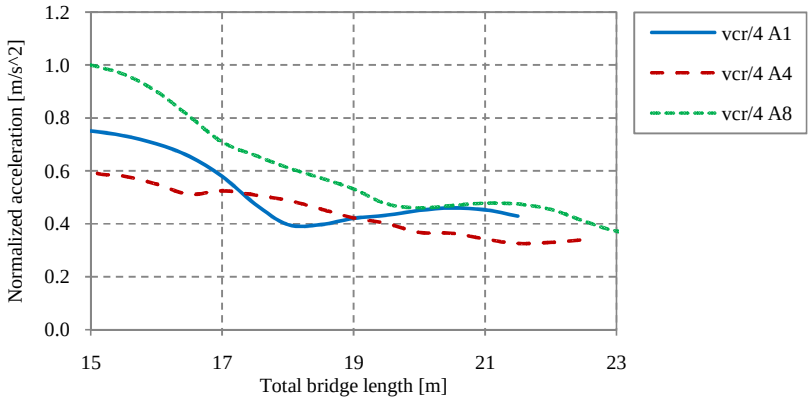

Figure B-29 *Normalized acceleration response in resonance peek at vcr/4 from the response shown by figures B-20-23*

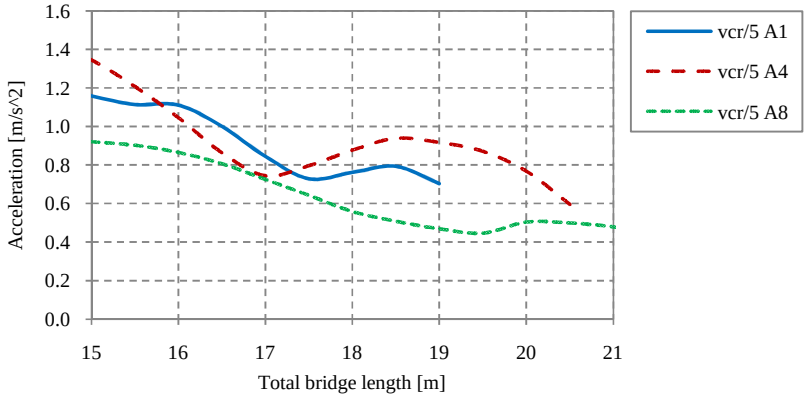

Figure B-30 *Acceleration response in resonance peek at vcr/5 from the response shown by figures B-20-23*

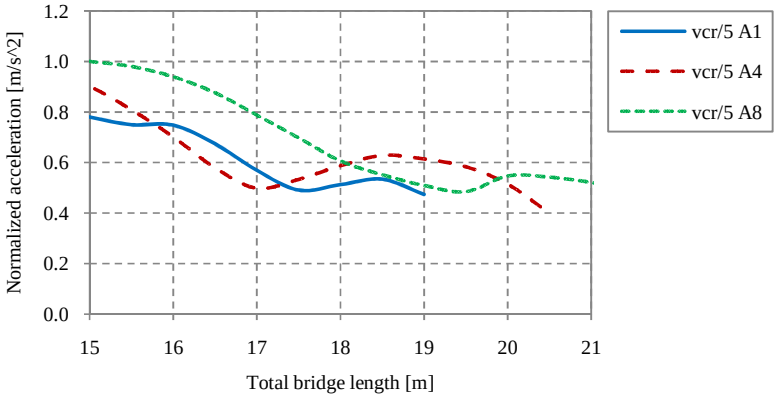

Figure B-31 *Normalized acceleration response in resonance peek at vcr/5 from the response shown by figures B-20-23*

B.5 Variation of damping, c, for a two-span bridge

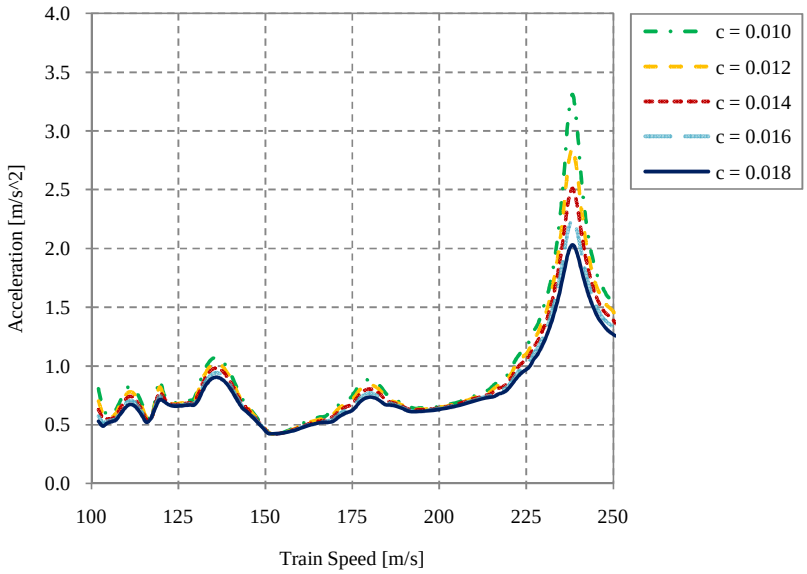

Figure B-32 *Acceleration response for a two-span bridge subjected to HSLM-A1 using E=40 GPa, μ=2, ρ=4000 kg/m^3 and Ltot=15 m*

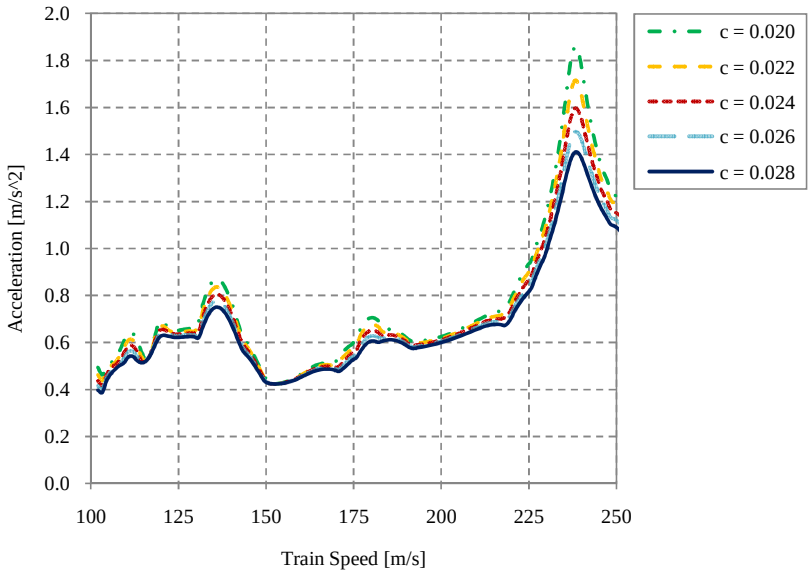

Figure B-33 *Acceleration response for a two-span bridge subjected to HSLM-A1 using E=40 GPa, μ=2, ρ=4000 kg/m^3 and Ltot=15 m*

B.6 Variation of module of elasticity, E, and density, ρ, for a three-span bridge

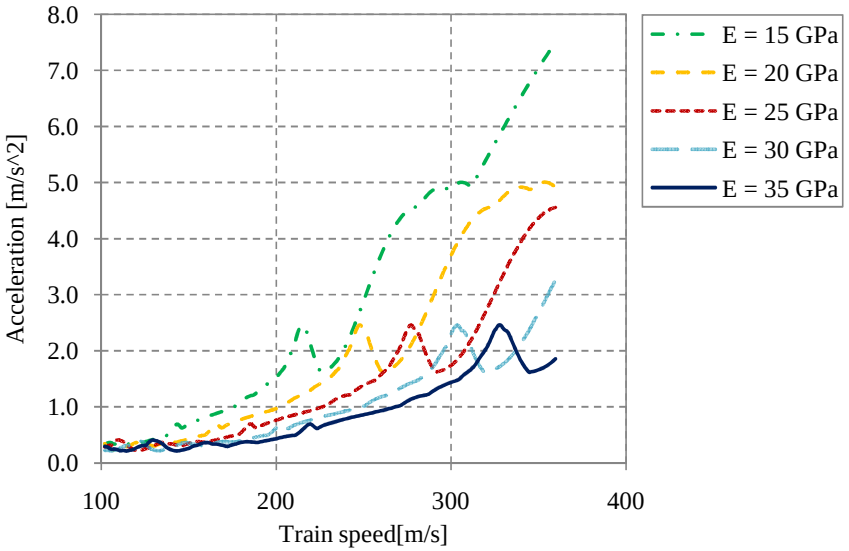

Figure B-34 *Acceleration response for a three-span bridge subjected to HSLM-A1 using ρ=3000 kg/m^3, μ=1, Ltot=25 m, , κ= 1 and c=0.02*

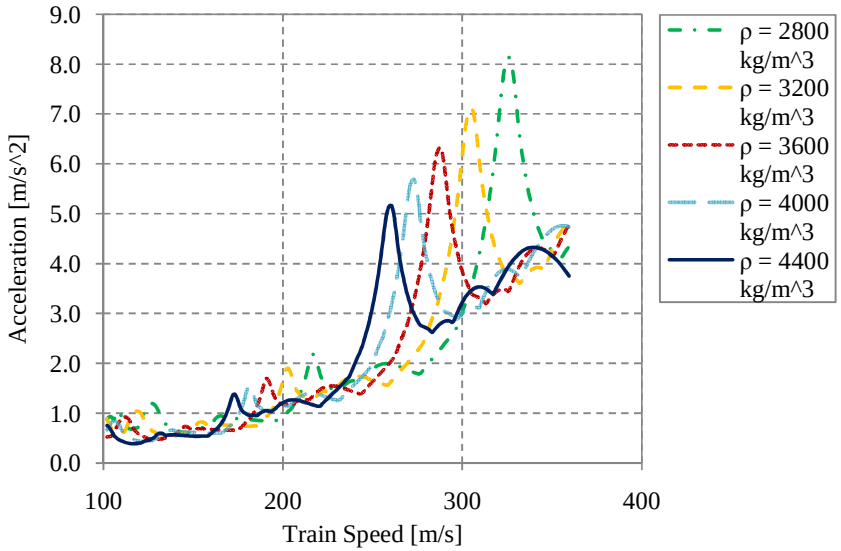

Figure B-35 *Acceleration response for a three-span bridge subjected to HSLM-A1 using E=40 GPa, μ=1, Ltot=25 m, , κ= 1 and c=0.02*

B.7 Variation of span relation, η, for a three-span bridge

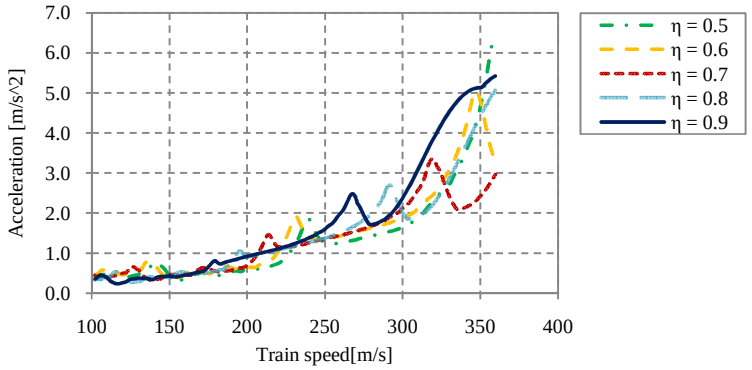

Figure B-36 *Acceleration response for a three-span bridge subjected to HSLM-A1 using E=20 GPa, L=20 m, ρ=2500 kg/m^3, κ= 1 and c=0.02*

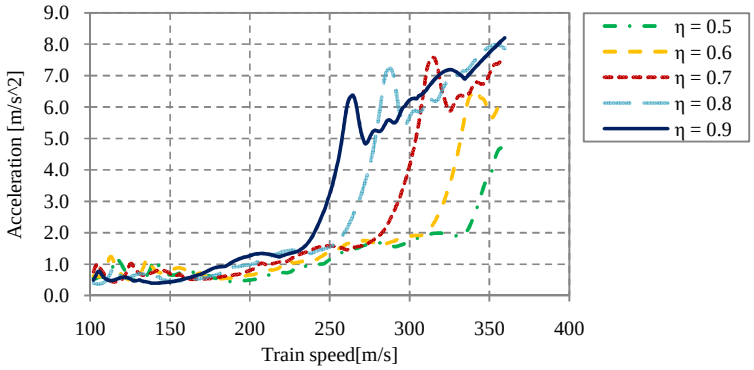

Figure B-37 *Acceleration response for a three-span bridge subjected to HSLM-A4 using E=14 GPa, L=20 m, ρ=2500 kg/m^3, κ= 1 and c=0.02*

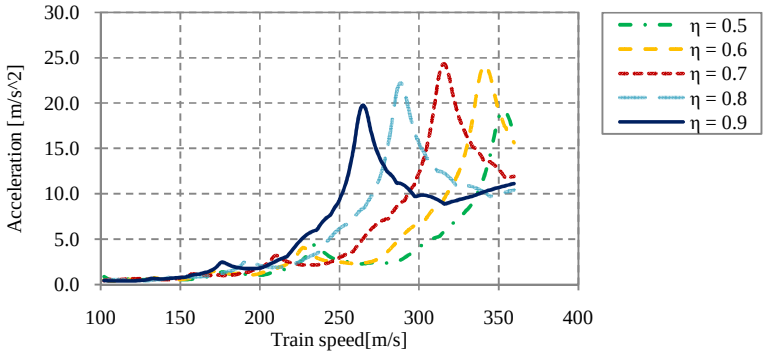

Figure B-38 *Acceleration response for a three-span bridge subjected to HSLM-A8 using E=10 GPa, L=20 m, ρ=2500 kg/m^3, κ= 1 and c=0.02*

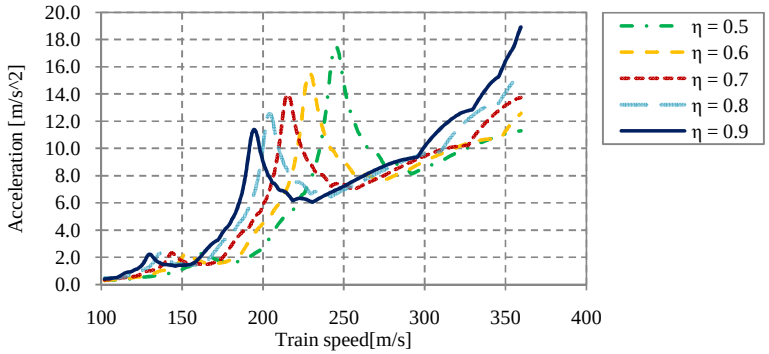

Figure B-39 *Acceleration response for a three-span bridge subjected to HSLM-A8 using E=10 GPa, L=20 m, ρ=2500 kg/m^3, κ= 1 and c=0.02*

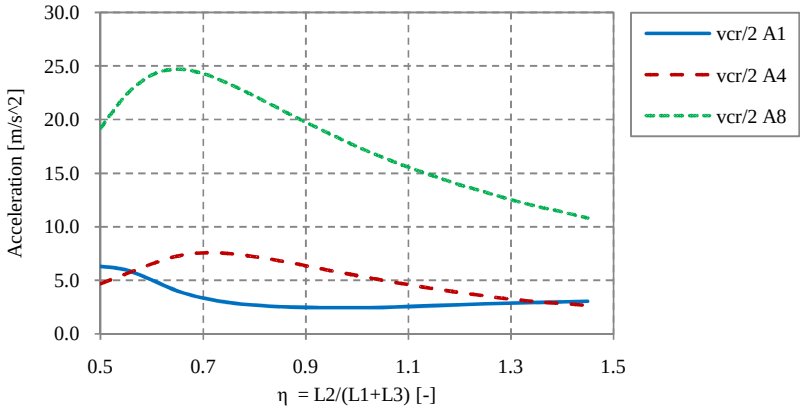

Figure B-40 *Acceleration response in resonance peek at vcr/2 from the response shown by figures B-36-39*

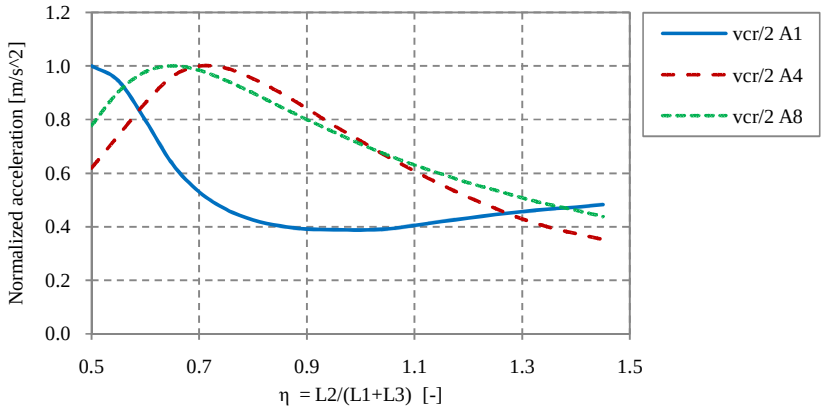

Figure B-41 *Normalized acceleration response in resonance peek at vcr/2 from the response shown by figures B-36-39*

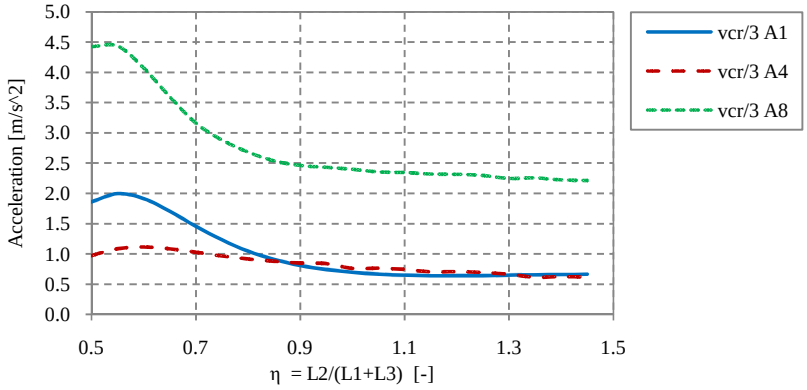

Figure B-42 *Acceleration response in resonance peek at vcr/3 from the response shown by figures B-36-39*

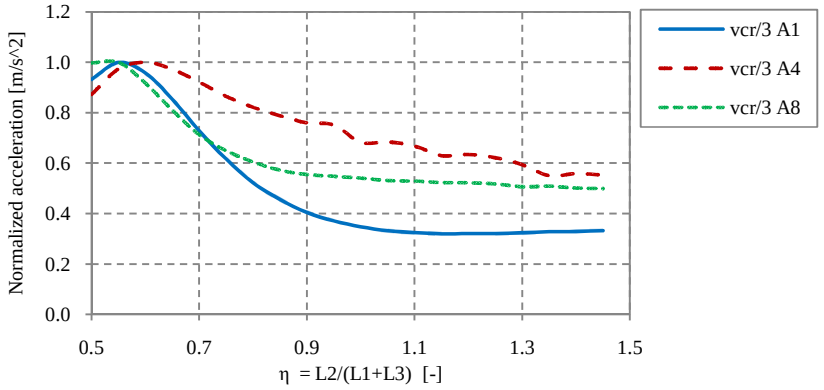

Figure B-43 *Normalized acceleration response in resonance peek at vcr/4 from the response shown by figures B-36-39*

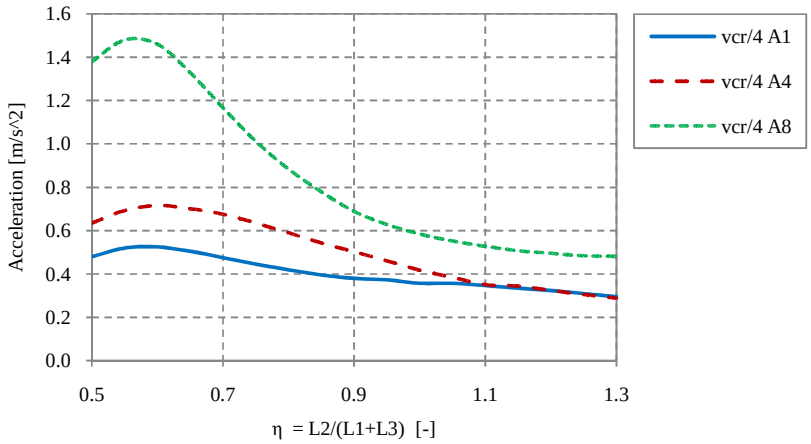

Figure B-44 *Acceleration response in resonance peek at vcr/4 from the response shown by figures B-36-39*

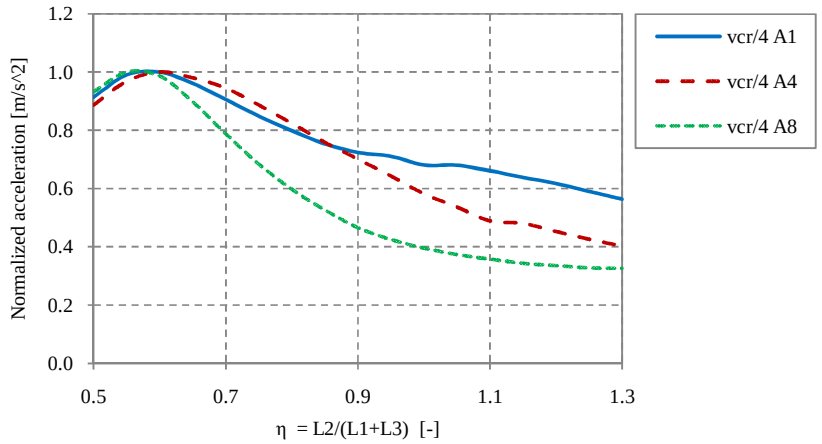

Figure B-45 *Normalized acceleration response in resonance peek at vcr/4 from the response shown by figures B-36-39*

C. Appendix C

The design curves from the three different case studies are gathered in this appendix. The different bridge configurations are:

- Single-span bridge – Section C.1
- Two-span bridge with equal span lengths – Section C.2
- Three-span bridge with equal span lengths – Section C.3

Further description and explanation of the three case studies can be found in section 3.6.4. The layout of each section in this appendix is first a summation of the design curves for all bridge lengths considered in the each case study, followed by the design curves for each specific bridge length with the possibility to see which load that governs the response at a specific choice of β.

C. APPENDIX C 133

C.1 Bridge with one span 134
C.1.1 Total length 7 m 135
C.1.2 Total length 8 m 136
C.1.3 Total length 10 m 138
C.1.4 Total length 11 m 139
C.1.5 Total length 12 m 140
C.1.6 Total length 13 m 141
C.1.7 Total length 14 m 142
C.1.8 Total length 15 m 143
C.1.9 Total length 16 m 144
C.1.10 Total length 17 m 145
C.1.11 Total length 18 m 146
C.1.12 Total length 19 m 147
C.1.13 Total length 20 m 148

C.2 Bridge with two equal spans 149
C.2.1 Total length 16 m 150
C.2.2 Total length 18 m 151
C.2.3 Total length 20 m 152
C.2.4 Total length 22 m 153
C.2.5 Total length 24 m 154
C.2.6 Total length 26 m 155
C.2.7 Total length 28 m 156
C.2.8 Total length 30 m 157

C.3 Bridge with three equal spans 158
C.3.1 Total length 30 m 159
C.3.2 Total length 31.5 m 160
C.3.3 Total length 33 m 161
C.3.4 Total length 34.5 m 162
C.3.5 Total length 36 m 163
C.3.6 Total length 37.5 m 164
C.3.7 Total length 39 m 165
C.3.8 Total length 40.5 m 166
C.3.9 Total length 42 m 167
C.3.10 Total length 43.5 m 168

C.1 Bridge with one span

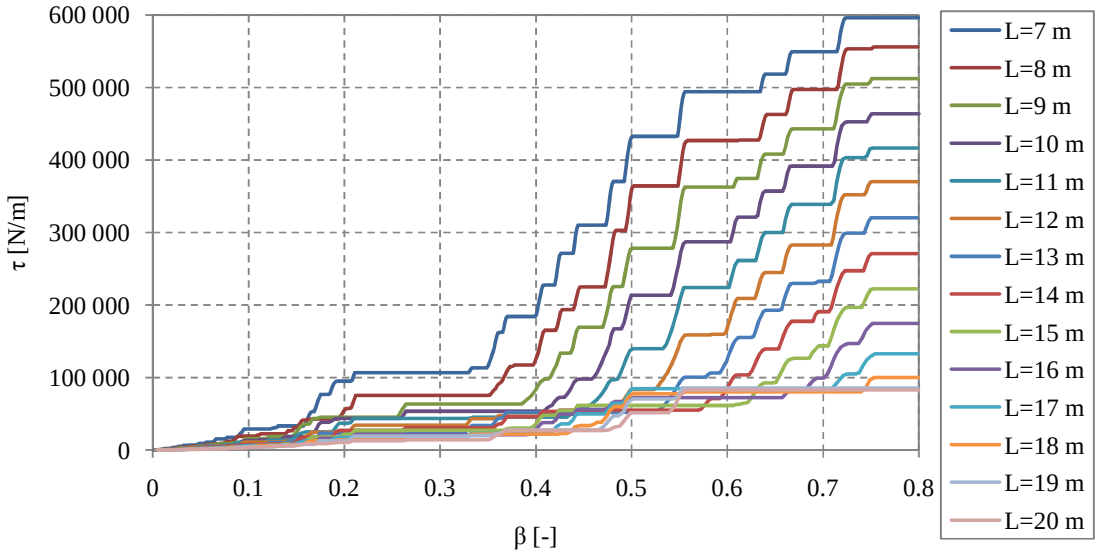

Figure C-1 *Design curves of the relation between β and τ for the HSLM-A loads of a bridge with one span and L_{tot}=7 m to L_{tot}=20 m .*

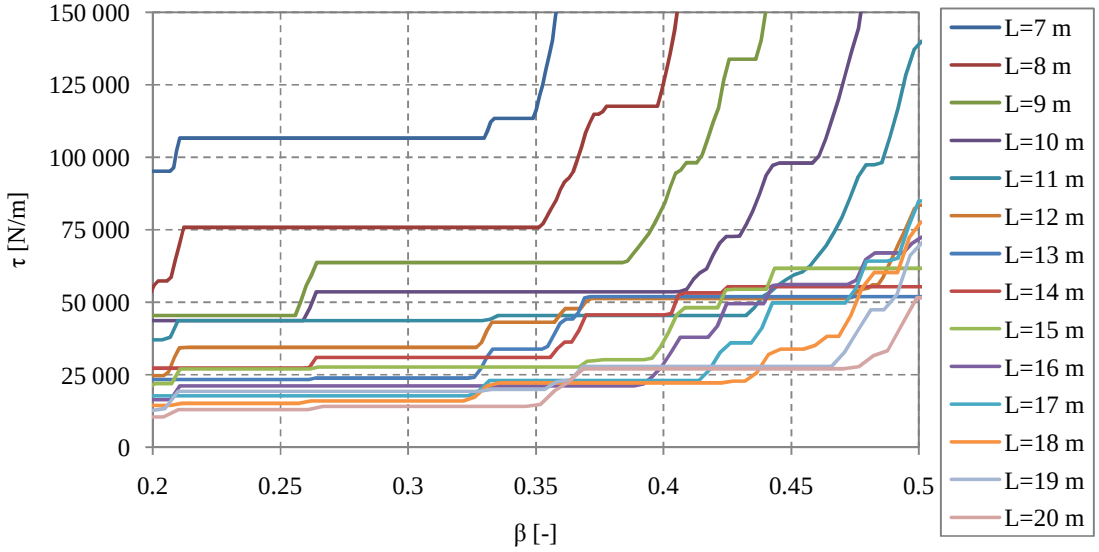

Figure C-2 *Design curves of the relation between β and τ for the HSLM-A loads of a bridge with one span and L_{tot}= 7 m to L_{tot}=20 m.*

C.1.1 Total length 7 m

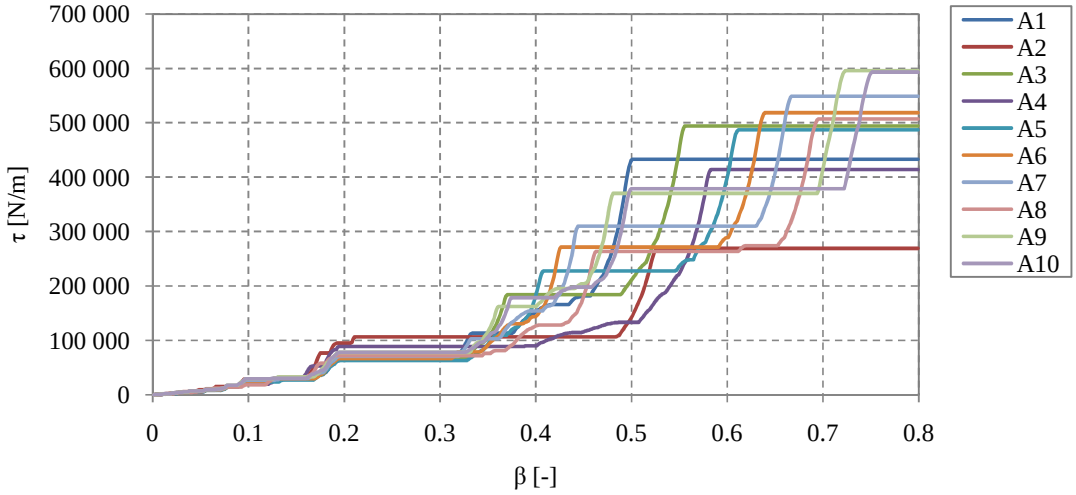

Figure C-3 *Relation between β and τ for load A1 to A10 for a bridge with one span and L_{tot}=7 m.*

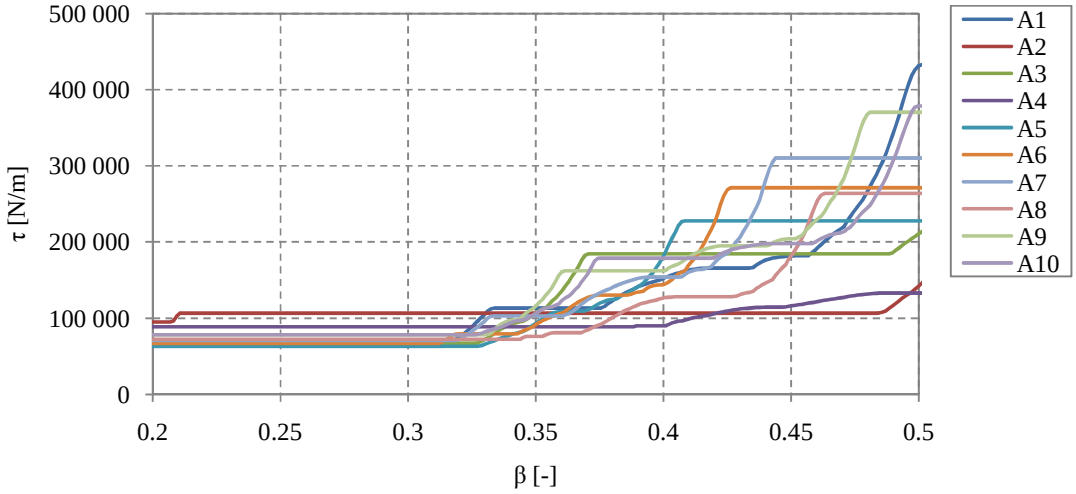

Figure C-4 *Relation between β and τ for load A1 to A10, with a zoom at β=0.2 to β=0.5, for a bridge with one span and L_{tot}=7 m.*

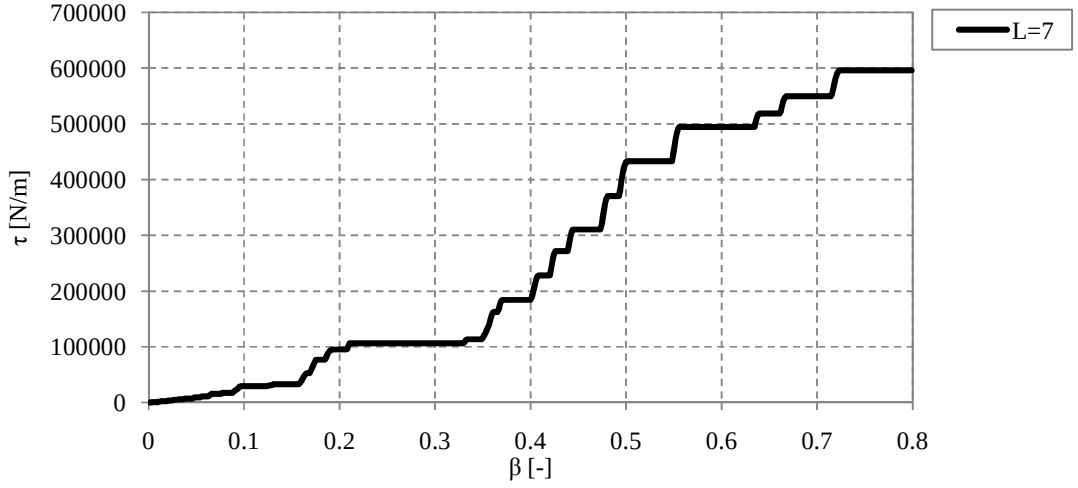

Figure C-5 *Design curve of the relation between β and τ for the HSLM-A loads of a bridge with one span and L_{tot}=7 m.*

C.1.2 Total length 8 m

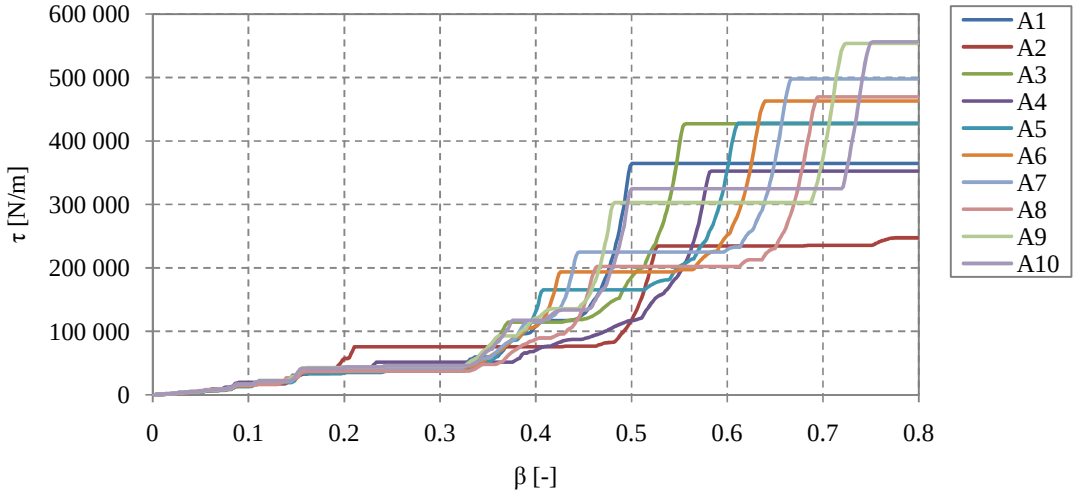

Figure C-6 *Relation between β and τ for load A1 to A10 for a bridge with one span and L_{tot}=8 m.*

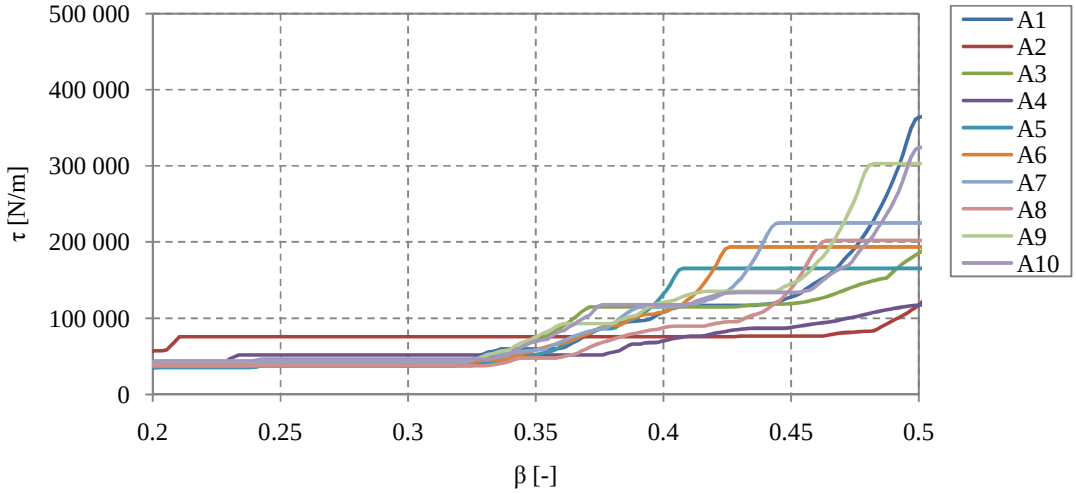

Figure C-7 *Relation between β and τ for load A1 to A10, with a zoom at β=0.2 to β=0.5, for a bridge with one span and L_{tot}=8 m.*

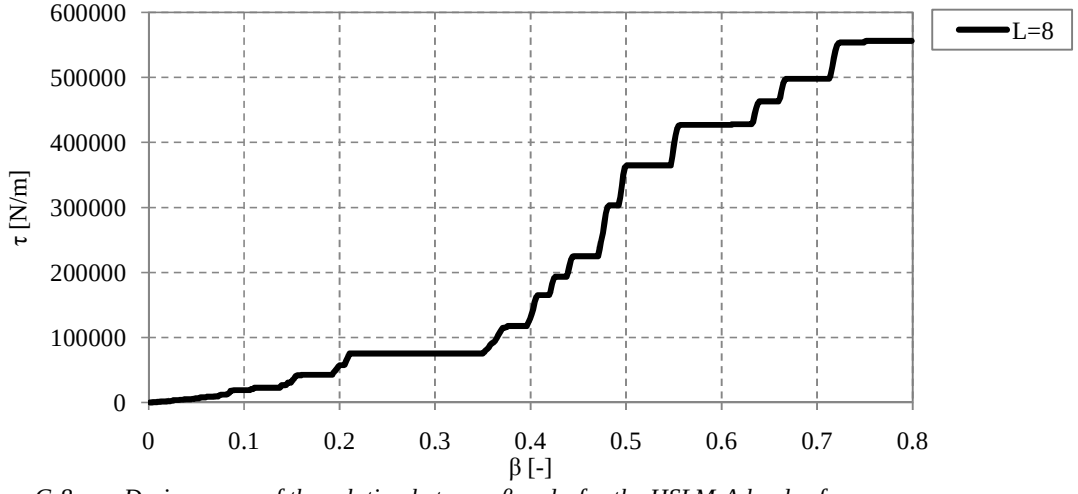

Figure C-8 *Design curve of the relation between β and τ for the HSLM-A loads of a bridge with one span and L_{tot}=8 m.*

Total length 9 m

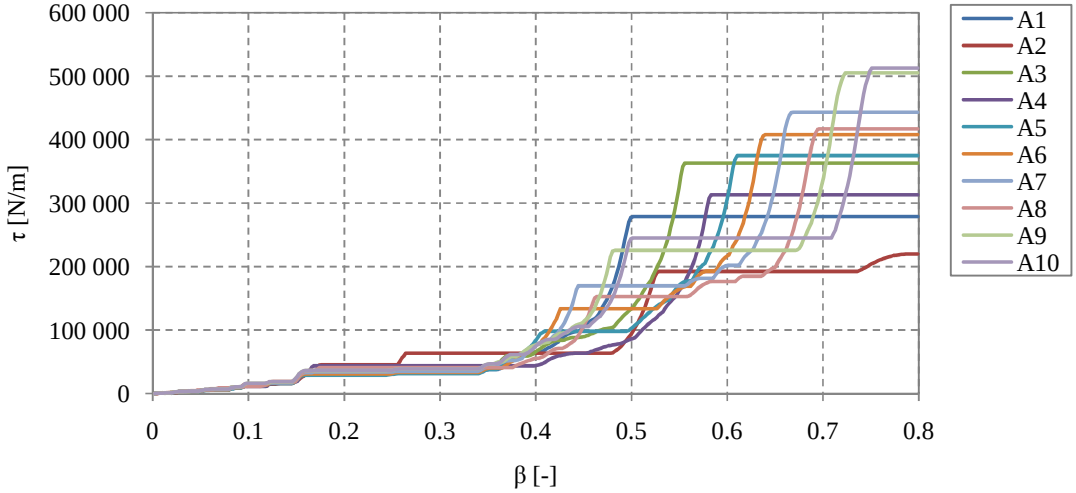

Figure C-9 *Relation between β and τ for load A1 to A10 for a bridge with one span and L_{tot}=9 m.*

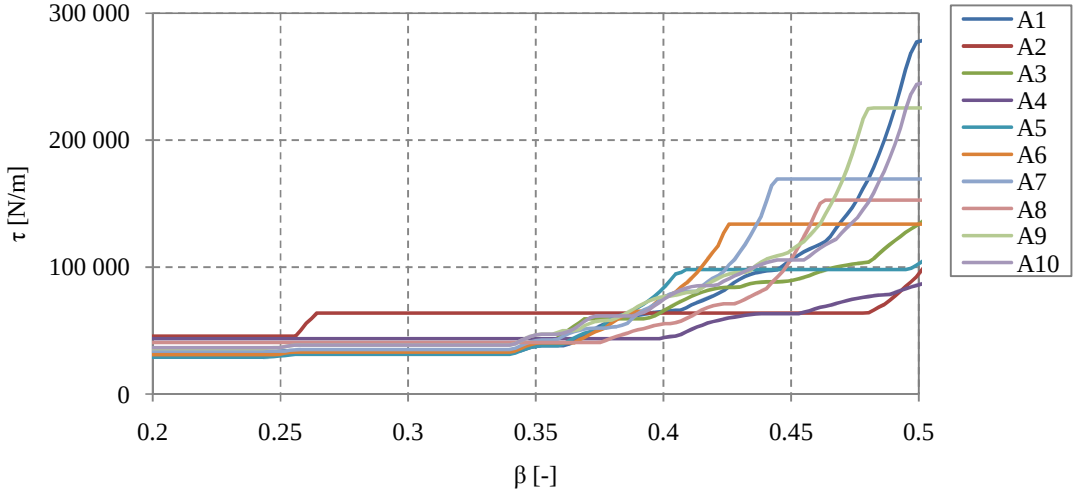

Figure C-10 *Relation between β and τ for load A1 to A10, with a zoom at β=0.2 to β=0.5, for a bridge with one span and L_{tot}=9 m.*

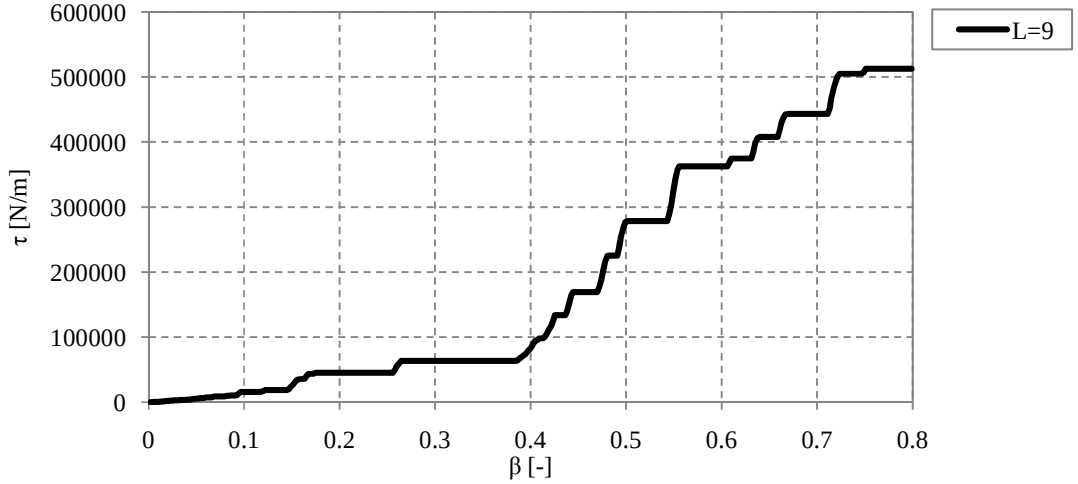

Figure C-11 *Design curve of the relation between β and τ for the HSLM-A loads of a bridge with one span and L_{tot}=9 m.*

C.1.3 Total length 10 m

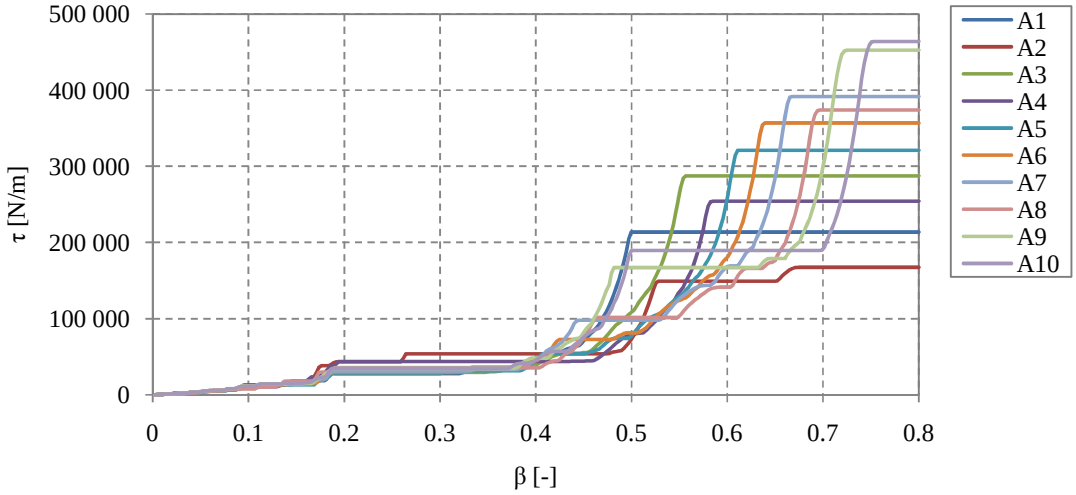

Figure C-12 *Relation between β and τ for load A1 to A10 for a bridge with one span and L_{tot}=10 m.*

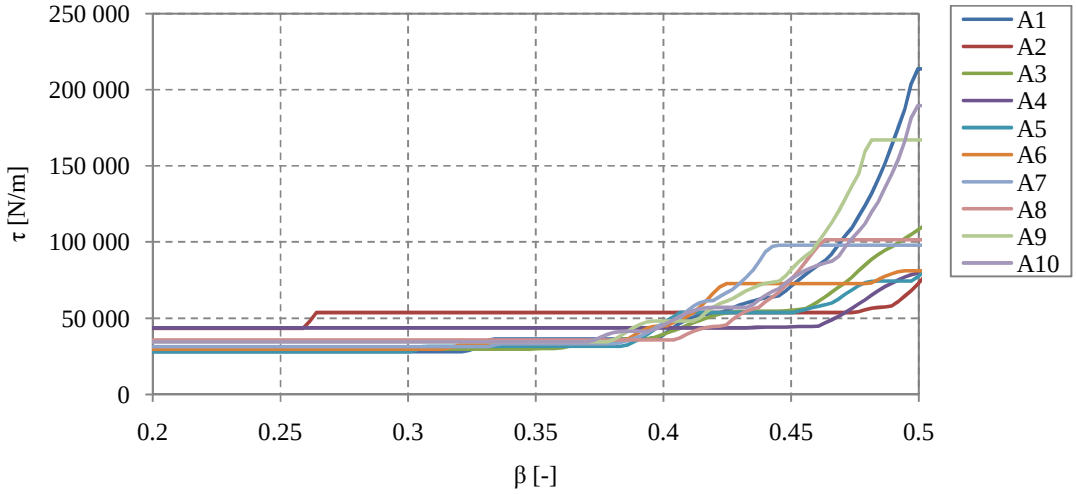

Figure C-13 *Relation between β and τ for load A1 to A10, with a zoom at β=0.2 to β=0.5, for a bridge with one span and L_{tot}=10 m.*

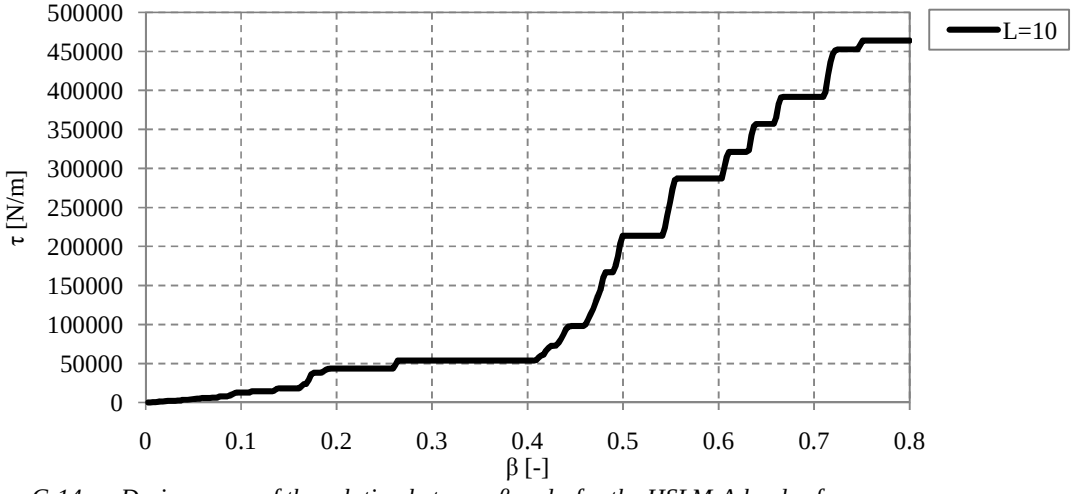

Figure C-14 *Design curve of the relation between β and τ for the HSLM-A loads of a bridge with one span and L_{tot}=10 m.*

C.1.4 Total length 11 m

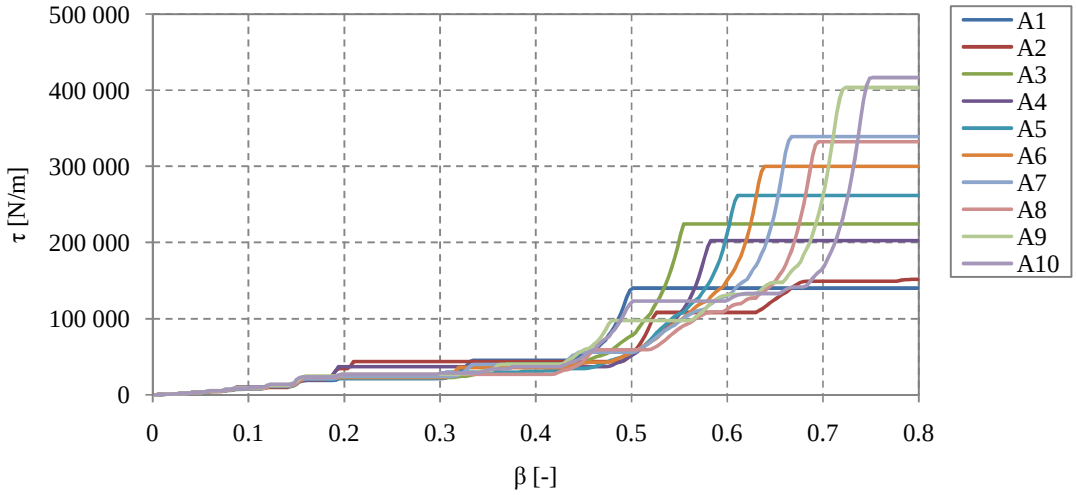

Figure C-15 *Relation between β and τ for load A1 to A10 for a bridge with one span and L_{tot}=11 m.*

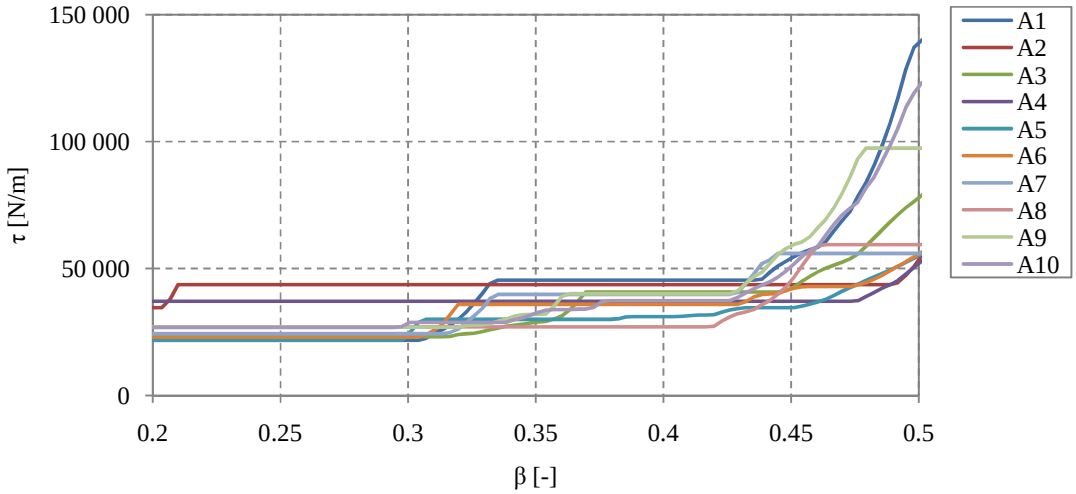

Figure C-16 *Relation between β and τ for load A1 to A10, with a zoom at β=0.2 to β=0.5, for a bridge with one span and L_{tot}=11 m.*

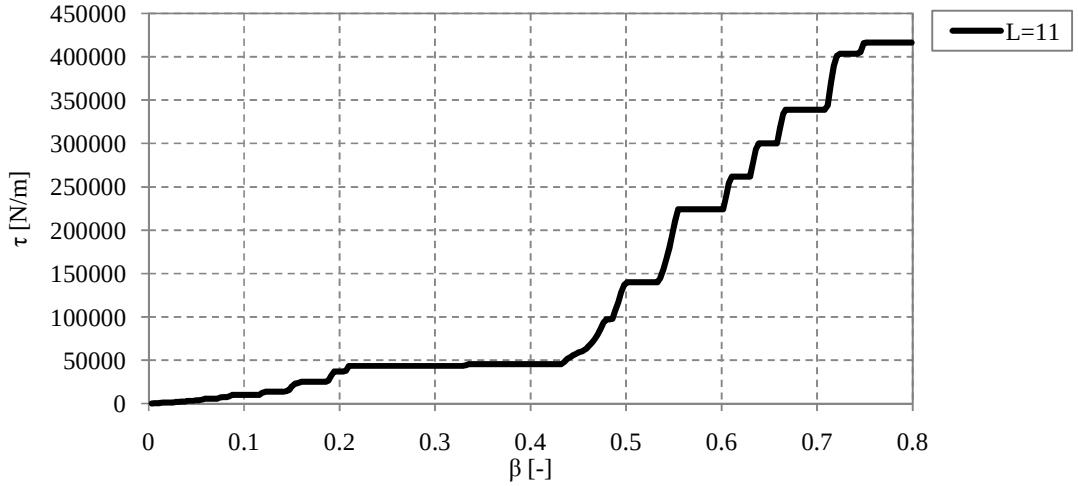

Figure C-17 *Design curve of the relation between β and τ for the HSLM-A loads of a bridge with one span and L_{tot}=11 m.*

C.1.5 Total length 12 m

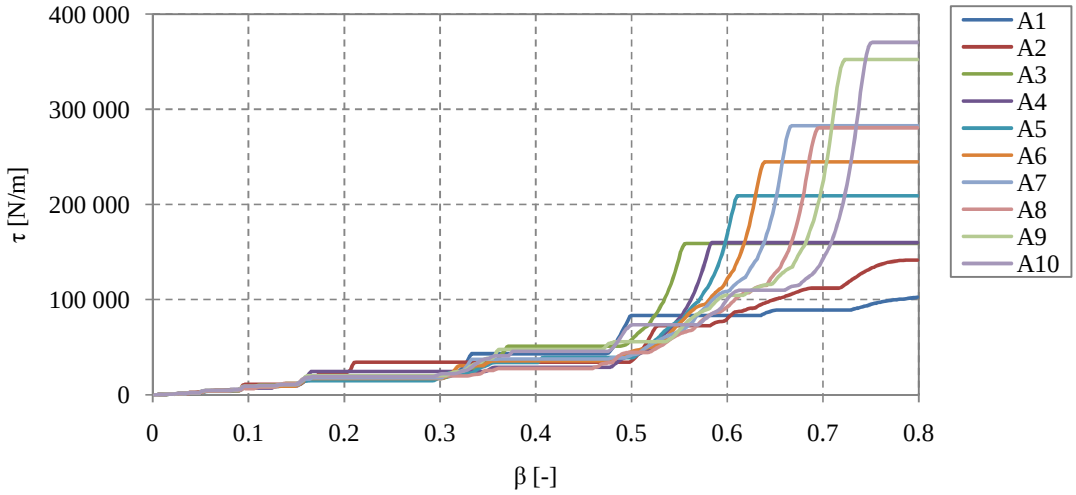

Figure C-18 *Relation between β and τ for load A1 to A10 for a bridge with one span and L_{tot}=12 m.*

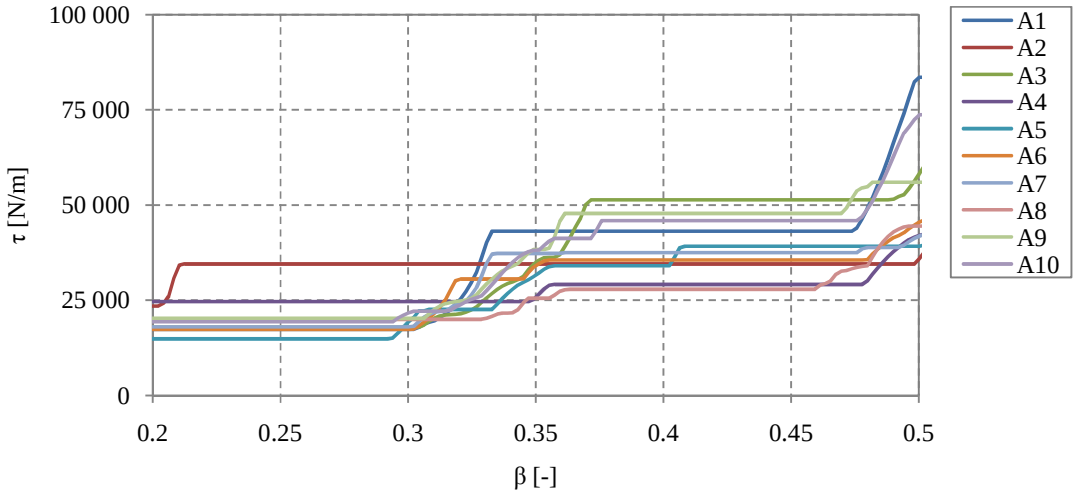

Figure C-19 *Relation between β and τ for load A1 to A10, with a zoom at β=0.2 to β=0.5, for a bridge with one span and L_{tot}=12 m.*

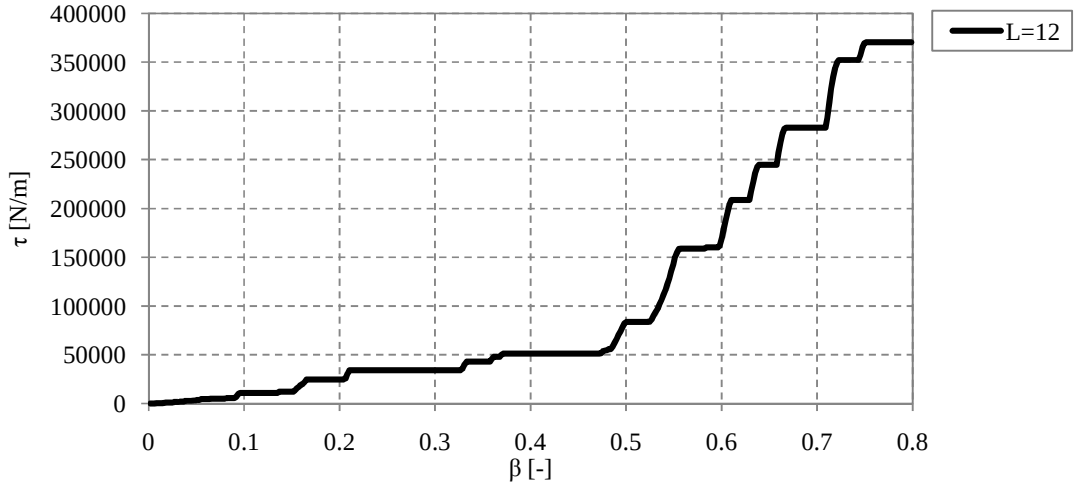

Figure C-20 *Design curve of the relation between β and τ for the HSLM-A loads of a bridge with one span and L_{tot}=12 m.*

C.1.6 Total length 13 m

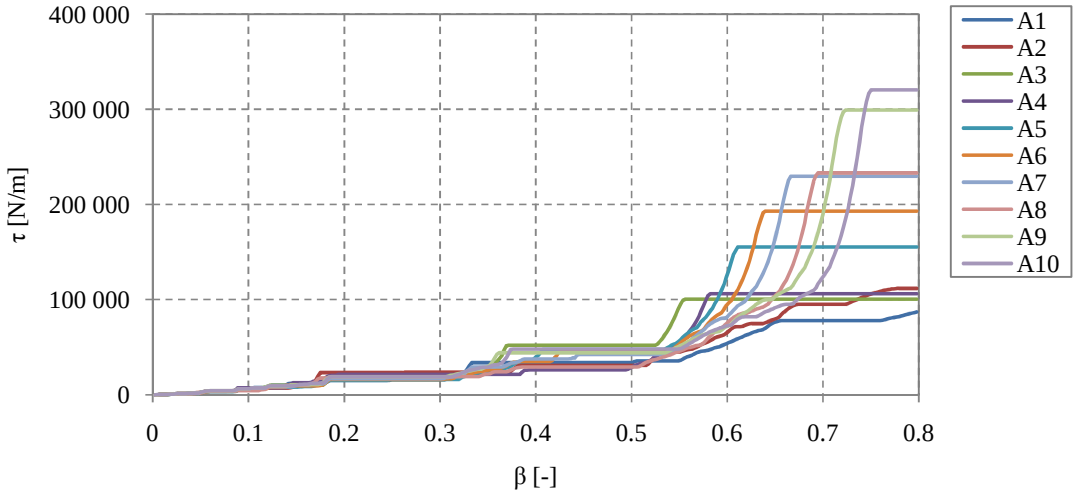

Figure C-21 *Relation between β and τ for load A1 to A10 for a bridge with one span and L_{tot}=13 m.*

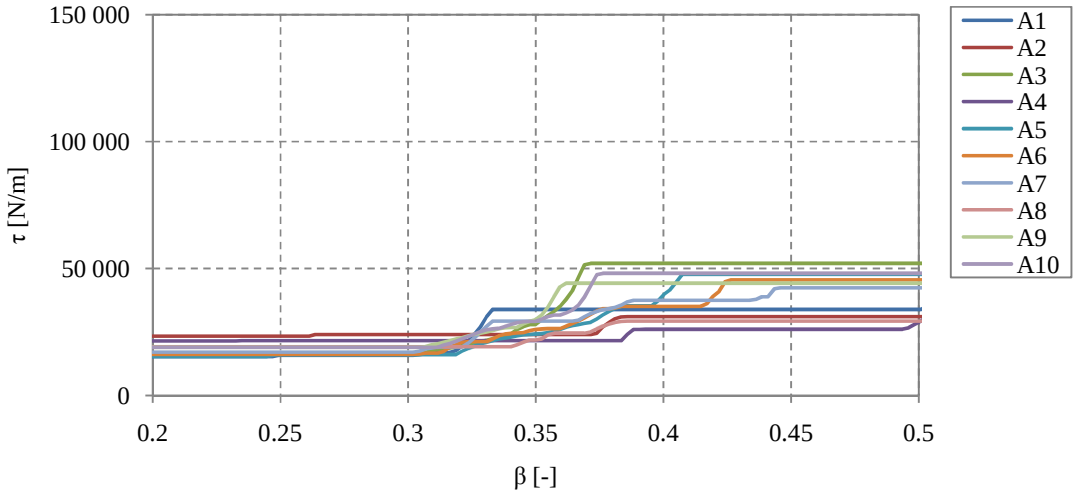

Figure C-22 *Relation between β and τ for load A1 to A10, with a zoom at β=0.2 to β=0.5, for a bridge with one span and L_{tot}=13 m.*

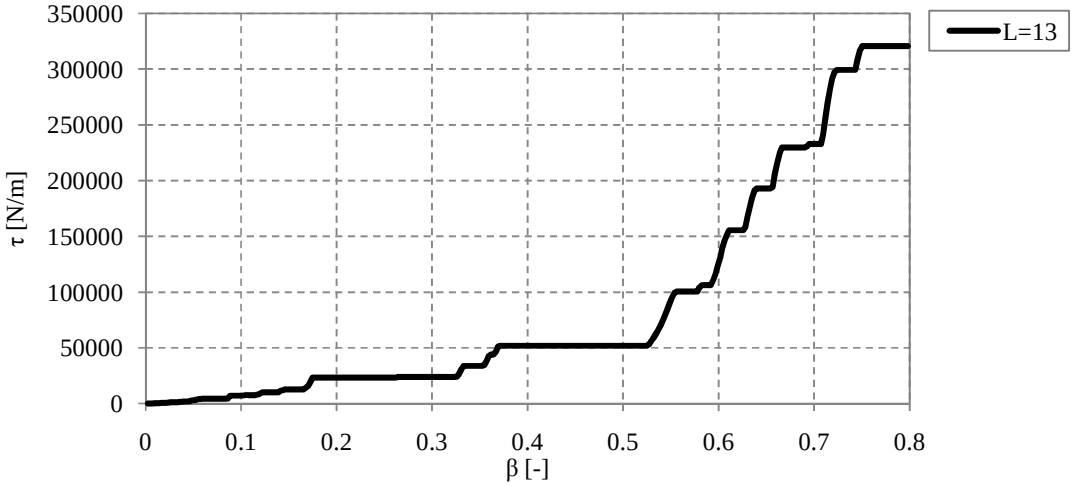

Figure C-23 *Design curve of the relation between β and τ for the HSLM-A loads of a bridge with one span and L_{tot}=13 m.*

C.1.7 Total length 14 m

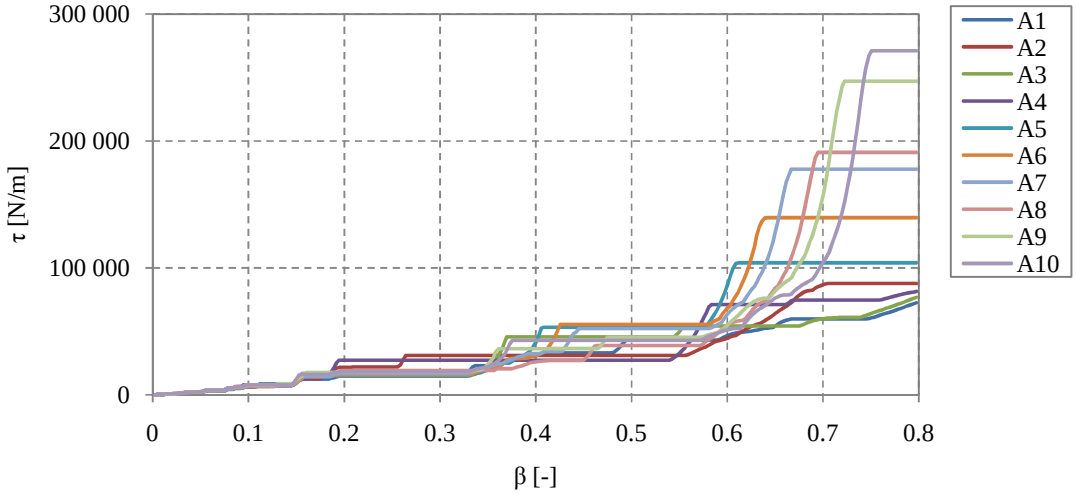

Figure C-24 *Relation between β and τ for load A1 to A10 for a bridge with one span and L_{tot}=14 m.*

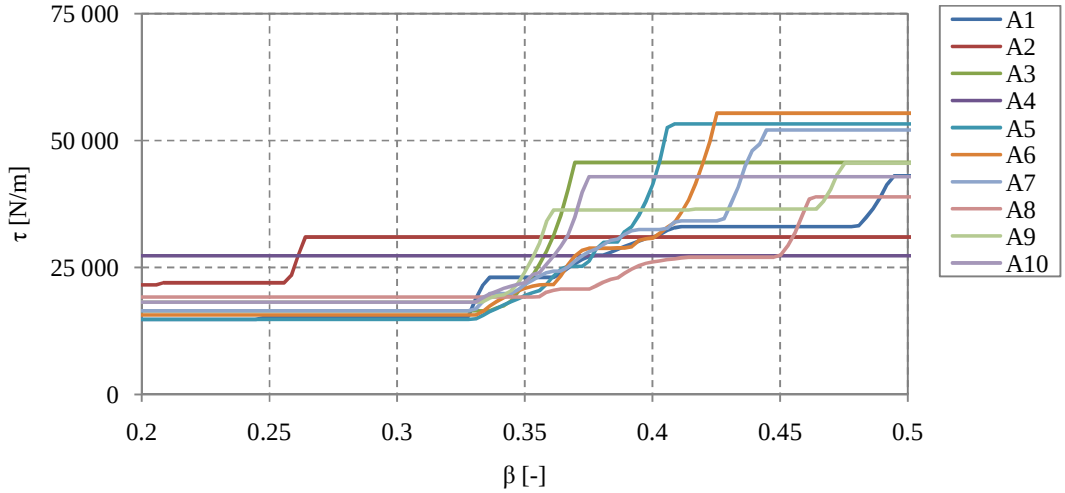

Figure C-25 *Relation between β and τ for load A1 to A10, with a zoom at β=0.2 to β=0.5, for a bridge with one span and L_{tot}=14 m.*

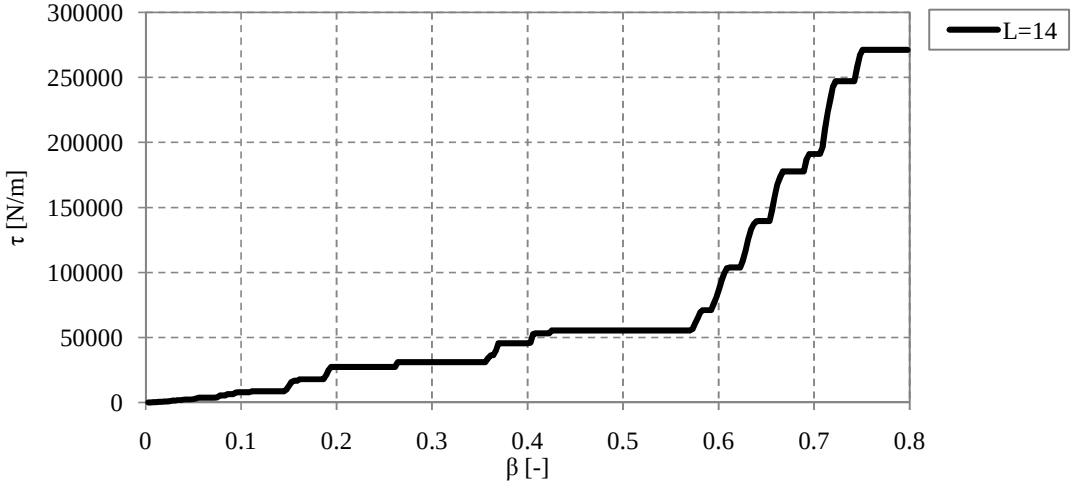

Figure C-26 *Design curve of the relation between β and τ for the HSLM-A loads of a bridge with one span and L_{tot}=14 m.*

C.1.8 Total length 15 m

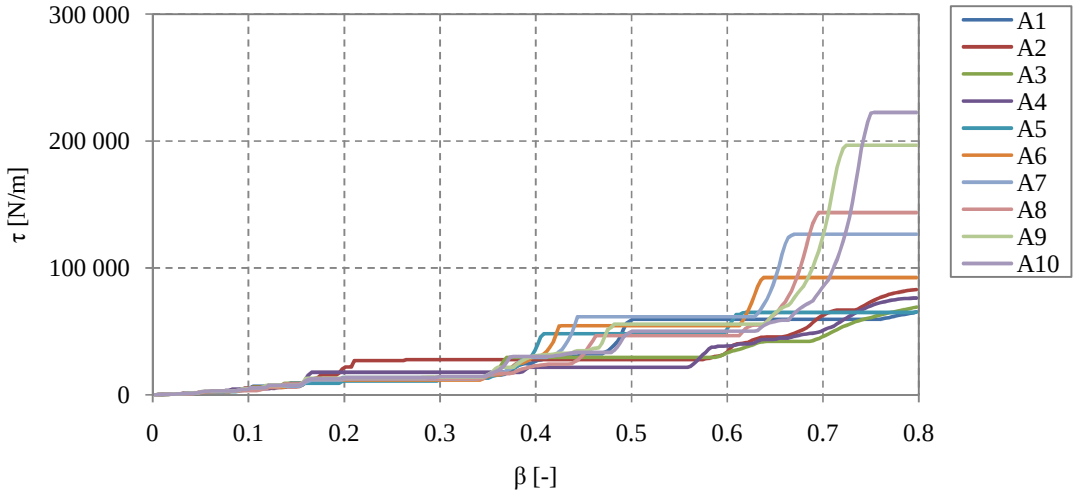

Figure C-27 *Relation between β and τ for load A1 to A10 for a bridge with one span and L_{tot}=15 m.*

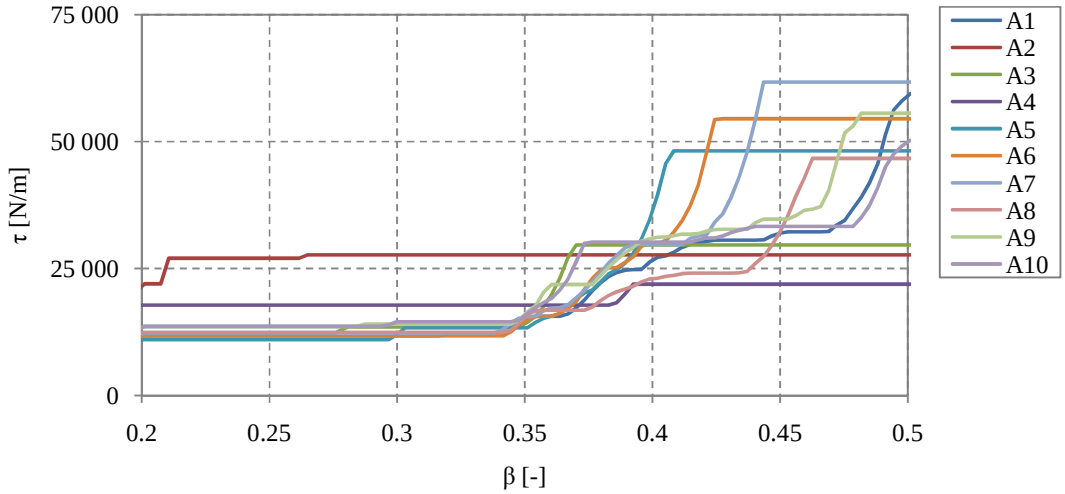

Figure C-28 *Relation between β and τ for load A1 to A10, with a zoom at β=0.2 to β=0.5, for a bridge with one span and L_{tot}=15 m.*

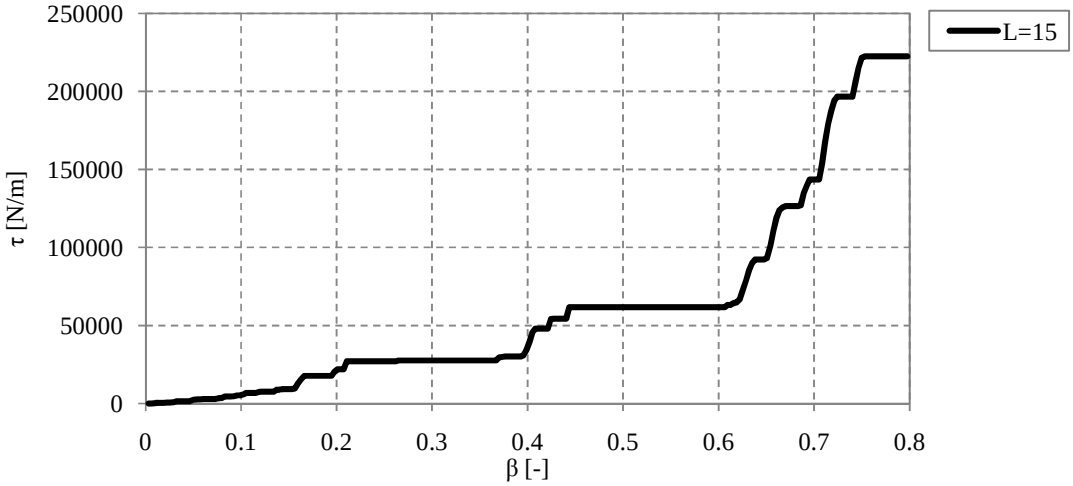

Figure C-29 *Design curve of the relation between β and τ for the HSLM-A loads of a bridge with one span and L_{tot}=15 m.*

C.1.9 Total length 16 m

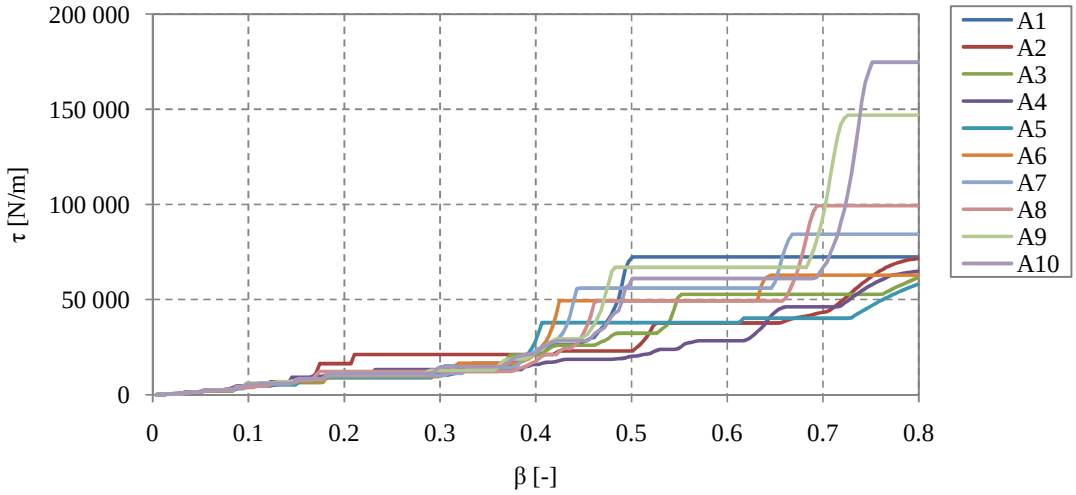

Figure C-30 *Relation between β and τ for load A1 to A10 for a bridge with one span and L_{tot}=16 m.*

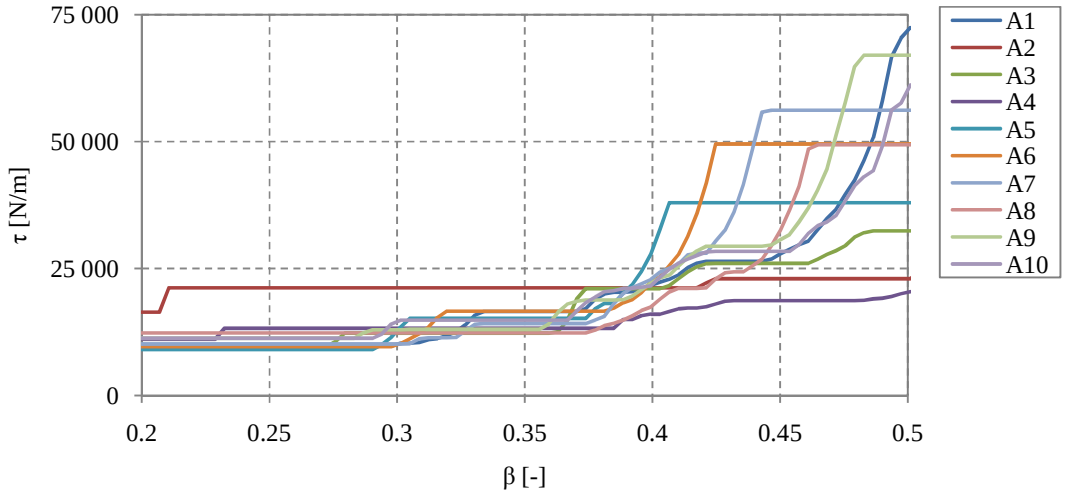

Figure C-31 *Relation between β and τ for load A1 to A10, with a zoom at β=0.2 to β=0.5, for a bridge with one span and L_{tot}=16 m.*

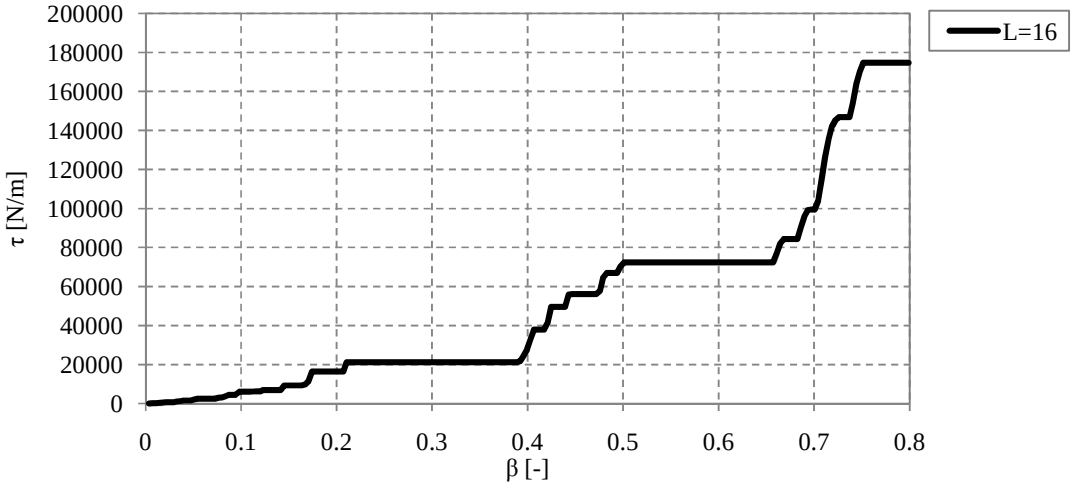

Figure C-32 *Design curve of the relation between β and τ for the HSLM-A loads of a bridge with one span and L_{tot}=16 m.*

C.1.10 Total length 17 m

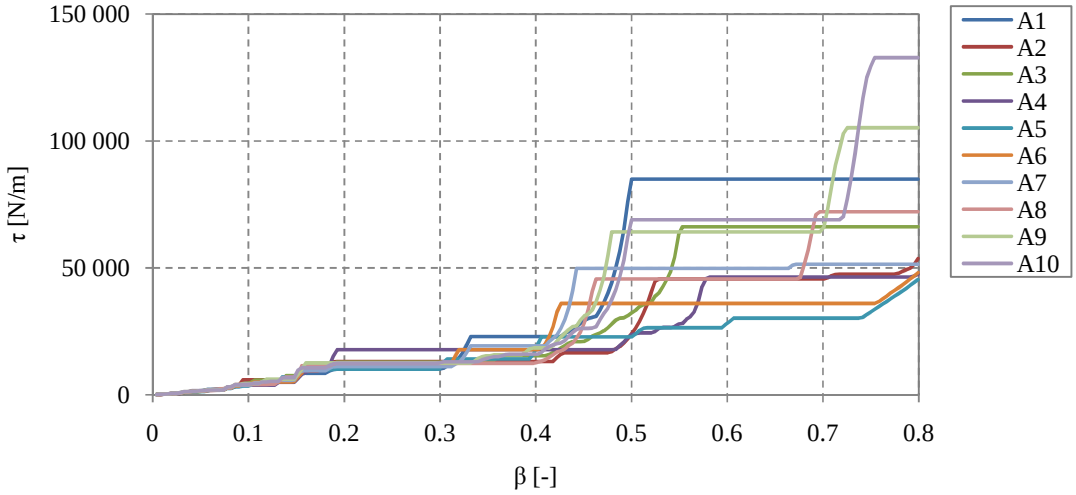

Figure C-33 *Relation between β and τ for load A1 to A10 for a bridge with one span and L_{tot}=17 m.*

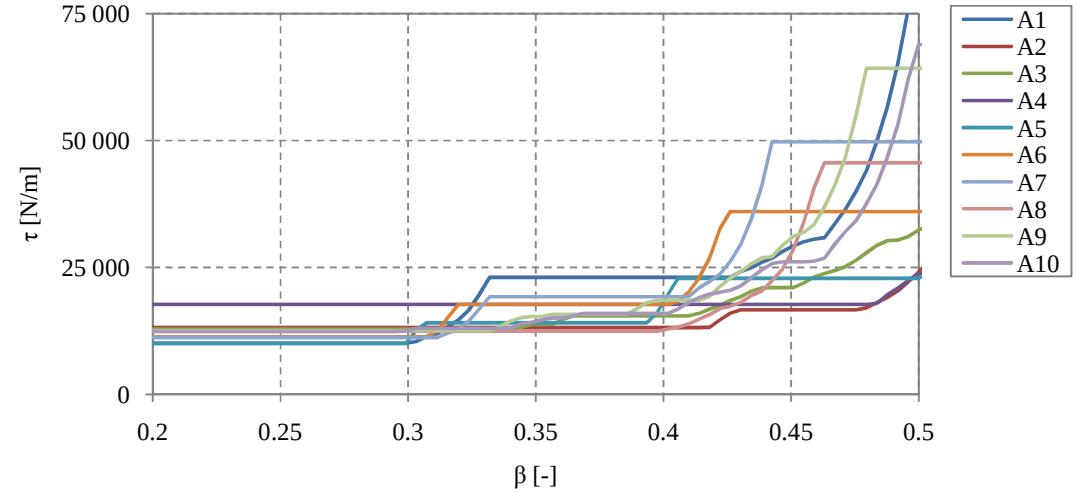

Figure C-34 *Relation between β and τ for load A1 to A10, with a zoom at β=0.2 to β=0.5, for a bridge with one span and L_{tot}=17 m.*

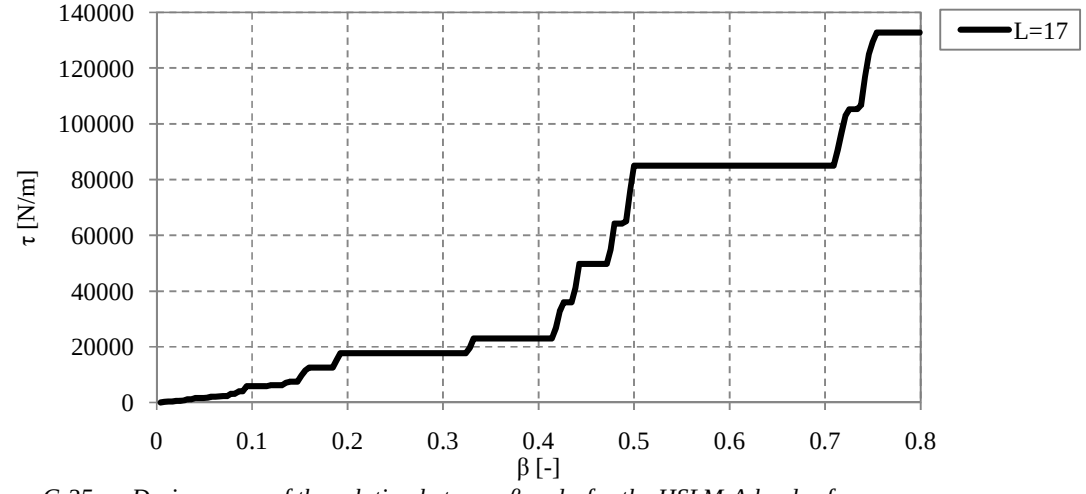

Figure C-35 *Design curve of the relation between β and τ for the HSLM-A loads of a bridge with one span and L_{tot}=17 m.*

C.1.11 Total length 18 m

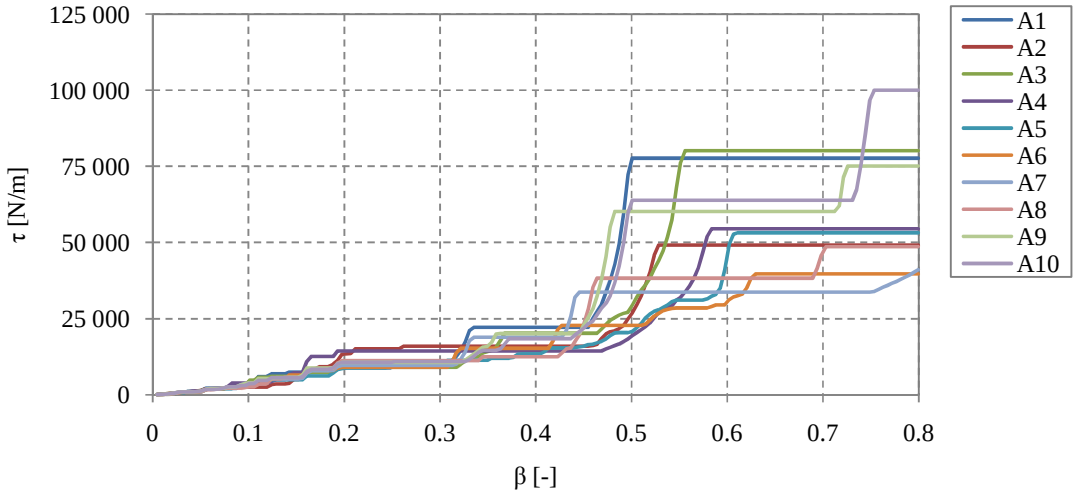

Figure C-36 *Relation between β and τ for load A1 to A10 for a bridge with one span and L_{tot}=18 m.*

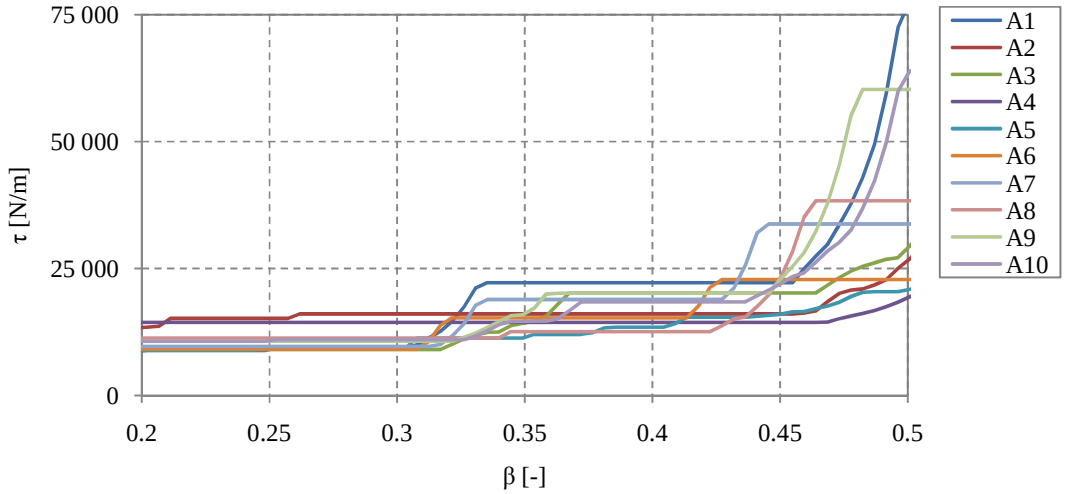

Figure C-37 *Relation between β and τ for load A1 to A10, with a zoom at β=0.2 to β=0.5, for a bridge with one span and L_{tot}=18 m.*

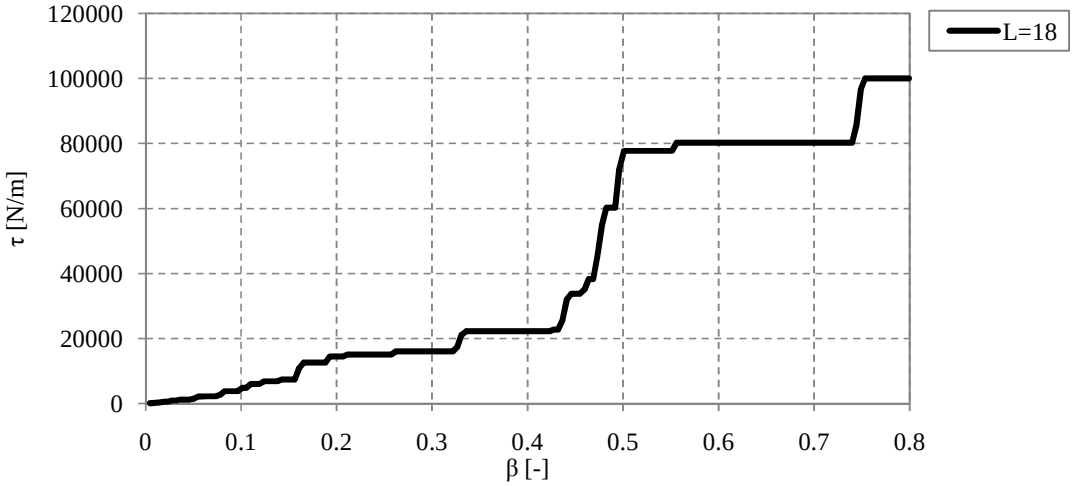

Figure C-38 *Design curve of the relation between β and τ for the HSLM-A loads of a bridge with one span and L_{tot}=18 m.*

C.1.12 Total length 19 m

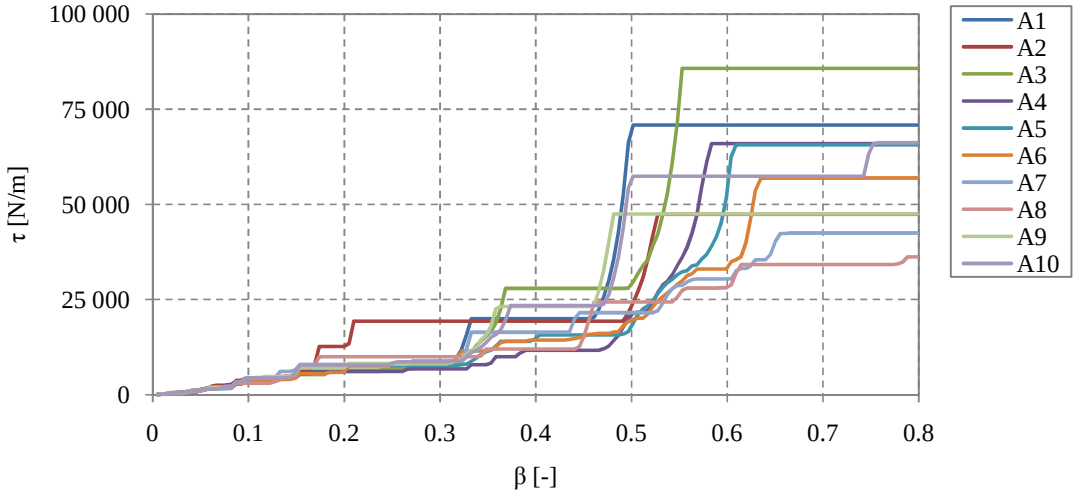

Figure C-39 *Relation between β and τ for load A1 to A10 for a bridge with one span and L_{tot}=19 m.*

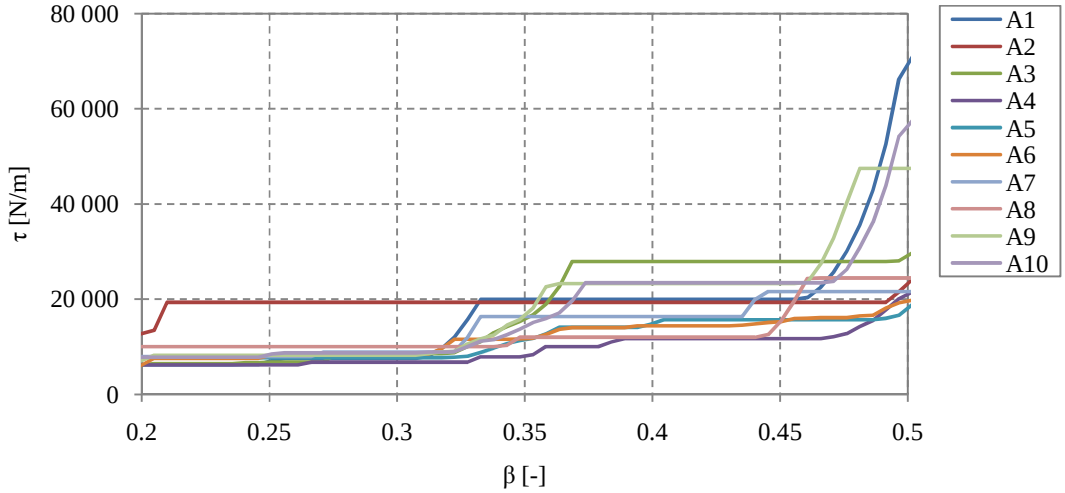

Figure C-40 *Relation between β and τ for load A1 to A10, with a zoom at β=0.2 to β=0.5, for a bridge with one span and L_{tot}=19 m.*

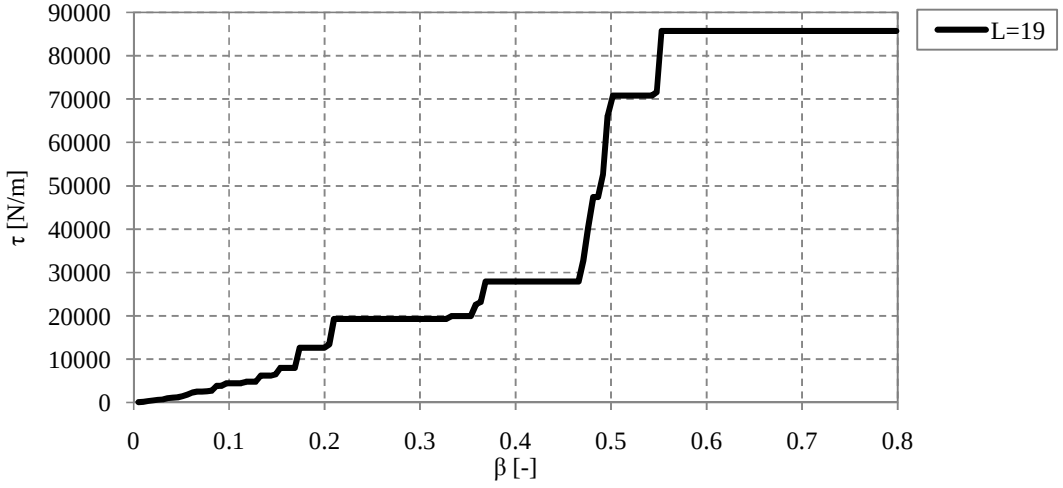

Figure C-41 *Design curve of the relation between β and τ for the HSLM-A loads of a bridge with one span and L_{tot}=19 m.*

C.1.13 Total length 20 m

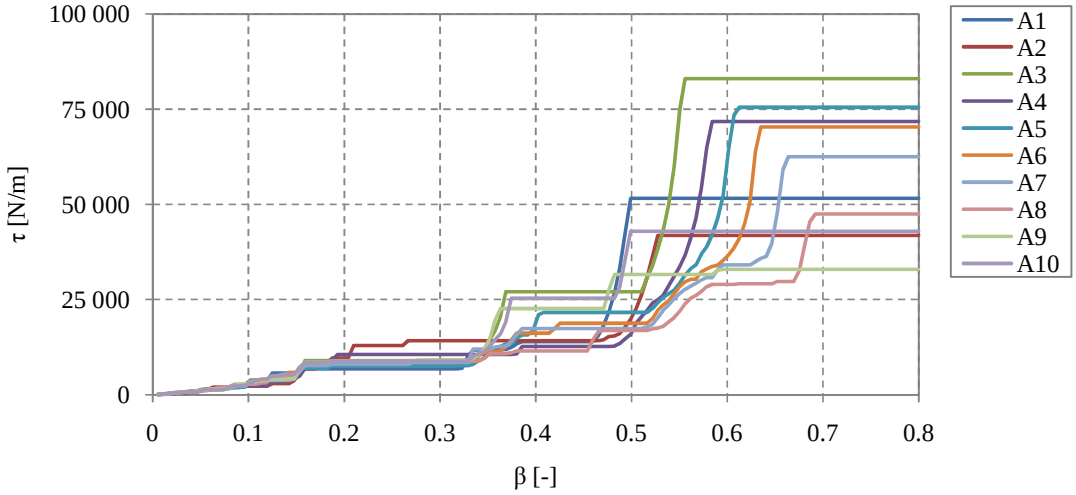

Figure C-42 *Relation between β and τ for load A1 to A10 for a bridge with one span and L_{tot}=20 m.*

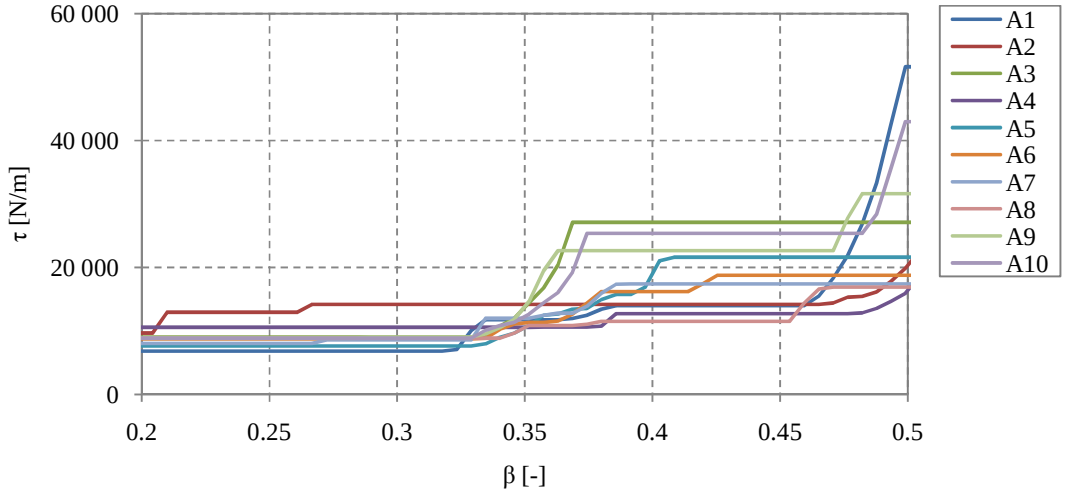

Figure C-43 *Relation between β and τ for load A1 to A10, with a zoom at β=0.2 to β=0.5, for a bridge with one span and L_{tot}=20 m.*

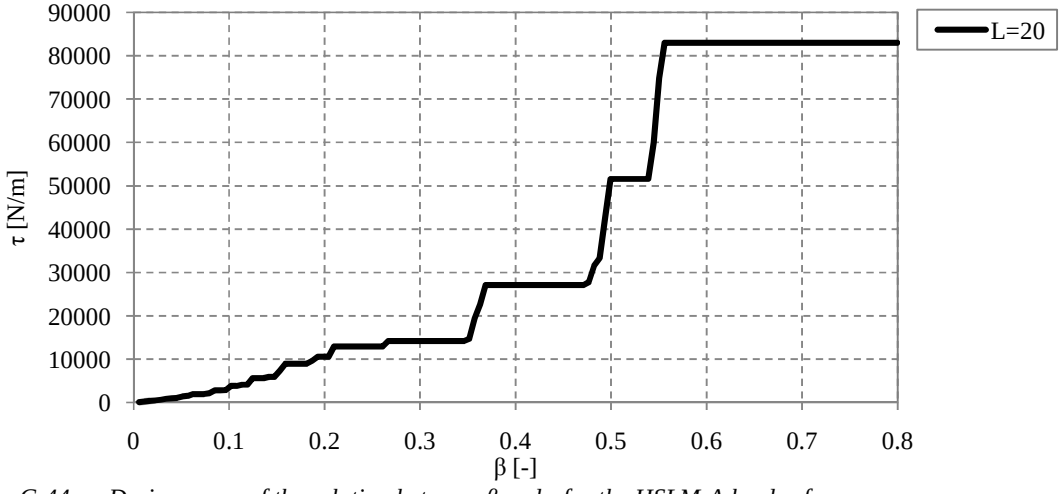

Figure C-44 *Design curve of the relation between β and τ for the HSLM-A loads of a bridge with one span and L_{tot}=20 m.*

C.2 Bridge with two equal spans

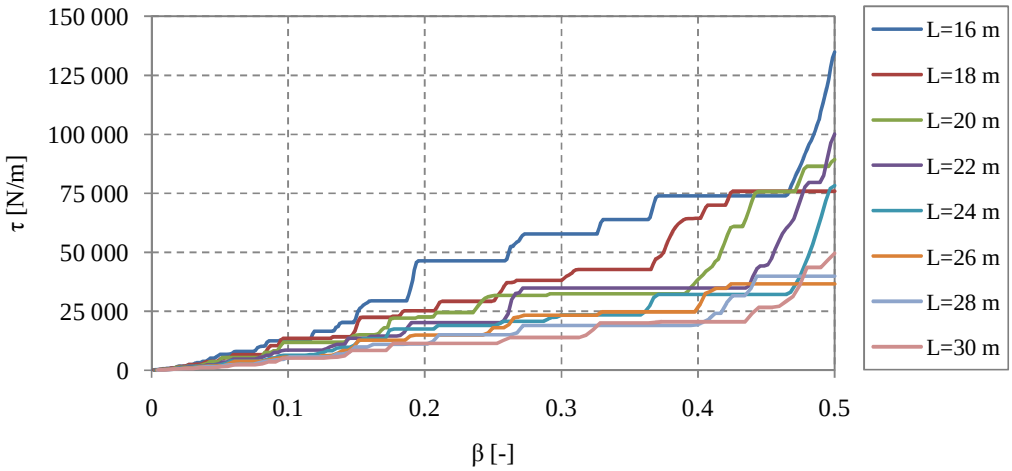

Figure C-45 *Design curves of the relation between β and τ for the HSLM-A loads of a bridge with two equal spans and L_{tot}=16 m to L_{tot}=30 m.*

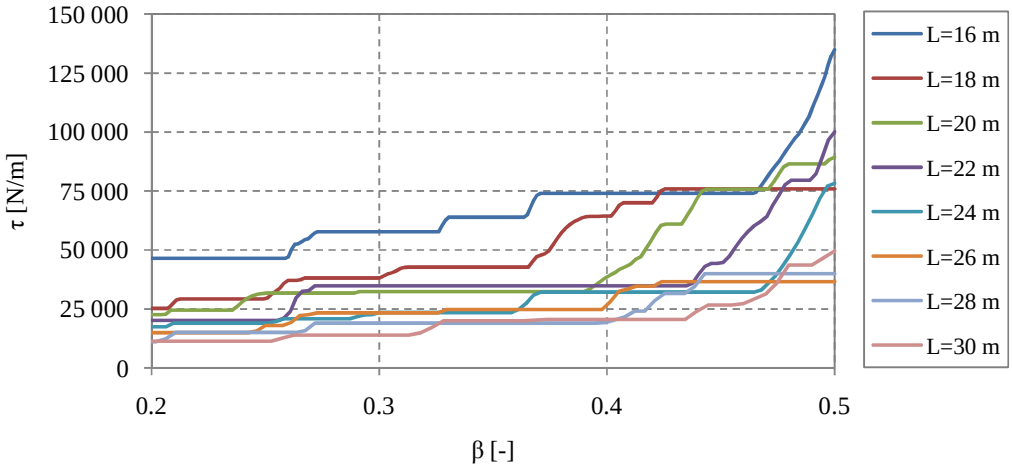

Figure C-46 *Design curves of the relation between β and τ for the HSLM-A loads of a bridge with two equal spans and L_{tot}=16 m to L_{tot}=30 m.*

C.2.1 Total length 16 m

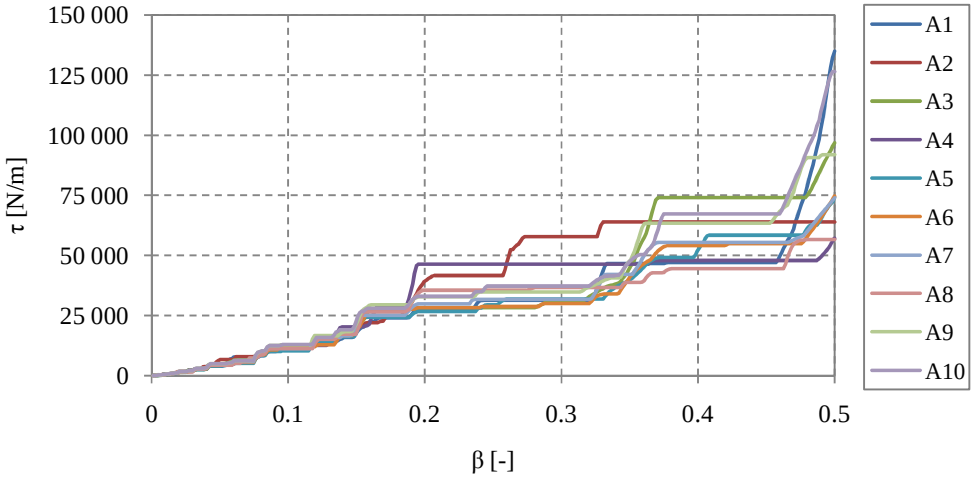

Figure C-47 *Relation between β and τ for load A1 to A10 for a bridge with two equal spans and L_{tot}=16 m.*

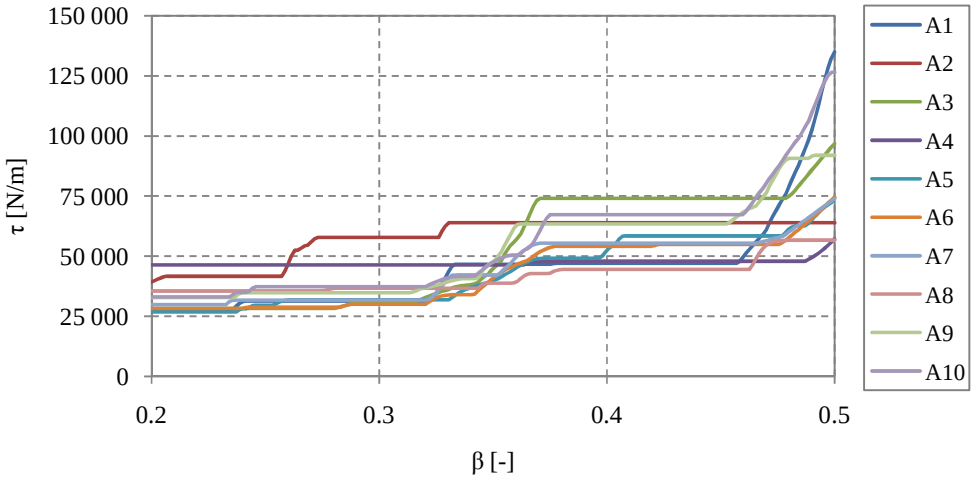

Figure C-48 *Relation between β and τ for load A1 to A10, with a zoom at β=0.2 to β=0.5, for a bridge with two equal spans and L_{tot}=16 m.*

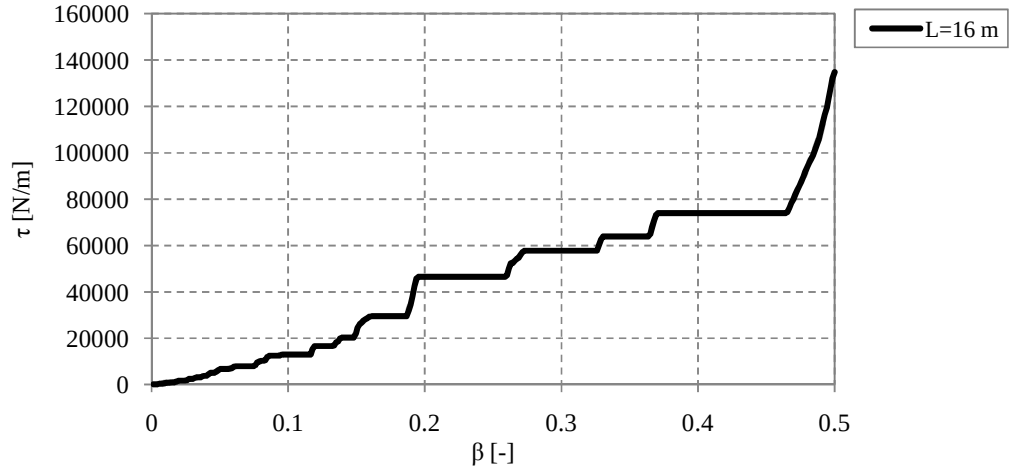

Figure C-49 *Design curve of the relation between β and τ for the HSLM-A loads of a bridge with two equal spans and L_{tot}=16 m.*

C.2.2 Total length 18 m

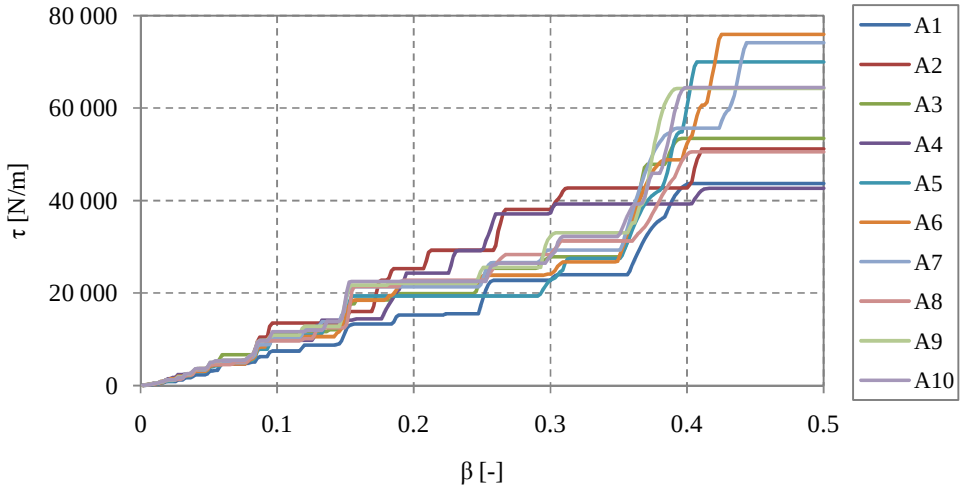

Figure C-50 *Relation between β and τ for load A1 to A10 for a bridge with two equal spans and L_{tot}=18 m.*

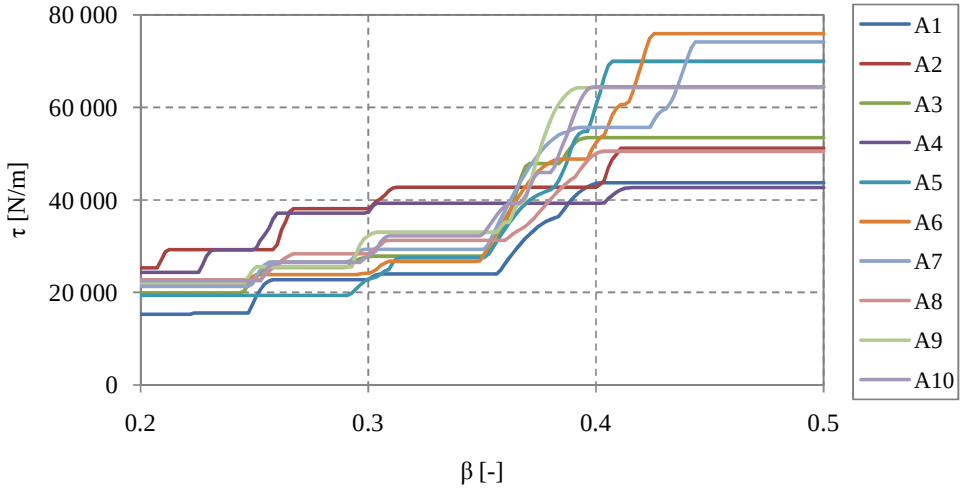

Figure C-51 *Relation between β and τ for load A1 to A10, with a zoom at β=0.2 to β=0.5, for a bridge with two equal spans and L_{tot}=18 m.*

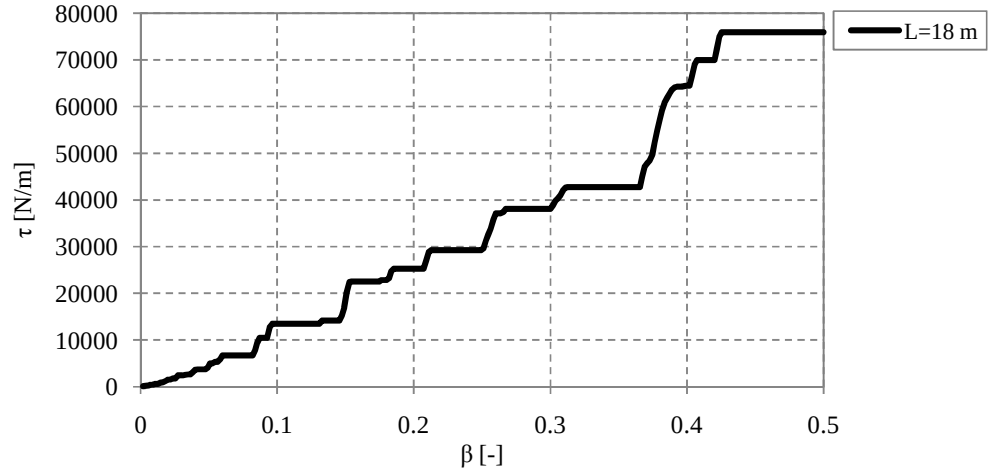

Figure C-52 *Design curve of the relation between β and τ for the HSLM-A loads of a bridge with two equal spans and L_{tot}=18 m.*

C.2.3 Total length 20 m

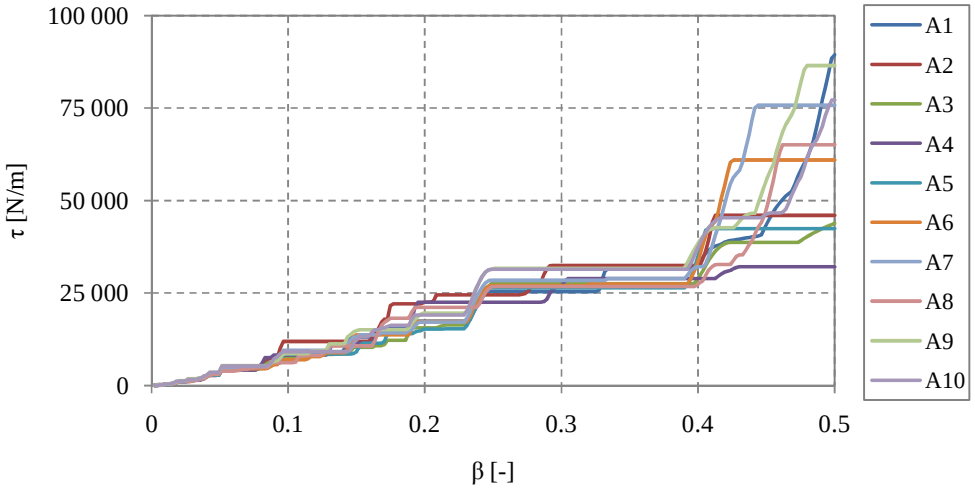

Figure C-53 *Relation between β and τ for load A1 to A10 for a bridge with two equal spans and L_{tot}=20 m.*

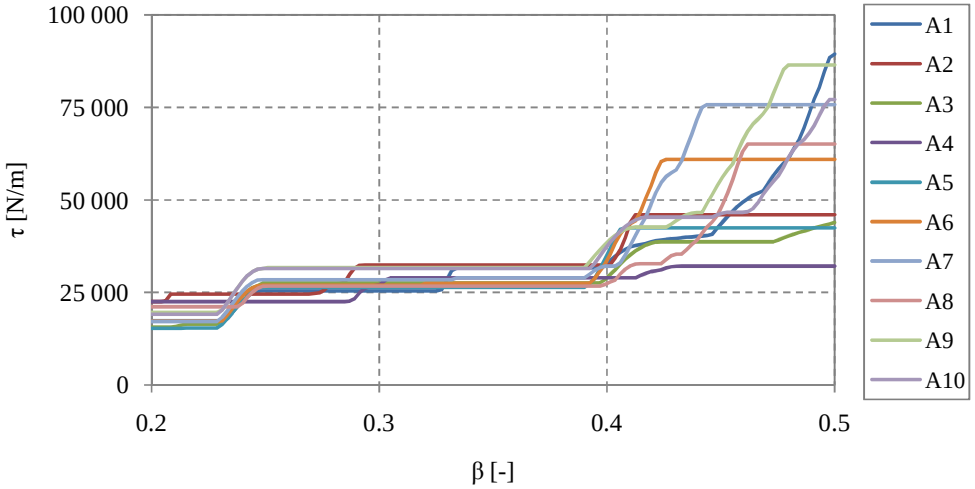

Figure C-54 *Relation between β and τ for load A1 to A10, with a zoom at β=0.2 to β=0.5, for a bridge with two equal spans and L_{tot}=20 m.*

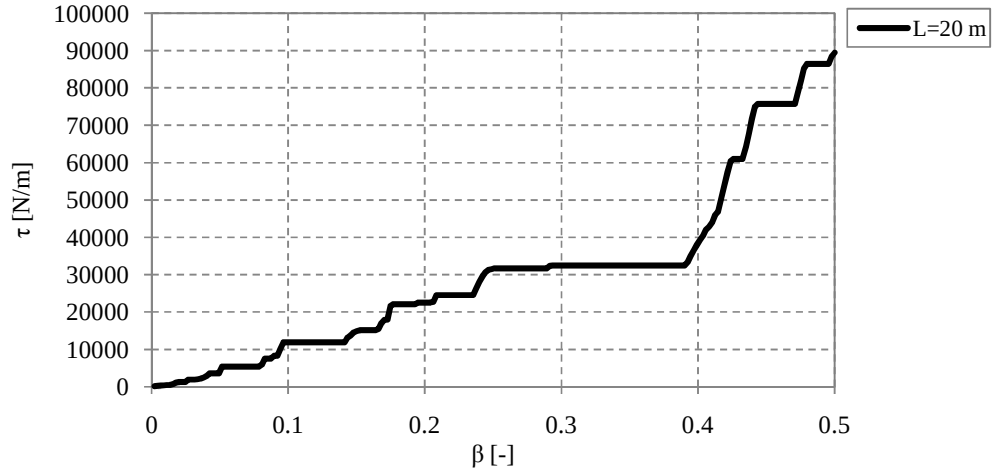

Figure C-55 *Design curve of the relation between β and τ for the HSLM-A loads of a bridge with two equal spans and L_{tot}=20 m.*

C.2.4 Total length 22 m

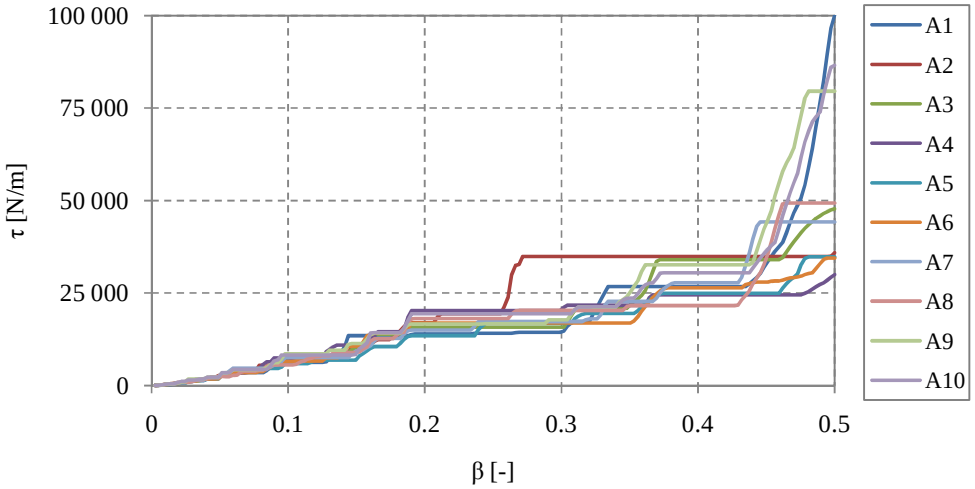

Figure C-56 *Relation between β and τ for load A1 to A10 for a bridge with two equal spans and L_{tot}=22 m.*

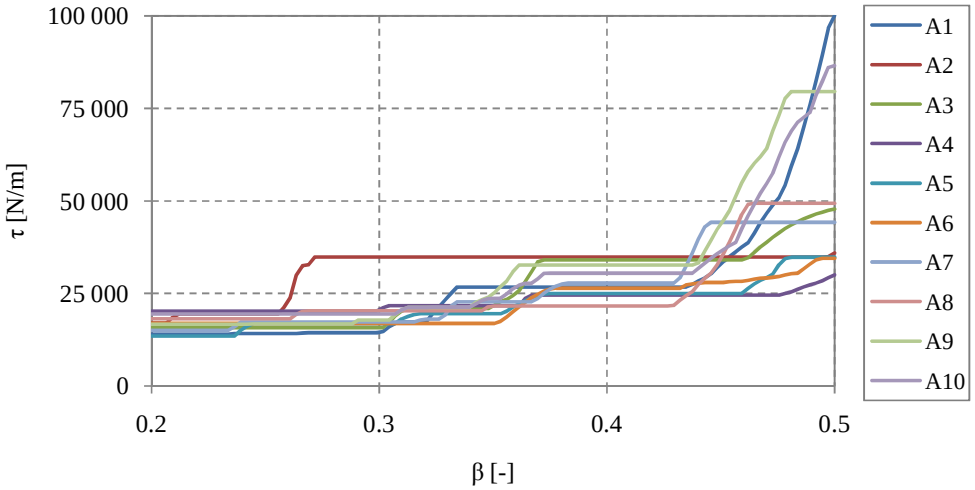

Figure C-57 *Relation between β and τ for load A1 to A10, with a zoom at β=0.2 to β=0.5, for a bridge with two equal spans and L_{tot}=22 m.*

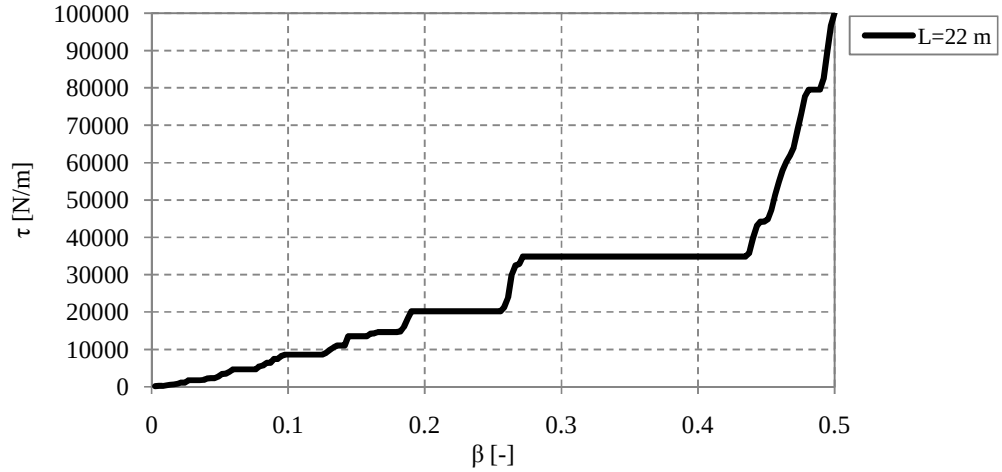

Figure C-58 *Design curve of the relation between β and τ for the HSLM-A loads of a bridge with two equal spans and L_{tot}=22 m.*

C.2.5 Total length 24 m

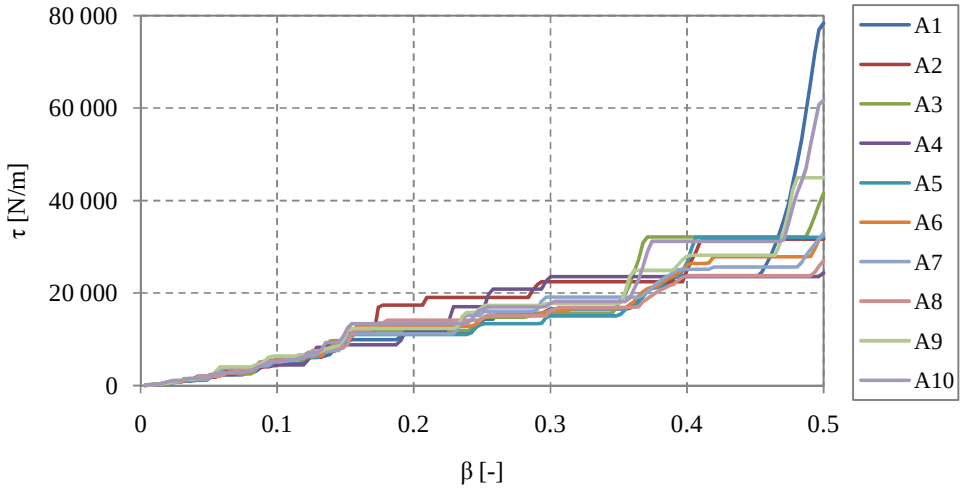

Figure C-59 *Relation between β and τ for load A1 to A10 for a bridge with two equal spans and L_{tot}=24 m.*

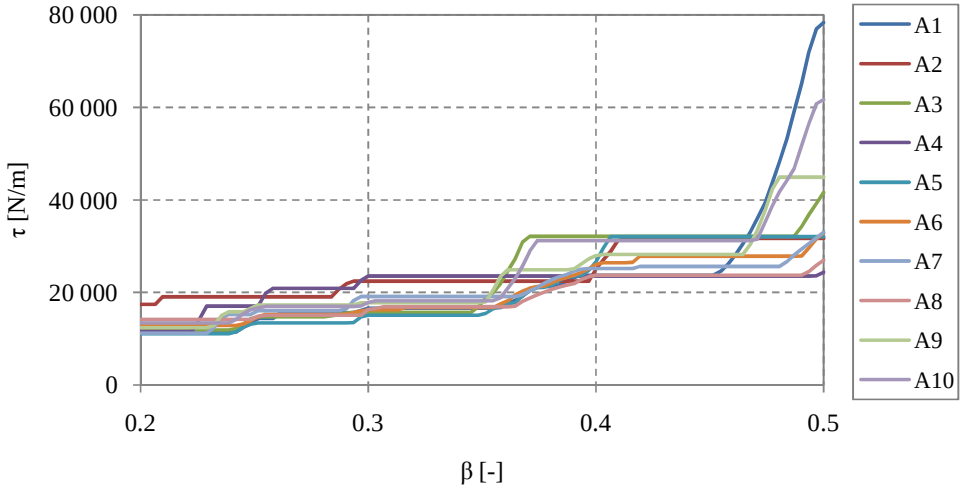

Figure C-60 *Relation between β and τ for load A1 to A10, with a zoom at β=0.2 to β=0.5, for a bridge with two equal spans and L_{tot}=24 m.*

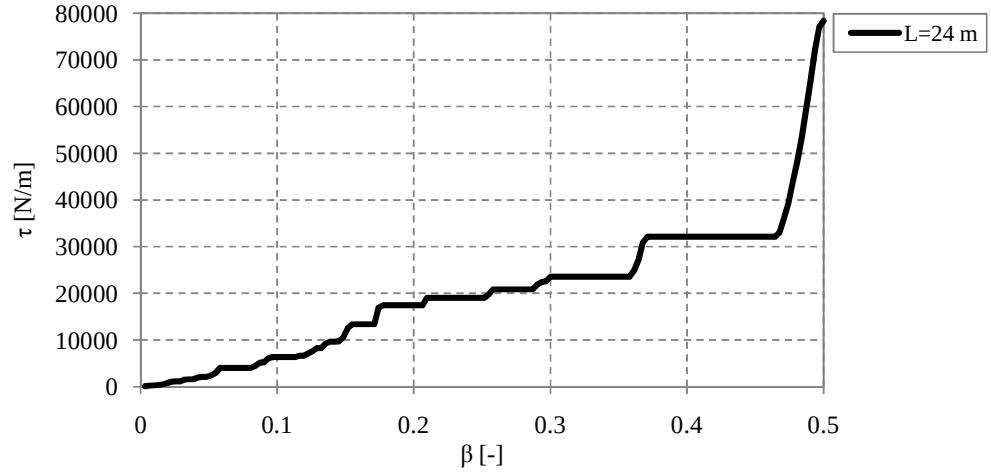

Figure C-61 *Design curve of the relation between β and τ for the HSLM-A loads of a bridge with two equal spans and L_{tot}=24 m.*

C.2.6 Total length 26 m

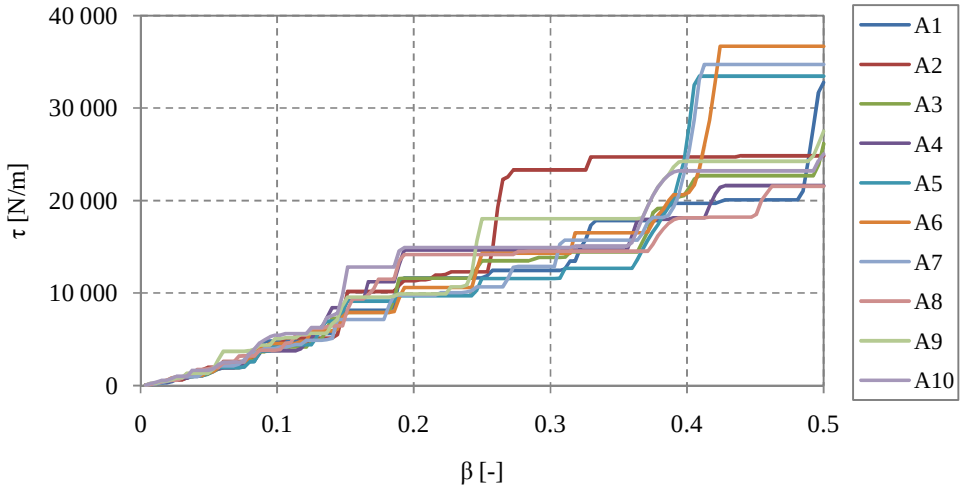

Figure C-62 *Relation between β and τ for load A1 to A10 for a bridge with two equal spans and L_{tot}=26 m.*

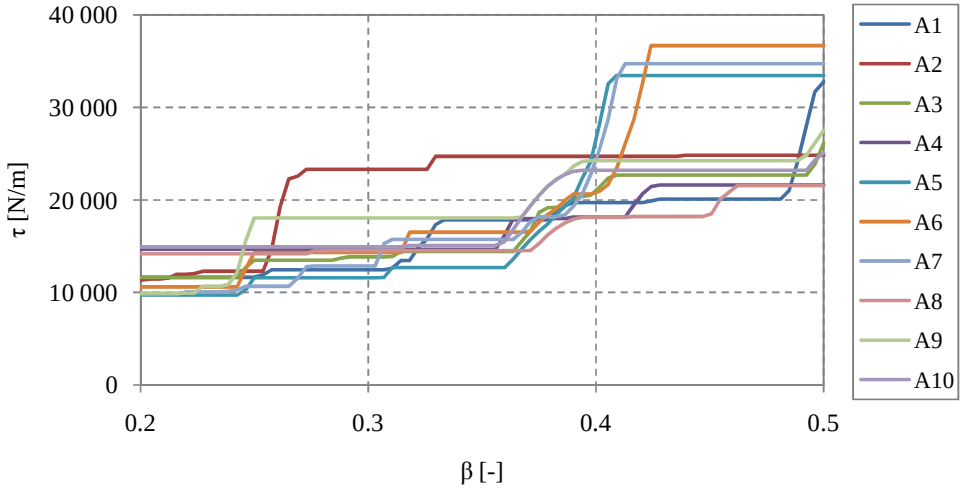

Figure C-63 *Relation between β and τ for load A1 to A10, with a zoom at β=0.2 to β=0.5, for a bridge with two equal spans and L_{tot}=26 m.*

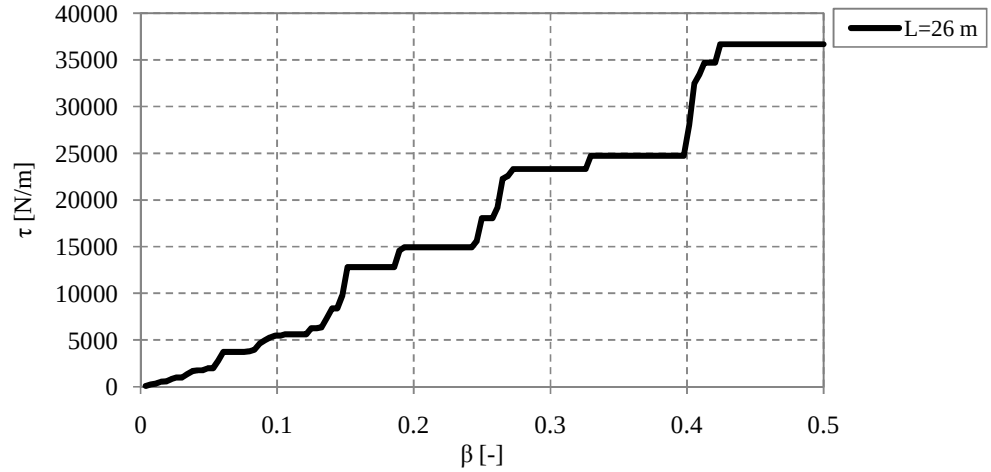

Figure C-64 *Design curve of the relation between β and τ for the HSLM-A loads of a bridge with two equal spans and L_{tot}=26 m.*

C.2.7 Total length 28 m

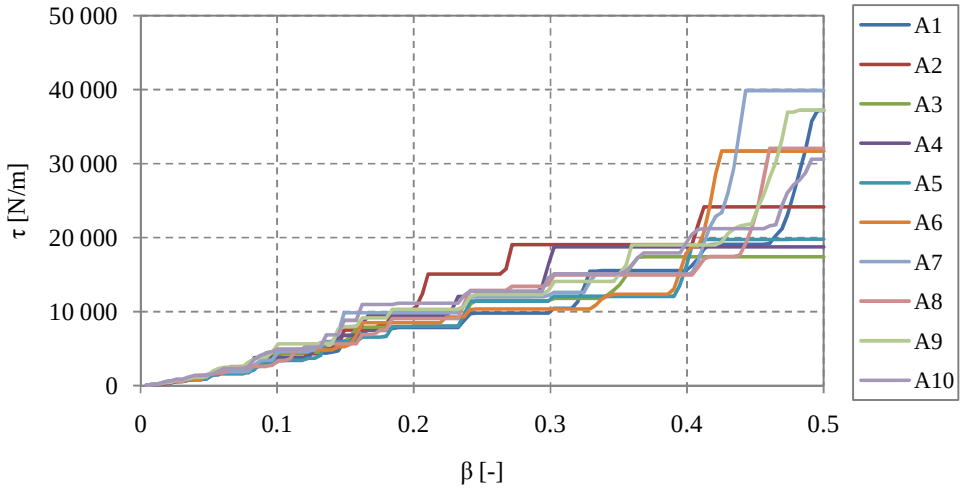

Figure C-65 *Relation between β and τ for load A1 to A10 for a bridge with two equal spans and L_{tot}=28 m.*

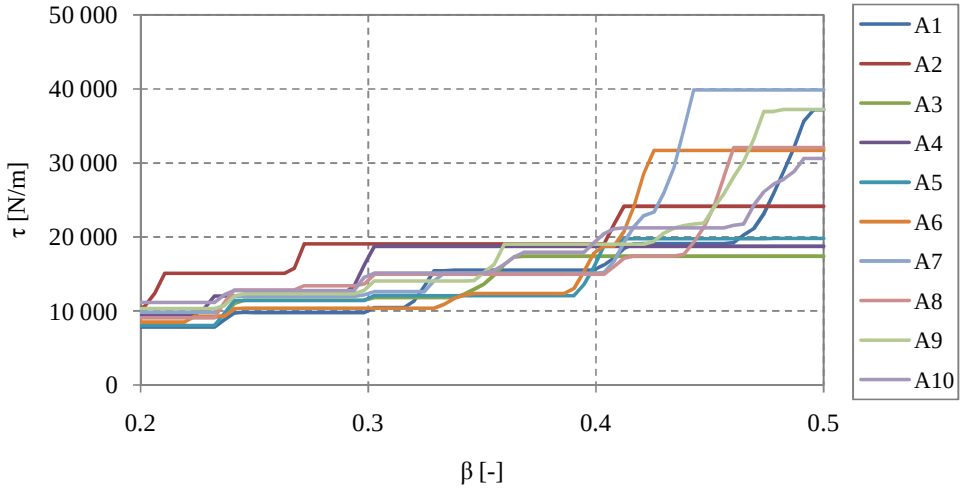

Figure C-66 *Relation between β and τ for load A1 to A10, with a zoom at β=0.2 to β=0.5, for a bridge with two equal spans and L_{tot}=28 m.*

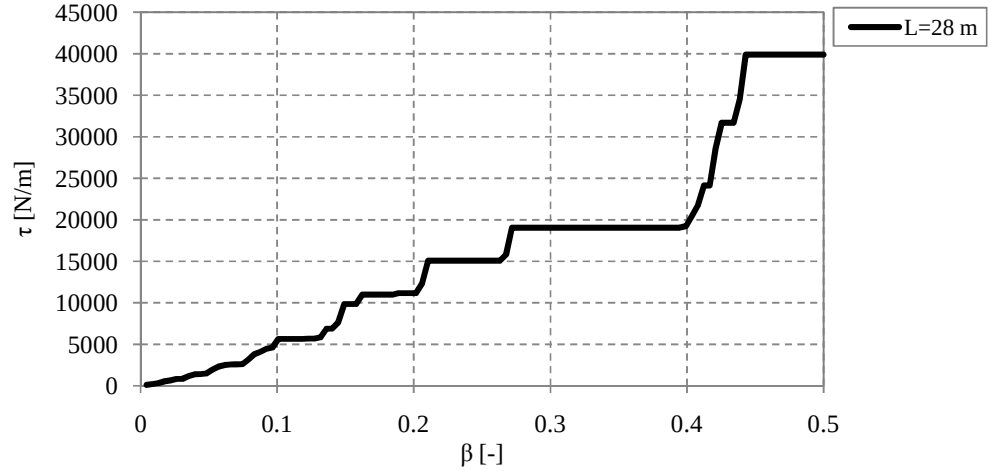

Figure C-67 *Design curve of the relation between β and τ for the HSLM-A loads of a bridge with two equal spans and L_{tot}=28 m.*

C.2.8 Total length 30 m

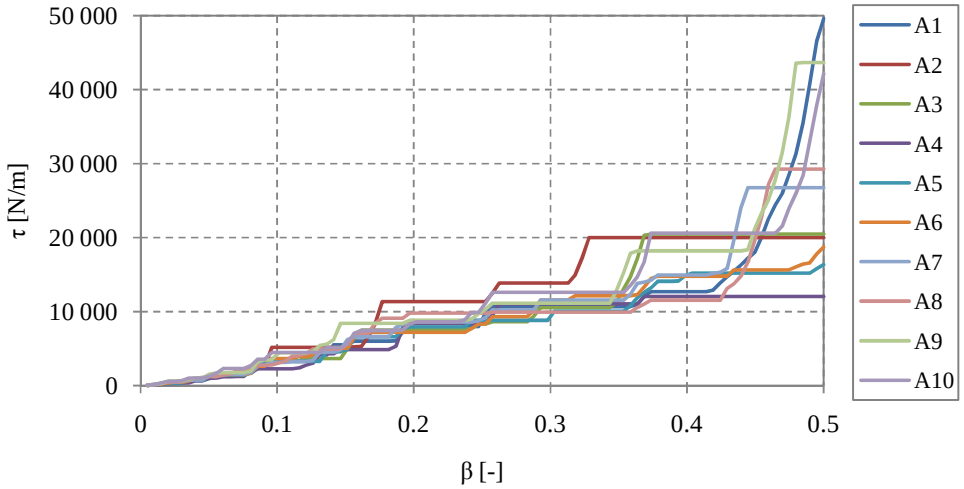

Figure C-68 *Relation between β and τ for load A1 to A10 for a bridge with two equal spans and L_{tot}=30 m.*

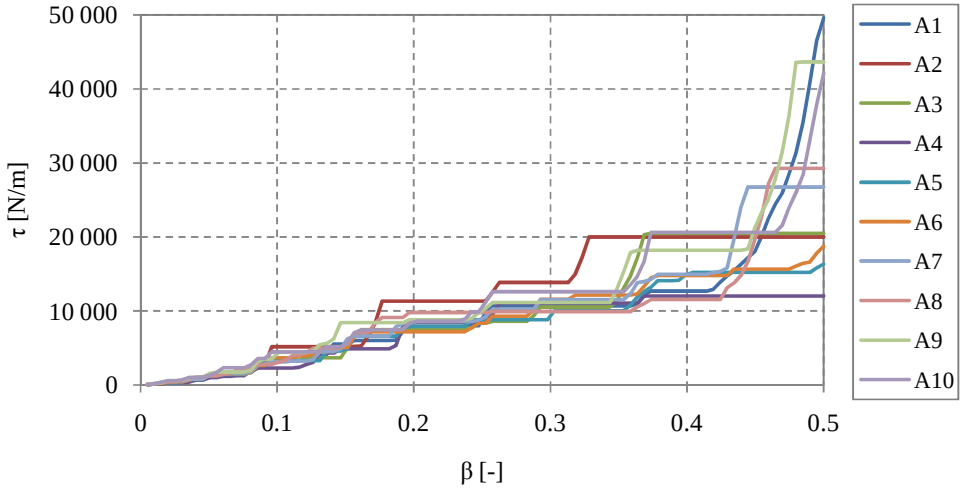

Figure C-69 *Relation between β and τ for load A1 to A10, with a zoom at β=0.2 to β=0.5, for a bridge with two equal spans and L_{tot}=30 m.*

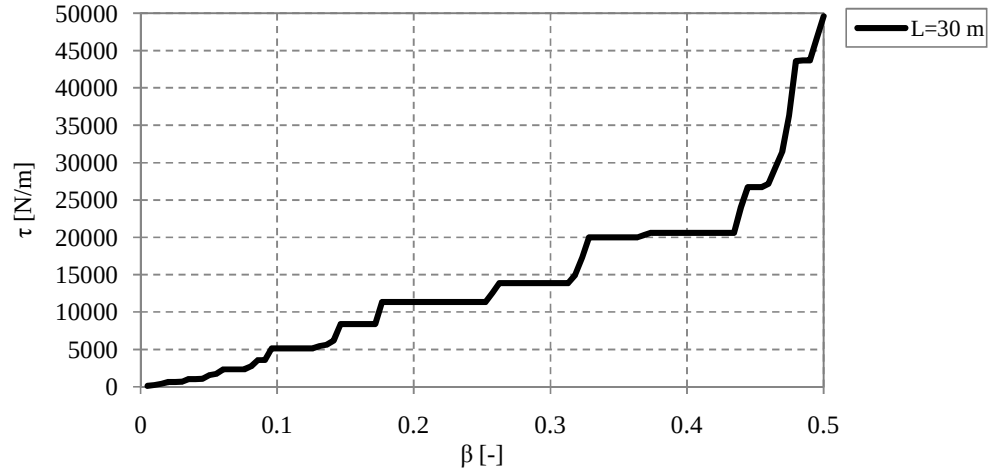

Figure C-70 *Design curve of the relation between β and τ for the HSLM-A loads of a bridge with two equal spans and L_{tot}=30 m.*

C.3 Bridge with three equal spans

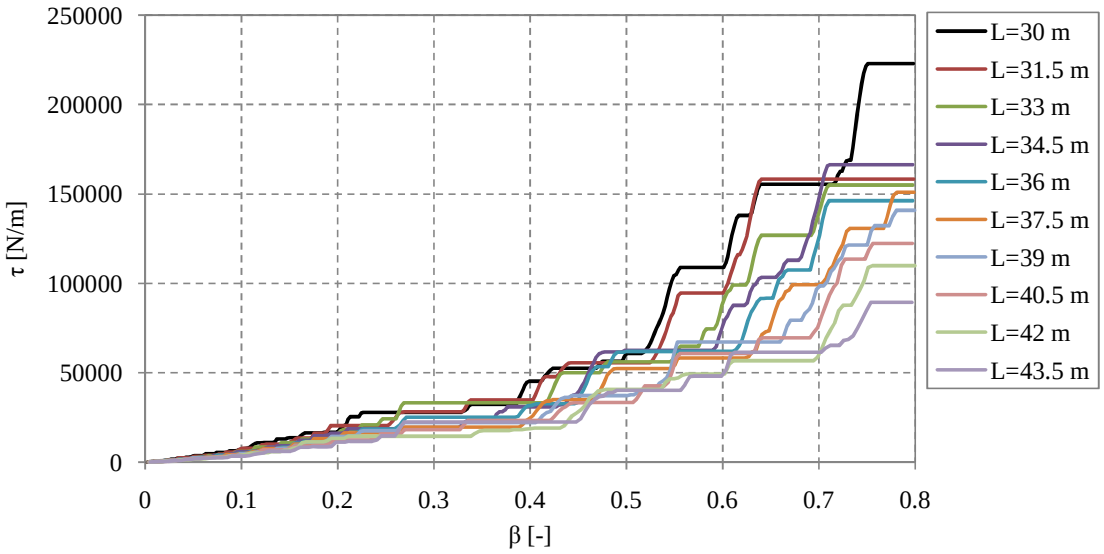

Figure C-71 *Design curves of the relation between β and τ for the HSLM-A loads of a bridge with three equal spans and L_{tot}=30 m to L_{tot}=43.5 m .*

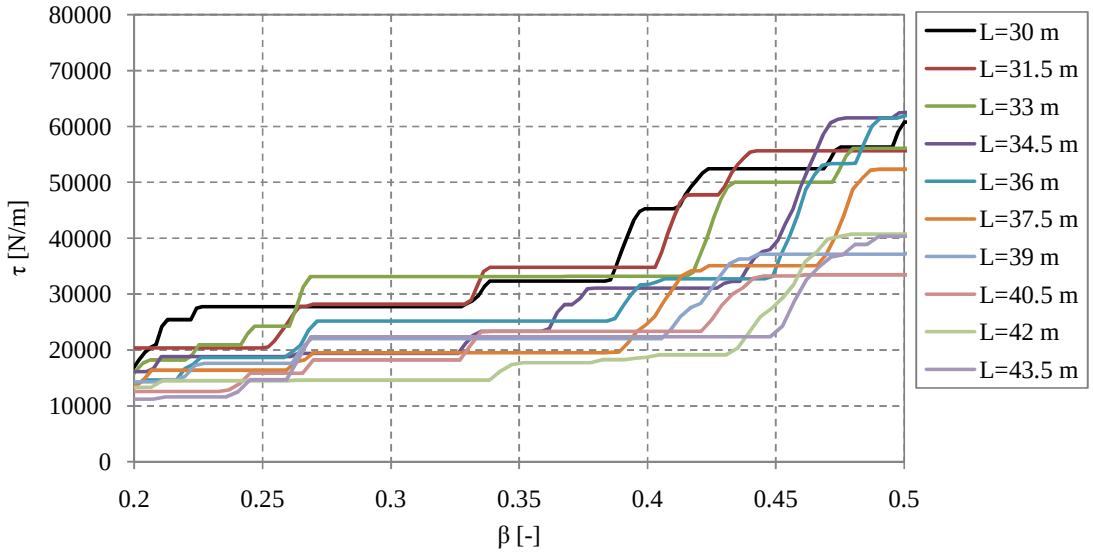

Figure C-72 *Design curves of the relation between β and τ for the HSLM-A loads of a bridge with three equal spans and L_{tot}=30 m to L_{tot}=43.5 m .*

C.3.1 Total length 30 m

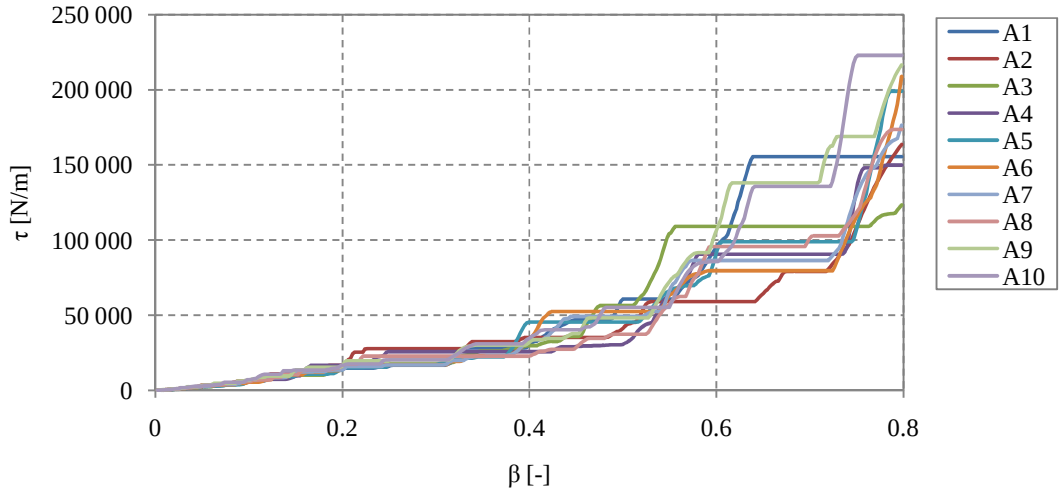

Figure C-73 *Relation between β and τ for load A1 to A10 for a bridge with three equal spans and L_{tot}=30 m.*

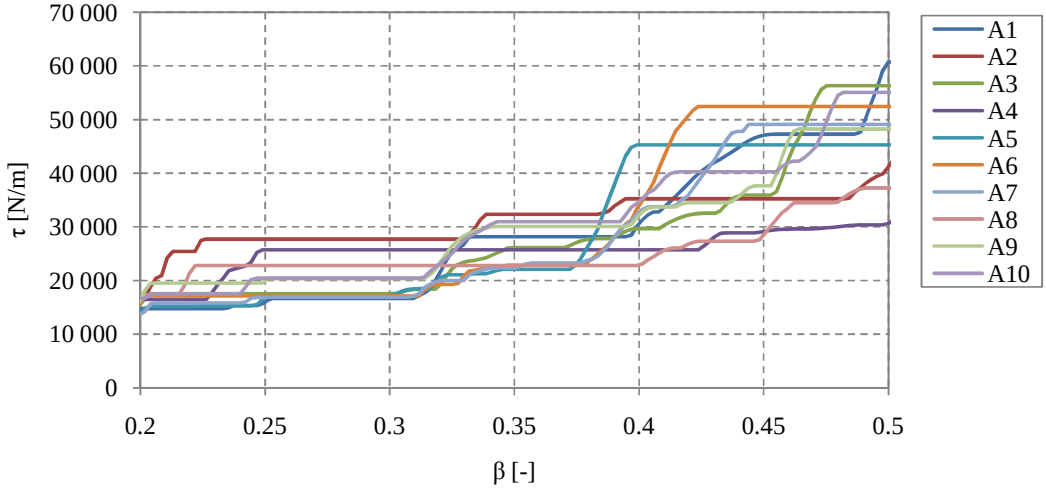

Figure C-74 *Relation between β and τ for load A1 to A10, with a zoom at β=0.2 to β=0.4, for a bridge with three equal spans and L_{tot}=30 m.*

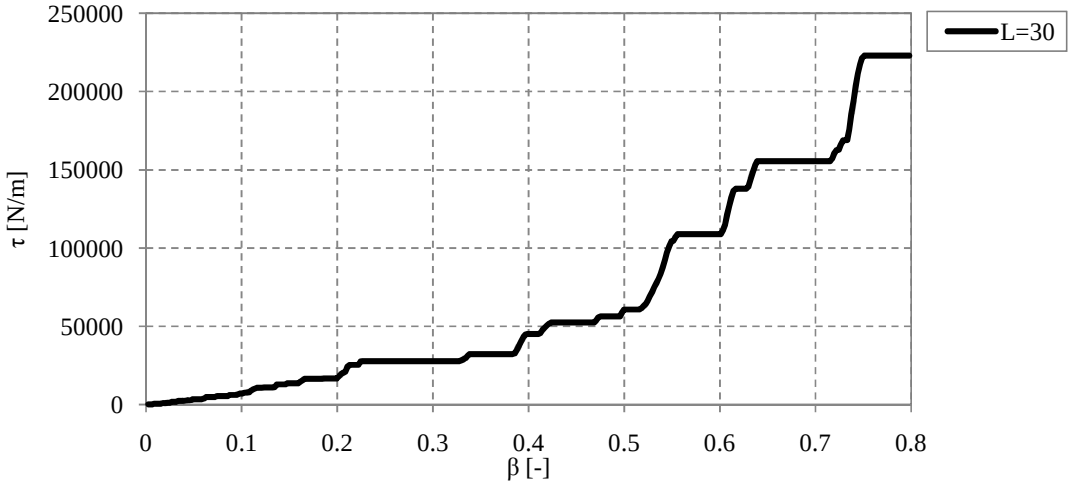

Figure C-75 *Design curve of the relation between β and τ for the HSLM-A loads of a bridge with three equal spans and L_{tot}=30 m.*

C.3.2 Total length 31.5 m

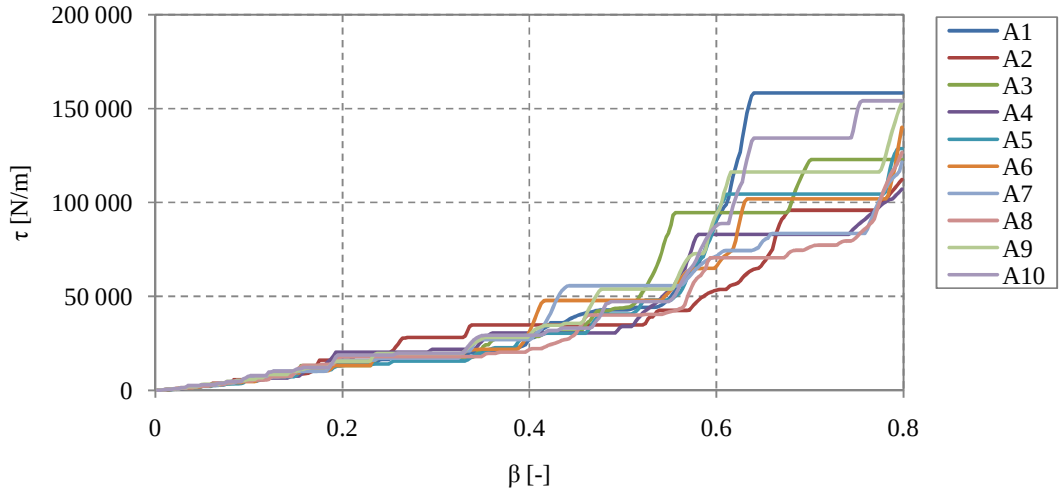

Figure C-76 *Relation between β and τ for load A1 to A10 for a bridge with three equal spans and L_{tot}=31.5 m.*

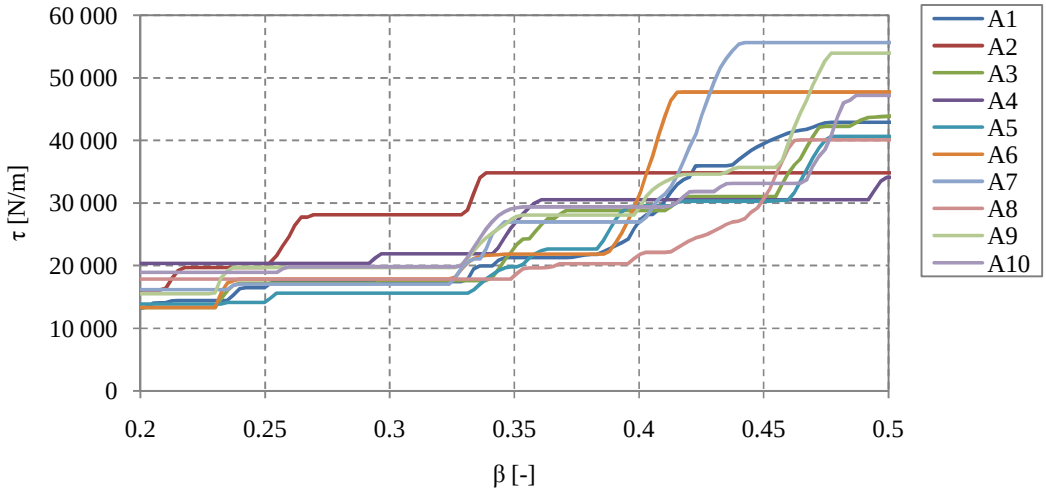

Figure C-77 *Relation between β and τ for load A1 to A10, with a zoom at β=0.2 to β=0.4, for a bridge with three equal spans and L_{tot}=31.5 m.*

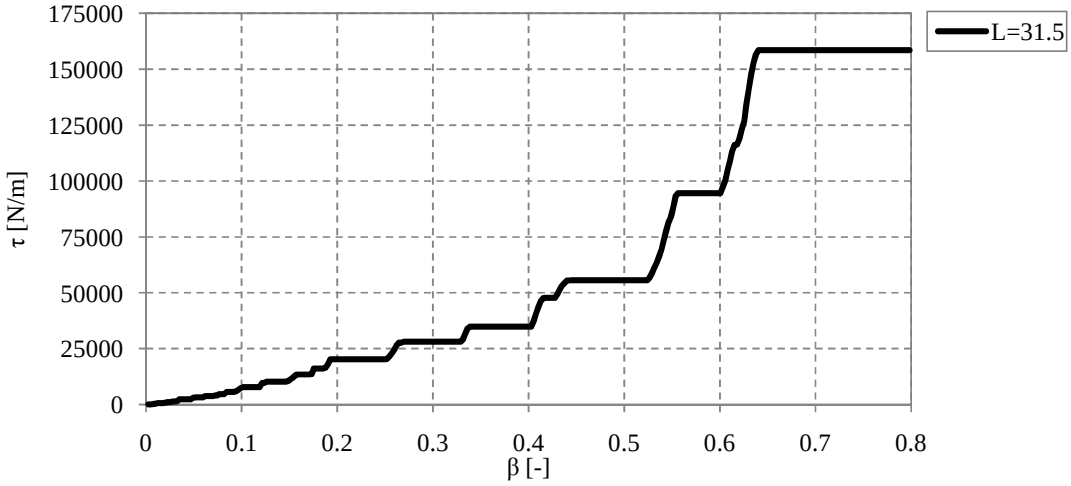

Figure C-78 *Design curve of the relation between β and τ for the HSLM-A loads of a bridge with three equal spans and L_{tot}=31.5 m.*

C.3.3 Total length 33 m

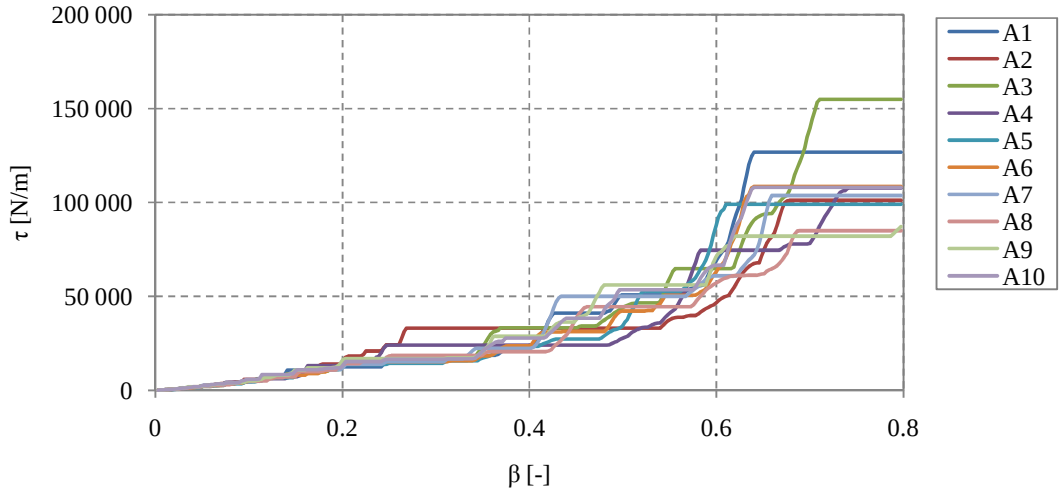

Figure C-79 *Relation between β and τ for load A1 to A10 for a bridge with three equal spans and L_{tot}=33 m.*

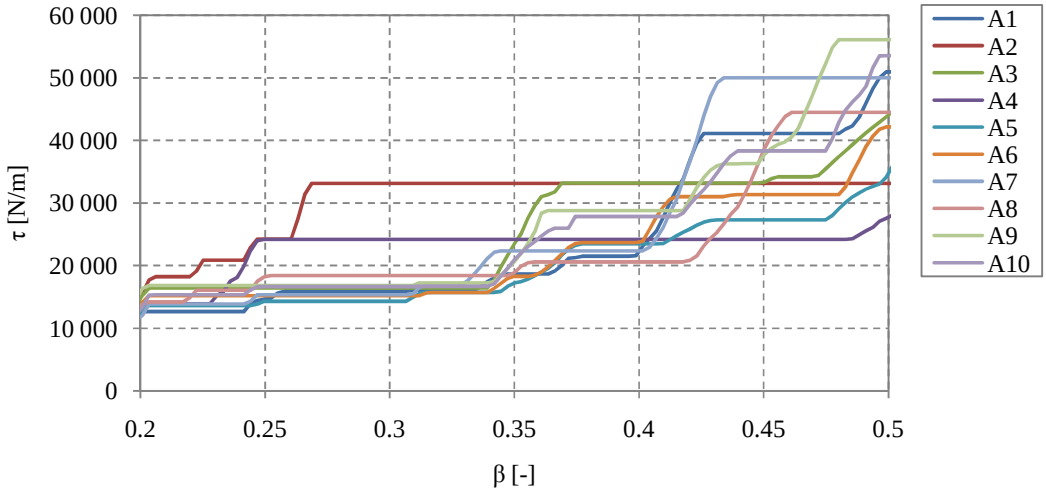

Figure C-80 *Relation between β and τ for load A1 to A10, with a zoom at β=0.2 to β=0.4, for a bridge with three equal spans and L_{tot}=33 m.*

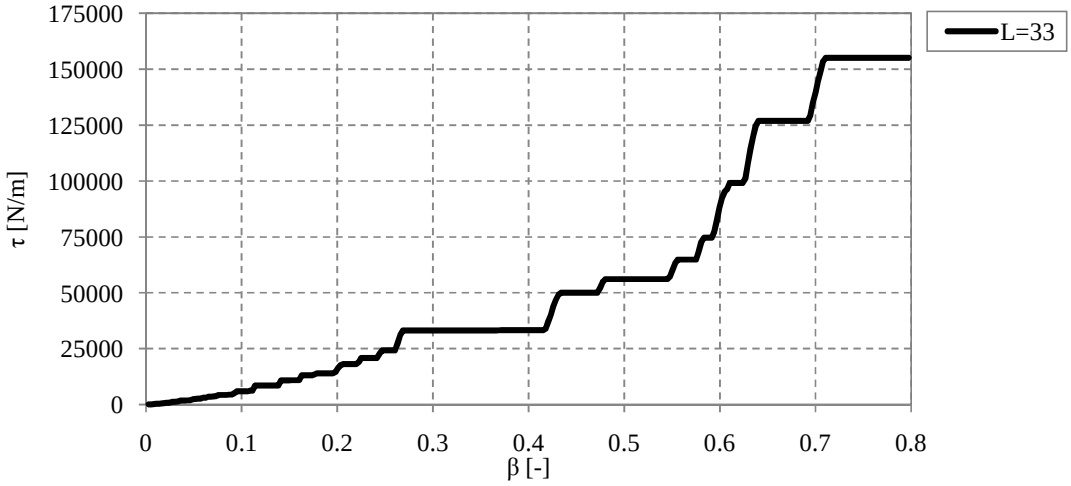

Figure C-81 *Design curve of the relation between β and τ for the HSLM-A loads of a bridge with three equal spans and L_{tot}=33 m.*

C.3.4 Total length 34.5 m

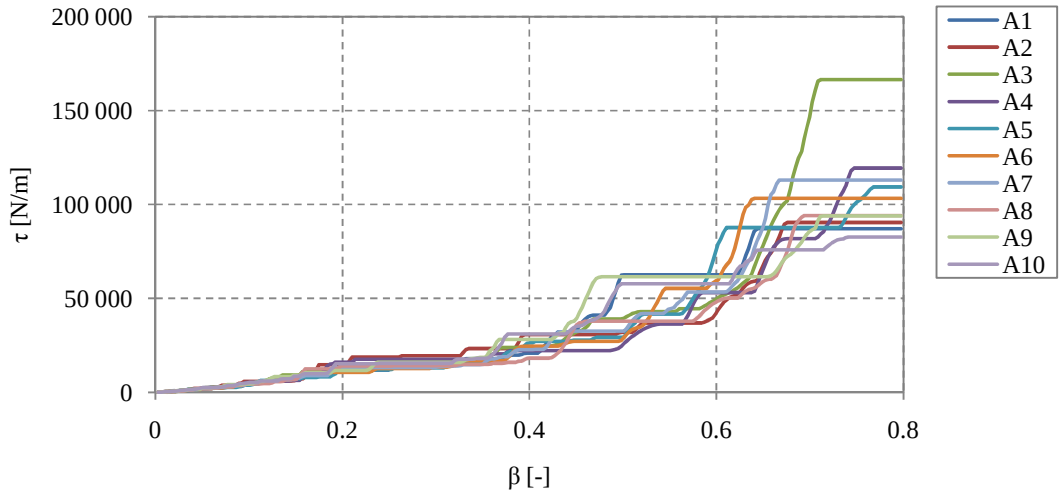

Figure C-82 *Relation between β and τ for load A1 to A10 for a bridge with three equal spans and L_{tot}=34.5 m.*

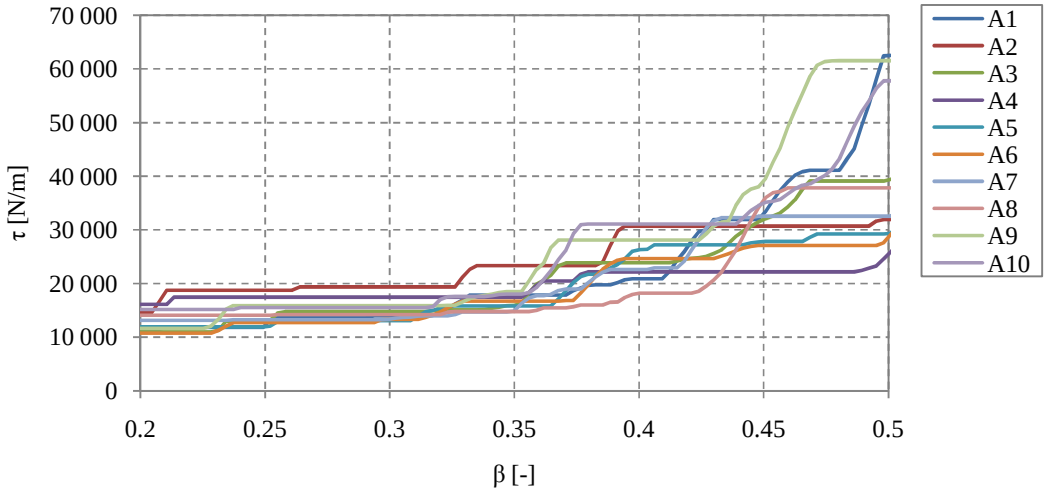

Figure C-83 *Relation between β and τ for load A1 to A10, with a zoom at β=0.2 to β=0.4, for a bridge with three equal spans and L_{tot}=34.5 m.*

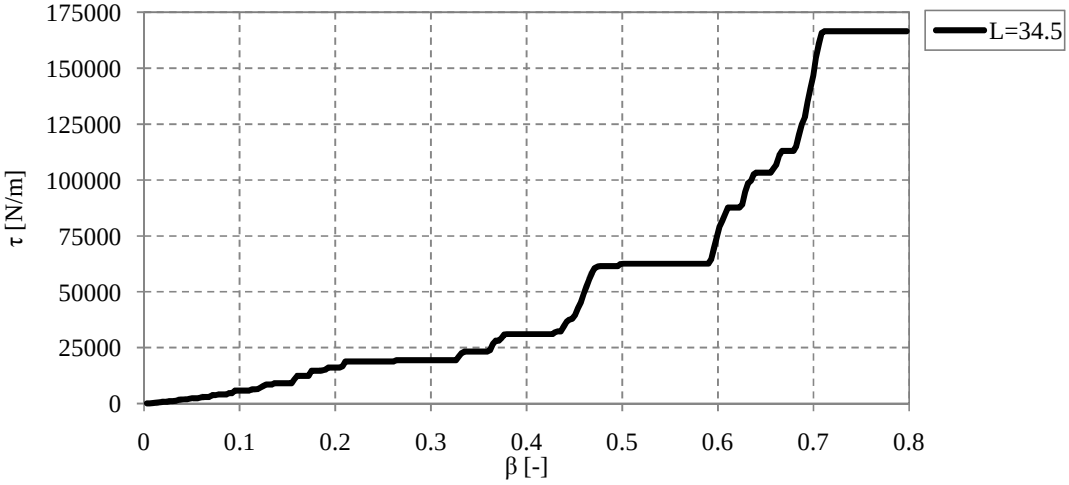

Figure C-84 *Design curve of the relation between β and τ for the HSLM-A loads of a bridge with three equal spans and L_{tot}=34.5 m.*

C.3.5 Total length 36 m

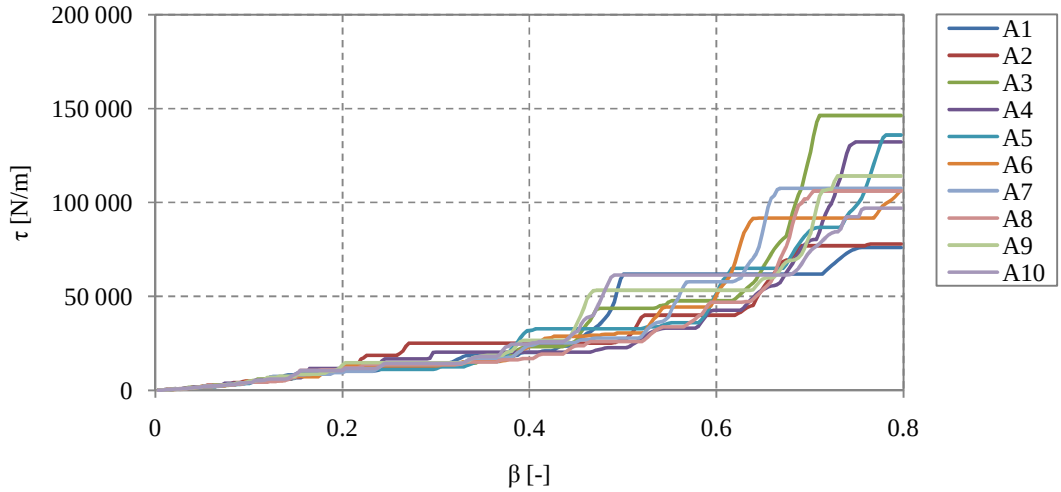

Figure C-85 *Relation between β and τ for load A1 to A10 for a bridge with three equal spans and L_{tot}=36 m.*

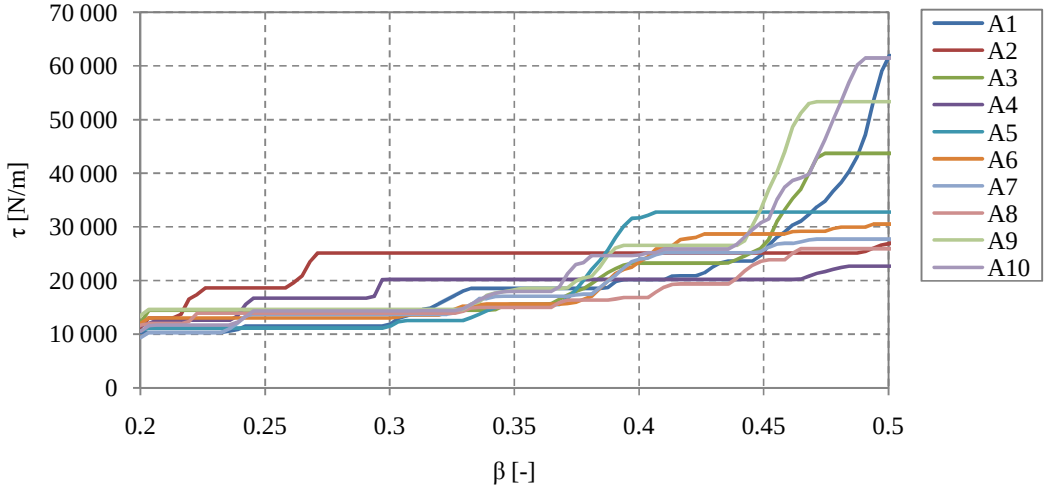

Figure C-86 *Relation between β and τ for load A1 to A10, with a zoom at β=0.2 to β=0.4, for a bridge with three equal spans and L_{tot}=36 m.*

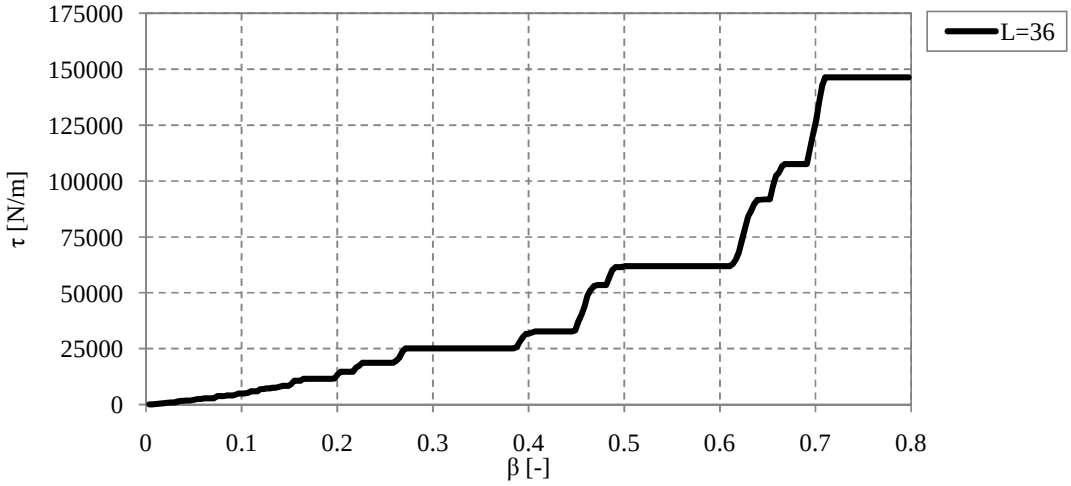

Figure C-87 *Design curve of the relation between β and τ for the HSLM-A loads of a bridge with three equal spans and L_{tot}=36 m.*

C.3.6 Total length 37.5 m

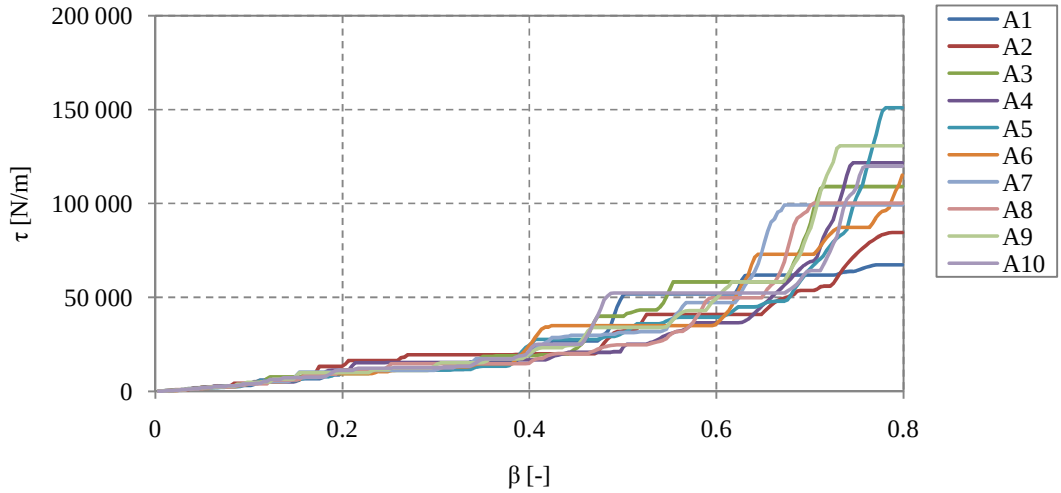

Figure C-88 *Relation between β and τ for load A1 to A10 for a bridge with three equal spans and L_{tot}=37.5 m.*

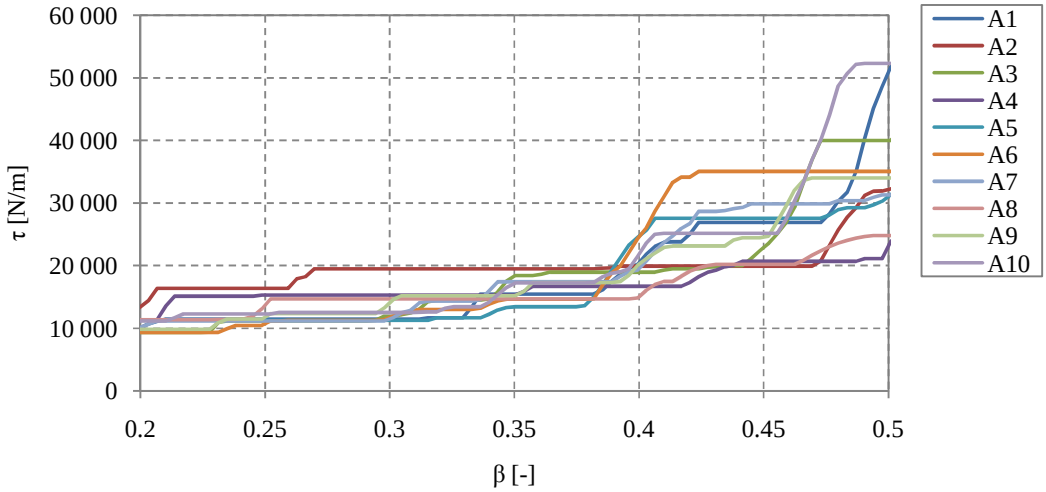

Figure C-89 *Relation between β and τ for load A1 to A10, with a zoom at β=0.2 to β=0.4, for a bridge with three equal spans and L_{tot}=37.5 m.*

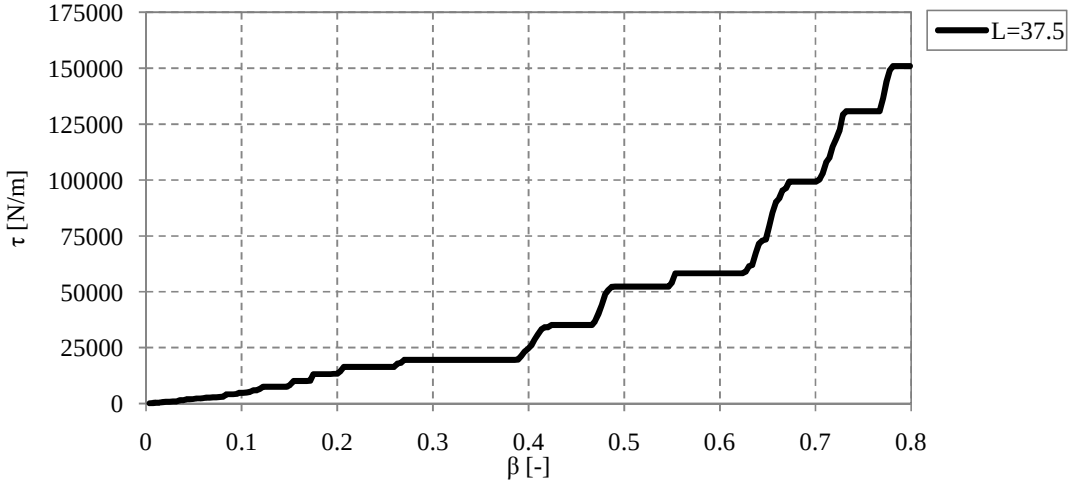

Figure C-90 *Design curve of the relation between β and τ for the HSLM-A loads of a bridge with three equal spans and L_{tot}=37.5 m.*

C.3.7 Total length 39 m

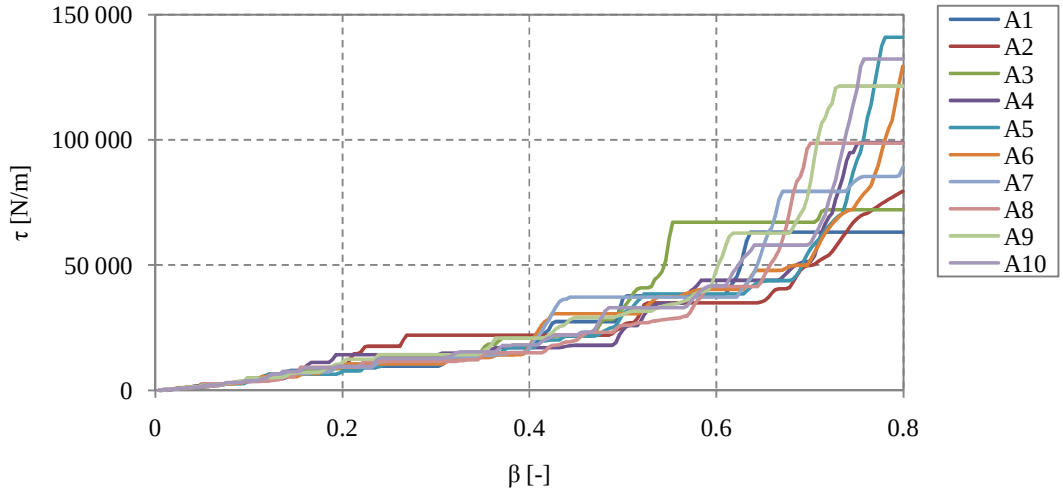

Figure C-91 *Relation between β and τ for load A1 to A10 for a bridge with three equal spans and L_{tot}=39 m.*

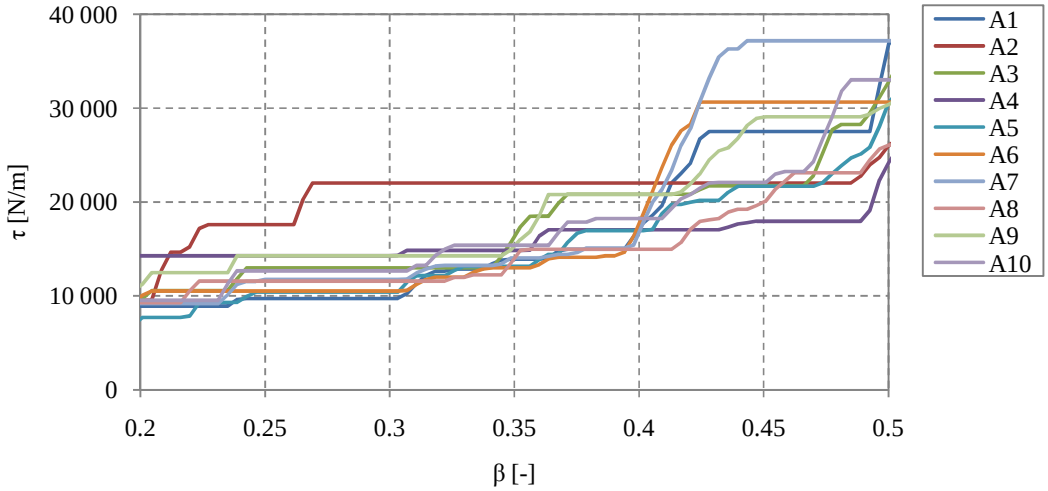

Figure C-92 *Relation between β and τ for load A1 to A10, with a zoom at β=0.2 to β=0.4, for a bridge with three equal spans and L_{tot}=39 m.*

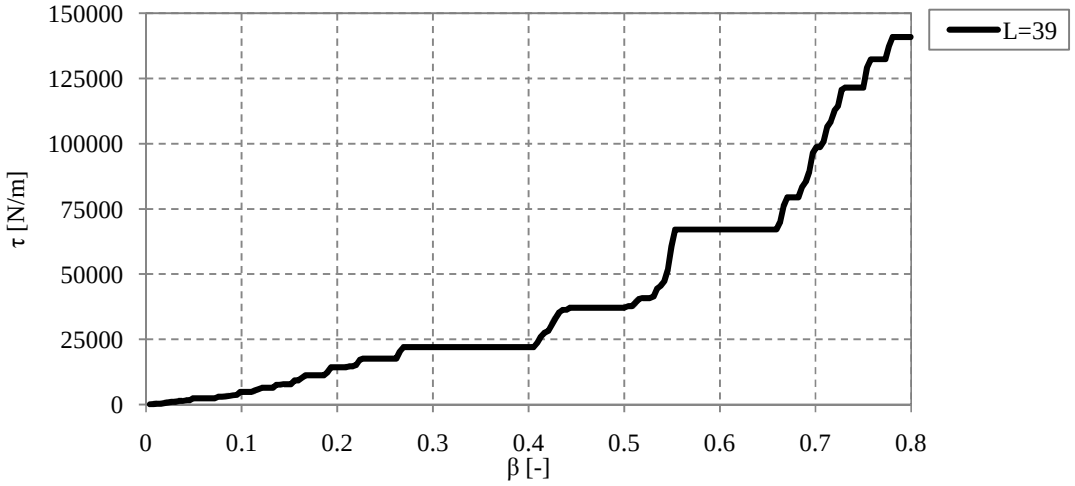

Figure C-93 *Design curve of the relation between β and τ for the HSLM-A loads of a bridge with three equal spans and L_{tot}=39 m.*

C.3.8 Total length 40.5 m

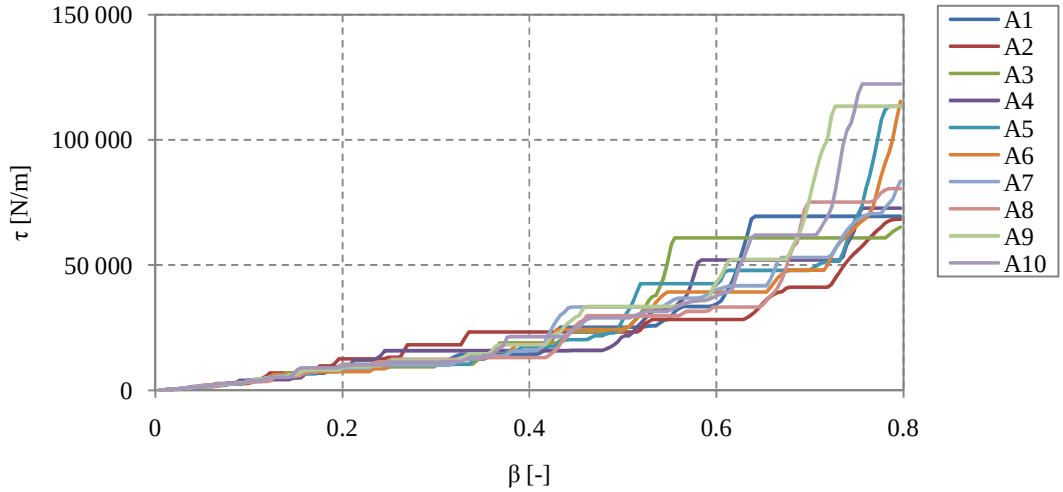

Figure C-94 *Relation between β and τ for load A1 to A10 for a bridge with three equal spans and L_{tot}=40.5 m.*

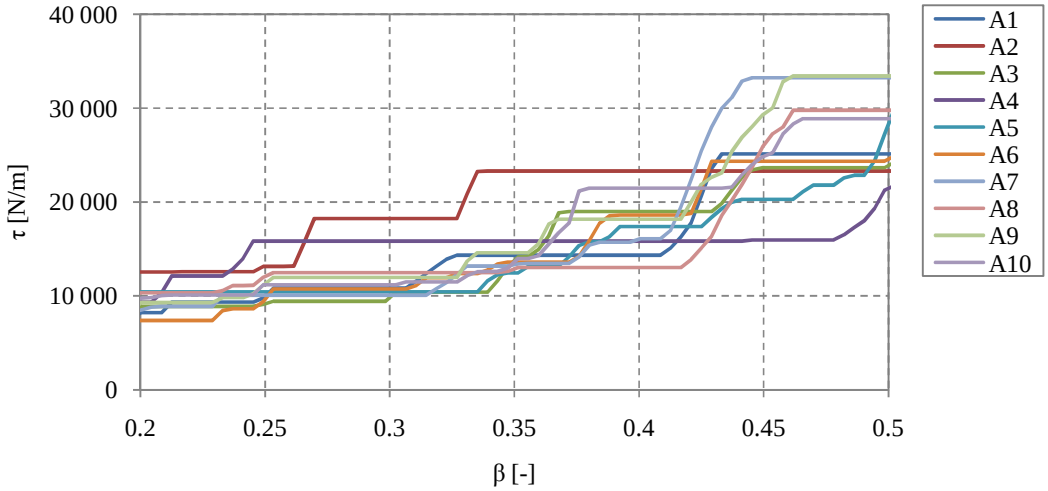

Figure C-95 *Relation between β and τ for load A1 to A10, with a zoom at β=0.2 to β=0.4, for a bridge with three equal spans and L_{tot}=40.5 m.*

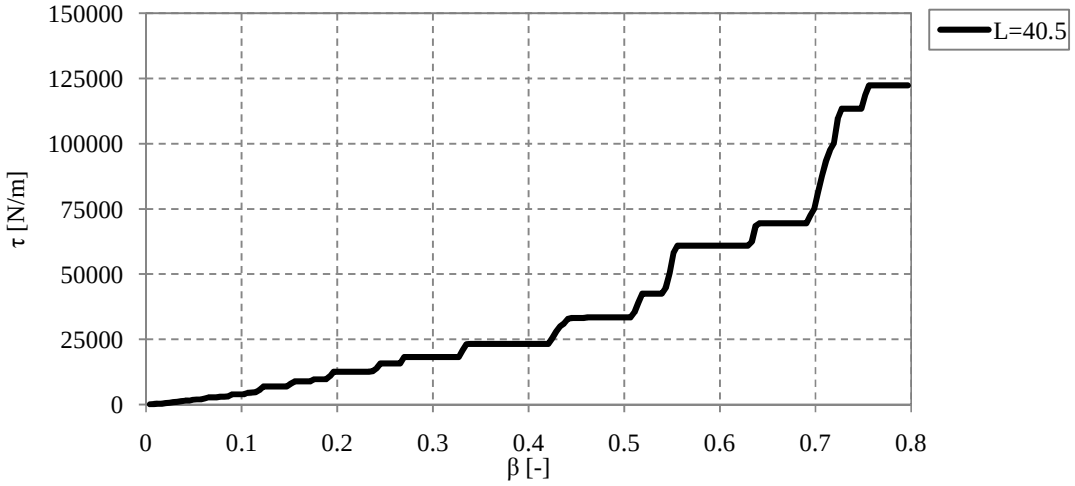

Figure C-96 *Design curve of the relation between β and τ for the HSLM-A loads of a bridge with three equal spans and L_{tot}=40.5 m.*

C.3.9 Total length 42 m

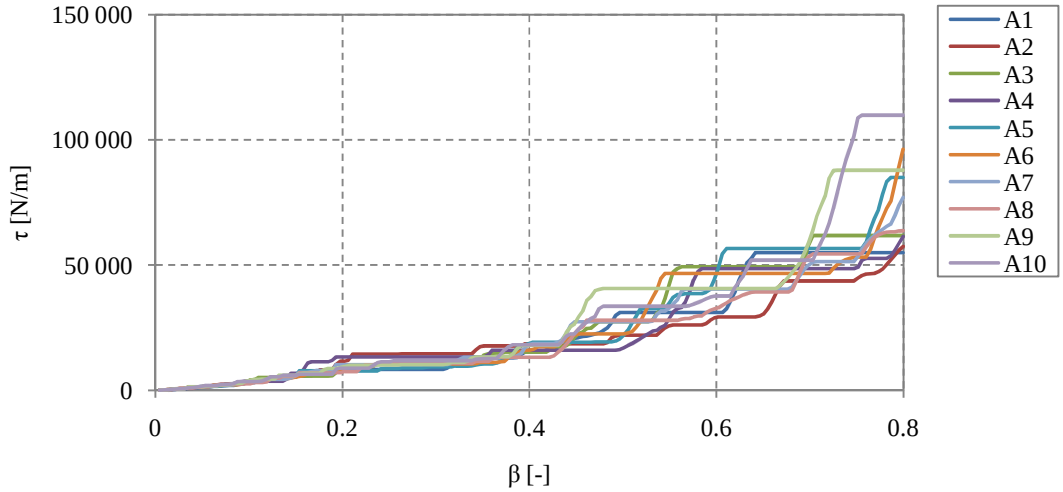

Figure C-97 *Relation between β and τ for load A1 to A10 for a bridge with three equal spans and L_{tot}=42 m.*

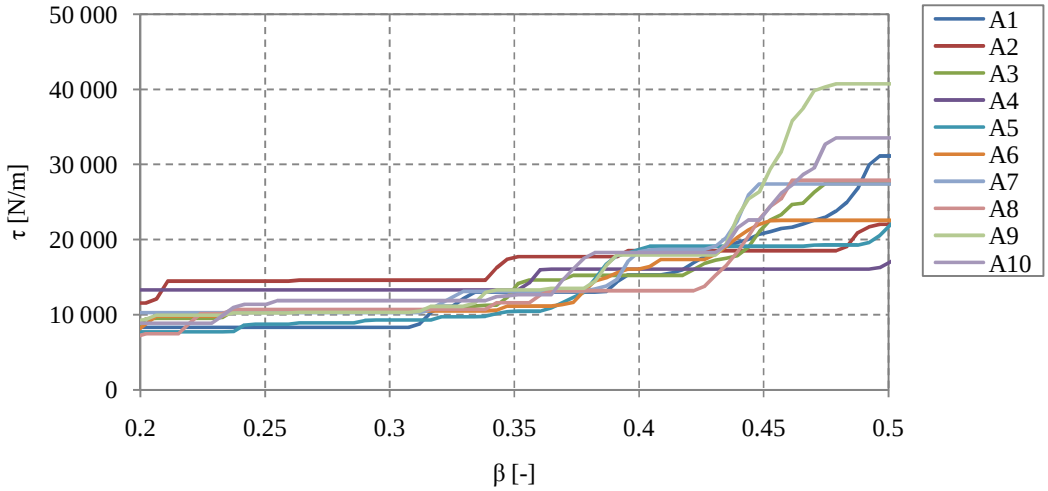

Figure C-98 *Relation between β and τ for load A1 to A10, with a zoom at β=0.2 to β=0.4, for a bridge with three equal spans and L_{tot}=42 m.*

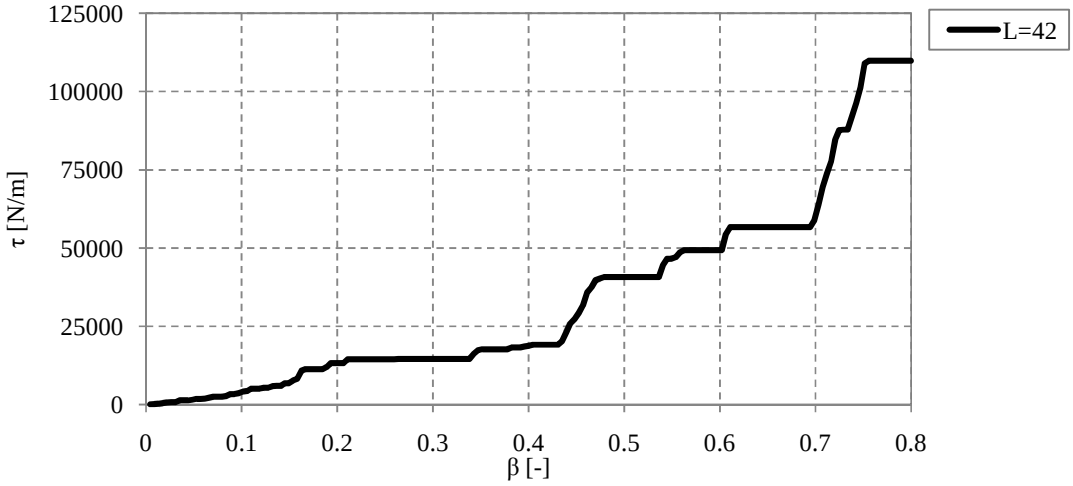

Figure C-99 *Design curve of the relation between β and τ for the HSLM-A loads of a bridge with three equal spans and L_{tot}=42 m.*

C.3.10 Total length 43.5 m

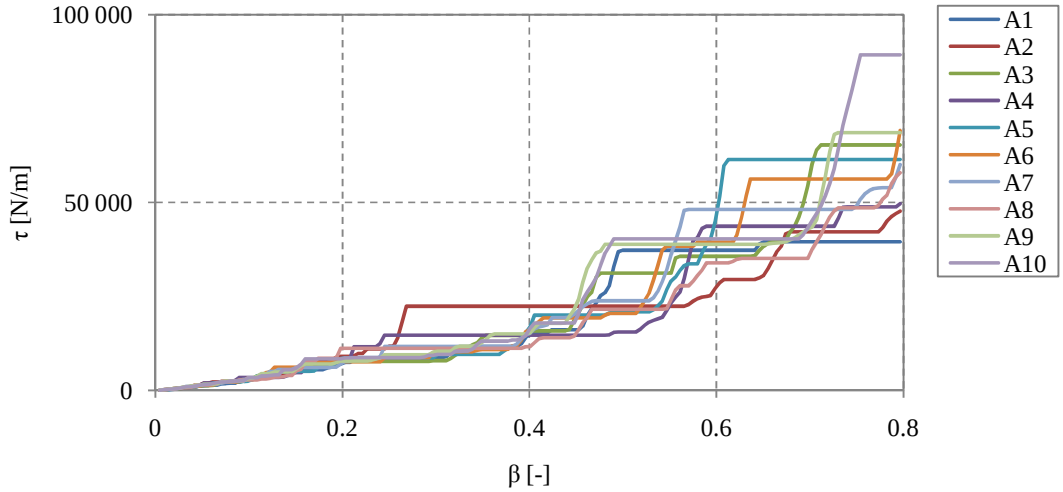

Figure C-100 *Relation between β and τ for load A1 to A10 for a bridge with three equal spans and L_{tot}=43.5 m.*

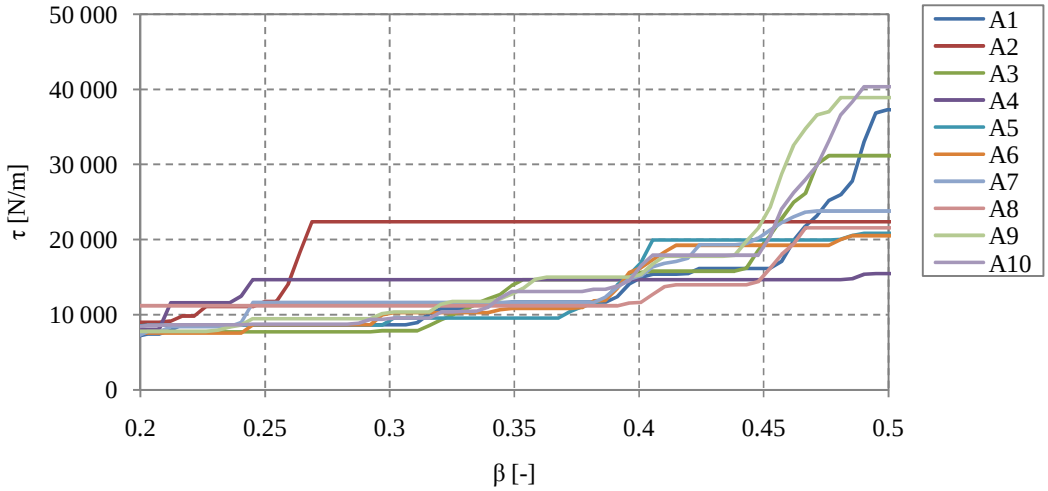

Figure C-101 *Relation between β and τ for load A1 to A10, with a zoom at β=0.2 to β=0.4, for a bridge with three equal spans and L_{tot}=43.5 m.*

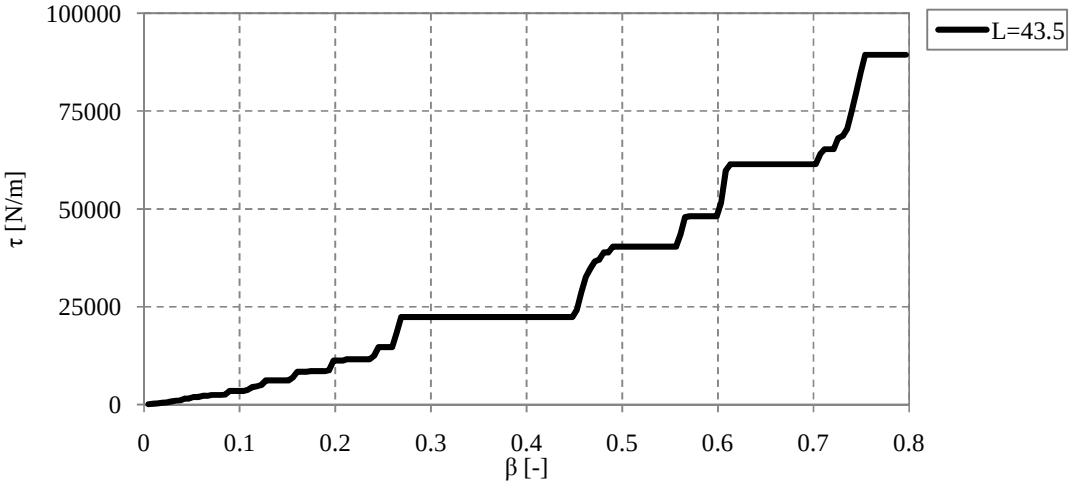

Figure C-102 *Design curve of the relation between β and τ for the HSLM-A loads of a bridge with three equal spans and L_{tot}=43.5 m.*

D. Appendix D Matlab Programs

In this appendix the layout of several Matlab programs used in the dynamic analysis of railway bridges will be presented. In the first three sections “main programs” are presented. With “main program” the authors refer to a program which purpose mainly is to gather the calculations from different function files to achieve a sought result. Used function files are presented in section D.4.

Each section starts with an overview of the created program and a description of the area of use for the program. In each section the code for the specific program will be printed and available to be copied into Matlab. Verifications for some of the programs are presented in the end of the sections.

D. APPENDIX D MATLAB PROGRAMS 169

D.1 SDOF 170
D.1.1 About the SDOF program 170
D.1.2 Code 170

D.2 Acceleration response in 2D 172
D.2.1 About the FE program 172
D.2.2 Matlab code 173
D.2.3 Verification 175

D.3 Acceleration response in 3D 179
D.3.1 About the FE program 179
D.3.2 Matlab code 180
D.3.3 Verification 183

D.4 Function files 186
D.4.1 Sdof Load 186
D.4.2 Train load 2D 187
D.4.3 Train load 3D 189
D.4.4 Mesh in 2D 191
D.4.5 Mesh in 3D 194
D.4.6 Newmark 196
D.4.7 Inverse iteration 197

D.1 SDOF

This section will present the “main program” for the transformation of a railway bridge into a SDOF model using the force scaling approach.

D.1.1 About the SDOF program

The force scaling approach is made in three steps. First the mass of the SDOF system is chosen arbitrary. Then the stiffness is calculated to get the first eigenfrequency equal to the first eigenfrequency of the railway bridge. Finally the load is scaled so that the static displacement of the SDOF system and the critical point in the railway bridge become equal.

The scaling of the load requires that the influence line for the displacement in the critical point of the bridge is calculated for a point load moving across the bridge. This is done in a function file called SdofLoad.m, see section D.4.1.

The Newmark-β method is used as the numerical time integration method, see section D.4.6.

D.1.2 Code

```
%-------------------------------------------------------------------------

%           MAIN PROGRAM
%           SDOF MODELING OF A RAILWAY BRIDGE

%-------------------------------------------------------------------------

%% STARTING DEFINITIONS
clear all

dof = 3;
neli = 20;

%% DEFINITION OF BRIDGE PARAMETERS
L_tot = 15;
kap = 1;
my = 2;
Li = L_tot*[1/(1+my) (1-1/(1+my))];
w=11.2;
h = 0.6;
E = 40*10^9;
Mass = 2400;
A = w*h;
I = w*h^3/12;
ep =[E A I Mass*w*h [0 0]];

%% EIGENFREQUENCIES
[Coord, Edof, Ndof, Elnod, Ex, Ey, nel, non, ndof, b] =...
    MeshTwoD(dof, neli, Li);

K = zeros(ndof);
M = zeros(ndof);
for i=1:nel
    [Ke,Me] = beam2d(Ex(i,:),Ey(i,:),ep);
    K = assem(Edof(i,:),K,Ke);
    M = assem(Edof(i,:),M,Me);
end

[L,X] = eigen(K,M,b);

%% MASS, STIFFNESS AND DAMPING OF THE SDOF SYSTEM

M_sdof = 1;
```

```
K_sdof = M_sdof * L(1);

damp = 0.02;
C_sdof = 2*damp*M_sdof*sqrt(L(1));

speed_step = 2.5/3.6;
max_speed = 100;

q = waitbar(0, 'Jag är en muffin..');
for i=1:((max_speed-28)/speed_step)

    speed = 28+i*speed_step; %Speed in m/s

    ntimes = 10000;

    [F_sdof,K_bridge,h]= SdofLoad(speed,ntimes,Li,E,I,4);
    %[F_sdof,K_bridge,h]= SdofLoadSimple(speed,ntimes,Li,E,I,1);

    S = K_sdof/K_bridge;

    F = S*F_sdof;

    u0 = 0;
    v0 = 0;
    bet = 0.25;
    gam = 0.5;
    [u,v,a,t] = NEWMARK(K_sdof,C_sdof,M_sdof,F,h,u0,v0,bet,gam);

    A_max(i) = max(a);
    V(i) = speed;

    waitbar(i/((max_speed-28)/speed_step))
end
close(q)
%% PLOT RESULTS

hold on
%plot(t,F)

plot(V.*3.6,A_max,'r')
%plot(t,a)
%plot(t,F)
```

D.2 Acceleration response in 2D

This section will present a "main program" for Matlab for calculating the acceleration response of a continuous railway bridge in 2D. The program has several areas of use. The main use is to calculate the maximum vertical acceleration in time in the railway bridge for the variation of train velocity and bridge parameters. But as several calculation procedures are required to achieve this it can also be used to produce the result of each separate calculation. With small modifications of the program code presented later it is possible to extract eigenfrequencies, eigenmodes and the time response concerning displacement, velocity and accelerations.

D.2.1 About the FE program

The program calculates the acceleration response using FE analysis. The analysis is based on mode-superposition, but numerical time integration is still used because of complexity in the train load. The calculation procedure can be divided in the following steps:

- Meshing
- Assembly of stiffness and mass matrix
- Calculation of eigenfrequencies, eigenmodes, modal mass matrix, modal stiffness matrix and modal damping
- Load creation
- Numerical time integration
- Data saving and plotting

The meshing is made using a function file called MeshTwoD.m. In short the mesh file creates a 2D beam with the possibility of choosing the number of spans, span lengths, degrees of freedom in each node and the number of elements in each span. The reader is referred to section D.4.4 for more information on the mesh function file.

Creation of each elements local stiffness and mass matrix and assembly into the global stiffness matrices is made using two Calfem files called beam2d.m and assem.m. The reader is referred to CALFEM (Austell P.–E., et. Al., 2004) for more information on Calfem and the used function files.

Calculation of eigenfrequencies and eigenmodes is also made using a Calfem file, called eigen.m. This file uses the built in eigensolver in Matlab but orders the output data in a correct way for the use of mode-superposition. It also normalizes the eigenmodes to get a modal mass matrix equal to a diagonal of ones.

Calculation of the train load is made using a function file called TrainTwoD.m. The function file calculates the load matrix representing the load in each node for every time step for an arbitrary HSLM-A load. The file has the possibilities of easily switching between different HSLM-A train loads and adjusting these loads to any choice of number of elements and time step length. The reader is referred to section D.4.2 for more information on the load function file.

The time integration function file uses the Newmark-β method with the parameters β and γ equal to 0.25 and 0.5 respectively to make it unconditionally stable. The time integration has been made using the function file Newmark.m, see D.4.6.

D.2.2 Matlab code

```
%--------------------------------------------------------------------------

%           MAIN PROGRAM
%           FE ANALYSIS ON A 2D CONTINUOUS BEAM

%--------------------------------------------------------------------------

%% INTRODUCTION
%--------------------------------------------------------------------------
%Program that calcualtes the response in time using Newmark integration.
%Mode superposition is used for fastening the calculation process. Meshing
%and load creation is made in function files.
%--------------------------------------------------------------------------

%% MAIN CALCULATIONS

%Clears all previous data
clear all
clc
clf

%Defines degrees of freedom in each node and number of elements in each
%span
dof = 3;
neli = 100;

%A loop that allows for the variation of any bridge parameter. Each loop
%defines a set of material, geometric and load parameters and calculates
%the response in time for a defined range of train velocities. The program
%can hence be used for smaller calculations like the response in time for
%one specific set of parameters but also extensive calculations like the
%maximum acceleration in time under the variation of train velocities for a
%chosen number of parameter sets.
for j=1:10
    %GEOMETRIC PARAMETERS
    %Total length
    L_tot = 15;
    %Relation between third and first span for three-sapn bridges
    kap = 1;
    %Relation between second and first span for two-span bridges
    my = 1.5;
    %Vector defining the length of each span. Has different definition
    %depending on the number of spans
    %Li = L_tot*[1/((1+my)*(1+kap)) (1-1/(1+my))  1/((1+my)*(1+1/kap))];
    Li = L_tot*[1/(1+my) (1-1/(1+my))];
    %Cross-section width
    w=11.2;
    %Cross-section height
    h = 0.6;
    %Area
    A = w*h;
    %Moment of inertia
    I = w*h^3/12;

    %MATERIAL PARAMETERS
    %Module of elasticity
    E = (20+5*j)*10^9;
    %Density
    Density = 2800;

    %Vector used in the creation of beam elements
    ep =[E A I Density*w*h [0 0]];

    %MESHING
    %Meshing is made using a separate function file
```

```
[Coord, Edof, Ndof, Elnod, Ex, Ey, nel, non, ndof, b] =...
    MeshTwoD(dof, neli, Li);

%ASSEMBLY OF BEAM ELEMENTS
%The Calfem function file beam2d is used for creating the local
%stiffness matrices and these are assembled using the Calfem file
%assem
K = zeros(ndof);
M = zeros(ndof);
for i=1:nel
    [Ke,Me] = beam2d(Ex(i,:),Ey(i,:),ep);
    K = assem(Edof(i,:),K,Ke);
    M = assem(Edof(i,:),M,Me);
end

%EIGENVALUES AND EIGENMODES
[L,X] = eigen(K,M,b);

%Cropping of the stiffness, mass and eigenvector matrices with
%consideration to boundary conditions.
K(b,:)=[];
K(:,b)=[];
M(b,:)=[];
M(:,b)=[];
X(b,:) = [];

%MODE SUPERPOSITION
%number of eigenmodes used
nmodes = 2;

%modal mass and stiffness matrix
M_diag = X(:,1:nmodes)'*M*X(:,1:nmodes);
K_diag = X(:,1:nmodes)'*K*X(:,1:nmodes);

%modal damping
damp = 0.02;
C_diag = diag(2*damp*sqrt(L(1:nmodes)));

%CONSIDERED RANGE OF TRAIN VELOCITY
speed_step = 1.25/3.6;
max_speed = 315;

%Loop that calculates the response in time using mode superposition
%for a chosen range of train velocities
q = waitbar(0, ['Iteration ' num2str(j)]);
for i=1:((max_speed)/speed_step)
    %Train velocity
    speed = i*speed_step;
    %Number of time steps
    ntimes = 10000;
    %Starting displacement and velocity
    u0 = zeros(nmodes,1);
    v0 = zeros(nmodes,1);

    %TRAIN LOAD
    [F_train] = TrainTwoD(speed,ntimes,ndof,Coord,Elnod,Edof,Li,1);
    F_train = [zeros(length(F_train(:,1)),1) F_train];
    F_train(b,:) = [];
    F = X(:,1:nmodes)'*F_train;

    %TIME INTEGRATION
    bet = 0.25;
    gam = 0.5;
    [u,v,a,t] = NEWMARK(K_diag,C_diag,M_diag,F,h,u0,v0,bet,gam);

    %Calculates the true displacements and accelerations and adds the
    %removed degrees of freedom
    u = X(:,1:nmodes)*u;
```

```
        a = X(:,1:nmodes)*a;
        e=1:1:ndof;
        e(b) = [];
        u_true = zeros(ndof,ntimes+1);
        a_true = zeros(ndof,ntimes+1);
        u_true(e,:) = u;
        a_true(e,:) = a;

        %MAXIMUM ACCELERATION
        Max = max(max(a_true));
        Min = min(min(a_true));
        A_maxmax(i,j) = max([Max abs(Min)]);

        V(i,j) = speed;
        waitbar(i/((max_speed)/speed_step))
    end
    close(q)
    %SAVES USED PARAMETERS FOR EACH ITERATION
    EE(j) = E;
    MASS(j) = Mass;
    L_TOT(j) = L_tot;
    MY(j) = my;
    DAMP(j) = damp;
end

%% PLOT RESULTS
% A huge variation of plot options can be used. The code below is just an
% example of possible plot options
hold on
colors = ['y', 'g', 'b', 'r', 'k'];
for k=1:5
plot(V(:,k)*3.6, A_maxmax(:,k), colors(k))
end
xlabel('Speed [km/h]')
ylabel('Acceleration [m/s^2]')
title('HSLM-A1')
vari = 'E = ';
legend([vari num2str(EE(1))], [vari num2str(EE(2))],...
   [vari num2str(EE(3))], [vari num2str(EE(4))],...
   [vari num2str(EE(5))])
```

D.2.3 Verification

Verification of the program has been made using the commercial software ADINA. A 2D model of a two-span bridge has been created in both ADINA and the Matlab FE program with the purpose of comparing the responses from the two programs. The geometry and boundary conditions in the model are shown by **Error! Reference source not found.**.

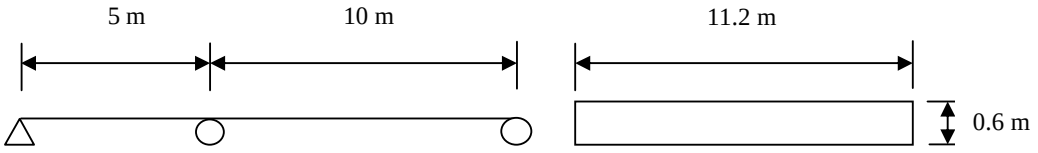

Figure D-1 Geometry and boundary conditions in the model used for the verification.

The material parameters in the form of module of elasticity and concrete density have been chosen to 30 GPa and 2400 kg/m^3 respectively.

The time integration is made using the Newmark-β method with the integration parameters β and γ equal to 0.25 and 0.5 respectively. 10000 time steps are used in the integration.

Both models use mode-superposition limited to the three eigenmodes with lowest corresponding eigenfrequency. Damping has been included through a modal damping of 2 % for all considered eigenmodes.

Beam elements are used in both programs. One hundred elements in each span have been used in the Matlab program, which corresponds to a length of 0.05 and 0.1 m. The element length in Adina has been chosen to 0.25 in both spans. The reason why the element lengths have been chosen differently between the models is because the Matlab model is built to choose the number of elements equally in every span, while the Adina model gets substantially easier to create with regard to the train load using equal span lengths.

As a first verification the frequencies from the two models are compared, see Table D.1.

Table D.1 Eigenfrequencies for the two models

	Frequencies	
Mode	ADINA	Matlab
1	14.21 Hz	14.2 Hz
2	44.17 Hz	44.17 Hz
3	61.71 Hz	61.71 Hz

The HSLM-A load case A1 and A4 have been used to verify the dynamic response of the program. The loads have been simulated with the velocities 180 km/h and 270 km/h respectively. The displacements and accelerations have been gathered in the middle of the second span. Figure D-2 to Figure D-5 show the comparison of responses between the two programs for the two first seconds.

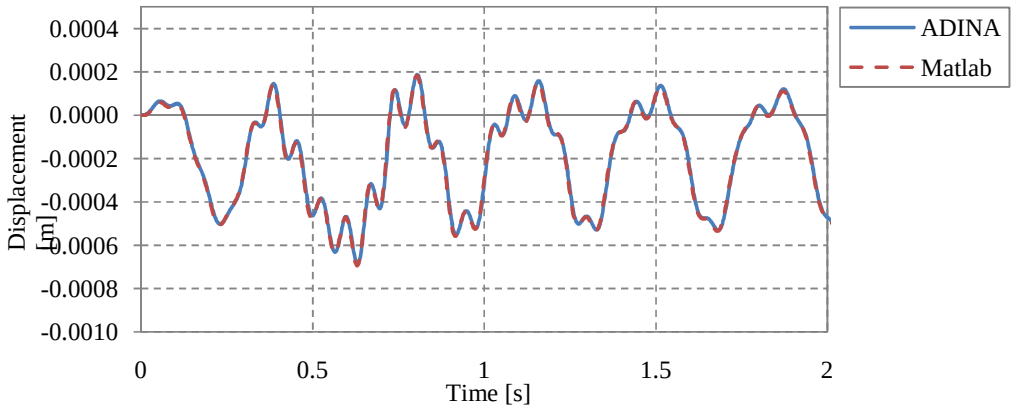

Figure D-2 *Comparison between displacements for the HSLM-A1 train load with velocity of 180 km/h*

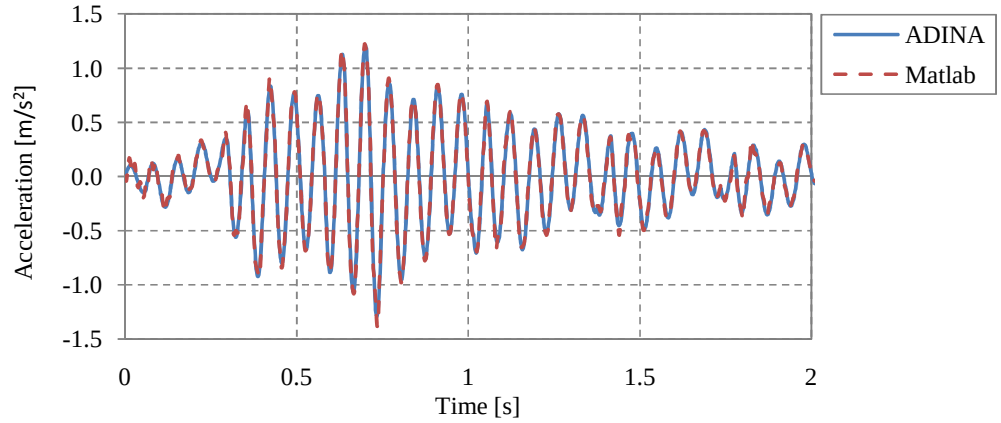

Figure D-3 *Comparison between accelerations for the HSLM-A1 train load with velocity of 180 km/h*

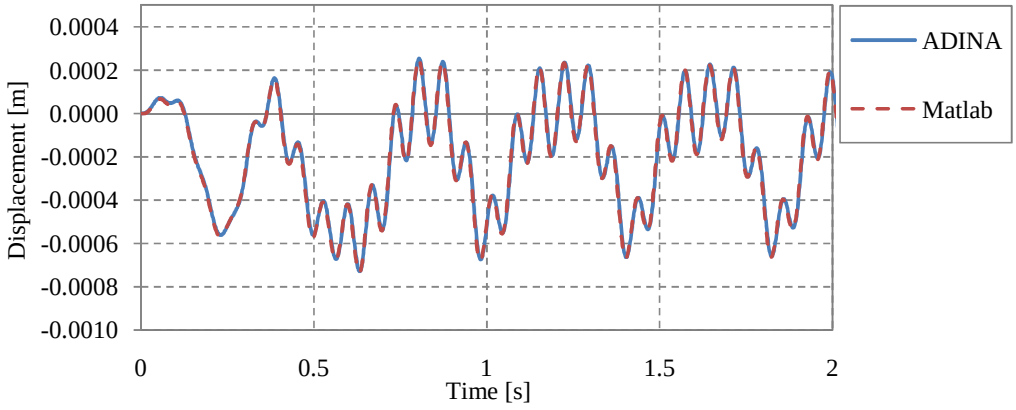

Figure D-4 *Comparison between displacements for the HSLM-A4 train load with velocity of 270 km/h*

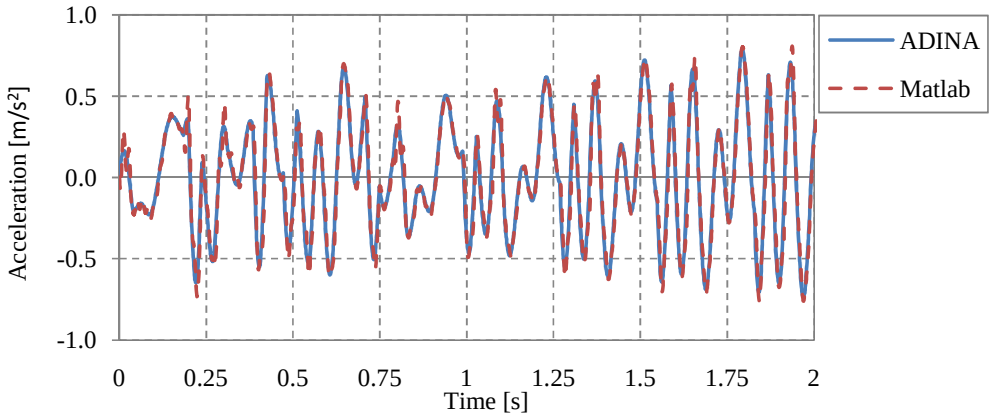

Figure D-5 *Comparison between accelerations for the HSLM-A4 train load with velocity of 270 km/h*

D.3 Acceleration response in 3D

The purpose with this "main program" is to calculate the maximum vertical acceleration in time considering a 3D model of railway bridges for the variation of load and bridge parameters. It is also possible to modify the program to calculate eigenfrequencies, eigenmodes and the time response concerning displacement, velocity and accelerations.

D.3.1 About the FE program

The program calculates the acceleration response for a railway bridge modelled as a simply supported plate with the possibility to use eccentric loading. The analysis uses mode-superposition and numerical time integration to get the vertical acceleration response in time. The program can be divided in several steps:

- Meshing
- Assembly of the stiffness matrix
- Calculation of eigenfrequencies, eigenmodes, modal mass matrix, modal stiffness matrix and modal damping
- Creation of HSLM train loads
- Numerical time integration
- Plot figures and saves data

The function file MeshThreeD.m is used for creating the mesh. The mesh file creates a 3D plate consisting of shell elements. It is possible to choose span length and the number of elements in both length of the span and the width. More information about the mesh function file can be found in section D.4.5.

The Calfem files platre.m, planre and assem.m have been used in the creation of each elements local stiffness and mass matrix and assembly into the global stiffness matrices. Further information about the Calfem files is found in CALFEM – A finite element toolbox version 3.4 (Austell P.–E., et. Al., 2004)

The 3D program uses a different method for calculating the eigenfrequencies and eigenmodes compared to the 2D "main program". Instead of using a Calfem file and the built in eigensolver in Matlab a method called inverse iteration and inverse iteration with shift is used. The method provides the possibility of calculating only a few of the lowest eigenmodes to save calculation time and can be used to choose specific eigenmodes. The gained eigenmodes from the function file Inverse_iteration.m are all normalized so it is possible to get a modal mass matrix equal to a diagonal of ones. The function file is described in detail in section D.4.7.

The train load in this program is defined by the function file TrainThreeD.m. It calculates the load representing the load in each node for every time step for an arbitrary HSLM-A load. It is possible to switch between different HSLM-A train loads and adjust to arbitrary choice of time steps and mesh size. The function file is described further in D.4.3.

As in the 2D program Newmark integration are used for the time integration, for more information see D.4.6.

D.3.2 Matlab code

```
%-------------------------------------------------------------------------
%
%           MAIN PROGRAM
%           FE ANALYSIS ON A 3D PLATE
%
%-------------------------------------------------------------------------

%% INTRODUCTION
%-------------------------------------------------------------------------
% Program that calculates the response in time using Newmark         %
integration.
% Mode superposition is used for fastening the calculation process.  %
Meshing, and load creation is made in function files.

%% MAIN CALCULATIONS

% Clear all previous data
clear all
clc
clf

%Indata
qz = 0;
ty = 0;

%Number of elements used in the length of the bridge
n11 = 16;

%Number of elements used in the width of the bridge
n2  = 16;

%% Mesh the geometry in separate file.
%A loop that allows for the variation of any bridge parameter. Each %loop
defines a set of material, geometric and load parameters and %calculates the
response in time for a defined range of train %velocities. The program can
therefore be used for the response in %time for one specific set of
parameters but also extensive %calculations like the maximum acceleration in
time under the %variation of train velocities for a chosen number of
parameter sets.
for j=1:10
    %GEOMETRIC PARAMETERS
    %Total length
    l1 = 15;
    Li = [l1 l2];
    %Cross-section width
    b=11;
    %Cross-section height
    h=0.7;
    %Area
    A = b*h;
    %Moment of inertia
    I = b*h^3/12;

    %MATERIAL PARAMETERS
    %Module of elasticity
    E = 40e9 ;
    %Density
    d=2800;
    %poisson's ratio
    v = 0.2;

    %MESHING
    %Meshing is made using a separate function file
    [B1,B2,B3,B4,P1,P2,P3,P4,Ex,Ey,ndof,nel,non,Edof]=MeshThreeD(l1,b,n11,n2)
    ;
```

```
%ASSEMBLY OF SHELL ELEMENTS
%The Calfem function files platre and planre are used for %creating the
local stiffness matrices and these are assembled %using the Calfem
function file assem
K = zeros(ndof);
f = zeros(ndof,1);
D = hooke(1,E,v);
ep = [1 h];
eq = [0 0 qz]';
for i=1:nel
     ex = Ex(i,:);
     ey = Ey(i,:);
     [Ke1,fe1]=platre(ex,ey,ep(2),D,eq(3));
     [Ke2,fe2]=planre(ex([1 2]),ey([2 3]),ep,D,eq([1 2]));
     Ke = zeros(20);
     fe = zeros(20,1);
     Ke([1 2 6 7 11 12 16 17],[1 2 6 7 11 12 16 17])=Ke2;
     Ke([3 4 5 8 9 10 13 14 15 18 19 20],[3 4 5 8 9 10 13 14 15 18 19
       20])=Ke1;
     fe([1 2 6 7 11 12 16 17])=fe2;
     fe([3 4 5 8 9 10 13 14 15 18 19 20])=fe1;
    [K,f] = assem(Edof(i,:),K,Ke,f,fe);
end
%% MASS MATRICE
%Mass for each element
M_el_1 = l1*b*d*h/nel;
%Rotational lumped mass (see ADINA manual)
M_rot_1 = (M_el_1/4)*(1/12)*(h*h);
k1 = [M_el_1/4 M_el_1/4 M_el_1/4 M_rot_1 M_rot_1...
      M_el_1/4 M_el_1/4 M_el_1/4 M_rot_1 M_rot_1...
      M_el_1/4 M_el_1/4 M_el_1/4 M_rot_1 M_rot_1...
      M_el_1/4 M_el_1/4 M_el_1/4 M_rot_1 M_rot_1];
Me_1 = diag(k1);
M = zeros(ndof);
for i=1:nel
    M = assem(Edof(i,:),M,Me_1);
end
%% BOUNDARY CONDITIONS
for i=1:length(B4(:,1))
    bc1((3*i-2):(3*i)) = B4(i,1:3)';
    bc2((2*i-1):(2*i)) = B2(i,2:3)';
    bc5((2*i-1):(2*i)) = B4(i,2:3)'+5*(n2+1)*n11/2;
end

bc3 = zeros(1,2);
for k=2:(length(B3(:,1))-1)
    b3 = B1(k,[1 2 3])+5*n2/2;
    bc3e = [b3; 0 0 0]';
    bc3 = [bc3;bc3e];
end
bc3(1,:)=[];

bc4 = zeros(1,2);
for k=2:(length(B3(:,1))-1)
    b4 = B1(k,4)+5*n2/2;
    bc4e = [b4; 0]';
    bc4 = [bc4;bc4e];
end
bc4(1,:)=[];

bc = [bc1';bc2'];
BC2 = [bc1';bc3(:,1);bc2'];
BC3 = [bc1';bc4(:,1);bc5';bc2'];


%% Solve the eigen-value problem
Ltot = l1;
[X,L]=Inverse_iteration(K,M,bc,BC2,BC3,ndof,Ltot,E,b*h^3/12,b*h,d);
```

```
    %SAVE USED PARAMETERS FOR EACH ITERATION
    EE(z,j) = E;
    L_TOT(z,j) = l1;
    MASS(z,j) = d;
    BB(z,j)=b;
    H(z,j) = h;

    %Cropping of the stiffness, mass and eigenvector matrices with
    %consideration to boundary conditions.
    K(bc,:)=[];
    K(:,bc)=[];
    M(bc,:)=[];
    M(:,bc)=[];
    X(bc,:) = [];

    %%MODE SUPERPOSITION
    %Number of eigenmodes used
    nmodes = 3;

    %% Creation of diagonal K,M and C for mode superposition

    M_diag = X(:,1:nmodes)'*M*X(:,1:nmodes);
    K_diag = X(:,1:nmodes)'*K*X(:,1:nmodes);

    %modal damping (According to BV Bro, Banverket 2006)
    if Ltot<=20
    damp = 0.015 + 0.0007*(20-Ltot);
    else
    damp = 0.015;
    end
    C_diag = diag(2*damp*2*pi*L(1:nmodes));

    %CONSIDERED RANGE OF TRAIN VELOCITY
    speed_step = 1.25/3.6;
    max_speed = 0.8*vcr;
    vcr = pi/2/Ltot^2*sqrt(E*I/(d*A))*18;

    %% Newmark integration
    bet = 0.25;
    gam = 0.5;
    %Number of time steps
    ntimes = 10000;
    %Starting displacements
    u0 = zeros(nmodes,1);
    v0 = zeros(nmodes,1);

    q = waitbar(0, ['Iteration' num2str(j)]);
    %Loop that calculate the response in time using mode
     %superposition for a chosen range of train velocities
        for i=1:(max_speed/speed_step)
            e = 3.5;
            %Train velocity
            speed = i*speed_step;
            %% Train load
            [F_train h] =
TrainLoadThreeD(Li,speed,ntimes,ndof,Ex,Ey,Edof,b,e,n2,n11,n12,j);
            F_train(bc,:) = [];
            F = X(:,1:nmodes)'*F_train;

            %TIME INTEGRATION
            [a,t] = NEWMARK(K_diag,C_diag,M_diag,F,h,u0,v0,bet,gam);
             %Calculate the true displacements and acceleration and %adds
             the removed degrees of freedom.
            e = 1:1:ndof;
            e(bc) = [];
            a = X(:,1:nmodes)*a;
            a_true = zeros(ndof,ntimes);
```

```
            a_true(e,:) = a;
            a = [];
            % MAX IN THE WHOLE BRIDGE
            % MaxMax = max(max(a_true));
            % MinMin = min(min(a_true));
            % A_maxmax(i,j) = max([MaxMax abs(MinMin)]);
            V(i,j) = speed;
            e2 = 3:5:(ndof-2);
            u_vert = u_true(e2,:);
            a_vert = a_true(e2,:);
            a_true = [];
            MaxVert = max(max(a_vert));
            MinVert = min(min(a_vert));
            A_maxvert(i,j) = max([MaxVert abs(MinVert)]);
        end
end

%% PLOT RESULTS
% A huge variation of plot options can be used. The code below is just an
% example of possible plot options
hold on
colors = ['y', 'g', 'b', 'r', 'k'];
for k=1:5
plot(V(:,k)*3.6, A_maxmax(:,k), colors(k))
end
xlabel('Speed [km/h]')
ylabel('Acceleration [m/s^2]')
title('HSLM-A1')
vari = 'E = ';
legend([vari num2str(EE(1))], [vari num2str(EE(2))],...
   [vari num2str(EE(3))], [vari num2str(EE(4))],...
   [vari num2str(EE(5))])
```

D.3.3 Verification

ADINA and the Matlab 3D FE program has been used to build a similar model of a one span bridge with the purpose of comparing the responses from the two programs. The boundary conditions and geometry used in the verification model can been seen in Figure D-6.

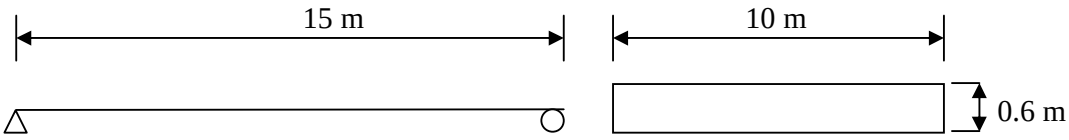

Figure D-6 Geometry and boundary conditions.

The material parameters in the form of module of elasticity and concrete density have been chosen to 30 GPa and 2400 kg/m^3 respectively.

The time integration is made using the Newmark-β method with the integration parameters β and γ equal to 0.25 and 0.5 respectively. 10000 time steps are used in the integration.

Both models use mode-superposition limited to the three eigenmodes with lowest corresponding eigenfrequency. Damping has been included through a modal damping of 2 % for all considered eigenmodes.

Plate elements are used in the Matlab program to create the model above and in ADINA shell elements are used. The element size in Adina has been chosen to $0.25 \cdot 0.25 m^2$. In Matlab the element size were chosen to 16·16 elements which correspond to $0.625 \cdot 0.9375\ m^2$. The reason why a much more coarse mesh was chosen for the Matlab program is because of the memory limit that the program has.

The result from comparing the frequencies from the two models can be seen in Table D-1 .

Table D-1 Comparison between the eigenfrequencies for the two programs.

	Frequencies	
Mode	ADINA	Matlab
1	4.3 Hz	4.3 Hz
2	9.93 Hz	10.03 Hz
3	17.25 Hz	17.26 Hz

The further verification of the FE Matlab 3D plate program is divided in two parts. First the total response is monitored for one specific train configuration, certain bridge parameters and a velocity of 180 km/h. The response gained from the Matlab FE program is compared to the response obtained from an analysis in ADINA with the same input parameters. After the total response is verified, for one single case, max accelerations for different bridge configurations and speeds for the trainload will be compared. It is mainly the width of the bridge that will be changed in the comparison but also two different velocities of the traveling train will be tested.

The load case HSLM-A1 has been used to represent the high-speed train. It has been simulated with the velocity 180 km/h and accelerations has been monitored in the middle of the span. Results from the comparison between total acceleration response in ADINA and Matlab are shown in Figure D-7 and Figure D-8. The response from each program shows very similar behavior and has only small deviations from one other.

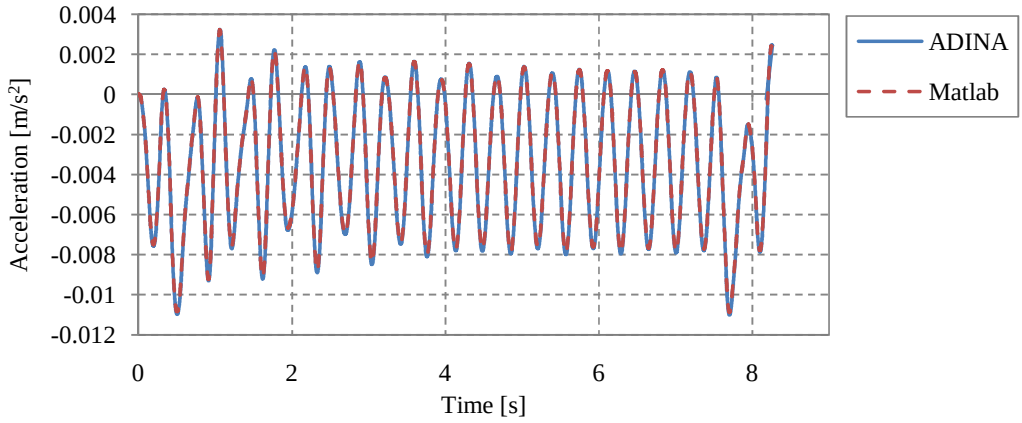

Figure D-7 Comparison between displacements for the HSLM-A1 train load with velocity of 180 km/h

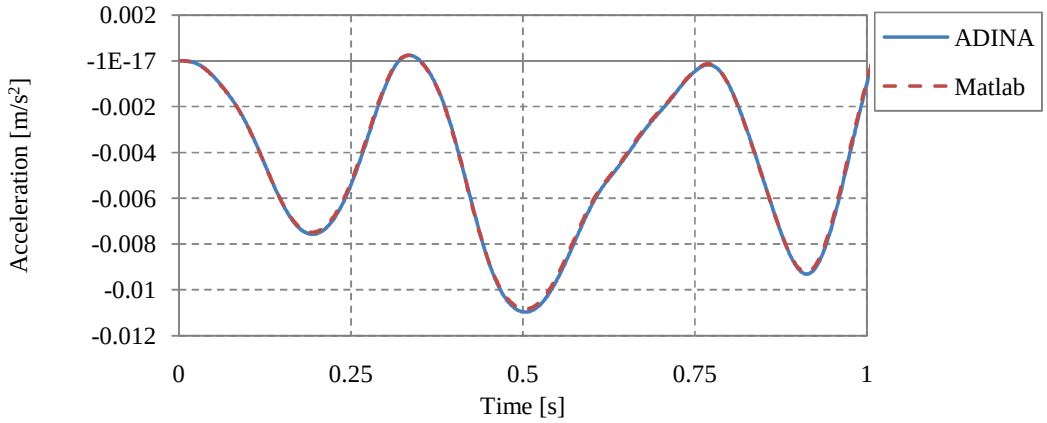

Figure D-8 *Comparison between displacements for the HSLM-A1 train load with velocity of 180 km/h.*

Since the response is nearly identical for this single case next step is to compare the maximum acceleration with some different input parameters. Results from the analysis in ADINA and Matlab are shown in Table D-2 and Table D-3 respectively. The comparison between the results in each program is shown in Table D-4.

Table D-2 *Max accelerations from the different input parameters in ADINA.*

ADINA		
HSLM-A1	L=10 m, b=6 m	L=10 m, b=10 m
180.0 km/h	2.925 m/s^2	1.239 m/s^2
242.5 km/h	15.446 m/s^2	9.177 m/s^2

Table D-3 *Max accelerations from the different input parameters in Matlab.*

Matlab		
HSLM-A1	L=10 m, b=6 m	L=10 m, b=10 m
180.0 km/h	2.816 m/s^2	1.262 m/s^2
242.5 km/h	15.439 m/s^2	8.897 m/s^2

Table D-4 *Comparison of max accelerations from the result in ADINA and Matlab.*

ADINA vs Matlab		
HSLM-A1	L=10 m, b=6 m	L=10 m, b=10 m
180.0 km/h	3.7%	1.8%
242.5 km/h	0.0%	3.0%

D.4 Function files

The “main programs” described earlier all gather calculations from several function files. Function files are used to mesh the geometry, calculate the travelling train load, calculate the dynamic response and for solving the eigenvalue-problem. Several of these function files have been made by the authors, and these are described in the following sub-chapters.

D.4.1 Sdof Load

The function file SdofLoad.m is used in the “Mina program” for transforming a railway bridge into a SDOF system.

The function file calculates the influence lines for the critical point of the railway bridge (in the middle of the largest span) for a two-span bridge considering static displacement when a point load moves across the bridge. The file also gathers the influence from all point loads in a HSLM-A train load into an influence line with consideration to a chosen train configuration.

D.4.1.1 Matlab code

```
%--------------------------------------------------------------------------
%           FUNCTION FILE
%           TRAIN LOAD IN 2D
%--------------------------------------------------------------------------
%% INTRODUCTION
function [F_sdof,K_bridge,h]= SdofLoad(v,ntimes,Li,E,I,A)
%--------------------------------------------------------------------------
%Pogram that calculates the load matrix for a FE analysis corresponding to
%a HSLM-A train load.

%       INDATA

%       v =         Train velocity
%       ntimes =    Number of time steps
%       Li =        Vector containing the length of each span. The function
%                   file is compatible with arbitrary number of spans.
%       E =         Module of elasticity.
%       I =         Moment of inertia.
%       A =         Number of the HSLM-A train load considered.

%       OUTPUT

%       F_sdof =    Vector where every value corresponds to the load for a
%                   time step.
%       K_bridge =  Stiffness of the railway bridge in the considered point
%       h =         time step
%--------------------------------------------------------------------------

N = [18 17 16 15 14 13 13 12 11 11];
D = [18 19 20 21 22 23 24 25 26 27];
d = [ 2 3.5 2 3 2 2 2 2.5 2 2];
P = [170 200 180 190 170 180 190 190 210 210]*10^3;

N = N(A);
D = D(A);
d = d(A);
P = P(A);

distance = zeros(1,(N+1)*2+12);
s = length(distance);
distance(1:6) = [0 3 14 17 20.525 20.525+d];

for i=1:(N+1)
    distance([5+2*i 6+2*i]) = [18.7625+D*i-d/2 18.7625+D*i+d/2];
```

```
end

distance((s-5):s) = [(N+2)*D+17-d (N+2)*D+17 (N+2)*D+20.525 ...
    (N+2)*D+23.525 (N+2)*D+34.525 (N+2)*D+37.525];

start = distance./v;
h = (sum(Li)+distance(s))/v/ntimes;
%%

defl_max = Li(2)^3/(48*E*I) - Li(2)^4/(64*E*I*sum(Li))*3/4;
F_sdof = zeros(1,ntimes+1);
for i=1:ntimes

    for j=1:length(start)

        a1 = v*(h*i-start(j));
        a2 = v*(h*i-start(j))-Li(1);
        b = Li(2)-a2;

        if a1<=0
            break
        end

        if b<=0
            continue
        end

        if v*(h*i-start(j)) <= Li(1)
            F_sdof(i+1) = F_sdof(i+1) + ...
                P*(a1*Li(1)*Li(2)^2/(32*E*I*sum(Li))*(1-a1^2/Li(1)^2));
        else if v*(h*i-start(j)) <= Li(1)+Li(2)/2
                F_sdof(i+1) = F_sdof(i+1) - ...
                    P*(a2*Li(2)^2/(48*E*I)*(3-4*a2^2/Li(2)^2)-b*Li(2)^3/...
                    (32*E*I*sum(Li))*(1-b^2/Li(2)^2));
            else
                F_sdof(i+1) = F_sdof(i+1) - ...
                    P*(b*Li(2)^2/(48*E*I)*(3-4*b^2/Li(2)^2)-b*Li(2)^3/...
                    (32*E*I*sum(Li))*(1-b^2/Li(2)^2));
            end
        end

    end
end

F_sdof = F_sdof./defl_max;
K_bridge = 1/defl_max;
```

D.4.2 Train load 2D

The function file is called TrainTwoD. It creates the load matrix of a HSLM-A train load. A load matrix is a matrix where every column corresponds to the load on every degree of freedom and one time step. The load matrix hence has rows equal to the degrees of freedom and columns equal to the number of time steps.

The procedure behind the calculations in the file is as follows:

- The load parameters are decided based on which HSLM-A train load that the user has chosen.
- Based on the load parameters a vector containing the distance between all point loads with the first load as reference is created. The vector is called “distance”.

- Based on the “distance” vector and the chosen train velocity a vector describing the time between loads is created. The vector is called “start” as it describes the time for which every point load starts affecting the bridge.
- When the “start” vector has been established a double loop is used for performing the calculations. The first loop corresponds to every time step and the second to every point load inside each time step. For one time step the program calculates where every point load is using the “start” vector and assembles the load on the corresponding elements vertical degrees of freedom.

The assembly of the load has been made on the vertical degrees of freedom, which means that an element affected by a point load is seen as simply supported. This solution will be correct if small element lengths are used as the moments become negligible.

D.4.2.1 Matlab code

```
%-------------------------------------------------------------------------
%           FUNCTION FILE
%           TRAIN LOAD IN 2D
%-------------------------------------------------------------------------
%% INTRODUCTION
function [F_train] = TrainTwoD(v,ntimes,ndof,Coord,Elnod,Edof,Li,A)
%-------------------------------------------------------------------------
%Pogram that calculates the load matrix for a FE analysis corresponding to
%a HSLM-A train load.

%       INDATA

%       v =         Train velocity
%       ntimes =    Number of time steps
%       ndof =      Number of degrees of freedom
%       Coord =     Vector with the x coordinate of each node
%       Elnod =     Matrix where each row contains the nodes for the
%                   corresponding element
%       Edof =      Matrix connecting dofs and elements according to Calfem
%       Li =        Vector containing the length of each span. The function
%                   file is compatible with arbitrary number of spans.
%       A =         Number of the HSLM-A train load considered.

%       OUTPUT

%       F_train =   Matrix where every column corresponds to the load for a
%                   time step. The size is ndof*ntimes.
%-------------------------------------------------------------------------

F_train = zeros(ndof,ntimes);

N = [18 17 16 15 14 13 13 12 11 11];
D = [18 19 20 21 22 23 24 25 26 27];
d = [ 2 3.5 2 3 2 2 2 2.5 2 2];
P = [170 200 180 190 170 180 190 190 210 210]*10^3;

N = N(A);
D = D(A);
d = d(A);
P = P(A);

distance = zeros(1,(N+1)*2+12);
s = length(distance);
distance(1:6) = [0 3 14 17 20.525 20.525+d];

for i=1:(N+1)
    distance([5+2*i 6+2*i]) = [18.7625+D*i-d/2 18.7625+D*i+d/2];
```

```
end

distance((s-5):s) = [(N+2)*D+17-d (N+2)*D+17 (N+2)*D+20.525 ...
    (N+2)*D+23.525 (N+2)*D+34.525 (N+2)*D+37.525];

start = distance./v;
load = P * ones(1,s);
h = (sum(Li)+distance(s))/v/ntimes;

for i=1:ntimes

    for j=1:length(start)

        s= v*(h*i-start(j));
        if s<=0
            break
        end

        if s>=sum(Li)
            continue
        end

        for k = 1:(length(Coord)-1)
            if s <= Coord(k+1)
                el = k;
                break
            end
        end

        a = s - Coord(Elnod(el,2));
        b = Coord(Elnod(el,3)) - s;
        L = Coord(Elnod(el,3)) - Coord(Elnod(el,2));

        P1 = load(j)*b/L;
        P2 = load(j)*a/L;

        F_train(Edof(el,[3 6]),i) = [-P1 -P2]';
    end
end
```

D.4.3 Train load 3D

The function file is called TrainThreeD. It creates the load matrix considering a three-dimensional geometry. The procedure behind the calculations is very similar to that in TrainTwoD, and the reader is referred to this description for a more thorough explanation of the calculation procedure.

The additional calculation that is required when considering a 3D geometry concerns the eccentricity of the load. The only addition is that when the “start” vector has been calculated an additional vector that describes the numbering of the elements that the train will pass through needs to be established before the double loop. The “Coord” vector was used for this purpose in the 2D load creation as it was known that the load would pass through all elements.

D.4.3.1 Matlab code

```
%-------------------------------------------------------------------------
%
%           FUNCTION FILE
%           TRAIN LOAD IN 3D
%
%-------------------------------------------------------------------------

%% INTRODUCTION
```

```
function [F_train h] = ...
    TrainThreeD(Li,speed,ntimes,ndof,Ex,Ey,Edof,b,e,n2,n11,n12,A)

%-------------------------------------------------------------------------
%Pogram that calculates the load matrix for a FE analysis corresponding to
%a HSLM-A train load.
%
%       INDATA
%
%       Li =        Vector containing the length of each span. The function
%                   file is compatible with arbitrary number of spans.
%       speed =     Train velocity
%       ntimes =    Number of time steps
%       ndof =      Number of degrees of freedom
%       Ex =        x-coordinates for every element. Each row corresponds
%                   to one element. The coordinates for one element are
%                   displaced in the following order:
%
%                   4-------------3
%                   |             |
%                   |             |
%                   |             |
%                   1-------------2
%
%       Ey =        y-coordinates for every element.
%       Edof =      Matrix connecting dofs and elements according to Calfem
%       b =         Width of the bridge
%       e =         Eccentricity of the load
%       n2 =        Number of elements perpendicular to the bridge length
%                   coordination
%       n11 =       Number of elements in the first span
%       n12 =       Number of elements in the second span
%       A =         Number of the HSLM-A train load considered.

%       OUTPUT

%       F_train =   Matrix where every column corresponds to the load for a
%                   time step. The size is ndof*ntimes.
%-------------------------------------------------------------------------

F_train = zeros(ndof,ntimes);

y_coord = b/2+e;

N = [18 17 16 15 14 13 13 12 11 11];
D = [18 19 20 21 22 23 24 25 26 27];
d = [ 2 3.5 2 3 2 2 2 2.5 2 2];
P = [170 200 180 190 170 180 190 190 210 210]*10^3;

N = N(A);
D = D(A);
d = d(A);
P = P(A);


distance = zeros(1,(N+1)*2+12);
s = length(distance);
distance(1:6) = [0 3 14 17 20.525 20.525+d];

for i=1:(N+1)
    distance([5+2*i 6+2*i]) = [18.7625+D*i-d/2 18.7625+D*i+d/2];
end

distance((s-5):s) = [(N+2)*D+17-d (N+2)*D+17 (N+2)*D+20.525 ...
    (N+2)*D+23.525 (N+2)*D+34.525 (N+2)*D+37.525];

start = distance./speed;
```

```
load = P * ones(1,s);
h = (sum(Li)+distance(s))/speed/ntimes;


%%

for i=1:n2
    if y_coord<=Ey(i,4)
        el_row_nr = i;
        break
    end
end

for i=1:(n11+n12)
    el_row(i) = el_row_nr + n2*(i-1);
end

%%

for i=1:ntimes

    for j=1:length(start)

        s= speed*(h*i-start(j));
        if s<=0
            break
        end

        if s>=sum(Li)
            continue
        end

        for j = 1:length(el_row)
            if s <= Ex(el_row(j),2)
                el = el_row(j);
                break
            end
        end
        a1 = s-Ex(el,1);
        a2 = Ex(el,2)-s;
        b1 = y_coord - Ey(el,1);
        b2= Ey(el,4) - y_coord;

        P1 = P*b2*a2/((Ey(el,3)-Ey(el,1))*(Ex(el,2)-Ex(el,1)));
        P2 = P*b2*a1/((Ey(el,3)-Ey(el,1))*(Ex(el,2)-Ex(el,1)));
        P3 = P*b1*a1/((Ey(el,3)-Ey(el,1))*(Ex(el,2)-Ex(el,1)));
        P4 = P*b1*a2/((Ey(el,3)-Ey(el,1))*(Ex(el,2)-Ex(el,1)));

        F_train(Edof(el,[4 9 14 19]) ,i) = F_train(Edof(el,[4 9 14 19])
        ,i)+[-P1 -P2 -P3 -P4]';
    end
end
```

D.4.4 Mesh in 2D

The function file is called MeshTwoD. Its purpose is to create a two-dimensional mesh of a continuous beam. Basically it creates a row of nodes placed with a spacing that depends on the requested span lengths and number of elements.

The program can create the mesh of a continuous beam with arbitrary span lengths and number of spans. It is however limited in the choice of spacing between nodes as the same number of elements is used for all spans.

Creating the mesh of a structure basically means establishing a number of matrices that describes coordinates and structure of the mesh. The created matrices are explained in the code below.

D.4.4.1 Matlab code

```
%-------------------------------------------------------------------------

%           FUNCTION FILE
%           MESH FOR 2D CONTINUOUS BEAM

%-------------------------------------------------------------------------

%% INTRODUCTION

function [Coord, Edof, Ndof, Elnod, Ex, Ey, nel, non, ndof, b] = ...
    MeshTwoD(dof, neli, Li)

%-------------------------------------------------------------------------
%Function file that creates the mesh of a 2D continuous beam

%       INDATA

%       dof =   degrees of freedom in each node
%       neli =  number of elements in every span
%       Li =    vector with the lengths of each span respectively. The
%               length Li defines the number of spans.

%       OUTPUT

%       Coord = A vector with the x coordinate of each node.
%       Edof =  Matrix connecting dofs and elements according to CALFEM.
%               Has the follwing form for the case of dof=3:

%               Edof = [1 1 2 3 4 5 6;
%                       2 4 5 6 7 8 9;
%                       3 7 8 9 ...

%       Ndof =  Dofs for each node. Has the following form:

%               Ndof = [1 1 .. dof;
%                       2 dof+1 .. dof*2;
%                       3 2*dof+1 .. dof*3;
%                       4 ..

%       Elnod = Nodes for each element. Has the following form:

%               Elnod = [1 1 2;
%                        2 2 3;
%                        3 ..

%       Ex =    x coordinates for each element.Each row correspond to one
%               element
%       Ey =    y coordinates for each element. The matrix is a zero matrix
%       nel =   number of elements
%       non =   number of nodes
%       ndof =  total number of degrees of freedom
%       b =     vector consisting of locked dofs

%-------------------------------------------------------------------------

%% Creation of Coord, nel, non
nel = length(Li) * neli;
Coord = 0;
for j=1:length(Li)
    for i=1:neli
        Coord = [Coord; Li(j)/neli*i+Coord((j-1)*neli+1)];
    end
```

```
end

non = length(Coord);

%% Creation of Elnod, Ex, Ey
for i=1:nel
    Elnod(i,:) = [i i i+1];
end

for i=1:length(Elnod)
    ex = [Coord(Elnod(i,2),1) Coord(Elnod(i,3),1)];
    Ex(i,:) = ex;
end

Ey = zeros(nel,2);

%% Creation of Ndof, ndof
for i=1:non
    for j=1:dof
        t(j) = (dof*i-dof)+j;
    end
    Ndof(i,:) = [i t];
end

ndof =  max(max(Ndof));

%% Creation of Edof
for i=1:nel
    Edof(i,:) = [i Ndof(Elnod(i,2), 2:(dof+1)) Ndof(Elnod(i,3), 2:(dof+1))];
end

%% Creation of b
b = [1 2]';
for i=1:length(Li)
    b = [b; dof*neli*i*[1 1]'+[1 2]'];
end
```

D.4.5 Mesh in 3D

The purpose with the 3D mesh file is to create a mesh for a rectangular domain which represents a one span bridge with simply supported boundary conditions. It will therefore create a rectangular mesh with the chosen mesh density of n11xn2 and a mesh size that depend on chosen size of the bridge and mesh density. It will assemble all necessary matrices needed to use the CALFEM-toolbox, this includes the following matrices:

- Edof – Describe the connection between elements
- Ex – Element wise x-coordinates
- Ey – Element wise y-coordinates
- Pi – Row vector containing x-dof (1st value) and y-dof (2nd value) for corner node i (i=1,2,3,4).
- Bi – Matrix containing x-dofs (1st column) and y-dofs (2nd column) for nodes on boundary segment i (i=1,2,3,4).

In excess of these matrices the function file also calculate and provide the main program with the number of elements (nel), number of nodes (non) and number of degrees of freedom (ndof) included in the model.

D.4.5.1 Matlab Code

```
function[B1,B2,B3,B4,P1,P2,P3,P4,Ex,Ey,ndof,nel,non,Edof]= MeshThreeD
(l1,b,n11,n2)
%-------------------------------------------------------------------------
%           Bridge Mesh 3D one span
%-------------------------------------------------------------------------
%PURPOSE:
% Generates a mesh for one rectangular domain with corners 1,2,3,4   % and
boundaries 1, 2, 3 and 4
%
%-------------------------------------------------------------------------
%
%  P4    B3    P3
%    *---------*
%    |         |
% B4 |         |B2
%    |         |
%    *---------*
%   P1    B1   P2
%
% Input:
% xcorner    - x-coordinates for the four corners of the domain (1x4)
% ycorner    - x-coordinates for the four corners of the domain (1x4)
% xcorner    - x-coordinates for the four corners of the domain (1x4)
% ycorner    - x-coordinates for the four corners of the domain (1x4)
% elemtype - Element type    "tria3"  - 3-node triangular element
%                            "quad4" - 4-node quadrilateral element
% n1    - number of elements along the boundaries 1 and 3
% n2    - number of elements along the boundaries 2 and 4
%
% Output:
% Edof  - Connectivity matrix for mesh
% Ex    - Elementwise x-coordinates, cf. Calfem Toolbox
% Ey    - Elementwise y-coordinates, cf. Calfem Toolbox
% Bi    - Matrix containing x-dofs (1st column) and y-dofs (2nd      %
column) for nodes on boundary segment i (i=1,2,3,4)
%
```

```
% Pi    - Row vector containing x-dof (1st value) and y-dof (2nd     %
value) for corner node i (i=1,2,3,4).
%
%-------------------------------------------------------------------
%AUTHORS: PATRIK ERIKSSON, EMANUEL TROLIN 2010-02-05
%
%-------------------------------------------------------------------

% Specify the geometry of the bridge with respectively
xcorner = [0 l1 l1  0];
ycorner = [0 0  b b];

% Specify the element type to use
elemtype = 'quad4';


% The program now calculates and define all geometrical parameters
nel = (n1+1)*(n2+1);
for k=1:nel
    ndof(k,:) = [1 2 3 4 5]+5*(k-1)*[1 1 1 1 1];
end

B1 = zeros(n1+1,5);
B2 = zeros(n2+1,5);
B3 = B1;
B4 = B2;
    for i=1:n1
        for j=1:n2
            sw=(i-1).*(n2+1)+j;
            nw=sw+1;
            se=sw+(n2+1);
            ne=se+1;
            xiw=((i-1)/n1);
            xie=(i/n1);
            etas=((j-1)/n2);
            etan=(j/n2);
            [xsw,ysw]=bilmap(xiw,etas,xcorner,ycorner);
            [xse,yse]=bilmap(xie,etas,xcorner,ycorner);
            [xne,yne]=bilmap(xie,etan,xcorner,ycorner);
            [xnw,ynw]=bilmap(xiw,etan,xcorner,ycorner);
            elno=(i-1)*n2+(j-1);

Edof(elno+1,:)=[elno+1,ndof(sw,:),ndof(se,:),ndof(ne,:),ndof(nw,:)];
            Ex(elno+1,:)=[xsw xse xne xnw];
            Ey(elno+1,:)=[ysw yse yne ynw];

            if j == 1
                B1([i i+1],:) = [ndof(sw,:);ndof(se,:)];
            end
            if i == n1
                B2([j j+1],:) = [ndof(se,:);ndof(ne,:)];
            end
            if j == n2
                B3([i i+1],:) = [ndof(nw,:);ndof(ne,:)];
            end
            if i == 1
                B4([j j+1],:) = [ndof(sw,:);ndof(nw,:)];
            end

        end
    end

P2=B1(end,:);
P1=B1(1,:);
P3=B3(end,:);
P4=B3(1,:);

function [x,y]=bilmap(xi,eta,xcorner,ycorner)
```

```
N=[(1-xi).*(1-eta) xi.*(1-eta) xi.*eta (1-xi).*eta];
x=N*xcorner';
y=N*ycorner';

nel = length(Edof(:,1));
ndof = max(max(Edof));
non = ndof/5;
```

D.4.6 Newmark

Newmark-β method is an unconditionally stable method if the parameters are chosen properly. The function file calculates the change in acceleration, velocity and displacement for each time step by first calculating the first initial acceleration and performs a LU factorization of the mass matrix. For each time step the function file calculates updated acceleration, velocity and displacements.

The time integration function file uses the Newmark-β method with the parameters β and γ equal to 0.25 and 0.5 respectively to make it unconditionally stable.

More information about the Newmark-β method can be found in section 2.3.1.1.

D.4.6.1 Matlab Code

```
function [u,v,a,t] = NEWMARK(K,C,M,F,h,u0,v0,bet,gam)
%--------------------------------------------------------------------
%
%           NEWMARK INTEGRATION
%
%--------------------------------------------------------------------
%PURPOSE:
%Function file that calculates the response in time using the Newmark
%integration method.
%
%--------------------------------------------------------------------
%IN DATA:
%K-Stiffness matrix
%C-Damping matrix
%M-Mass matrix
%F-Trainload
%h-Time step
%u0-displacement vector
%v0-velocity vector
%--------------------------------------------------------------------
%AUTHORS: PATRIK ERIKSSON, EMANUEL TROLIN 2010-02-05
%
%--------------------------------------------------------------------

%Calculate the initial acceleration from the equations of motion
a0 = inv(M)*(F(:,1)-C*v0-K*u0);

%Calculate the LU factorization of M
LU = M + gam*h*C + bet*h^2*K;

%Initial Acceleration, Velocity and displacement
u = zeros(size(F));
v = u;
a = u;
u(:,1) = u0;
v(:,1) = v0;
a(:,1) = a0;

%Loop for each time step
for i=1:length(F(1,:))-1
```

```
    RHS = -K*u(:,i) -(C+h*K)*v(:,i) - ...
        (h*(1-gam)*C+h^2/2*(1-2*bet)*K)*a(:,i) + F(:,i+1);

    %Solve for the second derivatives at the next time step
    a(:,i+1) = inv(LU)*RHS;

    %Evaluate the set of displacements and velocities
    u(:,i+1) = u(:,i) + h*v(:,i) +((1-2*bet)*a(:,i)+2*bet*a(:,i+1))*h^2/2;
    v(:,i+1) = v(:,i) + ((1-gam)*a(:,i)+gam*a(:,i+1))*h;

    %Continue to the next time step:
end

t = linspace(0,length(F(1,:))*h,length(F(1,:)));
%-------------------------------END---------------------------------
```

D.4.7 Inverse iteration

The largest difference between the 2D and 3D program, besides plate elements instead of beam elements, is that the Matlab FE 3D plate model uses another technique of solving the eigen-value problem. Instead of using the Calfem file eigen.m, which itself uses the built-in Matlab function file eigen, the eigenvalues and eigenvector is obtained by the inverse iteration method. The method is effective when only a few of the lowest eigenvalues and eigenvectors are desired (Craig and Kurdila, 2006). The benefit with using only a few eigenmodes is that the time required to perform the calculation is significantly reduced which is very important when the program is repeated many times.

D.4.7.1 Matlab Code

```
function [X1,L]=Inverse_iteration(K,M,bc,BC2,ndof)
%--------------------------------------------------------------------
%PURPOSE:
%Calculate the first eigenvalues (L) and eigenvectors (X1) by the vector
%iteration method inverse iteration.
%--------------------------------------------------------------------
%INDATA:
%K-Stiffness matrix
%M-Mass matrix
%bc-boundary condition for simply supported bridge (used to calculate the
%1st eigenvalue)
%BC2-boundary condition for simply supported bridge with locked mid row.
%(used to calculate the 2nd eigenvalue)
%ndof-number of degrees of freedom
%--------------------------------------------------------------------
%AUTHORS: PATRIK ERIKSSON, EMANUEL TROLIN 2010-03-03
%
%--------------------------------------------------------------------

%%------Remove the locked dofs for each boundary condition-----------
 K1=K;
 M1=M;
 K2=K;
 M2=M;

 K1(bc,:)=[];
 K1(:,bc)=[];
 M1(bc,:)=[];
 M1(:,bc)=[];

 K2(BC2,:)=[];
 K2(:,BC2)=[];
```

```
 M2(BC2,:)=[];
 M2(:,BC2)=[];

%%------Calculate the first eigen-value by Inverse Iteration---------
freedof = setdiff(1:ndof,bc);
unlockeddof=ndof-length(bc);
U0=ones(unlockeddof,1);
X1=zeros(ndof,2);

%Calculate the dynamic matrix
D=inv(K1)*M1;

%Calculate the Rayleigh quotient and shape U0 with 10 iterations
U(:,1)=U0;
for i=1:10
    V(:,i)=D*U(:,i);
    Lambda(i)=V(:,i)'*K1*V(:,i)/(V(:,i)'*M1*V(:,i));

    U(:,i+1)=Lambda(i)*V(:,i);
end

%Pick the first eigenvector
X1(freedof,1)=U(:,11);

%Calculate the first eigenfrequency
Freq1=sqrt(Lambda(i))/(2*pi);

%%------Calculate the second eigen-value by Inverse Iteration--------
freedof2 = setdiff(1:ndof,BC2);
unlockeddof2=ndof-length(BC2);
U02=ones(unlockeddof2,1);

%Calculate the dynamic matrix
D2=inv(K2)*M2;

%Calculate the Rayleigh quotient and shape U0 with 10 iterations
U2(:,1)=U02;
for i=1:10
    V2(:,i)=D2*U2(:,i);
    Lambda2(i)=V2(:,i)'*K2*V2(:,i)/(V2(:,i)'*M2*V2(:,i));

    U2(:,i+1)=Lambda2(i)*V2(:,i);
end

%Pick the second eigenvector
X1(freedof2,2)=U2(:,11);

%Calculate the second eigenfrequency
Freq2=sqrt(Lambda2(i))/(2*pi);

% Let L be a vector of 1st and 2nd eigenfrequencies
L=[Freq1 Freq2];

%%------Normalize the eigenvectors-----------------------------------
fdof=[1:ndof]';

[nfdof,nfdof]=size(X1);

for j=1:nfdof;
    mnorm=sqrt(X1(:,j)'*M(fdof,fdof)*X1(:,j));
    X1(:,j)=X1(:,j)/mnorm;
End
----------------------------END--------------------------
```

E. Appendix E

Analytical solution for the acceleration response of a SDOF model

In this document a shorter derivation of the acceleration response for a SDOF model in the form of a mass-spring system subjected to a sinusoidal load is presented. The derivation is meant to show how the acceleration is affected by the mass and the stiffness of the spring.

Consider the SDOF model as defined by Figure E-1.

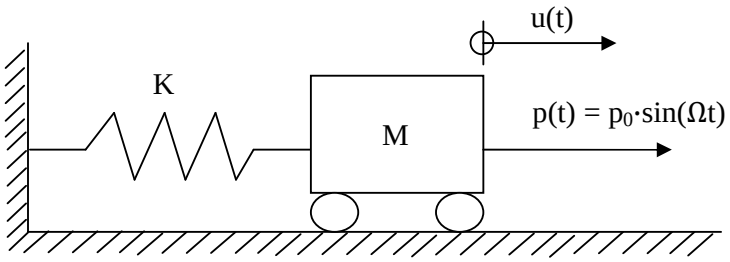

Figure E-1 SDOF model in the form of a mass-spring system

The following differential equation can be conducted for the SDOF model:

$$M\ddot{u} + Ku = p_0 \sin(\Omega t) \quad \text{(E.1)}$$

The solution to such a simple model can analytically be found to be:

$$u(t) = \frac{p_0}{(1-r^2)} * \frac{1}{K} \cos(\Omega t) \quad \text{(E.2)}$$

$$\ddot{u}(t) = a(t) = -\frac{p_0}{(1-r^2)} * \frac{\Omega^2}{K} \cos(\Omega t) \quad \text{(E.3)}$$

Where:

$$r = \frac{\Omega}{\omega} \quad \text{(E.4)}$$

$$\omega = eigenfrequency\ of\ the\ simple\ SDOF\ model$$

The stiffness can be expressed as:

$$K = M * \omega^2 \quad \text{(E.5)}$$

(E.3), (E.4) and (E.5) give us that:

$$a(t) = -\frac{p_0}{(1-r^2)} * \frac{r^2}{M} \cos(\Omega t) \quad \text{(E.6)}$$

Since r is a constant for any combination of load frequency and eigenfrequency we get from equation (E.6) that the acceleration amplitude has an inverse proportionality to the mass and is independent of the stiffness.

F. Appendix F
Tabled values of eigenfrequency functions and design curves

In this appendix tabled values of important results in the report are presented. The tabled values are presented to give the interest reader an opportunity of producing own figures of the results.

F.1 Eigenfrequency functions for two-span bridge

	Eigenfrequency function				
My	One	Two	Three	Four	Five
1	6.2832	9.8155	25.1328	31.8086	56.5488
1.06	6.2502	9.8804	24.879	32.1756	55.7353
1.12	6.164	10.055	24.2858	33.0796	54.0489
1.18	6.0448	10.3095	23.5717	34.2573	52.2394
1.24	5.9092	10.6195	22.8514	35.5431	50.5779
1.3	5.7681	10.9664	22.1722	36.8217	49.1763
1.36	5.6279	11.3368	21.5526	37.9718	48.1303
1.42	5.4924	11.7201	20.9992	38.8333	47.5711
1.48	5.3634	12.1069	20.5148	39.2439	47.6327
1.54	5.2415	12.4882	20.1015	39.1771	48.313
1.6	5.127	12.8543	19.7624	38.7748	49.4402
1.66	5.0197	13.194	19.5024	38.2008	50.814
1.72	4.9193	13.4954	19.3281	37.5603	52.2815
1.78	4.8254	13.7463	19.2465	36.9083	53.7173
1.84	4.7375	13.937	19.2628	36.2721	54.9889
1.9	4.6552	14.0629	19.3772	35.6652	55.9438
1.96	4.578	14.1261	19.5835	35.0942	56.4583
2.02	4.5056	14.1346	19.8697	34.5624	56.5288
2.08	4.4376	14.0996	20.2206	34.0713	56.2697
2.14	4.3736	14.0323	20.6208	33.6221	55.8145
2.2	4.3134	13.9424	21.0561	33.2157	55.2586
2.26	4.2566	13.8375	21.5138	32.8538	54.6589
2.32	4.2029	13.7233	21.9825	32.5384	54.0474
2.38	4.1522	13.6039	22.4517	32.2729	53.4419
2.44	4.1041	13.4821	22.9109	32.0615	52.8526
2.5	4.0586	13.36	23.3495	31.9097	52.2853
2.56	4.0154	13.239	23.7566	31.824	51.7432
2.62	3.9744	13.1199	24.1216	31.8112	51.2282
2.68	3.9354	13.0034	24.435	31.877	50.7414
2.74	3.8982	12.89	24.6901	32.0249	50.2835

F.2 Eigenfrequency functions for three-span bridge

	Eigenfrequency functions for my = 0.5-1.95						
My	One	Two	Three	Four	Five	Six	Seven
0.5	14.13717	18.117	26.45459	56.54905	64.44663	79.0665	127.2388
0.55	14.01267	19.07504	25.49564	55.50075	67.72738	76.9824	123.7507
0.6	13.6693	20.03279	25.20083	52.91896	70.96009	77.9157	116.3635
0.65	13.18384	20.97804	25.39332	49.91484	73.895	80.4455	109.2185
0.7	12.63619	21.89429	25.9178	47.10175	76.10762	83.7038	103.8394
0.75	12.08178	22.75925	26.662	44.68058	76.97044	87.2813	100.9446
0.8	11.55077	23.54341	27.55216	42.70102	76.12183	90.9396	100.7712
0.85	11.05657	24.20974	28.54045	41.17168	74.03129	94.4599	102.6927
0.9	10.60331	24.71713	29.59448	40.09387	71.44769	97.5436	105.8097
0.95	10.1905	25.03	30.69044	39.46398	68.82738	99.7387	109.5239
1	9.815544	25.13283	31.80867	39.26248	66.36893	100.5367	113.4927
1.05	9.475083	25.03972	32.93085	39.44487	64.14845	99.816	117.4733
1.1	9.165607	24.78938	34.03787	39.94621	62.19286	98.0317	121.214
1.15	8.88377	24.42957	35.1082	40.69602	60.51199	95.7483	124.3766
1.2	8.62651	24.00339	36.11662	41.63116	59.11245	93.327	126.5148
1.25	8.391089	23.54356	37.0337	42.70085	58.00347	90.9494	127.2532
1.3	8.175087	23.07245	37.82687	43.86596	57.19795	88.6999	126.6255
1.35	7.976383	22.60436	38.46414	45.09604	56.70958	86.6164	125.0562
1.4	7.793117	22.14798	38.92077	46.36624	56.54631	84.7152	122.9979
1.45	7.623664	21.70828	39.18675	47.65477	56.70282	83.0036	120.7492
1.5	7.466602	21.28783	39.27072	48.94078	57.15638	81.4864	118.4746
1.55	7.320686	20.88772	39.19715	50.20285	57.86941	80.1691	116.2597
1.6	7.18482	20.50808	38.99877	51.41775	58.7968	79.0596	114.1481
1.65	7.058044	20.1485	38.70869	52.5598	59.89347	78.1697	112.1619
1.7	6.939508	19.80824	38.35566	53.60109	61.1188	77.5143	110.312
1.75	6.828463	19.48636	37.96239	54.51306	62.43802	77.1102	108.6039
1.8	6.724242	19.18185	37.54582	55.26978	63.82153	76.9721	107.0412
1.85	6.626255	18.89368	37.1181	55.85261	65.2435	77.1084	105.6272
1.9	6.533973	18.62083	36.68778	56.25451	66.68033	77.5162	104.3662
1.95	6.446927	18.36231	36.26074	56.4819	68.10921	78.1798	103.2646

F.3 Design curves for a single-span railway bridges

L = 7 m	
β	τ
0.00127	160
0.00888	1013
0.01649	2169
0.02410	3922
0.03171	6202
0.03933	7196
0.04694	8523
0.05455	9710
0.06216	10981
0.06977	15660
0.07738	17650
0.08500	17650
0.09261	24059
0.10022	29188
0.10783	29188
0.11544	29188
0.12305	29188
0.13066	33337
0.13828	33337
0.14589	33337
0.15350	33337
0.16111	42056
0.16872	53221
0.17633	76736
0.18394	76736
0.19156	94614
0.19917	95210
0.20678	95210
0.21439	106667
0.22200	106667
0.22961	106667
0.23723	106667
0.24484	106667
0.25245	106667
0.26006	106667
0.26767	106667
0.27528	106667
0.28289	106667
0.29051	106667
0.29812	106667
0.30573	106667
0.31334	106667
0.32095	106667
0.32856	106667
0.33618	113391
0.34379	113391
0.35140	121003
0.35901	156235
0.36662	167236
0.37423	184274
0.38184	184274
0.38946	184274
0.39707	184274
0.40468	213465
0.41229	227754
0.41990	227754
0.42751	271397
0.43513	271397
0.44274	305367
0.45035	310382
0.45796	310382
0.46557	310382
0.47318	310382
0.48079	370509
0.48841	370509
0.49602	408038
0.50363	432852
0.51124	432852
0.51885	432852
0.52646	432852
0.53407	432852
0.54169	432852
0.54930	445842
0.55691	494090
0.56452	494090
0.57213	494090
0.57974	494090
0.58736	494090
0.59497	494090
0.60258	494090
0.61019	494090
0.61780	494090
0.62541	494090
0.63302	494090
0.64064	518744
0.64825	518744
0.65586	518744
0.66347	533238
0.67108	549191
0.67869	549191
0.68631	549191
0.69392	549191
0.70153	549191
0.70914	549191
0.71675	563450
0.72436	595947
0.73197	595947
0.73959	595947
0.74720	595947
0.75481	595947
0.76242	595947
0.77003	595947
0.77764	595947
0.78525	595947
0.79287	595947
0.79921	595947

L = 8 m	
β	τ
0.00166	175
0.00994	918
0.01823	1813
0.02651	3670
0.03480	4381
0.04308	5427
0.05136	6573
0.05965	8035
0.06793	9035
0.07622	12229
0.08450	14878
0.09279	19257
0.10107	19257
0.10936	20990
0.11764	22651
0.12593	22651
0.13421	22651
0.14250	26559
0.15078	34538
0.15907	41678
0.16735	42656
0.17563	42656
0.18392	42656
0.19220	42656
0.20049	57411
0.20877	69893
0.21706	75786
0.22534	75786
0.23363	75786
0.24191	75786
0.25020	75786
0.25848	75786
0.26677	75786
0.27505	75786
0.28333	75786
0.29162	75786
0.29990	75786
0.30819	75786
0.31647	75786
0.32476	75786
0.33304	75786
0.34133	75786
0.34961	75786
0.35790	88924
0.36618	103279
0.37447	115634
0.38275	117575
0.39104	117575
0.39932	128981
0.40760	165255
0.41589	165255
0.42417	190638
0.43246	193646
0.44074	210647
0.44903	224879
0.45731	224879
0.46560	224879
0.47388	247527
0.48217	302996
0.49045	302996
0.49874	361166
0.50702	364379
0.51530	364379
0.52359	364379
0.53187	364379
0.54016	364379
0.54844	378381
0.55673	427077
0.56501	427077
0.57330	427077
0.58158	427077
0.58987	427077
0.59815	427077
0.60644	427077
0.61472	427904
0.62301	427904
0.63129	427904
0.63957	462987
0.64786	462987
0.65614	462987
0.66443	489755
0.67271	497486
0.68100	497486
0.68928	497486
0.69757	497486
0.70585	497486
0.71414	502936
0.72242	552592
0.73071	553595
0.73899	553595
0.74727	553595
0.75556	556036
0.76384	556036
0.77213	556036
0.78041	556036
0.78870	556036
0.79698	556036

L = 9 m	
β	τ
0.00210	181
0.00839	602
0.01468	1287
0.02097	1889
0.02726	3173
0.03355	3629
0.03984	4062
0.04614	5418
0.05243	5614
0.05872	6590
0.06501	7674
0.07130	9131
0.07759	9131
0.08388	10060
0.09017	10388
0.09646	15759
0.10276	15986
0.10905	15986
0.11534	15986
0.12163	18547
0.12792	18908
0.13421	18908
0.14050	18908
0.14679	19867
0.15308	31209
0.15938	35915
0.16567	41183
0.17196	43598
0.17825	45447
0.18454	45447
0.19083	45447
0.19712	45447
0.20341	45447
0.20971	45447
0.21600	45447
0.22229	45447
0.22858	45447
0.23487	45447
0.24116	45447
0.24745	45447
0.25374	45447
0.26003	55689
0.26633	63702
0.27262	63702
0.27891	63702
0.28520	63702
0.29149	63702
0.29778	63702
0.30407	63702
0.31036	63702
0.31665	63702
0.32295	63702
0.32924	63702
0.33553	63702
0.34182	63702
0.34811	63702
0.35440	63702
0.36069	63702
0.36698	63702
0.37328	63702
0.37957	63702
0.38586	64196
0.39215	71279
0.39844	80577
0.40473	94460
0.41102	98133
0.41731	106397
0.42360	126652
0.42990	133752
0.43619	133752
0.44248	164395
0.44877	169448
0.45506	169448
0.46135	169448
0.46764	169448
0.47393	188508
0.48022	224716
0.48652	225401
0.49281	264472
0.49910	277091
0.50539	278485
0.51168	278485
0.51797	278485
0.52426	278485
0.53055	278485
0.53685	278485
0.54314	278485
0.54943	323346
0.55572	362810
0.56201	362810
0.56830	362810
0.57459	362810
0.58088	362810
0.58717	362810
0.59347	362810
0.59976	362810
0.60605	362810
0.61234	374711
0.61863	374711
0.62492	374711
0.63121	374711
0.63750	405662
0.64379	408092
0.65009	408092
0.65638	408092
0.66267	430016
0.66896	443197
0.67525	443197
0.68154	443197
0.68783	443197
0.69412	443197
0.70042	443197
0.70671	443197
0.71300	451391
0.71929	492183
0.72558	504929
0.73187	504929
0.73816	504929
0.74445	504929
0.75074	512454
0.75704	512454
0.76333	512454
0.76962	512454
0.77591	512454
0.78220	512454
0.78849	512454
0.79478	512454
0.79898	512454

L = 10 m	
β	τ
0.00259	149
0.01036	659
0.01812	1226
0.02589	1935
0.03366	2342
0.04142	3539
0.04919	4324
0.05696	5329
0.06472	6091
0.07249	6505
0.08026	7760
0.08802	8889
0.09579	12881
0.10356	12881
0.11132	14369
0.11909	14369
0.12686	14369
0.13463	15015
0.14239	18349
0.15016	18349
0.15793	18349
0.16569	23585
0.17346	35843
0.18123	38433
0.18899	42093
0.19676	43713
0.20453	43713
0.21229	43713
0.22006	43713
0.22783	43713
0.23559	43713
0.24336	43713
0.25113	43713
0.25890	43713
0.26666	53671
0.27443	53671
0.28220	53671
0.28996	53671
0.29773	53671
0.30550	53671
0.31326	53671
0.32103	53671
0.32880	53671
0.33656	53671
0.34433	53671
0.35210	53671
0.35986	53671
0.36763	53671
0.37540	53671
0.38316	53671
0.39093	53671
0.39870	53671
0.40647	53782
0.41423	60136
0.42200	70480
0.42977	72835
0.43753	87228
0.44530	98016
0.45307	98016
0.46083	100425
0.46860	120067
0.47637	144313
0.48413	167064
0.49190	174870
0.49967	213535
0.50743	213535
0.51520	213535
0.52297	213535
0.53073	213535
0.53850	213535
0.54627	239541
0.55404	284718
0.56180	287311
0.56957	287311
0.57734	287311
0.58510	287311
0.59287	287311
0.60064	287311
0.60840	314836
0.61617	321123
0.62394	321123
0.63170	323356
0.63947	357105
0.64724	357105
0.65500	357105
0.66277	381940
0.67054	391523
0.67831	391523
0.68607	391523
0.69384	391523
0.70161	391523
0.70937	391523
0.71714	436327
0.72491	452613
0.73267	452613
0.74044	452613
0.74821	458723
0.75597	463848
0.76374	463848
0.77151	463848
0.77927	463848
0.78704	463848
0.79481	463848
0.79999	463848

L = 11 m	
β	τ
0.00313	169
0.01253	732
0.02193	1275
0.03133	1973
0.04072	3326
0.05012	3893
0.05952	5586
0.06892	5586
0.07832	7267
0.08771	10376
0.09711	10376
0.10651	10376
0.11591	10376
0.12531	13824
0.13470	13824
0.14410	14431
0.15350	22930
0.16290	24988
0.17229	24988
0.18169	24988
0.19109	31668
0.20049	37058
0.20989	43640
0.21928	43640
0.22868	43640
0.23808	43640
0.24748	43640
0.25688	43640
0.26627	43640
0.27567	43640
0.28507	43640
0.29447	43640
0.30386	43640
0.31326	43640
0.32266	43640
0.33206	44119
0.34146	45409
0.35085	45409
0.36025	45409
0.36965	45409
0.37905	45409
0.38845	45409
0.39784	45409
0.40724	45409
0.41664	45409
0.42604	45409
0.43544	48041
0.44483	55919
0.45423	60406
0.46363	69369
0.47303	85998
0.48242	97348
0.49182	116997
0.50122	140011
0.51062	140011
0.52002	140011
0.52941	140011
0.53881	154806
0.54821	194081
0.55761	224258
0.56701	224258
0.57640	224258
0.58580	224258
0.59520	224258
0.60460	239108
0.61400	261609
0.62339	261609
0.63279	277935
0.64219	299945
0.65159	299945
0.66098	318079
0.67038	339039
0.67978	339039
0.68918	339039
0.69858	339039
0.70797	339039
0.71737	389450
0.72677	403413
0.73617	403413
0.74557	405438
0.75496	416448
0.76436	416448
0.77376	416448
0.78316	416448
0.79255	416448
0.79882	416448

L = 12 m	
β	τ
0.00204	106
0.01021	391
0.01838	940
0.02655	1530
0.03471	1948
0.04288	2835
0.05105	3971
0.05922	4706
0.06738	5025
0.07555	5025
0.08372	5785
0.09189	6963
0.10006	10937
0.10822	10937
0.11639	10937
0.12456	10937
0.13273	10937
0.14090	12141
0.14906	12141
0.15723	17024
0.16540	24669
0.17357	24669
0.18173	24669
0.18990	24669
0.19807	24669
0.20624	26043
0.21441	34498
0.22257	34498
0.23074	34498
0.23891	34498
0.24708	34498
0.25524	34498
0.26341	34498
0.27158	34498
0.27975	34498
0.28792	34498
0.29608	34498
0.30425	34498
0.31242	34498
0.32059	34498
0.32876	36111
0.33692	43127
0.34509	43127
0.35326	43127
0.36143	47805
0.36959	50179
0.37776	51333
0.38593	51333
0.39410	51333
0.40227	51333
0.41043	51333
0.41860	51333
0.42677	51333
0.43494	51333
0.44311	51333
0.45127	51333
0.45944	51333
0.46761	51333
0.47578	53690
0.48394	55998
0.49211	70288
0.50028	83540
0.50845	83540
0.51662	83540
0.52478	84122
0.53295	97337
0.54112	116551
0.54929	142862
0.55746	158997
0.56562	158997
0.57379	158997
0.58196	158997
0.59013	159987
0.59829	161810
0.60646	196696
0.61463	208956
0.62280	208956
0.63097	217740
0.63913	244756
0.64730	244756
0.65547	244756
0.66364	276480
0.67180	282864
0.67997	282864
0.68814	282864
0.69631	282864
0.70448	282864
0.71264	308704
0.72081	349804
0.72898	352252
0.73715	352252
0.74532	357152
0.75348	370239
0.76165	370239
0.76982	370239
0.77799	370239
0.78615	370239
0.79432	370239
0.79841	370239

L = 13 m	
β	τ
0.00240	86
0.00959	397
0.01678	618
0.02396	835
0.03115	1285
0.03834	1706
0.04553	2063
0.05272	3432
0.05991	4370
0.06710	4370
0.07429	4370
0.08148	4384
0.08867	7132
0.09586	7132
0.10305	7368
0.11024	7686
0.11743	8308
0.12462	10101
0.13181	10101
0.13900	10210
0.14618	12725
0.15337	12725
0.16056	12725
0.16775	14142
0.17494	23355
0.18213	23355
0.18932	23355
0.19651	23355
0.20370	23355
0.21089	23355
0.21808	23355
0.22527	23355
0.23246	23355
0.23965	23355
0.24684	23355
0.25403	23355
0.26121	23355
0.26840	23906
0.27559	23906
0.28278	23906
0.28997	23906
0.29716	23906
0.30435	23906
0.31154	23906
0.31873	23906
0.32592	24201
0.33311	33841
0.34030	33841
0.34749	33841
0.35468	34726
0.36187	44194
0.36906	51410
0.37625	52007
0.38343	52007
0.39062	52007
0.39781	52007
0.40500	52007
0.41219	52007
0.41938	52007
0.42657	52007
0.43376	52007
0.44095	52007
0.44814	52007
0.45533	52007
0.46252	52007
0.46971	52007
0.47690	52007
0.48409	52007
0.49128	52007
0.49847	52007
0.50565	52007
0.51284	52007
0.52003	52007
0.52722	53355
0.53441	62654
0.54160	74559
0.54879	90138
0.55598	100322
0.56317	100322
0.57036	100322
0.57755	100322
0.58474	106260
0.59193	106260
0.59912	123459
0.60631	146886
0.61350	155405
0.62069	155405
0.62787	157773
0.63506	184334
0.64225	193007
0.64944	193007
0.65663	194267
0.66382	224812
0.67101	229702
0.67820	229702
0.68539	229702
0.69258	230593
0.69977	232993
0.70696	232993
0.71415	269796
0.72134	297396
0.72853	299164
0.73572	299164
0.74291	299164
0.75009	320455
0.75728	320455
0.76447	320455
0.77166	320455
0.77885	320455
0.78604	320455
0.79323	320455
0.79802	320455

L = 14 m	
β	τ
0.00278	100
0.01112	379
0.01946	819
0.02779	1433
0.03613	2041
0.04447	2327
0.05281	3122
0.06115	3774
0.06948	3774
0.07782	5423
0.08616	6581
0.09450	7791
0.10284	7919
0.11117	8543
0.11951	8543
0.12785	8543
0.13619	8754
0.14453	8754
0.15286	15734
0.16120	17855
0.16954	17855
0.17788	17855
0.18622	18070
0.19455	27284
0.20289	27284
0.21123	27284
0.21957	27284
0.22791	27284
0.23624	27284
0.24458	27284
0.25292	27284
0.26126	27380
0.26960	30986
0.27793	30986
0.28627	30986
0.29461	30986
0.30295	30986
0.31129	30986
0.31962	30986
0.32796	30986
0.33630	30986
0.34464	30986
0.35298	30986
0.36131	36329
0.36965	45690
0.37799	45690
0.38633	45690
0.39467	45690
0.40300	46088
0.41134	53235
0.41968	53235
0.42802	55386
0.43636	55386
0.44469	55386
0.45303	55386
0.46137	55386
0.46971	55386
0.47805	55386
0.48638	55386
0.49472	55386
0.50306	55386
0.51140	55386
0.51974	55386
0.52807	55386
0.53641	55386
0.54475	55386
0.55309	55386
0.56143	55386
0.56976	55386
0.57810	64753
0.58644	71164
0.59478	75634
0.60312	93642
0.61145	103953
0.61979	104003
0.62813	116657
0.63647	136977
0.64481	139469
0.65314	139469
0.66148	167462
0.66982	177652
0.67816	177652
0.68650	177652
0.69483	190962
0.70317	190962
0.71151	210725
0.71985	242738
0.72819	247109
0.73652	247109
0.74486	257471
0.75320	271064
0.76154	271064
0.76988	271064
0.77821	271064
0.78655	271064
0.79489	271064
0.79767	271064

L = 15 m	
β	τ
0.00319	100
0.00957	287
0.01595	470
0.02233	617
0.02872	813
0.03510	1380
0.04148	1454
0.04786	2064
0.05424	2803
0.06062	2967
0.06700	2967
0.07338	2967
0.07976	3602
0.08615	4585
0.09253	4764
0.09891	5290
0.10529	6756
0.11167	6756
0.11805	7384
0.12443	7643
0.13081	7643
0.13719	8907
0.14358	9308
0.14996	9308
0.15634	9659
0.16272	15533
0.16910	17755
0.17548	17755
0.18186	17755
0.18824	17755
0.19462	17755
0.20101	21983
0.20739	21983
0.21377	26986
0.22015	26986
0.22653	26986
0.23291	26986
0.23929	26986
0.24567	26986
0.25205	26986
0.25844	26986
0.26482	27669
0.27120	27669
0.27758	27669
0.28396	27669
0.29034	27669
0.29672	27669
0.30310	27669
0.30948	27669
0.31587	27669
0.32225	27669
0.32863	27669
0.33501	27669
0.34139	27669
0.34777	27669
0.35415	27669
0.36053	27669
0.36691	27669
0.37330	29897
0.37968	30233
0.38606	30233
0.39244	30233
0.39882	34591
0.40520	45675
0.41158	48145
0.41796	48145
0.42434	54286
0.43073	54474
0.43711	54474
0.44349	61708
0.44987	61708
0.45625	61708
0.46263	61708
0.46901	61708
0.47539	61708
0.48177	61708
0.48816	61708
0.49454	61708
0.50092	61708
0.50730	61708
0.51368	61708
0.52006	61708
0.52644	61708
0.53282	61708
0.53920	61708
0.54559	61708
0.55197	61708
0.55835	61708
0.56473	61708
0.57111	61708
0.57749	61708
0.58387	61708
0.59025	61708
0.59663	61708
0.60302	61708
0.60940	63279
0.61578	64428
0.62216	66954
0.62854	78941
0.63492	90096
0.64130	92444
0.64768	92444
0.65406	101450
0.66045	118921
0.66683	125647
0.67321	126537
0.67959	126537
0.68597	127015
0.69235	139681
0.69873	143642
0.70511	143642
0.71149	167584
0.71788	187435
0.72426	196672
0.73064	196672
0.73702	196672
0.74340	205990
0.74978	221655
0.75616	222462
0.76254	222462
0.76892	222462
0.77531	222462
0.78169	222462
0.78807	222462
0.79445	222462
0.79764	222462

L = 16 m	
β	τ
0.00363	90
0.01089	284
0.01815	474
0.02541	699
0.03267	1199
0.03993	1553
0.04719	1564
0.05445	2527
0.06171	2527
0.06897	2527
0.07623	3023
0.08349	3748
0.09075	4522
0.09801	6123
0.10527	6123
0.11253	6181
0.11980	6181
0.12706	6964
0.13432	6964
0.14158	6964
0.14884	9239
0.15610	9239
0.16336	9239
0.17062	11421
0.17788	16432
0.18514	16432
0.19240	16432
0.19966	16432
0.20692	16432
0.21418	21229
0.22144	21229
0.22870	21229
0.23596	21229
0.24322	21229
0.25048	21229
0.25774	21229
0.26500	21229
0.27226	21229
0.27952	21229
0.28678	21229
0.29404	21229
0.30130	21229
0.30856	21229
0.31582	21229
0.32308	21229
0.33034	21229
0.33760	21229
0.34486	21229
0.35212	21229
0.35939	21229
0.36665	21229
0.37391	21229
0.38117	21229
0.38843	21229
0.39569	24403
0.40295	32699
0.41021	37975
0.41747	37975
0.42473	49512
0.43199	49512
0.43925	49512
0.44651	56123
0.45377	56123
0.46103	56123
0.46829	56123
0.47555	57675
0.48281	66975
0.49007	66975
0.49733	70339
0.50459	72417
0.51185	72417
0.51911	72417
0.52637	72417
0.53363	72417
0.54089	72417
0.54815	72417
0.55541	72417
0.56267	72417
0.56993	72417
0.57719	72417
0.58445	72417
0.59172	72417
0.59898	72417
0.60624	72417
0.61350	72417
0.62076	72417
0.62802	72417
0.63528	72417
0.64254	72417
0.64980	72417
0.65706	72417
0.66432	81832
0.67158	84356
0.67884	84356
0.68610	90426
0.69336	99148
0.70062	99424
0.70788	114683
0.71514	135827
0.72240	145421
0.72966	146857
0.73692	146857
0.74418	163991
0.75144	174632
0.75870	174632
0.76596	174632
0.77322	174632
0.78048	174632
0.78774	174632
0.79500	174632
0.79863	174632

L = 17 m	
β	τ
0.00410	95
0.01229	336
0.02049	570
0.02869	856
0.03688	1258
0.04508	1647
0.05328	1744
0.06147	2102
0.06967	2325
0.07786	3150
0.08606	4037
0.09426	5916
0.10245	5916
0.11065	5916
0.11884	6205
0.12704	6205
0.13524	7086
0.14343	7536
0.15163	9704
0.15983	12544
0.16802	12544
0.17622	12544
0.18441	12544
0.19261	17715
0.20081	17715
0.20900	17715
0.21720	17715
0.22540	17715
0.23359	17715
0.24179	17715
0.24998	17715
0.25818	17715
0.26638	17715
0.27457	17715
0.28277	17715
0.29096	17715
0.29916	17715
0.30736	17715
0.31555	17715
0.32375	17719
0.33195	23037
0.34014	23037
0.34834	23037
0.35653	23037
0.36473	23037
0.37293	23037
0.38112	23037
0.38932	23037
0.39751	23037
0.40571	23037
0.41391	23037
0.42210	32692
0.43030	36007
0.43850	41120
0.44669	49775
0.45489	49775
0.46308	49775
0.47128	49775
0.47948	64198
0.48767	64220
0.49587	76056
0.50407	84921
0.51226	84921
0.52046	84921
0.52865	84921
0.53685	84921
0.54505	84921
0.55324	84921
0.56144	84921
0.56963	84921
0.57783	84921
0.58603	84921
0.59422	84921
0.60242	84921
0.61062	84921
0.61881	84921
0.62701	84921
0.63520	84921
0.64340	84921
0.65160	84921
0.65979	84921
0.66799	84921
0.67619	84921
0.68438	84921
0.69258	84921
0.70077	84921
0.70897	84921
0.71717	96780
0.72536	105182
0.73356	105182
0.74175	116935
0.74995	129380
0.75815	132763
0.76634	132763
0.77454	132763
0.78274	132763
0.79093	132763
0.79913	132763

L = 18 m	
β	τ
0.00459	99
0.01378	334
0.02297	574
0.03216	989
0.04135	1262
0.05054	1509
0.05973	2173
0.06892	2216
0.07810	2726
0.08729	3823
0.09648	3823
0.10567	4882
0.11486	6034
0.12405	6902
0.13324	6902
0.14243	7462
0.15162	7462
0.16080	10986
0.16999	12654
0.17918	12654
0.18837	12654
0.19756	14420
0.20675	14420
0.21594	15133
0.22513	15133
0.23431	15133
0.24350	15133
0.25269	15133
0.26188	16033
0.27107	16033
0.28026	16033
0.28945	16033
0.29864	16033
0.30783	16033
0.31701	16033
0.32620	17430
0.33539	22235
0.34458	22235
0.35377	22235
0.36296	22235
0.37215	22235
0.38134	22235
0.39052	22235
0.39971	22235
0.40890	22235
0.41809	22235
0.42728	22791
0.43647	25712
0.44566	33784
0.45485	33784
0.46403	38320
0.47322	45343
0.48241	60261
0.49160	60261
0.50079	77727
0.50998	77727
0.51917	77727
0.52836	77727
0.53755	77727
0.54673	77727
0.55592	80193
0.56511	80193
0.57430	80193
0.58349	80193
0.59268	80193
0.60187	80193
0.61106	80193
0.62024	80193
0.62943	80193
0.63862	80193
0.64781	80193
0.65700	80193
0.66619	80193
0.67538	80193
0.68457	80193
0.69376	80193
0.70294	80193
0.71213	80193
0.72132	80193
0.73051	80193
0.73970	80193
0.74889	96785
0.75808	99984
0.76727	99984
0.77645	99984
0.78564	99984
0.79483	99984
0.79943	99984

L = 19 m	
β	τ
0.00512	101
0.01536	359
0.02560	646
0.03583	968
0.04607	1231
0.05631	1816
0.06655	2535
0.07679	2623
0.08702	3815
0.09726	4457
0.10750	4468
0.11774	4784
0.12798	4784
0.13821	6185
0.14845	6498
0.15869	7981
0.16893	7981
0.17917	12679
0.18941	12679
0.19964	12679
0.20988	19313
0.22012	19313
0.23036	19313
0.24060	19313
0.25083	19313
0.26107	19313
0.27131	19313
0.28155	19313
0.29179	19313
0.30203	19313
0.31226	19313
0.32250	19313
0.33274	19952
0.34298	19952
0.35322	19952
0.36345	23226
0.37369	27939
0.38393	27939
0.39417	27939
0.40441	27939
0.41464	27939
0.42488	27939
0.43512	27939
0.44536	27939
0.45560	27939
0.46584	27939
0.47607	40308
0.48631	47432
0.49655	66180
0.50679	70797
0.51703	70797
0.52726	70797
0.53750	70797
0.54774	71596
0.55798	85700
0.56822	85700
0.57845	85700
0.58869	85700
0.59893	85700
0.60917	85700
0.61941	85700
0.62965	85700
0.63988	85700
0.65012	85700
0.66036	85700
0.67060	85700
0.68084	85700
0.69107	85700
0.70131	85700
0.71155	85700
0.72179	85700
0.73203	85700
0.74227	85700
0.75250	85700
0.76274	85700
0.77298	85700
0.78322	85700
0.79346	85700
0.79857	85700

L = 20 m	
β	T
0.00567	100
0.01134	234
0.01702	347
0.02836	677
0.03403	859
0.03970	996
0.05105	1401
0.05672	1560
0.06239	1980
0.07374	1980
0.07941	2154
0.08508	2794
0.09643	2852
0.10210	3845
0.10777	3845
0.11911	4120
0.12479	5649
0.13046	5649
0.14180	5954
0.14747	5954
0.15315	7308
0.16449	8981
0.17016	8981
0.17584	8981
0.18718	9671
0.19285	10553
0.19852	10553
0.20987	12952
0.21554	12952
0.22121	12952
0.23256	12952
0.23823	12952
0.24390	12952
0.25524	12952
0.26092	12952
0.26659	14177
0.27793	14177
0.28360	14177
0.28928	14177
0.30062	14177
0.30629	14177
0.31197	14177
0.32331	14177
0.32898	14177
0.33465	14177
0.34600	14177
0.35167	14711
0.35734	19481
0.36869	27085
0.37436	27085
0.38003	27085
0.39137	27085
0.39705	27085
0.40272	27085
0.41406	27085
0.41974	27085
0.42541	27085
0.43675	27085
0.44242	27085
0.44810	27085
0.45944	27085
0.46511	27085
0.47078	27085
0.48213	31586
0.48780	33303
0.49347	42563
0.50482	51576
0.51049	51576
0.51616	51576
0.52751	51576
0.53318	51576
0.53885	51576
0.55019	74774
0.55587	82988
0.56154	82988
0.57288	82988
0.57855	82988
0.58423	82988
0.59557	82988
0.60124	82988
0.60691	82988
0.61826	82988
0.62393	82988
0.62960	82988
0.64095	82988
0.64662	82988
0.65229	82988
0.66364	82988
0.66931	82988
0.67498	82988
0.68632	82988
0.69200	82988
0.69767	82988
0.70901	82988
0.71468	82988
0.72036	82988
0.73170	82988
0.73737	82988
0.74304	82988
0.75439	82988
0.76006	82988
0.76573	82988
0.77708	82988
0.78275	82988
0.78842	82988
0.79977	82988

F.4 Design curves for a two-span railway bridges

L = 16 m		L = 18 m		L = 20 m		L = 22 m		L = 24 m		L = 26 m		L = 28 m		L = 30 m	
β	τ	β	τ	β	τ	β	τ	β	τ	β	τ	β	τ	β	τ
0.00144	112	0.00182	111	0.00224	106	0.00272	103	0.00323	93	0.00379	82	0.00439	85	0.00505	102
0.00575	374	0.00727	420	0.00673	290	0.00815	257	0.00968	300	0.00758	253	0.00877	210	0.01010	215
0.01006	649	0.01273	610	0.01121	493	0.01359	510	0.01613	517	0.01136	358	0.01316	305	0.01515	381
0.01437	980	0.01818	1184	0.01570	672	0.01902	817	0.02258	1050	0.01894	587	0.01754	523	0.02020	614
0.01868	1522	0.02364	1769	0.02018	1269	0.02446	1123	0.02903	1114	0.02273	815	0.02193	660	0.02525	614
0.02299	1780	0.02909	2436	0.02466	1269	0.02989	1766	0.03548	1582	0.02652	996	0.02632	839	0.03030	688
0.02730	2474	0.03455	2605	0.02915	1895	0.03533	1766	0.04194	2001	0.03409	1338	0.03070	839	0.03535	1032
0.03161	2943	0.04000	3658	0.03363	1963	0.04076	2273	0.04839	2083	0.03788	1654	0.03509	1149	0.04040	1032
0.03592	3200	0.04545	3716	0.03812	2500	0.04620	2325	0.05484	2960	0.04167	1761	0.03947	1382	0.04545	1093
0.04023	3780	0.05091	5038	0.04260	3579	0.05163	3471	0.06129	4042	0.04924	1979	0.04386	1403	0.05051	1566
0.04454	5065	0.05636	5321	0.04709	3579	0.05707	3978	0.06774	4042	0.05303	1979	0.04825	1469	0.05556	1720
0.04885	6263	0.06182	6706	0.05157	5360	0.06250	4688	0.07419	4042	0.05682	2808	0.05263	1965	0.06061	2306
0.05316	6762	0.06727	6706	0.05605	5360	0.06793	4688	0.08065	4042	0.06439	3714	0.05702	2303	0.06566	2306
0.05747	6882	0.07273	6706	0.06054	5360	0.07337	4688	0.08710	5115	0.06818	3714	0.06140	2490	0.07071	2306
0.06178	7934	0.07818	6706	0.06502	5360	0.07880	5415	0.09355	6116	0.07197	3714	0.06579	2551	0.07576	2306
0.06609	7934	0.08364	7741	0.06951	5360	0.08424	6390	0.10000	6389	0.07955	3787	0.07018	2551	0.08081	2733
0.07040	7934	0.08909	10458	0.07399	5360	0.08967	7492	0.10645	6389	0.08333	3965	0.07456	2609	0.08586	3570
0.07471	7934	0.09455	12737	0.07848	5360	0.09511	8295	0.11290	6389	0.08712	4632	0.07895	3167	0.09091	3570
0.07902	9994	0.10000	13512	0.08296	7538	0.10054	8584	0.11935	6637	0.09470	5270	0.08333	3797	0.09596	5161
0.08333	10541	0.10545	13512	0.08744	7538	0.10598	8584	0.12581	7577	0.09848	5454	0.08772	4068	0.10101	5161
0.08764	12526	0.11091	13512	0.09193	8299	0.11141	8584	0.13226	8268	0.10227	5454	0.09211	4437	0.10606	5161
0.09195	12526	0.11636	13512	0.09641	11920	0.11685	8584	0.13871	9643	0.10985	5637	0.09649	4604	0.11111	5161
0.09626	13074	0.12182	13512	0.10090	11920	0.12228	8584	0.14516	9704	0.11364	5637	0.10088	5648	0.11616	5161
0.10057	13074	0.12727	13512	0.10538	11920	0.12772	9109	0.15161	12547	0.11742	5637	0.10526	5648	0.12121	5161
0.10489	13074	0.13273	14149	0.10987	11920	0.13315	10500	0.15806	13387	0.12500	6276	0.10965	5648	0.12626	5161
0.10920	13074	0.13818	14149	0.11435	11920	0.13859	10989	0.16452	13387	0.12879	6276	0.11404	5648	0.13131	5456
0.11351	13074	0.14364	14149	0.11883	11920	0.14402	13478	0.17097	13387	0.13258	6380	0.11842	5648	0.13636	5630
0.11782	15282	0.14909	16914	0.12332	11920	0.14946	13478	0.17742	17463	0.14015	8410	0.12281	5671	0.14141	6203
0.12213	16589	0.15455	22502	0.12780	11920	0.15489	13478	0.18387	17463	0.14394	8410	0.12719	5671	0.14646	8404
0.12644	16589	0.16000	22502	0.13229	11920	0.16033	14243	0.19032	17463	0.14773	9796	0.13158	5821	0.15152	8404
0.13075	16589	0.16545	22502	0.13677	11920	0.16576	14593	0.19677	17463	0.15530	12803	0.13596	6887	0.15657	8404
0.13506	18208	0.17091	22502	0.14126	11920	0.17120	14593	0.20323	17463	0.15909	12803	0.14035	6887	0.16162	8404
0.13937	20272	0.17636	22846	0.14574	13787	0.17663	14593	0.20968	19029	0.16288	12803	0.14474	7630	0.16667	8404
0.14368	20272	0.18182	23207	0.15022	14880	0.18207	14814	0.21613	19029	0.17045	12803	0.14912	9836	0.17172	8404
0.14799	20272	0.18727	25302	0.15471	15127	0.18750	18373	0.22258	19029	0.17424	12803	0.15351	9836	0.17677	11344
0.15230	26148	0.19273	25302	0.15919	15127	0.19293	20222	0.22903	19029	0.17803	12803	0.15789	9836	0.18182	11344
0.15661	28214	0.19818	25302	0.16368	15129	0.19837	20222	0.23548	19029	0.18561	12803	0.16228	10971	0.18687	11344
0.16092	29520	0.20364	25302	0.16816	17040	0.20380	20222	0.24194	19029	0.18939	14553	0.16667	10971	0.19192	11344
0.16523	29520	0.20909	27019	0.17265	17957	0.20924	20222	0.24839	19029	0.19318	14921	0.17105	10971	0.19697	11344
0.16954	29520	0.21455	29238	0.17713	22082	0.21467	20222	0.25484	19753	0.20076	14921	0.17544	10971	0.20202	11344
0.17385	29520	0.22000	29238	0.18161	22082	0.22011	20222	0.26129	20869	0.20455	14921	0.17982	10971	0.20707	11344
0.17816	29520	0.22545	29238	0.18610	22082	0.22554	20222	0.26774	20869	0.20833	14921	0.18421	10971	0.21212	11344
0.18247	29520	0.23091	29238	0.19058	22082	0.23098	20222	0.27419	20869	0.21591	14921	0.18860	11157	0.21717	11344
0.18678	29520	0.23636	29238	0.19507	22560	0.23641	20222	0.28065	20869	0.21970	14921	0.19298	11157	0.22222	11344
0.19109	38217	0.24182	29238	0.19955	22560	0.24185	20222	0.28710	20869	0.22348	14921	0.19737	11157	0.22727	11344
0.19540	46465	0.24727	29238	0.20404	22560	0.24728	20222	0.29355	22427	0.23106	14921	0.20175	11157	0.23232	11344
0.19971	46465	0.25273	31314	0.20852	24532	0.25272	20222	0.30000	23532	0.23485	14921	0.20614	12311	0.23737	11344
0.20402	46465	0.25818	35808	0.21300	24541	0.25815	21253	0.30645	23532	0.23864	14921	0.21053	15078	0.24242	11344
0.20833	46465	0.26364	37156	0.21749	24541	0.26359	29883	0.31290	23532	0.24621	15646	0.21491	15078	0.24747	11344
0.21264	46465	0.26909	38099	0.22197	24541	0.26902	32790	0.31935	23532	0.25000	18062	0.21930	15078	0.25253	11344
0.21695	46465	0.27455	38099	0.22646	24541	0.27446	34874	0.32581	23532	0.25379	18062	0.22368	15078	0.25758	12598
0.22126	46465	0.28000	38099	0.23094	24541	0.27989	34874	0.33226	23532	0.26136	19243	0.22807	15078	0.26263	13877
0.22557	46465	0.28545	38099	0.23543	24541	0.28533	34874	0.33871	23532	0.26515	22268	0.23246	15078	0.26768	13877
0.22989	46465	0.29091	38099	0.23991	28061	0.29076	34874	0.34516	23532	0.26894	22564	0.23684	15078	0.27273	13877
0.23420	46465	0.29636	38099	0.24439	30678	0.29620	34874	0.35161	23532	0.27652	23310	0.24123	15078	0.27778	13877
0.23851	46465	0.30182	38844	0.24888	31478	0.30163	34874	0.35806	23532	0.28030	23310	0.24561	15078	0.28283	13877
0.24282	46465	0.30727	41011	0.25336	31736	0.30707	34874	0.36452	27268	0.28409	23310	0.25000	15078	0.28788	13877
0.24713	46465	0.31273	42745	0.25785	31736	0.31250	34874	0.37097	32094	0.29167	23310	0.25439	15078	0.29293	13877
0.25144	46465	0.31818	42745	0.26233	31736	0.31793	34874	0.37742	32094	0.29545	23310	0.25877	15078	0.29798	13877
0.25575	46465	0.32364	42745	0.26682	31736	0.32337	34874	0.38387	32094	0.29924	23310	0.26316	15078	0.30303	13877
0.26006	47095	0.32909	42745	0.27130	31736	0.32880	34874	0.39032	32094	0.30682	23310	0.26754	15778	0.30808	13877
0.26437	52510	0.33455	42745	0.27578	31736	0.33424	34874	0.39677	32094	0.31061	23310	0.27193	19054	0.31313	13877
0.26868	54718	0.34000	42745	0.28027	31736	0.33967	34874	0.40323	32094	0.31439	23310	0.27632	19054	0.31818	14975
0.27299	57812	0.34545	42745	0.28475	31736	0.34511	34874	0.40968	32094	0.32197	23310	0.28070	19054	0.32323	17290
0.27730	57812	0.35091	42745	0.28924	31736	0.35054	34874	0.41613	32094	0.32576	23310	0.28509	19054	0.32828	19995
0.28161	57812	0.35636	42745	0.29372	32409	0.35598	34874	0.42258	32094	0.32955	24716	0.28947	19054	0.33333	19995
0.28592	57812	0.36182	42745	0.29821	32409	0.36141	34874	0.42903	32094	0.33712	24716	0.29386	19054	0.33838	19995
0.29023	57812	0.36727	45019	0.30269	32409	0.36685	34874	0.43548	32094	0.34091	24716	0.29825	19054	0.34343	19995
0.29454	57812	0.37273	48486	0.30717	32409	0.37228	34874	0.44194	32094	0.34470	24716	0.30263	19054	0.34848	19995
0.29885	57812	0.37818	54905	0.31166	32409	0.37772	34874	0.44839	32094	0.35227	24716	0.30702	19054	0.35354	19995
0.30316	57812	0.38364	60766	0.31614	32409	0.38315	34874	0.45484	32094	0.35606	24716	0.31140	19054	0.35859	19995
0.30747	57812	0.38909	63645	0.32063	32409	0.38859	34874	0.46129	32094	0.35985	24716	0.31579	19054	0.36364	19995
0.31178	57812	0.39455	64262	0.32511	32409	0.39402	34874	0.46774	33017	0.36742	24716	0.32018	19054	0.36869	20332
0.31609	57812	0.40000	64457	0.32960	32409	0.39946	34874	0.47419	39313	0.37121	24716	0.32456	19054	0.37374	20593
0.32040	57812	0.40545	69046	0.33408	32409	0.40489	34874	0.48065	48241	0.37500	24716	0.32895	19054	0.37879	20593
0.32471	57812	0.41091	69956	0.33857	32409	0.41033	34874	0.48710	59063	0.38258	24716	0.33333	19054	0.38384	20593
0.32902	62602	0.41636	69956	0.34305	32409	0.41576	34874	0.49355	71913	0.38636	24716	0.33772	19054	0.38889	20593
0.33333	63900	0.42182	72354	0.34753	32409	0.42120	34874	0.50000	78358	0.39015	24716	0.34211	19054	0.39394	20593
0.33764	63900	0.42727	75925	0.35202	32409	0.42663	34874			0.39773	24716	0.34649	19054	0.39899	20593
0.34195	63900	0.43273	75925	0.35650	32409	0.43207	34874			0.40152	28022	0.35088	19054	0.40404	20593
0.34626	63900	0.43818	75925	0.36099	32409	0.43750	35815			0.40530	32505	0.35526	19054	0.40909	20593
0.35057	63900	0.44364	75925	0.36547	32409	0.44293	43037			0.41288	34721	0.35965	19054	0.41414	20593
0.35489	63900	0.44909	75925	0.36996	32409	0.44837	44221			0.41667	34721	0.36404	19054	0.41919	20593
0.35920	63900	0.45455	75925	0.37444	32409	0.45380	47305			0.42045	34721	0.36842	19054	0.42424	20593
0.36351	63900	0.46000	75925	0.37892	32409	0.45924	54875			0.42803	36668	0.37281	19054	0.42929	20593
0.36782	70900	0.46545	75925	0.38341	32409	0.46467	60273			0.43182	36668	0.37719	19054	0.43434	20593
0.37213	74013	0.47091	75925	0.38789	32409	0.47011	64108			0.43561	36668	0.38158	19054	0.43939	24021
0.37644	74013	0.47636	75925	0.39238	33287	0.47554	73180			0.44318	36668	0.38596	19054	0.44444	26728
0.38075	74013	0.48182	75925	0.39686	36496	0.48098	79552			0.44697	36668	0.39035	19054	0.44949	26728
0.38506	74013	0.48727	75925	0.40135	39282	0.48641	79552			0.45076	36668	0.39474	19054	0.45455	26728
0.38937	74013	0.49273	75925	0.40583	41999	0.49185	82370			0.45833	36668	0.39912	19217	0.45960	27164
0.39368	74013	0.49818	75925	0.41031	43985	0.49728	96649			0.46212	36668	0.40351	20443	0.46465	29258
0.39799	74013	0.50000	75925	0.41480	47018	0.50000	100133			0.46591	36668	0.40789	21715	0.46970	31445
0.40230	74013			0.41928	53735					0.47348	36668	0.41228	24126	0.47475	36286
0.40661	74013			0.42377	60390					0.47727	36668	0.41667	24126	0.47980	43584
0.41092	74013			0.42825	60991					0.48106	36668	0.42105	28584	0.48485	43656
0.41523	74013			0.43274	60991					0.48864	36668	0.42544	31699	0.48990	43656
0.41954	74013			0.43722	67721					0.49242	36668	0.42982	31699	0.49495	46564
0.42385	74013			0.44170	74991					0.49621	36668	0.43421	31699	0.50000	49599
0.42816	74013			0.44619	75777					0.50000	36668	0.43860	34510		
0.43247	74013			0.45067	75777							0.44298	39887		
0.43678	74013			0.45516	75777							0.44737	39887		
0.44109	74013			0.45964	75777							0.45175	39887		
0.44540	74013			0.46413	75777							0.45614	39887		
0.44971	74013			0.46861	75777							0.46053	39887		
0.45402	74013			0.47309	78739							0.46491	39887		
0.45833	74013			0.47758	85157							0.46930	39887		
0.46264	74013			0.48206	86462							0.47368	39887		
0.46695	76391			0.48655	86462							0.47807	39887		
0.47126	82072			0.49103	86462							0.48246	39887		
0.47557	87548			0.49327	86462							0.48684	39887		
0.47989	93846			0.49552	86462							0.49123	39887		
0.48420	98911			0.50000	89424							0.49561	39887		
0.48851	106099											0.50000	39887		
0.49282	116435														
0.49713	128341														
0.50000	134908														

F.5 Design curves for a three-span railway bridge

L = 30 m		L = 31.5 m		L = 33 m		L = 34.5 m		L = 36 m		L = 37.5 m		L = 39 m		L = 40.5 m		L = 42 m		L = 43.5 m	
β	τ	β	τ	β	τ	β	τ	β	τ	β	τ	β	τ	β	τ	β	τ	β	τ
0.002242	116.2585	0.002472	102.9108	0.002713	96.62865	0.002965	97.47153	0.003229	108.8065	0.003503	118.6441	0.003789	106.3135	0.004086	95.48939	0.004395	108.4476	0.004714	89.8916
0.008968	523.5175	0.009888	446.4143	0.010852	431.9652	0.011861	445.38	0.009686	275.7452	0.01051	355.9948	0.011367	354.9664	0.012259	353.3344	0.013184	322.835	0.014142	323.7149
0.015695	654.173	0.017303	675.5032	0.018991	617.6315	0.020756	768.5169	0.016143	507.3154	0.017516	636.0863	0.018946	570.4226	0.020431	570.9336	0.021973	705.8436	0.02357	540.0452
0.022421	1222.764	0.024719	1083.903	0.027129	1175.115	0.029652	1102.548	0.0226	816.9627	0.024523	870.7022	0.026524	1030.499	0.028604	921.3637	0.030762	798.656	0.032998	975.8854
0.029147	1657.914	0.032135	1511.036	0.035268	1801.994	0.038547	1772.889	0.029058	927.6	0.031529	933.5443	0.034102	1364.993	0.036776	1223.927	0.039551	1400.427	0.042426	1507.089
0.035874	2291.726	0.039551	2493.666	0.043407	1868.109	0.047443	2170.185	0.035515	1599.72	0.038536	1427.013	0.041681	1662.552	0.044948	1540.826	0.04834	1506.934	0.051854	1943.059
0.0426	2791.472	0.046966	2493.666	0.051546	2612.694	0.056338	2447.445	0.041972	1715.338	0.045543	1913.929	0.049259	2456.931	0.053121	1936.714	0.057129	1816.966	0.061282	2240.409
0.049326	3428.53	0.054382	3259.332	0.059685	3161.418	0.065234	2963.162	0.048429	2004.547	0.052549	2264.75	0.056837	2456.931	0.061293	2346.848	0.065918	2188.127	0.07071	2456.256
0.056052	3519.524	0.061798	3814.478	0.067823	3530.805	0.074129	3732.116	0.054887	2601.103	0.059556	2433.026	0.064415	2456.931	0.069466	2746.571	0.074707	2508.274	0.080138	2468.999
0.062779	4752.455	0.069214	3835.656	0.075962	4338.856	0.083025	4051.167	0.061344	2828.286	0.066562	2744.046	0.071994	2486.47	0.077638	2978.072	0.083496	2700.46	0.089566	3443.74
0.069505	4752.455	0.076629	4666.247	0.084101	4338.856	0.09192	4743.905	0.067801	2828.286	0.073569	2841.485	0.079572	3037.914	0.085811	3115.145	0.092285	3403.181	0.098994	3443.74
0.076231	5412.912	0.084045	5644.819	0.09224	5061.093	0.100816	5808.86	0.074258	3762.7	0.080575	3167.63	0.08715	3400.239	0.093983	3927.128	0.101074	4127.702	0.108422	3804.579
0.082958	5412.912	0.091461	5644.819	0.100379	5929.631	0.109712	5808.86	0.080716	3762.7	0.087582	4217.125	0.094729	3665.302	0.102156	3927.128	0.109863	5132.154	0.11785	4722.025
0.089684	6227.773	0.098877	7431.03	0.108518	6142.925	0.118607	6431.733	0.087173	4088.297	0.094588	4303.01	0.102307	4825.444	0.110328	4624.145	0.118652	5132.154	0.127278	6148.335
0.09641	6707.287	0.106292	7774.616	0.116656	8455.796	0.127503	8493.045	0.09363	4510.725	0.101595	4812.522	0.109885	4825.444	0.1185	5550.994	0.127441	5354.236	0.136706	6148.335
0.103136	7543.619	0.113708	7774.616	0.124795	8455.796	0.136398	9187.112	0.100087	4982.699	0.108602	5229.263	0.117463	5835.043	0.126673	6922.597	0.13623	5941.833	0.146134	6148.335
0.109863	8976.76	0.121124	9734.305	0.132934	8455.796	0.145294	9187.112	0.106545	5219.374	0.115608	5986.295	0.125042	6499.988	0.134845	6922.597	0.145019	6790.933	0.155562	6914.119
0.116589	10746.86	0.12854	10232.45	0.141073	10771.72	0.154189	9187.112	0.113002	5959.318	0.122615	7557.29	0.13262	6499.988	0.143018	6922.597	0.153808	7723.014	0.16499	8364.992
0.123315	10923.15	0.135955	10232.45	0.149212	10771.72	0.163085	12372.66	0.119459	6849.97	0.129621	7557.29	0.140198	7567.581	0.15119	7963.458	0.162597	10904.21	0.174418	8573.748
0.130042	10923.15	0.143371	10232.45	0.15735	10971.57	0.17198	12372.66	0.125916	7234.196	0.136628	7557.29	0.147777	7857.357	0.159363	8936.625	0.171386	11308.06	0.183846	8573.748
0.136768	12948.06	0.150787	11249.89	0.165489	13062.57	0.180876	14612.01	0.132374	7513.355	0.143634	7557.29	0.155355	9239.27	0.167535	8936.625	0.180175	11308.06	0.193274	8803.226
0.143494	12948.06	0.158203	13453.88	0.173628	13062.57	0.189771	15229.77	0.138831	7935.919	0.150641	8376.664	0.162933	10273.79	0.175708	9677.676	0.188964	11987.79	0.202702	11215.63
0.15022	13672.11	0.165618	13453.88	0.181767	13979.36	0.198667	16133.51	0.145288	8297.098	0.157647	10132.89	0.170511	11170.66	0.18388	9677.676	0.197753	13306.52	0.21213	11605.98
0.156947	13672.11	0.173034	13649.88	0.189906	13979.36	0.207562	16700.51	0.151745	9127.746	0.164654	10132.89	0.17809	11170.66	0.192052	10800.42	0.206542	13306.52	0.221558	11605.98
0.163673	15637.24	0.18045	16129.84	0.198045	14525.99	0.216458	18784.41	0.158203	10697.7	0.17166	10240.32	0.185668	11170.66	0.200225	12557.53	0.215331	14475.32	0.230987	11605.98
0.170399	16452.53	0.187865	16588.22	0.206183	18237.1	0.225353	18784.41	0.16466	11577.87	0.178667	13158.28	0.193246	14287.51	0.208397	12557.53	0.22412	14475.32	0.240415	12481.29
0.177126	16452.53	0.195281	20353.94	0.214322	18237.1	0.234249	18784.41	0.171117	11577.87	0.185674	13158.28	0.200825	14287.51	0.21657	12579.15	0.232909	14475.32	0.249843	14666.03
0.183852	16452.53	0.202697	20353.94	0.222461	19092.43	0.243145	18784.41	0.177574	11577.87	0.19268	13158.28	0.208403	14287.51	0.224742	12579.15	0.241698	14475.32	0.259271	14666.03
0.190578	16668.3	0.210113	20353.94	0.2306	20877.56	0.25204	18784.41	0.184031	11577.87	0.199687	13318.13	0.215981	14648.6	0.232915	12579.15	0.250487	14475.32	0.268699	22362.31
0.197304	16668.3	0.217528	20353.94	0.238739	20877.56	0.260936	18784.41	0.190489	11577.87	0.206693	16362.41	0.223559	17192.99	0.241087	13987.01	0.259276	14475.32	0.278127	22362.31
0.204031	19545.53	0.224944	20353.94	0.246877	24229.67	0.269831	19400.01	0.196946	11731.29	0.2137	16362.41	0.231138	17602.16	0.24926	15844.07	0.268065	14594.87	0.287555	22362.31
0.210757	24180.35	0.23236	20353.94	0.255016	24229.67	0.278727	19400.01	0.203403	14617.36	0.220706	16362.41	0.238716	17602.16	0.257432	15844.07	0.276854	14594.87	0.296983	22362.31
0.217483	25446.65	0.239776	20353.94	0.263155	27536.41	0.287622	19400.01	0.20986	14617.36	0.227713	16362.41	0.246294	17602.16	0.265604	15844.07	0.285643	14594.87	0.306411	22362.31
0.22421	27474.51	0.247191	20353.94	0.271294	33125.83	0.296518	19400.01	0.216318	14617.36	0.234719	16362.41	0.253873	17602.16	0.273777	18231.83	0.294432	14594.87	0.315839	22362.31
0.230936	27754.45	0.254607	21620.76	0.279433	33125.83	0.305413	19400.01	0.222775	17421.04	0.241726	16362.41	0.261451	17602.16	0.281949	18231.83	0.303221	14594.87	0.325267	22362.31
0.237662	27754.45	0.262023	26515.68	0.287571	33125.83	0.314309	19400.01	0.229232	18645.28	0.248733	16362.41	0.269029	22042.27	0.290122	18231.83	0.31201	14594.87	0.334695	22362.31
0.244388	27754.45	0.269439	28155.82	0.29571	33125.83	0.323204	19400.01	0.235689	18645.28	0.255739	16362.41	0.276607	22042.27	0.298294	18231.83	0.320799	14594.87	0.344123	22362.31
0.251115	27754.45	0.276854	28155.82	0.303849	33125.83	0.3321	22609.67	0.242147	18645.28	0.262746	17897.95	0.284186	22042.27	0.306467	18231.83	0.329588	14594.87	0.353551	22362.31
0.257841	27754.45	0.28427	28155.82	0.311988	33125.83	0.340995	23332.09	0.248604	18645.28	0.269752	19488.88	0.291764	22042.27	0.314639	18231.83	0.338377	14594.87	0.362979	22362.31
0.264567	27754.45	0.291686	28155.82	0.320127	33125.83	0.349891	23332.09	0.255061	18645.28	0.276759	19488.88	0.299342	22042.27	0.322812	18231.83	0.347166	17397.4	0.372407	22362.31
0.271294	27754.45	0.299102	28155.82	0.328266	33125.83	0.358786	23332.09	0.261518	19602.21	0.283765	19488.88	0.30692	22042.27	0.330984	20875.27	0.355955	17729.59	0.381835	22362.31
0.27802	27754.45	0.306517	28155.82	0.336404	33125.83	0.367682	28125.47	0.267976	23523.44	0.290772	19488.88	0.314499	22042.27	0.339156	23303.24	0.364744	17729.59	0.391263	22362.31
0.284746	27754.45	0.313933	28155.82	0.344543	33125.83	0.376577	30958.59	0.274433	25143.44	0.297778	19488.88	0.322077	22042.27	0.347329	23303.24	0.373533	17729.59	0.400691	22362.31
0.291473	27754.45	0.321349	28155.82	0.352682	33125.83	0.385473	31085.66	0.28089	25143.44	0.304785	19488.88	0.329655	22042.27	0.355501	23303.24	0.382322	18269.29	0.410119	22362.31
0.298199	27754.45	0.328765	28155.82	0.360821	33125.83	0.394369	31085.66	0.287347	25143.44	0.311791	19488.88	0.337234	22042.27	0.363674	23303.24	0.391111	18269.29	0.419547	22362.31
0.304925	27754.45	0.33618	34050.29	0.36896	33200.38	0.403264	31085.66	0.293805	25143.44	0.318798	19488.88	0.344812	22042.27	0.371846	23303.24	0.3999	18703.69	0.428975	22362.31
0.311651	27754.45	0.343596	34812.38	0.377098	33200.38	0.41216	31085.66	0.300262	25143.44	0.325805	19488.88	0.35239	22042.27	0.380019	23303.24	0.408689	19115.63	0.438403	22362.31
0.318378	27754.45	0.351012	34812.38	0.385237	33200.38	0.421055	31085.66	0.306719	25143.44	0.332811	19488.88	0.359968	22042.27	0.388191	23303.24	0.417478	19115.63	0.447831	22362.31
0.325104	27754.45	0.358428	34812.38	0.393376	33200.38	0.429951	31949.53	0.313176	25143.44	0.339818	19488.88	0.367547	22042.27	0.396364	23303.24	0.426267	19115.63	0.457259	28716.89
0.33183	28830.66	0.365843	34812.38	0.401515	33200.38	0.438846	34561.99	0.319634	25143.44	0.346824	19488.88	0.375125	22042.27	0.404536	23303.24	0.435056	20301.64	0.466687	34801.26
0.338557	32315.05	0.373259	34812.38	0.409654	33200.38	0.447742	37975.76	0.326091	25143.44	0.353831	19488.88	0.382703	22042.27	0.412708	23303.24	0.443845	25929.95	0.476115	37028.25
0.345283	32315.05	0.380675	34812.38	0.417793	33855.72	0.456637	45216.3	0.332548	25143.44	0.360837	19488.88	0.390282	22042.27	0.420881	23303.24	0.452634	29360.69	0.485543	38909.85
0.352009	32315.05	0.388091	34812.38	0.425931	43889.87	0.465533	55433.18	0.339005	25143.44	0.367844	19488.88	0.39786	22042.27	0.429053	27985.99	0.461423	35823	0.494971	40331.52
0.358735	32315.05	0.395506	34812.38	0.43407	50018.16	0.474428	61349.02	0.345463	25143.44	0.37485	19488.88	0.405438	22042.27	0.437226	31112.28	0.470212	39834.45	0.504399	40331.52
0.365462	32315.05	0.402922	34812.38	0.442209	50018.16	0.483324	61549.3	0.35192	25143.44	0.381857	19488.88	0.413016	26070.63	0.445398	33233.88	0.479001	40736.92	0.513827	40331.52
0.372188	32315.05	0.410338	43913.34	0.450348	50018.16	0.492219	61549.3	0.358377	25143.44	0.388864	19626.84	0.420595	28300.98	0.453571	33233.88	0.48779	40736.92	0.523255	40331.52
0.378914	32315.05	0.417753	47752.75	0.458487	50018.16	0.501115	62518.61	0.364834	25143.44	0.39587	23290.49	0.428173	33191.58	0.461743	33444.56	0.496579	40736.92	0.532683	40331.52
0.385641	32599.66	0.425169	47752.75	0.466625	50018.16	0.51001	62518.61	0.371292	25143.44	0.402877	26025.97	0.435751	36301.74	0.469916	33444.56	0.505368	40736.92	0.542111	40331.52
0.392367	40679.86	0.432585	51593.12	0.474764	52195.8	0.518906	62518.61	0.377749	25143.44	0.409883	30988.15	0.44333	37165.44	0.478088	33444.56	0.514157	40736.92	0.551539	40331.52
0.399093	45272.68	0.440001	55382.79	0.482903	56123.05	0.527801	62518.61	0.384206	25143.44	0.41689	34156.16	0.450908	37165.44	0.48626	33444.56	0.522946	40736.92	0.560967	43500.84
0.405819	45272.68	0.447416	55622.98	0.491042	56123.05	0.536697	62518.61	0.390663	28023.93	0.423896	35070.47	0.458486	37165.44	0.494433	33444.56	0.531735	40736.92	0.570395	48143.4
0.412546	45805.24	0.454832	55622.98	0.499181	56123.05	0.545593	62518.61	0.397121	31590.29	0.430903	35070.47	0.466064	37165.44	0.502605	33444.56	0.540524	44584.07	0.579823	48143.4
0.419272	50467.06	0.462248	55622.98	0.50732	56123.05	0.554488	62518.61	0.403578	32149.83	0.437909	35070.47	0.473643	37165.44	0.510778	35423.7	0.549313	46640.69	0.589251	48143.4
0.425998	52466.85	0.469664	55622.98	0.515458	56123.05	0.563384	62518.61	0.410035	32762.22	0.444916	35070.47	0.481221	37165.44	0.51895	42586.88	0.558102	48608.16	0.598679	48143.4
0.432725	52466.85	0.477079	55622.98	0.523597	56123.05	0.572279	62518.61	0.416492	32762.22	0.451922	35070.47	0.488799	37165.44	0.527123	42586.88	0.566891	49310.28	0.608107	59825.12
0.439451	52466.85	0.484495	55622.98	0.531736	56123.05	0.581175	62518.61	0.42295	32762.22	0.458929	35070.47	0.496378	37165.44	0.535295	42586.88	0.57568	49310.28	0.617535	61448.62
0.446177	52466.85	0.491911	55622.98	0.539875	56123.05	0.59007	62518.61	0.429407	32762.22	0.465936	35070.47	0.503956	37680.23	0.543468	44727.49	0.584469	49310.28	0.626963	61448.62
0.452903	52466.85	0.499327	55622.98	0.548014	57420.45	0.598966	74741.76	0.435864	32762.22	0.472942	40064.61	0.511534	38962.32	0.55164	58262.42	0.593258	49310.28	0.636391	61448.62
0.45963	52466.85	0.506742	55622.98	0.556152	64870.4	0.607861	85152.56	0.442321	32762.22	0.479949	48711.41	0.519112	40883.97	0.559812	60845.01	0.602047	49310.28	0.645819	61448.62
0.466356	52466.85	0.514158	55622.98	0.564291	64870.4	0.616757	87659.57	0.448779	33182.32	0.486955	52188.37	0.526691	40883.97	0.567985	60845.01	0.610837	56678.67	0.655247	61448.62
0.473082	55653.06	0.521574	55622.98	0.57243	64870.4	0.625652	89098.57	0.455236	40191.34	0.493962	52323.58	0.534269	44364.52	0.576157	60845.01	0.619626	56678.67	0.664675	61448.62
0.479809	56327.11	0.52899	58736.74	0.580569	72659.87	0.634548	99686.48	0.461693	48711.71	0.500968	52323.58	0.541847	47307.48	0.58433	60845.01	0.628415	56678.67	0.674103	61448.62
0.486535	56327.11	0.536405	66265.03	0.588708	74649.19	0.643443	103262	0.46815	53031.69	0.507975	52323.58	0.549426	60619.78	0.592502	60845.01	0.637204	56678.67	0.683532	61448.62
0.493261	56327.11	0.543821	77551.23	0.596846	82511.67	0.652339	103262	0.474608	53352.91	0.514981	52323.58	0.557004	67123.35	0.600675	60845.01	0.645993	56678.67	0.69296	61448.62
0.499987	60775.34	0.551237	88137.16	0.604985	95198.11	0.661234	106844.2	0.481065	53404.14	0.521988	52323.58	0.564582	67123.35	0.608847	60845.01	0.654782	56678.67	0.702388	61448.62
0.506714	60775.34	0.558653	94640.41	0.613124	99100.82	0.67013	113015.1	0.487522	60106.01	0.528995	52323.58	0.57216	67123.35	0.61702	60845.01	0.663571	56678.67	0.711816	65299.02
0.51344	60775.34	0.566068	94640.41	0.621263	99100.82	0.679026	113015.1	0.493979	61486.79	0.536001	52323.58	0.579739	67123.35	0.625192	60845.01	0.67236	56678.67	0.721244	65299.02
0.520166	62939.7	0.573484	94640.41	0.629402	107684.9	0.687921	124782	0.500437	61915.18	0.543008	52323.58	0.587317	67123.35	0.633364	62445.78	0.681149	56678.67	0.730672	68613.86
0.526893	69211.43	0.5809	94640.41	0.637541	124621.1	0.696817	141040.5	0.506894	61915.18	0.550014	54287.12	0.594895	67123.35	0.641537	69555.24	0.689938	56678.67	0.7401	74954.28
0.533619	77572.38	0.588316	94640.41	0.645679	126861	0.705712	161027.7	0.513351	61915.18	0.557021	58210.61	0.602474	67123.35	0.649709	69555.24	0.698727	58894.42	0.749528	84811.85
0.540345	87511.93	0.595731	94640.41	0.653818	126861	0.714608	166499.4	0.519808	61915.18	0.564027	58210.61	0.610052	67123.35	0.657882	69555.24	0.707516	69456.9	0.758956	89374.52
0.547071	101446.6	0.603147	97437.62	0.661957	126861	0.723503	166499.4	0.526265	61915.18	0.571034	58210.61	0.61763	67123.35	0.666054	69555.24	0.716305	77752.04	0.768384	89374.52
0.553798	107199.4	0.610563	108749.4	0.670096	126861	0.732399	166499.4	0.532723	61915.18	0.57804	58210.61	0.625208	67123.35	0.674227	69555.24	0.725094	87711.76	0.777812	89374.52
0.560524	108952.1	0.617979	116197.2	0.678235	126861	0.741294	166499.4	0.53918	61915.18	0.585047	58210.61	0.632787	67123.35	0.682399	69555.24	0.733883	87862.99	0.78724	89374.52
0.56725	108952.1	0.625394	126738.6	0.686373	126861	0.75019	166499.4	0.545637	61915.18	0.592053	58210.61	0.640365	67123.35	0.690572	69555.24	0.742672	96347.73	0.796668	89374.52
0.573977	108952.1	0.63281	147560	0.694512	129142.7	0.759085	166499.4	0.552094	61915.18	0.59906	58210.61	0.647943	67123.35	0.698744	75172.51	0.751461	108937.5		
0.580703	108952.1	0.640226	158414.1	0.702651	144483.3	0.767981	166499.4	0.558552	61915.18	0.606067	58210.61	0.655522	67123.35	0.706917	87715.14	0.76025	109836.2		
0.587429	108952.1	0.647641	158414.1	0.71079	155056.2	0.776876	166499.4	0.565009	61915.18	0.613073	58210.61	0.6631	69899.2	0.715089	97615.24	0.769039	109836.2		
0.594155	108952.1	0.655057	158414.1	0.718929	155056.2	0.785772	166499.4	0.571466	61915.18	0.62008	58305.08	0.670678	79488.05	0.723261	109830	0.777828	109836.2		
0.600882	108952.1	0.662473	158414.1	0.727068	155056.2	0.794667	166499.4	0.577923	61915.18	0.627086	59071.87	0.678256	79488.05	0.731434	113524	0.786617	109836.2		
0.607608	121524.1	0.669889	158414.1	0.735206	155056.2	0.797633	166499.4	0.584381	61915.18	0.634093	61966.71	0.685835	83334.08	0.739606	113524	0.795406	109836.2		
0.614334	136389.6	0.677304	158414.1	0.743345	155056.2			0.590838	61915.18	0.641099	71592.4	0.693413	89230.65	0.747779	113524	0.7998	109836.2		
0.621061	138038.8	0.68472	158414.1	0.751484	155056.2			0.597295	61915.18	0.648106	73483.05	0.700991	98716.85	0.755951	122399.1				
0.627787	138038.8	0.692136	158414.1	0.759623	155056.2			0.603752	61915.18	0.655112	85337.46	0.70857	100870.7	0.764124	122399.1				
0.634513	148821.6	0.699552	158414.1	0.767762	155056.2			0.61021	61915.18	0.662119	91697.71	0.716148	108613.4	0.772296	122399.1				
0.64124	155418.7	0.706967	158414.1	0.7759	155056.2			0.616667	64901.05	0.669125	96276.6	0.723726	114500.9	0.780469	122399.1				
0.647966	155418.7	0.714383	158414.1	0.784039	155056.2			0.623124	73509.42	0.676132	99232.82	0.731304	121536	0.788641	122399.1				
0.654692	155418.7	0.721799	158414.1	0.792178	155056.2			0.629581	84067.03	0.683139	99232.82	0.738883	121536	0.796813	122399.1				
0.661418	155418.7	0.729215	158414.1	0.797604	155056.2			0.636039	89669.47	0.690145	99232.82	0.746461	121536						
0.668145	155418.7	0.73663	158414.1					0.642496	91593.06	0.697152	99232.82	0.754039	129133.7						
0.674871	155418.7	0.744046	158414.1					0.648953	91771.53	0.704158	100244.5	0.761618	132346.8						
0.681597	155418.7	0.751462	158414.1					0.65541	97415.31	0.711165	107835.4	0.769196	132346.8						
0.688324	155418.7	0.758878	158414.1					0.661868	103748.9	0.718171	114936.5	0.776774	137391.1						
0.69505	155418.7	0.766293	158414.1					0.668325	107592.1	0.725178	122255.2	0.784352	140939.1						
0.701776	155418.7	0.773709	158414.1					0.674782	107592.1	0.732184	130757.9	0.791931	140939.1						
0.708502	155418.7	0.781125	158414.1					0.681239	107592.1	0.739191	130757.9	0.799509	140939.1						
0.715229	155418.7	0.788541	158414.1					0.687697	107592.1	0.746198	130757.9								
0.721955	162525	0.795956	158414.1					0.694154	114211.7	0.753204	130757.9								
0.728681	168687.3	0.798428	158414.1					0.700611	126961.5	0.760211	130757.9								
0.735408	175731.3							0.707068	142556.4	0.767217	130757.9								
0.742134	203755.7							0.713526	146314.7	0.774224	143894.2								
0.74886	221491.5							0.719983	146314.7	0.78123	150975.4								
0.755586	222950.1							0.72644	146314.7	0.788237	150975.4								
0.762313	222950.1							0.732897	146314.7	0.795243	150975.4								
0.769039	222950.1							0.739355	146314.7	0.798747	150975.4								
0.775765	222950.1							0.745812	146314.7										
0.782492	222950.1							0.752269	146314.7										
0.789218	222950.1							0.758726	146314.7										
0.795944	222950.1							0.765184	146314.7										
								0.771641	146314.7										
								0.778098	146314.7										
								0.784555	146314.7										
								0.791013	146314.7										
								0.79747	146314.7										